TEMPORAL VARIATION IN AEROSOL COMPOSITION AT NORTHWESTERN TURKEY

A THESIS SUBMITTED TO
THE GRADUATE SCHOOL OF NATURAL AND APPLIED SCIENCES
OF
MIDDLE EAST TECHNICAL UNIVERSITY

BY

D. DENİZ GENÇ TOKGÖZ

IN PARTIAL FULFILLMENT OF THE REQUIREMENTS
FOR
THE DEGREE OF DOCTOR OF PHILOSOPHY
IN
ENVIRONMENTAL ENGINEERING

FEBRUARY 2013

Approval of the thesis:

TEMPORAL VARIATION IN AEROSOL COMPOSITION AT NORTHWESTERN TURKEY

submitted by **D. DENİZ GENÇ TOKGÖZ** in partial fulfillment of the requirements for the degree of **Doctor of Philosophy in Environmental Engineering Department, Middle East Technical University** by,

Prof. Dr. Canan Özgen _____
Dean, Graduate School of **Natural and Applied Sciences**

Prof. Dr. F. Dilek Sanin _____
Head of Department, **Environmental Engineering**

Prof. Dr. Gürdal Tuncel _____
Supervisor, **Environmental Engineering Dept., METU**

Examining Committee Members:

Prof. Dr. Göksel N. Demirer _____
Environmental Engineering Dept., METU

Prof. Dr. Gürdal Tuncel _____
Environmental Engineering Dept., METU

Prof. Dr. O. Yavuz Ataman _____
Chemistry Dept., METU

Assoc. Prof. Dr. Ayşegül Aksoy _____
Environmental Engineering Dept., METU

Assoc. Prof. Dr. Eftade E. Gaga _____
Environmental Engineering Dept., Anadolu University

Date: _____

I hereby declare that all information in this document has been obtained and presented in accordance with academic rules and ethical conduct. I also declare that, as required by these rules and conduct, I have fully cited and referenced all material and results that are not original to this work.

Name, Last name: D. Deniz Genç Tokgöz
Signature:

ABSTRACT

TEMPORAL VARIATION IN AEROSOL COMPOSITION AT NORTHWESTERN TURKEY

Genç Tokgöz, D. Deniz
Ph.D., Department of Environmental Engineering
Supervisor: Prof. Dr. Gürdal Tuncel

February 2013, 177 pages

Daily aerosol samples (PM) were collected at a rural station, which is 5 km away from the Turkish-Bulgarian border between April 2006 and March 2008. Aerosol samples were analyzed for elements by ICPMS, ions by IC and black carbon by aethalometer to provide a multi-species aerosol data set, which can represent aerosol population for Northwestern Turkey and Eastern Europe. Average concentration of SO_4^{2-}, NO_3^- and NH_4^+ was 5.8, 2.9 and 2.0 µg m^{-3}, respectively, while total aerosol mass was 66 µg m^{-3}. Seasonal variation of crustal species had maxima in summer, while most of the anthropogenic species had maxima in winter. Rainfall was found as the only local meteorological parameter affecting aerosols concentrations. The dominant sectors of air masses arriving the Northwestern Turkey were northeast in summer and west-northwest in winter. Air masses were classified into five clusters regarding their wind speed and direction. Most species indicated significant differences between clusters. The influence of forest fires in Ukraine and Russian Federation was identified by cluster analysis using soluble K as tracer. Source apportionment of PM was carried out by EPA PMF model and five sources were resolved. Crustal emissions were found to be the major contributor to PM (41%). The second largest source was distant anthropogenic sources with a contribution of 26%. Traffic was also a remarkable source with 16% contribution. Sea salt and stationary combustion sources accounted for 9% and 8% of PM, respectively. Potential source regions of resolved sources were determined by potential source contribution function (PSCF).

Keywords: Rural Station, Eastern Europe, Cluster Analysis, Positive Matrix Factorization, Potential Source Contribution Function.

ÖZ

TÜRKİYE'NİN KUZEYBATISINDAKİ AEROSOL KOMPOZİSYONUNUN ZAMANSAL DEĞİŞİMİ

Genç Tokgöz, D. Deniz
Doktora, Çevre Mühendisliği Bölümü
Tez Danışmanı: Prof. Dr. Gürdal Tuncel

Şubat 2013, 177 sayfa

Türkiye - Bulgaristan sınırına 5 km uzaklıkta konuşlandırılan kırsal bir istasyonda Nisan 2006 ve Mart 2008 zaman aralığında partikül madde örnekleri günlük olarak toplanmıştır. Örneklerin element içeriği Endüktif Eşleşmiş Plazma Kütle Spektrometresi (ICPMS), iyon içeriği İyon Kromotografi (IC) cihazı ve siyah karbon içeriği Atelometre cihazı ile analiz edilmiştir. Böylece Türkiye'nin kuzeybatısı ve Doğu Avrupa'daki partikül maddeyi temsil eden çok parametreli bir veri seti elde edilmiştir. Sülfat, NO_3^- ve NH_4^+ iyonlarının aritmetik ortalama derişimleri sırasıyla 5.8, 2.9 ve 2.0 µg m^{-3} iken toplam partikül madde derişimi 66 µg m^{-3} olarak bulunmuştur. En yüksek derişimler toprak kaynaklı kirleticilerde yaz mevsiminde, insan kaynaklı kirletilerin çoğunda ise kış mevsiminde ölçülmüşür. Yerel meteorolojik faktörlerden sadece yağmurun partikül madde derişimini etkilediği tesbit edilmiştir. Türkiyenin kuzeybatısına ulaşan hava kütlelerinin hakim yönü yazın kuzeybatı, kışın ise batı-kuzeybatı sektörüdür. Hava kütleleri geliş yönleri ve rüzgar hızlarına göre beş farklı kümeye ayrılmıştır. Çoğu kirletici derişimi kümeler arasında farklılık göstermiştir. Kümeleme analizinde suda çözünebilir K'un orman yangınları belirticisi olarak kullanılmasıyla, Ukrayna ve Rusya Federasyonundaki orman yangınlarının etkisi gösterilmiştir. Partikül maddeyi etkileyen kaynakları bulmak için EPA'nın PMF modeli kullanılmış ve beş kaynak ayrıştırılmıştır. Toprak emisyonları partikül kütlesinin %41'ini oluşturarak en büyük katkıya sahiptir. Katkısı ikinci sırada yer alan uzun mesafeli kirletici emisyonları partikül kütlesinin %26 lık bir kısmını oluşturmaktadır. Trafik emisyonları %16 lık bir katkı ile dikkat çekmektedir. Deniz emisyonları ve sabit kaynaklarda yakıt yanması kaynaklı emisyonlar ise partikül kütleye sırasıyla %9 ve %8 lik bir katkıda bulunmaktadır. PMF ile ayrıştırılan kaynakların kaynak bölgeleri kaynak etki fonksiyonu yöntemi (PSCF) ile belirlenmiştir.

Anahtar Kelimeler: Kırsal İstasyon, Doğu Avrupa, Kümeleme Analizi, Pozitif Matriks Faktörizasyonu, Kaynak Etki Fonksiyonu Yöntemi.

To MyMoon…

ACKNOWLEDGMENTS

TABLE OF CONTENTS

LIST OF TABLES

TABLES

LIST OF FIGURES

FIGURES

CHAPTER 1

BACKGROUND

As the climatic effects and deleterious health effects of aerosols have been documented in the literature, ambient air quality standards have become stricter. Authorities have to formulate optimal abatement strategies to achieve these standards. In order to formulate optimal abatement strategies emission sources contributing to ambient aerosols, their quantitative contribution and geographical locations should be known. Not only local emission sources but also distant emission sources (hundreds or thousands kilometers away) can contribute to observed aerosols in an area. Hence contribution of both distant sources (natural+ anthropogenic sources) and local sources (natural+ anthropogenic sources) must be delineated, and then control strategies should be developed for controlling anthropogenic local sources. Distinguishing between local and distant source contribution is a crucial step and requires extensive aerosol data in terms of multiple species and multiple time periods.

The effect of long range transported (LRT) aerosols emitted from distant sources (natural and anthropogenic) particularly on rural areas, where influence of local sources is less, has been well documented. Therefore chemical composition of aerosols particularly in rural areas is now monitored in most of the EU countries. However there are few studies in Turkey and eastern European countries. The studies conducted in Turkey are discussed in Section 2.9.

The most comprehensive rural studies were conducted at the Mediterranean and the Black Sea coast of Turkey. These previous studies had increased our knowledge on LRT of aerosols over Turkey. However the measurements up to now were conducted in the locations where air masses traveled some distance over Turkey before they reached to the sampling points. Therefore, measured aerosols in these stations were composed of pollutants transported from abroad, plus pollutants picked up by air masses while transporting over Turkey prior the sampling points. Because of the fact that air masses originate from abroad may pick up the emissions from Turkey, differentiation of foreign emissions from those emitted within the country is very difficult for these studies.

There are few LRT studies conducted in northwestern part of Turkey and most of them were conducted in Istanbul which is Turkey's mega city with a population over 13 million. Beside population, Istanbul is one of the industrial centers of Turkey with numerous point sources (textile, automotive, pharmaceuticals, electronics, oil products and etc.) within and around the city. Istanbul is also close to the Turkey's other industrial centers, namely Kocaeli, Bursa and Tekirdağ. Most of the air pollution studies conducted in Istanbul indicated that accompanied with the prevailing weak dispersion conditions, observed air pollution in Istanbul is mostly affected from local sources. Therefore isolation of the local sources from transported aerosols in Istanbul can be difficult and even impossible if the adverse meteorological conditions and/or atmospheric chemistry mask the source signatures which can be defined as the variability in the impacts of sources at the receptor. In conclusion lack of extensive aerosol measurements in rural area of northwestern Turkey limits determination of the long range transported aerosols into Turkey.

Black carbon (BC) is a globally important aerosol species that affect global warming and visibility by absorbing light. There are few studies focusing on the BC concentration of aerosols in Eastern Europe and Turkey. Therefore there is a gap on the BC concentrations of aerosols in rural sites of Turkey and particularly in Eastern Europe in the literature.

1.1. Aim of the Study

The general purpose of this study is to investigate the chemical composition of aerosols, factors affecting their temporal variations, sources and potential source locations of aerosols at a rural site in Northwestern Turkey. This general purpose can be subdivided into more specific scopes as below:

1. To determine the chemical composition of northwestern Turkey aerosols at a rural area in where air masses are not influenced form Turkey's own emissions.
2. To characterize the short and long-term variations of aerosol species and investigate the factors controlling these variations.
3. To investigate the dependence of aerosol species on local meteorological conditions to distinguish between locally generated aerosol species and aerosol species transported into the area.
4. To investigate the relation between concentration of aerosol species and local rain events to determine the scavenging efficiency of species.
5. To assess the pollution level of the region by comparing the aerosol species with those reported in other parts of Turkey and literature.
6. To determine the influence of desert dust intrusions on northwestern Turkey aerosol chemical composition using trajectory statistics, satellite images and model simulations.
7. To determine the general flow climatology of the northwestern Turkey by analyzing the back trajectories between 2006 and 2008.
8. To assess the relation between general flow patterns of back trajectories and concentrations of aerosol species.
9. To use trajectory statistics for marker species whose source may be tracked back in time (such as soluble K as forest fire marker).
10. To identify the sources of aerosols affecting aerosol composition at northwestern Turkey.
11. To quantitatively determine the contribution of identified sources to the northwestern Turkey aerosols.
12. To find the potential source regions influencing the chemical composition of northwestern Turkey aerosols.

CHAPTER 2

LITERATURE REVIEW

Aerosol is defined as a complex mixture of solid particles and liquid droplets suspended in the air. Although only the solid part of aerosol is defined as particulate matter (PM), aerosol and PM is used interchangeably. Because aerosols undergo chemical and physical reactions in the atmosphere and finally they are transformed into PM.

Particle size, concentration and chemical composition are known as the main properties of aerosols; however aerosols are generally characterized by their size (aerodynamic diameter). Aerodynamic diameter is an expression of a particle's aerodynamic behavior as if it were a perfect sphere with unit-density and diameter equal to the aerodynamic diameter. Since particles larger than 30 µm to 70 µm remain suspended for a very short period before deposition, particulate matter in the ambient air generally range from less than 0.01 µm to more than 50 µm in diameter (Englert, 2004). Total suspended particles (TSP) is the most comprehensive term including particles of any size suspended in air and defined as the particulate matter with an aerodynamic diameter less than 100 µm. PM10 and PM2.5 is particulate matter with an aerodynamic diameter less than 10 µm and 2.5 µm, respectively. The PM10 fraction is called as respirable suspended particulate (RSP) and the PM2.5 fraction is called as fine particles. The fraction between 10 µm and 2.5 µm are called as coarse particles.

Regarding the size distribution aerosols are divided into four modes, namely aitken, nucleation, accumulation and coarse mode. The aitken mode contains particles with diameter up to 10 nm, while particles with diameter between 10 nm and 0.1 µm constitute the nucleation mode. The accumulation mode comprises particles in a size range from 0.1 to 2.5 µm. Particles larger than 2.5 µm make the coarse mode. Aitken, nucleation and accumulation mode particles together called as fine particles (PM2.5). Aerosols in each size mode have different formation and removal mechanisms in the atmosphere, and different chemical composition as well. As Seinfeld and Pandis, 2006 have stated size distribution of aerosols is the fundamental one when discussing any field related to aerosols.

2.1. Sources of Aerosols

Aerosols are emitted into atmosphere both from natural (biogenic) sources and anthropogenic (human activity) sources. The routes of incorporation of chemical species into atmospheric particulate matter is illustrated in Figure 2.1.1 (Meng et al., 1997). Emission from volcanoes, soil and sea spray are the most important natural sources of aerosols. The major aerosol species emitted from volcanoes are volcanic dust and SO_4^{2-} which is originally emitted as SO_2 gas and then oxidized to SO_4^{2-} in the atmosphere (Seinfeld and Pandis, 2006). The contribution of volcanoes to the ambient PM as volcanic dust is estimated to be 30 Tg (teragram, 10^{12} gram) per year (Seinfeld and Pandis, 2006, Kiehl and Rodhe, 1995). Estimates of volcanic sulfur emissions are more uncertain, ranging from 0.75 Tg to 25 Tg per year (Andres and Kasgnoc, 1998, Berresheim and Jaeschke, 1983, Graf et al., 1997, Lambert et al., 1988, Stoiber et al., 1987).

The other natural source of aerosols is mineral dust which arises from uplifting of soil particles by winds and suspension of them in the air. The Sahara-Sahel region of northern Africa and central Asia are the largest global mineral dust sources. The major species of soil dust are crustal species such as Fe, Ca, Si, Al and Ti. Mineral dust contribution estimates are highly uncertain and ranges from 1000-3000 Tg per year to the global aerosol mass (Dentener et al., 1996, Todd et al., 2008, Zender et al., 2004).
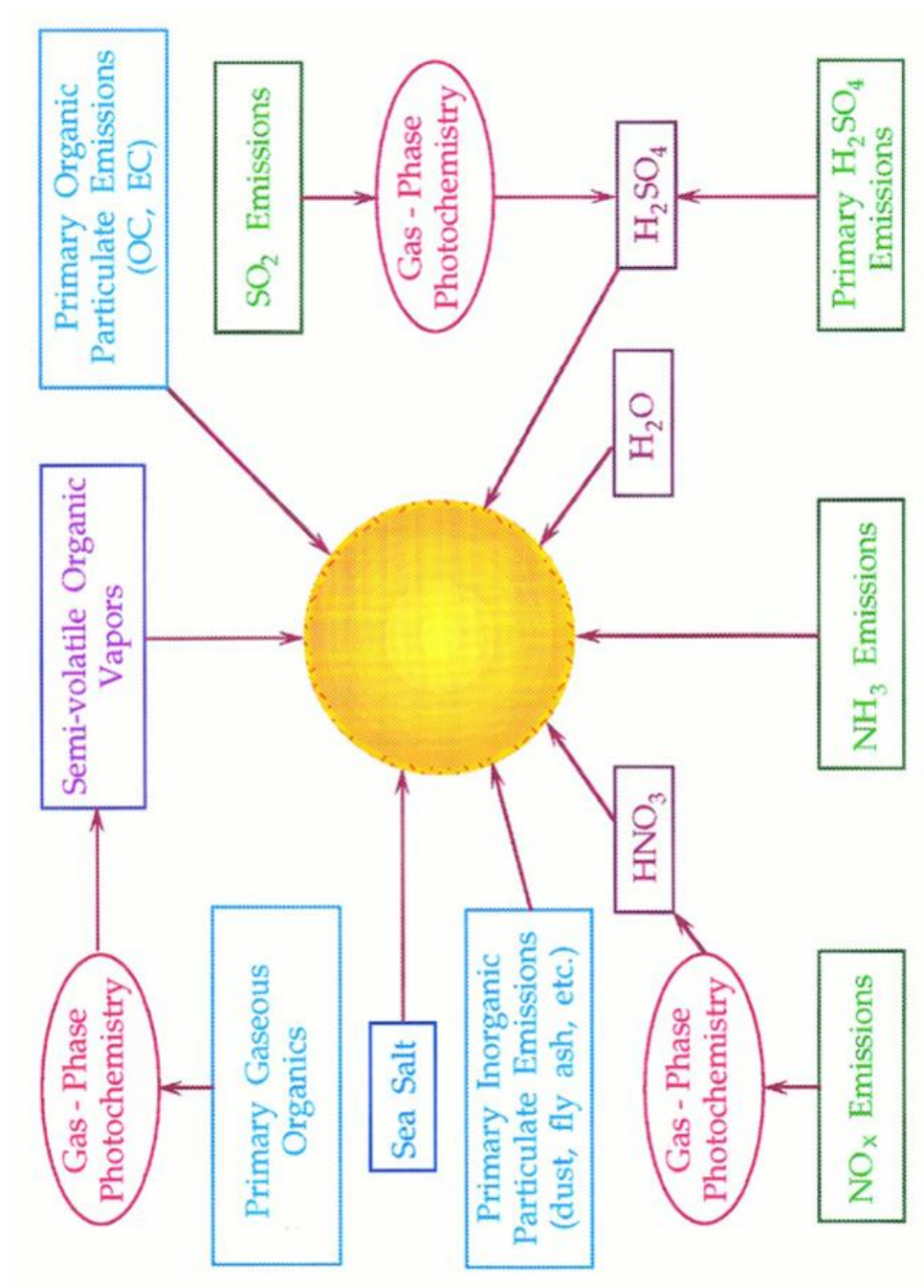
Figure 2.1.1 Sources and transformation mechanisms for atmospheric PM (Meng et al., 1997)

Sea spray is also a significant natural source of aerosols. The major species of sea spray are Na^+, Cl^-, Mg^{2+}, SO_4^{2-} and K^+ (Song and Carmichael, 1999, Murphy et al., 1997, Keene et al., 1986). The contribution of sea spray to the total aerosol mass is estimated as 300-2000 Tg per year (Pueschel, 1995, Gong et al., 1997, Liao et al., 2003). Pollens, seeds and forest fires are also natural aerosol sources but their contributions are very less compared to the major sources.

There are various anthropogenic sources that emit aerosols and/or precursor gases into the atmosphere. Human activities such as fossil fuel combustion, biomass burning, industrial processes and agricultural activities are the major ones. The size of the anthropogenic aerosols is generally less than 1 µm. Note that contribution of anthropogenic fraction to the total aerosol mass is small in the coarse fraction, while the contribution is dominated by anthropogenic species in the fine fraction.

Aerosols can either be directly emitted from sources, such as mineral dust or produced in the atmosphere. The former one is called as primary aerosol while the latter is called as secondary aerosol. Secondary aerosols can be formed in the atmosphere both by homogeneous and heterogeneous nucleation processes. When aerosol is formed by aggregation of gas molecules, this process is called as homogeneous nucleation. Gas phase oxidation of SO_2 to SO_4^{2-} can be given as an example for homogeneous nucleation. If low saturation vapor pressure gases condense on the surface of pre-existing particles and could not evaporate afterwards, this process is called as heterogeneous nucleation. Sea salt and mineral dust particles can act as reaction surface for nitrogen, sulfur and other low saturation vapor gases, hence they influence the atmospheric chemistry and biogeochemical cycle (Andreae and Crutzen, 1997, Song and Carmichael, 1999).

2.2. Formation of secondary aerosols

The mechanisms and pathways for the formation of secondary aerosols are extremely complex and not fully understood, therefore only formation mechanisms of the well-known secondary aerosol species, namely SO_4^{2-}, NO_3^- and NH_4^+ will be explained here. There are several gas-phase (homogeneous nucleation) reactions that can oxidize SO_2 but based on the rate of these reactions, reaction with the OH (hydroxyl) radical is the most important and dominant one in the atmosphere (Gleason et al., 1987, Margitan, 1984, Stockwell and Calvert, 1983). These reactions are given in Equation 2.2.1 to Equation 2.2.3. Once H_2SO_4 is produced, it should condense and dissociate to form SO_4^{2-} ion (Equation 2.2.4).

$$SO_2 + OH \cdot + M \rightarrow HSO_3 \cdot + M \qquad \text{Equation 2.2.1}$$

$$HSO_3 \cdot + O_2 \rightarrow HO_2 \cdot + SO_3 \qquad \text{Equation 2.2.2}$$

$$SO_3 + H_2O + M \rightarrow H_2SO_4 + M \qquad \text{Equation 2.2.3}$$

$$H_2SO_4 \rightarrow H_2SO_{4(aq)} \leftrightarrow H^+ + HSO_4^- \leftrightarrow 2H^+ + SO_4^{2-} \qquad \text{Equation 2.2.4}$$
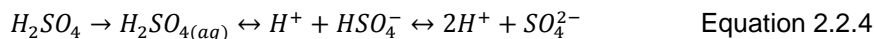
Sulfate is also produced by the heterogeneous nucleation processes (aqueous-phase reactions). In the literature there are several aqueous-phase reactions, of the most important ones are oxidation by O_3 (ozone), H_2O_2 (hydrogen peroxide), O_2 (oxygen) catalyzed by Mn^{2+} and Fe^{3+}, OH (hydroxyl radical), HCHO (formaldehyde) and Cl_2^- (dichloride) (Pandis and Seinfeld, 1989). The reactions given in Equation 2.2.5 to Equation 2.2.8 depend on pH. At pH value of 6 or less, Equation 2.2.8 is the most important reaction that produces sulfate. At pH value greater than 6, reaction given in Equation 2.2.9 is the most important one producing sulfate. Note that most aqueous-phase SO_2 oxidation occurs in clouds.

$$SO_2 + H_2O_{(aq)} \leftrightarrow H_2SO_{3(aq)}$$ Equation 2.2.5

$$H_2SO_{3(aq)} \leftrightarrow H^+ + HSO_3^-$$ Equation 2.2.6

$$HSO_3^- \leftrightarrow H^+ + SO_3^{2-}$$ Equation 2.2.7

$$HSO_3^- + H_2O_{2(aq)} + H^+ \leftrightarrow H_2O + 2H^+ + SO_4^{2-}$$ Equation 2.2.8

$$SO_3^{2-} + O_{3(aq)} \leftrightarrow O_{2(aq)} + SO_4^{2-}$$ Equation 2.2.9
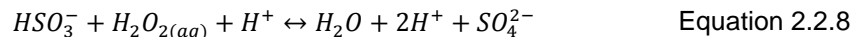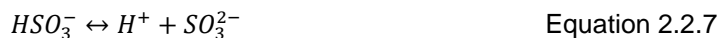
The gas-phase oxidation of oxides of nitrogen ($NO_x = NO+NO_2$) is dominant in the atmosphere because of the small solubility of NO and NO_2 in water (Carslaw et al., 1997, Jacob, 2000, Russell et al., 1986). The oxidation of NO_2 occurs directly by OH (Equation 2.2.10) or through a series of reactions with O_3 and $HCHO$. Depending on the pH, relative humidity (RH) and temperature, some of produced HNO_3 condenses on pre-existing particle surfaces and other portion remains in the gas phase (Wang et al., 2006, Tang and Munkelwitz, 1993).

$$NO_2 + OH \cdot + M \rightarrow HNO_3 + M$$ Equation 2.2.10

$$HNO_3 \leftrightarrow HNO_{3(aq)} \leftrightarrow H^+ + NO_3^-$$ Equation 2.2.11
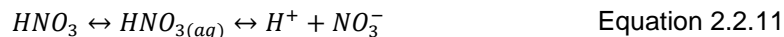
The gas-phase reaction of ammonia gas (NH_3) is very slow and assumed to be insignificant. The aqueous-phase reaction of NH_3 is given in Equation 2.2.12 and Equation 2.2.13. Firstly NH_3 condenses and then dissociates to form ammonium ion (NH_4^+). Once formed NH_4^+ reacts with sulfate, nitrate or chloride on the aerosols and neutralizes them. The amount of NH_4^+ highly depends on the relative amount of NH_3, H_2SO_4, relative humidity and pH (Nenes et al., 1999).

$$NH_3 + H_2O_{(aq)} \leftrightarrow NH_3 \cdot H_2O$$ Equation 2.2.12

$$NH_3 \cdot H_2O \leftrightarrow NH_4^+ + OH^-$$ Equation 2.2.13

At very acidic conditions i.e. NH_3/H_2SO_4 molar ratio less than 0.5, H_2SO_4 constitute the aerosol composition, while HSO_4^- (bisulfate) is the major aerosol species at acidic conditions in where NH_3/H_2SO_4 molar ratio is between 0.5-1.5. If there is enough NH_3 to neutralize the H_2SO_4, then aerosols exist as SO_4^{2-}.

Ammonia reacts with HNO_3 to form NH_4NO_3 at high NH_3 and HNO_3 concentrations and low H_2SO_4 concentrations. However the stability of NH_4NO_3 depends on temperature and RH, for example at low temperatures NH_4NO_3 prefers to be in solid phase, while at high temperatures it tends to be in gas phase as NH_3 and HNO_3. Therefore measurements of NH_4NO_3 in aerosols are highly uncertain.

In the atmosphere NH_3, H_2SO_4 and HNO_3 exist together. In this case there is a competition between H_2SO_4 and HNO_3 to react with NH_3. Due to extremely low vapor pressure of H_2SO_4, aerosols in the form of sulfate is preferred (Pandis and Seinfeld, 1989).

2.3. Removal Processes of Aerosols

Airborne aerosols can be scavenged by sedimentation, dry deposition and wet deposition (precipitation), and finally return to the earth's surface. Sedimentation removes larger particles, while dry deposition can usually remove smaller ones (diameter less than 0.5 µm). Dry deposition is defined as the removal of particles from the atmosphere in the absence of wet deposition due to transport to the ground or a surface in terms of molecular diffusion, turbulent diffusion or advection. Dry deposition is important for particles having low water solubility and for regions in where the amount and frequency of precipitation is less.

Wet deposition can be defined as the removal of aerosols from the atmosphere by hydrometeors (cloud and fog droplets, rain and snow) (Seinfeld and Pandis, 2006). Wet deposition can be described by below cloud processes and in-cloud processes. If a particle removed from the atmosphere due to collision of raindrop and particle, this process is called as wash-out or below-cloud scavenging. However if a particle acts as cloud condensation nuclei and forms cloud droplet, then subsequent removal of this cloud droplet is called as rain-out or in-cloud scavenging. Note that wash-out is a local removal process, whereas rain-out can be a regional and/or long range transport removal process.

2.4. Effects of Aerosols on Environment and Human Health

Particulate matters have adverse effects on human health (Anderson, 2009), materials (Grossi and Brimblecombe, 2002, Tidblad and Kucera, 1998), visibility (Watson, 2002), ecosystem (Bergin et al., 2001) and earth's climate (IPCC, 2001, Lelieveld et al., 2002). The adverse health effect of aerosols has been studied in the literature (Dockery et al., 1993, Pope et al., 1992, Pope, 2000, Schwartz et al., 1996, Samet et al., 2000). Although the mechanism by which particles influence human health are poorly understood, particle size and composition are known to be the most important factors that influence the human health (Englert, 2004). Epidemiological studies have shown an association between respiratory and cardiovascular related mortality and morbidity and levels of particulate matter (Adler et al., 1994, Singh et al., 2002). It has been well-documented that one of the main factors determining health effect is exposure length (Pope, 2000, Pope and Dockery, 2006). Pope et al. (1995) have found that there may be no lower threshold value of PM for health related problems. Most of the studies in the literature stated that small particles result in more problems than do larger particles. Particles having potentially toxic trace metals, such as Pb, Cd, V, Fe, Zn, Cr, Ni, Mn and Cu have been found to adversely affect human health if they present in elevated concentrations (Ghio et al., 1999, Hlavay et al., 1992, Natusch et al., 1974). However Karthikeyan et al. (2006) stated that the toxicity of these metals depend on their solubility and reactivity.

The climatic effects of aerosols are based on their radiative forcing. Radiative forcing is defined as the net change in the difference between the incoming radiation energy and the outgoing radiation energy at the tropopause and is measured in watts per square meter. A positive forcing indicates more incoming energy and thus tends to warm the system, while a negative forcing indicates more outgoing energy, thus tends to cool it. Direct effects of aerosols are due to their scattering and absorbing solar and infrared radiation in the atmosphere. Aerosols have indirect effect on climate by changing the cloud properties in a way of altering the formation and precipitation efficiency of liquid water, ice and mixed-phase clouds. In overall aerosols have a negative contribution to global warming (radiative forcing), but this contribution cannot compensate the radiative forcing of greenhouse gases because of the short residence time of aerosols in the atmosphere (IPCC, 2001, Haywood and Boucher, 2000).

Aerosols cause visibility reduction due to their absorbing and scattering of light properties. Aerosols in the size range of 0.4 and 0.7 µm which is close to the wavelength of visible light scatter light efficiently than other size aerosols. Aerosols can also reduce visibility by absorbing visible light, black carbon (BC) is known as the most significant light absorbing aerosol in the atmosphere (Japar et al., 1986).

Deposition of aerosols especially those rich in sulfur and nitrogen content may cause acidification problem in water bodies and soil (Krug and Frink, 1983, Likens et al., 1996). This acidification is harmful to ecosystems i.e., when the pH of the water body decreases solubility of toxic metals increases, eventually fish and other aquatic species are adversely impacted. The degree of acidification problem in a region depends on the balance between acidic species and alkali metals hence show high variation from region to region.

2.5. Determination of Chemical Composition of Aerosols

Sources have specific emissions that some of the chemical species found in emissions can be used as fingerprints of these specific sources. For example Duce et al. (1975) showed that anthropogenic V in aerosol is a result of combustion of heavy fuel oil containing V-porphyron complex. Sciare et al. (2003) and Alves et al. (2010) demonstrated that potassium can be used as a marker of biomass burning activities i.e., agricultural waste burning and forest fires. Therefore determination of chemical composition of aerosols is the fundamental of source apportionment studies.

Many analytical techniques have been used for the determination of chemical composition of aerosols. Inductively Coupled Plasma Mass Spectrometry (ICPMS), Atomic Absorption Spectrometry (AAS), Proton-Induced X-Ray Emission Spectrometry (PIXE), Instrumental Neutron Activation Analyser (INAA) and X-Ray Fluorescence (XRF) are generally used for trace element analyses while ions analyses are analyzed by Ion Chromatography (IC). There are advantages and disadvantages of each technique. Nowadays microwave digestion of aerosols followed by chemical analysis by ICPMS is widely used and accepted method for determining trace elements in aerosol samples (Karthikeyan et al., 2006, Kulkarni et al., 2007, Pekney and Davidson, 2005, Sandroni et al., 2003, Yang et al., 2002).

The choice of analytical method is very important and should be selected according to the target compounds and desired detection limits. In this study TSP is collected. It is well known that in TSP crustal source is predominant therefore it diminishes the contrast of combustion and industrial sources (Hien et al., 2001). However high volume sampler collects more material because of its higher flow rates and fine particulate matter which are mainly originate from anthropogenic emissions can be detected if appropriate analytical methods are used even if the ambient concentrations of these anthropogenic compounds are very low. ICPMS technique has low detection limit therefore allows the determination of low concentrations and allows the simultaneous analysis of multi-elements. In aerosol studies the number of samples and target compounds are generally high and the concentrations of most of the elements are low, therefore ICPMS technique is popular in aerosol studies.

2.6. The Long Range Transport of Aerosols

Atmosphere is the major pathway of air pollutants. Air pollutant that is emitted at a location may influence the other parts of the world by circulating around the globe within a few days to a few weeks depending on regional and global wind circulation patterns (Hegde et al., 2007, Savoie et al., 1987). This transport of pollutants in the atmosphere is called as long range transport (LRT). Regarding the scale of transport (i.e. hundreds kilometers to thousand kilometers) and time (i.e. a few days to a few weeks), different names can be used in the literature for referring LRT of air pollutants such as continental, transboundary, regional and country-to-country transport of air pollution.

Air pollution caused by transport of air pollutants between countries which is called as transboundary air pollution is known as one of the major problem in Europe. The transboundary air pollution problem is firstly recognized in the 1960s when acidification of aquatic ecosystems especially lakes were reported in remote areas of UK and Scandinavia (Mylona, 1996 and references therein). There was no emission sources such as sulfur dioxide emissions that may result in acidification problem in these areas, hence transported pollution from other regions were blamed for the acidification problem. After the relationship between sulfur dioxide emissions from continental Europe and acidification of Scandinavian

lakes were proven scientifically, a need for an international cooperation emerged to solve this problem. As a result, The Convention on Long-range Transboundary Air Pollution (CLRTAP) was signed in Geneva in 1979. At present, 34 countries in the United Nations Economic Commission for Europe (UNECE) region and the European Community (EC) have signed the CLRTAP. This convention is very important because it was the first international legally binding agreement dealing with the air pollution problems on larger scale (URL 1). Eight legally binding protocols have been adopted to control specific pollutants, namely sulfur dioxide (SO_2), nitrogen oxides (NO_x), ammonia (NH_3), volatile organic compounds (VOCs), ozone (O_3), persistent organic pollutants (POPs) and heavy metals (i.e. Pb, Cd and Hg). In these protocols emission reduction targets are set for specific pollutants, and all Parties who signed and ratified the protocols have to achieve these targets. Since 1980s about 75%, 30% and 40% reductions have been achieved for SO_2, NO_x and VOCs, respectively (UNECE, 2007).

Among these 8 protocols, Turkey just signed the 1984 Geneva Protocol on Long-term Financing of the Cooperative Programme for Monitoring and Evaluation of the Long-range Transmission of Air Pollutants in Europe (EMEP). The main aim of the EMEP is to monitor the emission reductions by monitoring the relevant pollutants and to provide a platform for the review and assessment of these pollutants using modeling tools. Note that leaded gasoline was banned in Turkey in 2006 based on the requirement of 98/70/EC directive, not due to protocols in CLRTAP.

Turkey signed some other international agreements related to air quality. These are Vienna Convention for the Protection of Ozone Layer (signed in 1990), the Montreal Convention (signed in 1990), United Nations Framework Convention on Climate Change (signed in 2003) and the Kyoto Protocol to the United Nations Framework Convention on Climate Change (signed in 2009).

2.7. National and International Ambient Air Quality Standards

Country, region or the globe based regulatory standards are established to protect human health and environment from adverse effects of air pollution. These regulatory standards are usually established for different exposure times, i.e. hourly average (1 hour, 8 hour or 24 hour) and annual average. Hourly average standards are called as short-term standards and are established to avoid acute effects of high level of pollution on human health in a short exposure time. Annual average standards are called as long-term standards and are used to avoid cumulative effects of air pollution when exposed over long period of times.

Ambient air quality in Turkey is regulated under the Air Quality Assessment and Management Regulation (AQAMR) which has been updated in 2008 to comply with the 96/62/EC, 99/30/EC, 2000/69/EC, 2002/3/EC and 2004/107/EC directives and to achieve the targets of the international protocols (Government, 2008). Turkish ambient air quality standards for bulk PM, heavy metals and polycyclic aromatic hydrocarbons (PAHs) are given in Table 2.7.1. Note that SO_2, NO_2 and NO_x are also presented in Table 2.7.1 because these pollutants are the main sources of sulfate and nitrate aerosols.

EU Air Quality Directives (AQD) and WHO Air Quality Guidelines (AQG) are the two international ambient air quality standards used for air quality assessments. Updated version of AQAMR complies with AQD and AQS from 2014 and 2020 on. Both EU and WHO has standard for fine particles (PM2.5) whose annual average standard values are 25 µg m^{-3} and 10 µg m^{-3} for EU and WHO, respectively. In AQAMR any standard has been established for PM2.5 yet.

Table 2.7.1 Turkish Ambient Air Quality Standards of PM and PM related pollutants

	Hourly	Daily	Annual	Unit	*From on
SO$_2$	150	125	20	µg m^{-3}	2014
NO$_2$	100		20	µg m^{-3}	2014
NOx			30	µg m^{-3}	2014
PM10		50	20	µg m^{-3}	2014
Pb			0.5	µg m^{-3}	2014
As			6	ng m^{-3}	2020
Cd			5	ng m^{-3}	2020
Ni			20	ng m^{-3}	2020
Benzo(a)pyrene			1	ng m^{-3}	2020

[*]Denotes the year of entry into force

2.8. Modeling of Aerosols

Atmospheric models are divided into two as physical models and mathematical models. The use of physical model is limited to small scale applications; hence mathematical atmospheric models are preferred for larger atmospheric scales (Seinfeld and Pandis, 2006). Mathematical atmospheric models are further divided into two as chemical transport models (also called as source models) and statistical models (also called as receptor models). Chemical transport models (CTMs) are numerical models that simulate receptor concentrations given information about topography, source emissions and meteorology.

Receptor models, on the other hand, do not require information about emissions, topography or meteorology. In receptor modeling, chemical species measured in the receptor is used as natural tracers of sources and these fingerprints are statistically resolved to determine the sources and their contributions. It is advised to use both models for air quality assessment studies as one compensate the weakness of the other (Watson et al., 2002).

There are numerous CTMs and receptor models that are used for modeling of aerosols. Here only receptor models will be explained. Receptor models that are currently used for aerosol studies are Chemical Mass Balance (CMB), enrichment factors (EF), principal component analysis (PCA), factor analysis (FA), positive matrix factorization (PMF) (these last three are different forms of eigenvector analysis), multilinear engine, multiple linear regression, neural networks, cluster analysis and Fourier Transform time series. Although there are a number of other multivariate data analysis methods, these are the most commonly used ones in air pollution research (Watson et al., 2002). The PMF is developed relatively recently (Paatero and Tapper, 1994) compared to FA and CMB, which are the oldest receptor models and are in use since early 80's. Although it is developed more recently, PMF found very wide application (Kim et al., 2003, Karanasiou et al., 2009, Liu et al., 2003, Reff et al., 2007, Viana et al., 2008a) owing to several advantages it offered over more conventional receptor models, such as FA, PCA or CMB. These advantages will be briefly discussed in Section 4.5.1. Receptor models which are used in the literature are given in Figure 2.8.1 based on the degree of knowledge needed about the pollution sources for running the model (Viana et al., 2008a). As seen from the figure less knowledge required for multivariate models, while source types and source profiles are required for CMB.
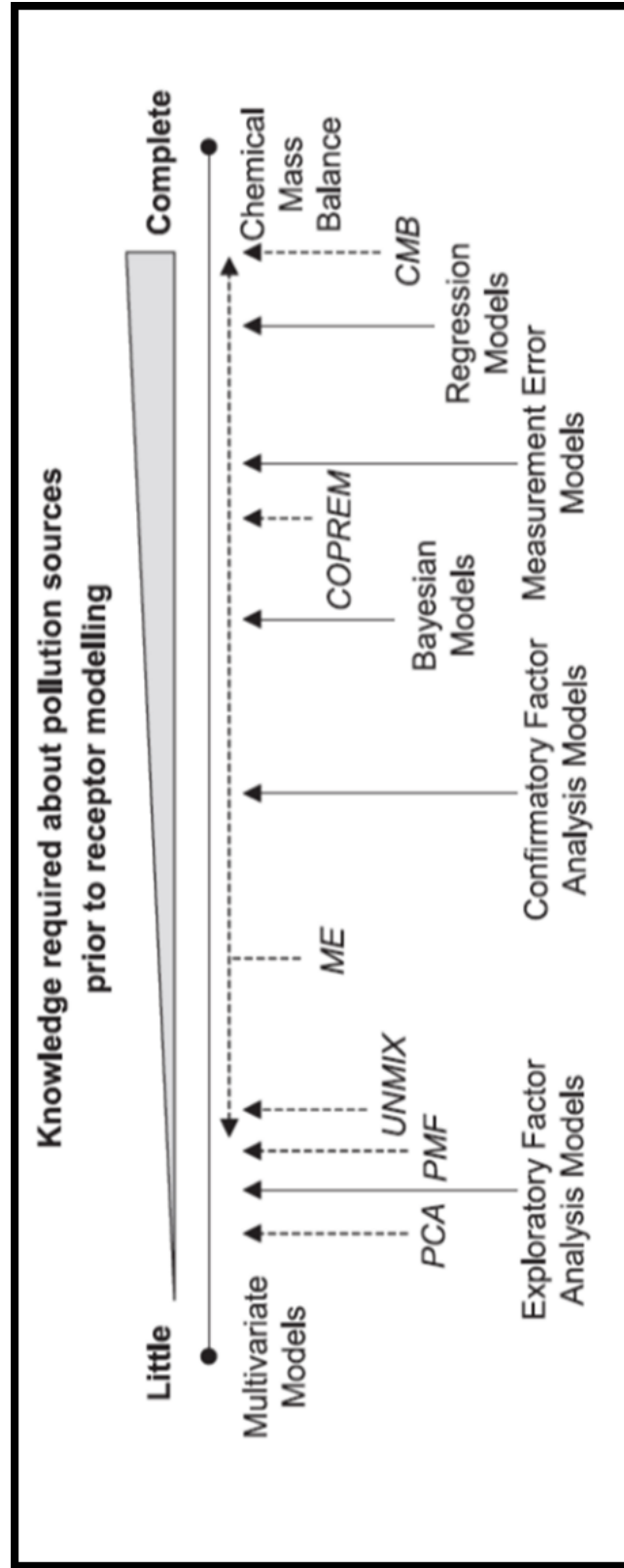
Figure 2.8.1 Receptor models for source apportionment (adapted from Viana et al., 2008). Specific models are shown in italics and with dotted arrows

Receptor models alone cannot determine geographical location of pollutant sources. Therefore in many studies receptor models are combined with trajectories and meteorological data to identify the potential regions from where emissions originate (Lee and Hopke, 2006, Zhao and Hopke, 2006, Xie et al., 1999, Gildemeister et al., 2007).

2.9. Aerosol Studies in Turkey

Most of the aerosol studies conducted in Turkey was focused on mass concentrations of particulate matter. In these studies usually relation between PM mass concentration and meteorological factors were investigated. A few studies focused on chemical characterization of aerosols and source apportionment as well. In this part aerosol studies in different parts of Turkey are presented but more focus is given to the studies on the northwestern Turkey.

Studies conducted in the Mediterranean part of Turkey were a few and limited to Eastern Mediterranean; however these studies were the most comprehensive ones in terms of number of parameters determined in Turkey (AlMomani et al., 1997, Gullu et al., 1998, Güllü et al., 2000, Kubilay et al., 2000, Bardouki et al., 2003, Gunaydin et al., 2003, Sciare et al., 2003, Gullu et al., 2004, Kocak et al., 2004, Gullu et al., 2005, Kubilay et al., 2005, Sciare et al., 2005, Kocak et al., 2007a, Kocak et al., 2007c, Kocak et al., 2007b, Turkum et al., 2008, Kocak et al., 2009, Dogan et al., 2010, Theodosi et al., 2010b, Im et al., 2012, Koçak et al., 2012, Öztürk et al., 2012). In most of these studies contribution of long range transport of Saharan dust and anthropogenic pollution sources to observed aerosols in the Eastern Mediterranean of Turkey has been indicated and high sulfate concentrations even higher than most of the EMEP stations has been reported.

Studies conducted in the Black Sea part of Turkey were few (Çelik and Kadi, 2007, Dogan et al., 2010, Gunaydin et al., 2003, Hacisalihoglu et al., 1992, Karakas et al., 2004, Tecer et al., 2012, Turk and Kavraz, 2010) and even some were conducted in urban sites. Among the urban studies (Çelik and Kadi, 2007, Tecer et al., 2012, Turk and Kavraz, 2010), only Tecer et al. (2012) investigated the chemical composition of aerosols and applied PMF to identify the sources. Studies that can be used as rural aerosol studies were collected by Hacisalihoglu et al. (1992) on shipboard and Karakas et al. (2004) in a rural site in the Western Black Sea Coast of Turkey. In both studies aerosols were chemically characterized and source apportionment methods were applied. Gunaydin et al. (2003) and Dogan et al. (2010a) furthermore used the aerosol data in the Western Black Sea Coast of Turkey and applied more sophisticated methods to investigate the potential source regions. Dogan et al. (2010a) compared the source regions affecting sulfate and nitrate concentrations at the Black Sea coast and the Eastern Mediterranean of Turkey, and demonstrated the Middle East, Aegean and Mediterranean coast of Turkey, Ukraine and Russia as common source regions.

Studies in the northwestern Turkey were mainly focused on Istanbul, although there were two studies that chemical composition of aerosol in Bursa which is a city in the south part of northwestern Turkey was determined. One of them was conducted in urban site of Bursa, and the other was in rural site (Karakaş and Tuncel, 1997, Samura et al., 2003). In these studies contribution of LRT to observed aerosol was emphasized. Sen(1997), Sen (1998) and Sen et al. (1997) investigated the relation between meteorological conditions and air pollution in Istanbul metropolitan area, and indicated that air pollution in Istanbul is affected by the weak dispersion conditions observed in the lower atmosphere over the city. They also showed the main sources of air pollution in Istanbul were fossil fuel combustion for residential activities, industrial activities and traffic. Tayanc et al. (1998) found that very high concentrations of PM (particulate matter) accompanied by westerly winds in İstanbul. Karaca et al. (2005) compared PM10 levels with PM2.5 levels in a suburban area of Istanbul and found high correlation (r=0.88) between them in winter, in the contrary, relatively low correlation (r=0.54) in summer. They concluded that in winter coarse and fine aerosols were affected from same sources and were influenced form the same meteorological conditions. Kindap et al. (2006), Kindap and Karaca (2006), Kindap et al. (2007) and Kindap (2008) investigated the long-range transport of aerosols from Europe to Turkey for a PM10 episode

observed between 5 and 12 January 2002 in Istanbul. They used CMAQ, which is a source model, to simulate PM10 concentrations during the episode period. They indicated that Istanbul was under the influence of transboundary transported pollution from Eastern Europe. They also applied sensitivity tests to emissions and indicated that contributions of individual Eastern European countries to PM10 in Istanbul could range from 0.5-13%.

Source apportionment of chemically speciated fine and coarse fractions of PM was conducted in suburban Istanbul by Karaca et al. (2008). They used correlation analysis and FA for source apportionment of PM and explained the resolved sources locally. Although contribution of secondary ions is expected to be dominant especially in the fine fraction, major ions were not determined. They did not apply back trajectory statistics. They did not observed LRT of pollution except Saharan dust intrusion.

Chen et al. (2008) developed an online tracer model based on MM5 meteorological model, then used it for simulation of two pollution episodes observed in Istanbul in January 2002. They showed that some of the pollution observed in Istanbul was from sources other than local. This transported pollution trapped in the boundary layer and transported to Istanbul by dominant northwesterly winds. Alp and Komurcu (2009) investigated the relation between PM10 and meteorology and speculated about the pollution problem in Istanbul is due to either local or long range transport. Anil et al. (2009) used hourly PM10 concentrations of 10 regular monitoring stations distributed through Istanbul in 2008. They obtained data from Istanbul Metropolitan Municipality. Their aim was to determine the effect of LRT on PM10 level of Istanbul. They used back trajectories to prove this. In their study, they stated that PM10 levels were higher than air quality standards in all the stations used, so they could not select a background station. This finding shows that Istanbul is under the effect of pollution, so stations used as rural sites are not rural anymore. They speculated about source regions. Europe, Mediterranean and Africa were speculated to be more important contributor to Istanbul than Balkans and Russia. But it should be noted that in their work, they did not apply any trajectory statistics. Karaca et al. (2009) used the same data but this time they applied trajectory statistics to define potential source regions affecting Istanbul. They chose potential LRT based on episode duration and occurrence in most of the stations. If PM10 level were higher than specified threshold value more than 10 hour in most of the stations, then that particular day was chosen as polluted day for use in PSCF. They used 72-h back trajectories at 500 m arrival height and applied PSCF seasonally. They found in spring and winter Istanbul was mostly influenced by LRT. Potential source regions were determined in spring were Mediterranean countries and Northern Africa, while in winter Balkan countries, Greece, Bulgaria, Serbia, Croatia, northern Italy, eastern France, southern Germany, Austria, Russia and the Aegean part of Turkey. Karaca and Camci (2010) used back trajectory cluster analysis to assess contribution of LRT to the PM10 polluted days, and found that back trajectories originating from Europe and southwest had significantly higher PM10 contribution than others. Elbir et al. (2010) used CALPUFF/CALMET modeling system to develop a model for forecasting SO_2, NO_X, CO and PM10 concentrations throughout Istanbul.

Im et al. (2010) used EPA's CMAQ model to simulate the PM episode observed between 13 and 17 January 2008 in Istanbul. In this study sulfate, nitrate and sulfate concentrations were also simulated as well. They used the high spatially and temporally resolved emission inventory for the greater Istanbul area (Markakis et al., 2012). They applied some sensitivity tests on emissions and indicated that contribution of local sources to observed PM10 episodes was significant; hence emission reductions on local scales can be applied as effective control strategies.

Theodosi et al. (2010a) conducted a study on chemically speciated PM10. They determined elements, ions, EC and OC. This study was the first study for Istanbul having fully characterized PM composition. To determine sources they applied FA and resolved 6 factors describing PM10. These were traffic/industry, crustal, sea salt, fuel oil combustion, secondary and ammonium sulfate. Study conducted between November 2007 and June 2009, so some samples coincided with our sampling period. Kocak et al. (2011) applied PMF2 to the same data set and resolved seven factors for PM10. These were secondary

factor (sulfate and ammonium), refuse incineration, traffic, fuel oil, solid fuel, crustal and sea salt. They indicated that 80% of PM10 in İstanbul was from anthropogenic sources. Besides PSCF, they also investigated the effect of Istanbul on other regions using forward trajectories and found that western Black sea, Bulgaria, Romania, Moldova, Ukraine and Belarus were influenced in winter, while Aegean and Levantine (eastern Mediterranean Sea) seas in summer.

Uygur et al. (2010) collected rain samples between October 2007 and May 2008 in Istanbul, applied FA and resolved 5 factors. PSCF indicated source regions for anthropogenic pollutants were Europe, Russia, southern and northern Mediterranean countries, and west of Turkey as well. Szigeti et al. (2012) collected PM2.5 samples in urban site of Budapest and Istanbul between June 2010 and May 2011 simultaneously. They compared PM2.5 mass and chemical composition of aerosols between the two cities and indicated that Istanbul was a factor of 1.2-20 times polluted than Budapest for all measured elements.

CHAPTER 3

METHODS

3.1. Sampling

3.1.1. Sampling Location

The sampling station (41° 57.996′ N and 27° 23.670′ E) is located in a rural area, approximately 30 km from the city of Kırklareli and 5 km from Bulgarian border of Turkey (Figure 3.1.1). The altitude of the station is 574 m above sea level. The wind rose, which shows the direction of potential surface transport of pollutants, is also included in Figure 3.1.1. The sampling station is located intentionally both in rural area and very near the Bulgarian border of Turkey. There are no adjacent anthropogenic sources on the windward side of the station, note that Kırklareli city is located downwind from the station (Figure 3.1.1). Therefore anthropogenic species measured in this study are not affected from nearby emission sources and can be used as indicators of regional and/or long range transport of pollution. Influence or lack of influence of local sources on measured concentrations of trace elements will be further discussed later in Section 4.5. As mentioned before, station was intentionally situated at the Bulgarian border, because 70% of the time air masses affecting Turkey come from Northwest (General Directorate of Meteorology, unpublished data) and the current location of the station is the entry point of these air masses to Turkey. Consequently, composition of particles measured in this study will provide an idea about the composition of aerosol when they enter to country. These air masses then travel within Turkey and intercepted and sampled at other stations located in other parts of the country. The difference can provide information on modification of aerosol composition as air masses travel within Turkey. The possible local sources affecting the sampling point is discussed in Section 4.5.

3.1.2. Aerosol Sampler

Particulate matter (PM) samples were collected daily using a High Volume Air Sampler (SIERRA-ANDERSEN Model SAUV-1H) given in Figure 3.1.2. The sampler consists of a protective housing, an inlet, a filter holder, a vacuum pump, a mass flow controller and a gas meter. Sampler inlet used in this study is not a size-selective inlet; hence particles of any size suspended in the air up to 25 to 50 μm (EPA, 1983) called as total suspended particulate matter (TSP) were collected. Filter holder is used for holding the collection medium which is 20x25 cm Whatman®41 (Whatman Inc., Clifton, NJ) cellulose filter. Copper contamination during sampling, which renders Cu data useless when regular pumps with copper brushes are used, is minimized by using a brushless motor to drive the pump. A mass flow controller was used to maintain the flow rate constant over the 24 hour sampling duration. There was no continuous flow recorder in the sampler; therefore exhaust of the sampler was connected to a high-volume dry gas meter to determine the air volume passed through the filter. The average flow rate of TSP sampler was calculated as 1.1 m^3 min^{-1} during the study period.
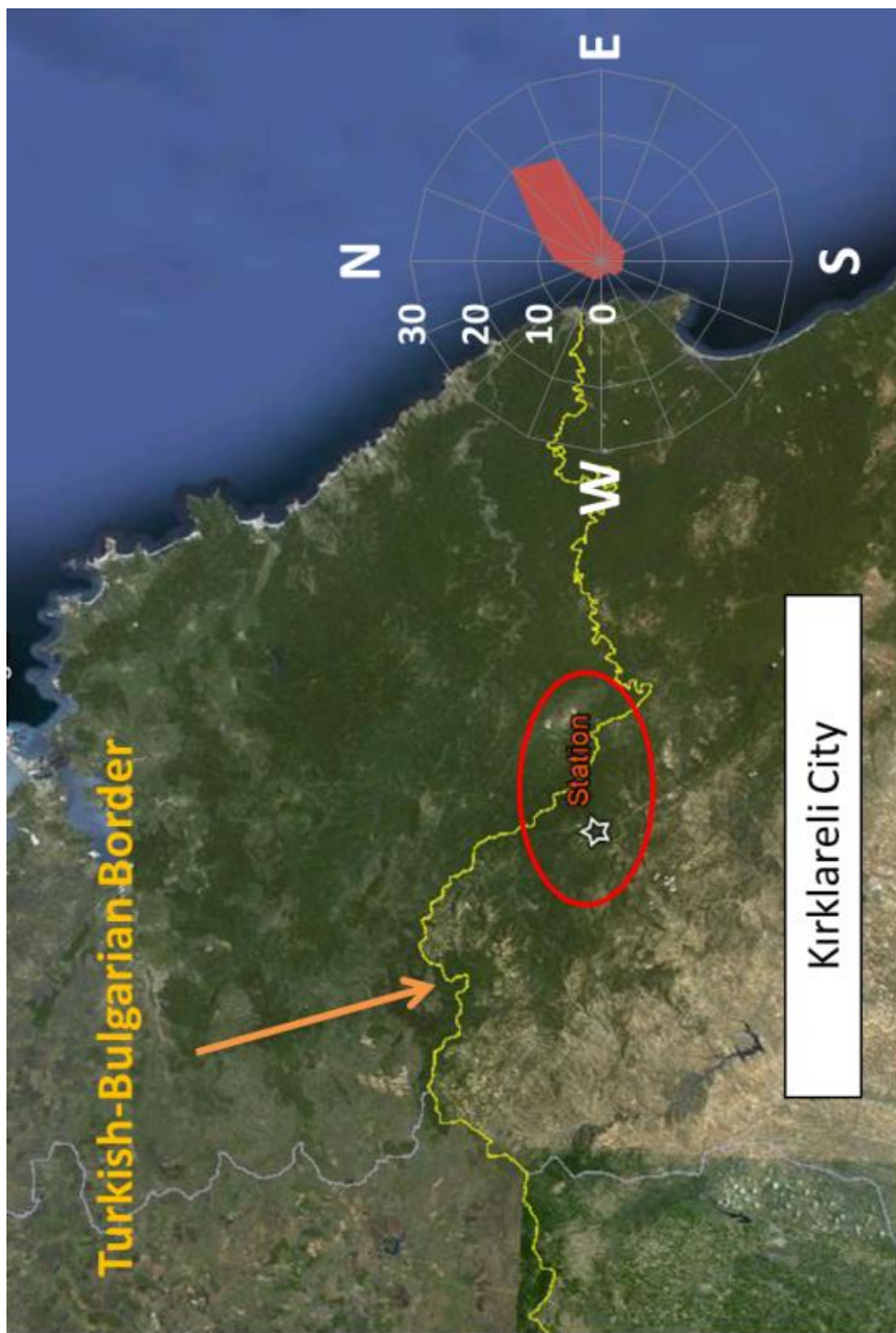
Figure 3.1.1 Location of sampling point and prevailing wind direction

3.1.3. **Aerosol Sampling**

All filters were handled carefully to minimize contamination. Non-powdered gloves and stainless steel forceps were used to touch filters. All filters were visually inspected with a backlight before sampling and defected filters with either pin holes or non-uniformity were not used in sampling. Filters passing from visual inspection were conditioned in a constant temperature $(25\pm5)^{\circ}$C and humidity (26 ± 4)% chamber for at least 24 hour. Un-exposed filters were weighted using an analytical balance (Sartorius A210P), with 0.1 mg sensitivity, and heat-sealed into polyethylene bags before they were shipped to the station. In the sampling station, non-powdered gloves were worn at all times when filters were handled. Sampling was started with an un-exposed filter at around 08:00 am and stopped at 08:00 am on the following day. When sampler was stopped, exposed filter was removed from the filter holder and heat-sealed into its original polyethylene bag (the bag in which it came to the station). A new un-exposed filter was placed on the filter holder and sampling was started for that particular day. Sampling duration for each sample was limited to 24±1 hours as required by EPA (1983). We tried to stick with this EPA procedure to be able to compare generated data with data generated in other studies conducted in Turkey and around the world. A sampling form, which includes gas-meter readings before and after the sampling, meteorological conditions during that particular sampling period (24 hours) and any noteworthy event that occurred (such as power cuts, any malfunctioning etc.) during that 24 hours were also filled and shipped to the laboratory along with the filter.

Daily PM sampling was started on 17 April 2006 and ended on 4 March 2008. During this duration 350 samples (255 samples on weekdays and 95 samples on weekends) were collected. Although our intention in the beginning was to collect approximately 300 samples in a 1-yr long sampling program, it did not materialized owing to serious logistic problems encountered. Approximately planned number of samples (350) were collected, but in two years instead of one year.

Exposed filters were shipped to the laboratory once in approximately every 15 days. When they arrive to the laboratory, exposed filters were conditioned, under the same conditions used for un-exposed filters, before they were weighted. The concentration of TSP in the ambient air, hereafter called as PM is determined by the net gain of filters (exposed filter weight minus un-exposed filter weight) divided by the volume of air sampled (V_s) and expressed in μgm^{-3}. The volume of air sampled is determined by the difference between the gas meter reading before and after each sampling. In this study, the volume of air sampled is corrected to EPA standard conditions (760 mmHg and 298 K) by the following formula:

$$V_{std} = V_s \frac{P_{atm}}{P_{std}} \frac{T_{std}}{T_{atm}}$$

Equation 3.1.1

In Equation 3.1.1, volume of air sampled (m^3) at EPA standard conditions (760 mmHg and 298 K) and ambient air conditions are represented by V_{std} and V_s, respectively. EPA standard atmospheric pressure (760 mmHg) and standard temperature (298 K) are denoted by P_{std} and T_{std}, respectively. Average atmospheric pressure (mmHg) and average atmospheric temperature (K) during sampling is denoted by P_{atm} and T_{atm}, respectively.

As different analytical techniques are used in this study to determine the chemical composition of aerosols, once weighed exposed filters were cut into eight equal parts using stainless steel knife blades. The first part was used for ICPMS analyses, the second part was used for IC analyses, the third part was used for BC analyses, and remaining parts were archived in case of reanalyzes of the sample or for analyses of different parameters in the same samples. Note that all weighing and laboratory manipulation of samples were performed in a clean area under twice HEPA filtered air.

Figure 3.1.2. High Volume Air Sampler used in this study

3.2. Analytical Procedures

In this study collected aerosol samples are analyzed for trace elements using an inductively coupled plasma spectrometer coupled to a mass selective detector (ICPMS), for water soluble ions by ion chromatography (IC) and for black carbon (BC) by optical spectrometry. Analytical techniques and sample requirements for these analyses are discussed in the following sections.

3.2.1. Trace Element Determinations by ICPMS

In aerosol studies accurate determination of trace elements had always been a challenge, because they generally are in very low concentrations in atmospheric particles. Atomic absorption spectrometry (AAS) had been the method of choice for a long time owing to its low detection limits, particularly in graphite furnace atomization mode. However, AAS was capable of measuring one element at a time. This was a serious drawback in atmospheric source apportionment studies where hundreds, sometimes thousands of samples are routinely analyzed for 20 – 60 elements and ions. Development of ICP technique in general and ICPMS technique in particular was refreshing for atmospheric scientists, because ICPMS has low enough detection limits that allowed the detection of up to 50+ elements in high and low volume aerosol samples.

The key components of ICPMS instrument is sample introduction system, plasma, mass analyzer (quadrupole), detector and computer. Sample introduction system consists of nebulizer, spray chamber and ICP-torch. Analyte is pumped from the sample vial into the nebulizer where it mixes with Argon (Ar) gas to form aerosol. Larger droplets are removed

from the aerosol as they pass through the cool spray chamber. The fine aerosol is swept into the central channel of the plasma which is a stream of Ar contained in a quartz tube or torch. Aerosol droplets are dried, decomposed, vaporized and atomized as they travel through the high temperature Ar plasma. By the removal of one electron from each atom, positively charged ions are produced in the plasma. The ions are extracted from the plasma into the interface through the sampling orifice, and then through the skimmer cone (metal plates) into the high vacuum region containing the ion lenses and mass analyzer. Electrostatic lenses focus the ion beam and separate the positive ions from the unwanted neutral species by bending them into the mass analyzer system. The ions are separated based on their mass-to-charge ratio (m/z) by a quadrupole mass spectrometer. The quadrupole scans rapidly across the mass range and passes each mass of interest sequentially to the detector, which is usually an electron multiplier detector. The detector counts and stores the electronic signal and creates a mass spectrum where the intensity of the given mass is proportional to concentration of isotope at that mass.

In this study, parts of filter samples allocated for trace element analysis were first digested using a microwave digestion procedure. Then digested samples were analyzed using a Perkin Elmer DRC II Model ICPMS in the METU Central Laboratory for 50 elements, including Li, Be, Na, Mg, Al, P, K, Ca, Ti, V, Cr, Mn, Fe, Ni, Cu, Zn, Ge, As, Se, Rb, Sr, Y, Mo, Cd, Sn, Sb, Cs, La, Ce, Pr, Nd, Eu, Sm, Gd, Tb, Dy, Ho, Er, Tm, Yb, Lu, Hf, W, Pt, Au, Tl, Pb, Bi, Th and U.

3.2.1.1. Preparation of Samples for ICPMS

One-eighth of the aerosol filter was placed into the PTFE (polytetrafluoroethylene) digestion vessel, and then 6.0 ml HNO_3 (nitric acid) and 1.0 ml of HF (hydrofluoric acid) were added. Note that Merck Suprapur analytical grade 65% HNO_3 and HF acids were used as digestion reagent in digestion process. Five samples and a reagent blank were digested in each batch. The closed vessel microwave, ETHOS 900 Milestone Microwave Digestion Oven was used for the digestion. The program used in microwave digestion is given in Table 3.2.1. The program consisted of 5 steps and completed in 30 min (Table 3.2.1).

Table 3.2.1 Program used in ETHOS 900 MW

Step	Time (min)	Power (W)
1	6	250
2	6	400
3	6	650
4	6	250
5	5	Ventilation

This digestion method has been developed in our group and used to digest aerosol samples since 1998. Prior to opening the vessels, microwave rotor having 6 vessels was placed into water bath for at least 45 minutes to cool down to room temperature. If vessels were opened immediately after digestion, some species may be lost and even samples may blow out due to high temperature and pressure existed in the vessels. After cooling to room temperature, vessels were opened in a fume-hood. The removal of HF after digestion is essential, because even a small quantity of HF injected to ICP spectrometer can etch the silica-based sampling tube of ICP torch and corrode the Ni cone interface. Therefore, HF in the mixture was completely evaporated by placing the vessels on the hot plate at 80°C till the white smoke from the analytes are ceased. Then 5 mL of HNO_3 was added and contents of the vessels were evaporated to near-dryness on the hot plate, this procedure of adding HNO_3 and evaporating was repeated for three times to ensure complete removal of HF. The solution was made to 50 mL with nanopure water which was produced by Milli-Q water purification system meeting ASTM Type 1 water requirements (18.2 MΩ – cm at 25 °C). Then diluted solution was filtered through 0.45 mm pore Millipore mixed cellulose ester filters

(Sartorius AG) to remove residues of soot carbon if present. Finally analytes were placed into high density polyethylene (HDPE) sample bottles and stored at $4^{o}C$ till the ICPMS analyses. Reagent and filter blanks were processed with the same procedure.

3.2.2. **Ion Determinations by IC**

Ion chromatography (IC) is a chemical separation and detection technique that provides qualitative and quantitative determination of ions. Like all other chromatographic methods the working principles of IC relies on the difference in the equilibrium distribution of analyte ions between the mobile phase (eluent) and stationary phase (ion-exchange column). Analyte species are separated based on their affinities relative to the functional group on the ion-exchange column. Each analyte species is identified by its retention time within the ion exchange column. If the affinity of a species is high, it will take more time to separate it from the column and if the affinity of a species is less, then its separation will be easy, hence taking shorter time to leave the column. The amount of each species is measured by detector as they leave the column. Electrochemical and spectroscopic detection methods have been applied in IC (Landsberger and Creatchman, 1999). Conductometry is one of the widely used electrochemical detection method in IC. Because all ionic solutions conduct electricity and conductivity of ionic solutions are generally linear with ion concentrations at some levels. Eluent also contains ions and create a background conductivity that may mask the conductivity of analyte ions. Therefore to reduce the background conductance of the eluent and increase the conductivity of analyte ions suppressor column is generally used before the detector.

In this study, ionic compositions of collected aerosol samples were determined using a DIONEX DX-120 Model Ion Chromatography at the General Directorate of Meteorology laboratory. Experimental conditions used in IC analysis are given Table 3.2.2. Dionex AG9-HC separation column with ASRS-ULTRA suppressor column was used for analysis of anions (Cl^{-}, NO_3^{-} and SO_4^{2-}). 10 mM solution of Na_2CO_3 at flow rate of 1.0 mL min^{-1} was used as eluent. Dionex CS12A separation column and CSRS-ULTRA suppressor column was used for the cation analysis (Na^{+}, NH_4^{+}, K^{+}, Mg^{2+}, Ca^{2+}), where 18 mM methanesulfanic acid (MSA) at 1.0 mL min^{-1} flow rate was used as eluent.

Table 3.2.2 Apparatus and conditions of the DX 120 Model Ion Chromatography system

Apparatus, solutions and conditions	Anions	Cations
Pre-columns	AG9-HC (4×50 mm)	CG12A (4×50 mm)
Separation columns	AS9-HC (4×250 mm)	CS12A (4×250 mm)
Suppressor columns	ASRS$^{®}$-ULTRA(4mm)	CSRS-ULTRA(4mm)
Eluent solution	10 mM Na$_2$CO$_3$	18 mM MSA
Flow rate	1.0 mL/min	1.0 mL/min
Injection volume	75 µL	10 µL

3.2.2.1. Preparation of Samples for IC

Major ions on one-eighth of the aerosol filter were first solubilized by sonication in 50 mL of nanopure water for an hour. Resulting solution was filtered through 0.2 μm pore size cellulose-acetate membrane filter, to avoid clogging the IC column by insoluble particles on filters. Finally, 100 μL of filtered solution was injected to IC for analysis of anions and cations. Separate columns were used for analysis of anions and cations. It should be noted that water soluble fractions of major ions (SO_4^{2-}, NO_3^-, NH_4^+, Ca^{2+}, K^+, Mg^{2+} and Na^+) were measured with IC, whilst total concentrations (water soluble + insoluble fraction) of elements were measured with ICPMS (remember that samples were totally digested before they were analyzed by ICPMS). If species is measured with both ICPMS and IC (Na, Ca, K and Mg) concentrations measured by ICPMS were used in statistical treatment of data for consistency.

3.2.3. BC Determination

Since Whatman®41 filter is made up of cellulose [$(C_6H_{10}O_5)_n$], its carbon content is very high (44%). That is why thermal-optical methods are not suitable for direct BC (black carbon) analysis for filters with cellulose matrix. Li et al. (2002) proposed a new technique for BC determination on cellulose filters. In his method cellulose filter is dissolved in $ZnCl_2$ and then filtered through a quartz fiber filter. In this way BC on cellulose filter is transferred to quartz filter that can be used for BC determination by thermal optical methods. Ahmed et al. (2009) has shown that BC concentrations on Whatman®41 filters can be successfully and rapidly determined via optical method and results are comparable to the results of thermal-optical measurements performed in the same filters. Since samples in the current study are collected on cellulose filters, method proposed by Li et al. (2002) was used to transfer carbon particles on one-eighth of the sample filter onto a quartz fiber filter. Final measurement of black carbon were made by Optical Transmissometer (OT-21, Magee Scientific), at the State University of New York at Albany, Department of Environmental Health Sciences.

The working principle of Optical Transmissometer is based on BC's black-body radiation optical properties. The light attenuation through the sample filter and reference (blank) filter at 880 nm was calculated by Equation 3.2.1, where T represents transmission intensity in aerosol sample and T_o represents transmission intensity in reference (blank filter). Like all other optical methods, it was assumed that attenuation through the filter is proportional to the BC loading on the filter. BC density ($\mu g\ cm^{-2}$) in the aerosol filters were determined by Equation 3.2.2, where σ represents the specific attenuation coefficient, which was given by the manufacturer as 16.6 $m^2\ g^{-1}$ for 880 nm channel optical BC measurements. BC density is then converted to BC concentration in ambient air ($\mu g\ m^{-3}$) by multiplying the exposed area of the filter fraction (A_F) analyzed, and then dividing by the volume of air passed through corresponding filter fraction (V_F) as given in Equation 3.2.3. Note that resulting BC concentration was multiplied by a correction factor of 1.1 (c_f) because the overall collection efficiency of Whatman®41 filter for BC has been reported as 90% (Khan et al., 2010).

$$Attenuation = 100 * ln\left(\frac{T_o}{T}\right)$$

Equation 3.2.1

$$BC\ density\ (\mu g\ cm^{-2}) = \frac{Attenuation}{\sigma}$$

Equation 3.2.2

$$BC\ (\mu g\ m^{-3}) = \frac{BC\ density\ (\mu g\ cm^{-2}) * A_F}{V_F} * c_f$$

Equation 3.2.3

Although black carbon is a very clear indicator of combustion sources of all types, BC measurement in Turkey are few. This study is the first measurement of BC concentration in rural area of northwestern Turkey.

3.2.3.1. Preparation of Samples for BC Determination

The method proposed by Li et al., 2002 was used for the preparation of Whatman®41 filters prior to determination of BC by optical method (OT-21, Magee Scientific). Firstly one-eighth of the Whatman 41 filter was dissolved in a 70% solution of $ZnCl_2$ at $50^{o}C$ and then solution was filtered through a quartz fiber filter (QMA, 47 mm diameter, 99.999% retention for particles). By this way BC on Whatman®41 filter was transferred to quartz filter that can directly be used for BC determination by optical methods. Recoveries of BC by this method were reported to be 93 ± 4% (Li et al., 2002).

3.3. Quality Assurance and Quality Control

3.3.1. Blanks

Two different types of blanks were used. These were laboratory blanks and field blanks. Laboratory blanks were prepared and analyzed to determine the contribution of laboratory procedures and material used to the measured concentrations of trace elements. Reagent blanks and filter blanks were the two types of laboratory blanks used in this study. Reagent blanks were prepared for each batch of acid digestion and water extraction (for ions) processes to determine the contribution of used reagents/supplies to measured concentrations of elements and to monitor potential contamination from them. One filter blank was prepared for each box of 100 filters, to monitor batch-to-batch variability of trace element concentrations in Whatman cellulose filters. Field blanks were the main blanks that included possible contamination from all field and laboratory processes applied to the samples. Field blanks were regular sample filters, which are selected as blanks. They are prepared and sent to field like sample filters, in the field they were loaded to sampler like regular sample filter, and sampler was operated for only 5 minutes, before the blank filter is removed. From that point on the field-blank filter is processed and analyzed exactly like a sample filter. One field blank was collected nearly once in each week. Field and lab blanks were treated as if they were sample and analyzed for trace elements, ions and BC. Average mass of each species in field blanks was subtracted from the mass of corresponding species in the sample. By this way contribution of filter itself and contamination due to sampling and filter handling is accounted for and actual concentrations of elements in ambient air are determined. Sample to blank ratio of each species measured in this study is given in Table 3.3.1.

Among 60 parameters measured in this study, ten had sample-to-blank ratios smaller than 5.0, which is our tentative criterion to identify species as having high and low blank values. These ten species are Se, Bi, Pt, Cr, P, Cl⁻, Fe, Zn, Cd and Er. Note that these species are not excluded from the data set, because some of them are good markers of different sources such as Se and Zn. High potential uncertainties associated with detection of these species are kept in mind, when they are used throughout the study.

3.3.2. Cleaning

PTFE vessels, HDPE sample bottles and all laboratory plasticware were soaked at least 24 hours into 5% HNO_3, and then rinsed several times by nanopure water prior to each use.

3.3.3. Quality Assurance

Detection limits of trace elements, water soluble ions and BC were calculated as the concentrations corresponding to $3x\sigma$ of 10 replicate measurements of the field blanks. Calculated detection limits of species determined in this study are given in Table 3.3.1, along with the blank values.

The accuracy of the ICPMS was verified using the Standard Reference Materials (SRMs). NIST urban particulate matter SRM (SRM 1648) was digested by the same procedure applied to samples and then analyzed by ICPMS. Measured and certified concentrations of

elements are given in Table 3.3.2. Measured concentrations are within ±10% of certified concentrations of elements.

Dionex Seven Anion Standard-II and Dionex Six Cation-II Standard were used for calibration of IC for anions and cations, respectively. Ion measurements were tested by dissolution of Merck high purity salts ($NaCl$, K_2SO_4, $NaNO_3$, KCl, $CaCl_2$ and NH_4Cl) in nanopure water. Reasonable agreement was obtained between the measured and calculated concentrations for Na^+, K^+, Ca^{2+}, Cl^-, NO_3^- and SO_4^{2-}, as shown in Table 3.3.3.

Table 3.3.1 Summary of the average sample to blank ratios and detection limit of each species in ambient air

Species	Sample to blank ratio average	Delection Limit ng m^{-3}
Al	24	13
As	5.91	0.00589
Au	5.14	0.11
Be	7.22	0.00192
Bi	1.58	0.00977
Ca	5.9	216
Cd	4.71	0.01144
Ce	28	0.03268
Cr	2.62	0.66
Cs	101	0.00233
Cu	6.91	0.12
Dy	34	0.00039
Er	4.89	0.00043
Eu	21	0.00559
Fe	3.43	35
Gd	56	0.00171
Ge	56	0.00156
Hf	18	0.00804
Ho	35	0.00047
K	16	19
La	42	0.018
Li	10	0.029
Lu	54	0.00013
Mg	24	17
Mn	18	0.198
Mo	13	0.03024
Na	6.17	83
Nd	45	0.012

Table 3.3.1cont. Summary of the average sample to blank ratios and detection limit of each species in ambient air

Species	Sample to blank ratio average	Delection Limit ng m^{-3}
Ni	9.41	0.76
P	2.72	6.2
Pb	17	0.65
Pr	47	0.00326
Pt	2.13	0.00121
Rb	48	0.017
Sb	9.93	0.022
Se	1.57	0.024
Sm	27	0.00265
Sn	7.8	0.0818
Sr	5.55	0.04536
Tb	76	0.00032
Th	12	0.00676
Ti	16	1.15
Tl	146	0.0016
Tm	21	0.00019
U	7.35	0.0157
V	118	0.053
W	6.54	0.024
Y	33	0.00702
Yb	62	0.00067
Zn	3.76	1.81
(Soluble Na) Na$^+$	7.46	5.55
NH$_4^+$	9.82	24
(Soluble K) K$^+$	13	6.21
(Soluble Mg) Mg^{2+}	35	2.32
(Soluble Ca) Ca^{2+}	7.86	13
Cl$^-$	3.12	23
NO$_3^-$	45	7
SO$_4^{2-}$	73	6
BC	100	10

Table 3.3.2 Certified and measured values of elements for the SRM analyses

Element	Unit	SRM 1648 certified	SRM 1648 measured
Al	%	3.22±0.16	3.49±0.05
Ca	%	5.83±0.33	6.38±0.03
Fe	%	3.92±0.24	3.63±0.05
Cd	mg/kg	72±2	74±1.87
Ce	mg/kg	55±4	58±0.37
Cs	mg/kg	3.5±0.2	3.6±0.04
K	mg/kg	1.03±0.5	1.06±0.03
La	mg/kg	39±3	39±0.04
Mn	mg/kg	822±45	769±20
Na	mg/kg	4230±230	4565±63
Sb	mg/kg	44±2	42±0.4
Se	mg/kg	24±2	22±2.2
Sr	mg/kg	207±15	214±4.1

Table 3.3.3 Calculated and IC measured concentrations of Merck high purity salts

Ion	Unit	Calculated conc.	Measured conc.
Cl^-	mg/L	6.0±0.3	6.26±0.05
NO_3^-	mg/L	6.0±0.3	6.36±0.12
SO_4^{2-}	mg/L	6.0±0.3	6.25±0.1
Na^+	mg/L	3.01±0.15	2.96±0.27
NH_4^+	mg/L	2.94±0.15	3.1±0.28
K^+	mg/L	3.05±0.15	2.93±0.3
Ca^{2+}	mg/L	3.1±0.16	3.04±0.24

3.4. Calculation of Back Trajectories

Atmosphere is the major pathway of air pollutants. Air pollutant that is emitted at a location may influence the other parts of the world by circulating around the globe at a time-scale ranging between few days and few weeks depending on regional and global circulation patterns (Hegde et al., 2007, Savoie et al., 1987). Such transport of pollutants in the atmosphere is called long range transport (LRT).

One of the aims of this study is to identify, and if possible quantify aerosol species reaching to our sampling point from distant sources through LRT. This requires examination of back trajectories, which are the paths followed by air masses before they were intercepted at the station. Since air masses pick up pollutants from sources on their transport path to receptor, back trajectory information can be related to observed concentrations of elements. This can be done either one-by-one investigation of trajectories or by investigating the relation between concentrations and segments of ensemble of trajectories. This later approach is known as "trajectory statistics".

There are large numbers of software programs that can be used to calculate back trajectories. However, three of them are used more frequently than the others. The first one is the FLEXTRA, which is developed by the University of Agricultural Sciences in Vienna and the Technical University of Munich (Stohl et al., 1995) and used extensively in the European Monitoring and Evaluation Programme (EMEP). The second one is the European Centre for Medium-Range Weather Forecasts (ECMWF) trajectory model (Molteni et al., 1996) which is the most widely used trajectory model before the HYSPLIT became freely available on internet (Stohl and Koffi, 1998). The third one is the HYbrid Single-Particle Lagrangian Integrated Trajectory Model (HYSPLIT) (Draxier and Hess, 1998) which is the model developed by the U.S. National Oceanic and Atmospheric Administration (NOAA). ECMWF is an intergovernmental organization and its services (forecasted and archived meteorological data and models as well) are only available to the Parties and World Meteorological Organization (WMO) members. To run the FLEXTRA model input meteorological data from ECMWF is required. Although all three of these models are three dimensional (3D) trajectory models, the use of ECMWF and FLEXTRA model against the HYSPLIT model is limited because the latter is freely available via internet and more user-friendly.

In this study back trajectories are calculated using the HYSPLIT model. If one wants to calculate back trajectories by HYSPLIT for each day of a year, then HYSPLIT will have to be run 365 times. However a new and Geographical Information System (GIS) based software, namely TrajStat (Wang et al., 2009) calculates monthly back trajectories using calculation module of HYSPLIT in a single run. TrajStat also enables some GIS functions for mapping and applies different statistical analysis methods for trajectories. Therefore back trajectories in this study were calculated using TrajStat software.

Choosing the trajectory length is one of the most important issues in trajectory models. While choosing the trajectory length one should consider the residence time of pollutants. Trajectory length should not be shorter or longer than the life time of measured species. It should cover the residence time of all measured species. Residence times of inorganic species range from 3 to 20 days. Another criterion in choosing trajectory length is the minimization of trajectory errors. Trajectory model may contain some uncertainty since the accuracy of trajectories depends on the input meteorological data. Spatial and temporal errors exist in meteorological data and these errors increase with increasing trajectory length (McQueen and Draxler, 1994, Draxler, 1991, Stohl, 1998, Fast and Berkowitz, 1997). Errors in trajectory calculations are reported to be on the order of 20% of the distance travelled (Stohl, 1998). Although five days may seem to be a long period for trajectory calculations regarding the uncertainties which increase considerably with such a long period, in this study trajectory calculations were performed for five days backward in time. Because trajectories calculated for shorter periods do not include distant parts of Europe in our trajectory statistics, so we had to accept this drawback. Fortunately ensembles of trajectories are used

in this study and it is known that uncertainty of individual trajectory is overcome to some extent when large number of trajectories used in statistical analyses. In the literature generally 3-7 day trajectory lengths are applied.

Arrival height of trajectory is another important issue in trajectory modeling. In aerosols studies only airflows that arrive within or below the boundary layer is assumed to contribute air quality in the sampling station, hence arrival height is chosen to be representative of flow within the boundary layer. The boundary layer for the Kırklareli is calculated by EPA's PCRAMMET software. The average boundary layer heights are found as 700 m and 1200 m for winter and summer, respectively. Three different arrival heights were chosen as 100 m, 500 m and 1500 m which are below and near the boundary layer.

Five-day back trajectories, extending 5 days back in time and starting at the sampling point at 19:00 UTC (Coordinate Universal Time), at altitudes of 100 m, 500 m and 1500 m from the surface were calculated for each day in the years 2006, 2007 and 2008. Reanalysis meteorological data archive (horizontal resolution of 2.5 degree latitude) of the NOAA was used as input data to TrajStat. Isentropic trajectory type which assumes air parcels to move along constant potential temperature (in contrast to earlier isobaric trajectory models where air parcels were assumed to move along a constant pressure) was chosen and hourly position of air masses with latitude, longitude and pressure coordinates along the trajectory's path was calculated by TrajStat.

3.5. Source Apportionment

In this study Enrichment Factor was used for preliminary source apportionment of aerosols. Positive Matrix Factorization (PMF) was used as receptor model to resolve the sources of aerosols and contribution of these sources on aerosols. As PMF alone cannot determine geographical location of pollutant sources, Potential Source Contribution Function (PSCF) was used to determine the possible locations of PMF resolved sources.

3.5.1. Enrichment Factor (EF)

Enrichment factor (EF) which is a double normalization technique, is generally used for the preliminary source apportionment of aerosol species in the atmosphere. The EF of an element is calculated by Equation 3.5.1(Chester and Stoner, 1973, Zoller et al., 1974) in where C_x represents the concentration of the target element and C_R represents the concentration of the reference element which can be used as a marker of its source. The ratio of the C_x to C_R in aerosol sample to that in the reference source constitutes the double normalization.

$$EF = \frac{\left(\frac{C_x}{C_R}\right)_{aerosol}}{\left(\frac{C_x}{C_R}\right)_{Reference}}$$

Equation 3.5.1

If crust is used as the reference source, calculated EF is called as crustal enrichment factor (EFc) and if marine source is used as the reference source, then calculated EF is called as marine EF (EFm). Since crustal and marine particles are the most abundant particle types in the atmosphere, crustal enrichment factor (EFc) and marine enrichment factor (EFm) are the most widely used enrichment factor calculations. For EFm calculations Na is used as reference element. For EFc calculations Al, Fe, Li, Sc, Zr, Mn and Ti which are enriched in crustal material, and do not have sources other than soil, can be used (Reimann and de Caritat, 2005 and references therein).

3.5.2. **Positive Matrix Factorization (PMF)**

Positive Matrix Factorization (PMF) is developed by Paatero and Tapper (1993, 1994) and Paatero (1997). Although it is relatively new technique, among the multivariate receptor models, it is one of the most common applied techniques in aerosol source apportionment studies. PMF, like other multivariate receptor models, is based on the idea that time dependency of a chemical species measured at a receptor site is the same for species from the same source. Therefore species of similar variability are grouped together in a minimum number of factors (sources) that explain the variability of the data set. It is assumed that each factor is associated with a source or source type (Chueinta et al., 2000).

PMF solves the general receptor modeling problem using constrained, weighted, least-square minimization scheme. The general model assumes that there are p sources, source types or source regions (termed factors) impacting a receptor, and linear combinations of the impacts from the p factors give rise to the observed concentrations of the various species. Mathematical representation of PMF model is given in Equation 3.5.2 in where X_{ij} is the concentration of jth species on the ith day at a receptor, g_{ik} is the contribution of the kth factor to the receptor on the ith day, f_{kj} is the fraction of the kth factor that is species j, e_{ij} is the residual for the jth species on the ith day.

$$x_{ij} = \sum_{k=1}^{p} g_{ik} f_{kj} + e_{ij}$$
Equation 3.5.2

In PMF, it is assumed that only the x_{ij}'s are known and that the goal is to estimate the contributions (g_{ik}) and the fractions (or profiles) (f_{kj}). It is assumed that the contributions ($g_{ik} \geq 0$) and mass fractions ($f_{kj} \geq 0$) are all non-negative, this forms the "constrained" part of the least-squares and means that sources cannot have negative species concentration and sample cannot have a negative source contribution. This is one of the most important advantages of PMF over conventional FA. In FA source contributions can be negative, which, of course, does not make sense physically.

In "weighted" part of PMF, data points that have high uncertainties (missing values, below detection limit values or negative values) are down weighted in order to reduce the effect of them in source apportionment. This is the second most important advantage of PMF over FA or PCA. In conventional FA, missing points (below detection limits or parameters that are not measured in a particular sample) are not allowed. There is large number of missing points in atmospheric trace element data sets, due to low concentrations of some of the elements, either large number of elements and samples has to be excluded from FA exercise, or a value is imputed for each missing data points. Neither of them are ideal approaches, because there is no ideal data filling method that generates correct concentration values and sample exclusion may result in excluding information. In PMF, on the other hand, any samples or elements are excluded from PMF analysis. Missing data points are dealt with by value imputing and very high uncertainties are assigned to these imputed values, so that their contribution to the model fit is down weighted.

In "least square" part of PMF, the Q value which is the object function in PMF problem is minimized by least squares solution according to the Equation 3.5.3 in where s_{ij} is the uncertainty in the jth species for i^{th} day. If the model is appropriate for the data and if the uncertainties specified are truly reflective of the uncertainties in the data, then Q should be approximately equal to the number of data points in the concentration data set (EPA, 2008).

$$Q = \sum_{i=1}^{n} \sum_{j=1}^{m} \left(\frac{X_{ij} - \sum_{k=1}^{p} g_{ik} f_{kj}}{s_{ij}} \right)^2$$
Equation 3.5.3

28

EPA PMF version 3.0.2.2 (hereafter called as PMF) was used in this study, since it is more user friendly compared to other programs that solves the PMF problem. Species concentrations in each sample and their corresponding uncertainties must be provided as input to PMF. Once the PMF run, two files must be prepared: a file containing concentrations and another file containing uncertainty values. PMF requires that there is no blank in the data set, so missing species measurements have to be dealt with. Approaches used for missing species measurements are summarized by Reff et al. (2007) as: 1). Samples with missing species measurements are totally excluded, 2). Only the species with missing measurements are excluded, 3). A value is imputed for each species with missing measurements and high uncertainties are assigned for them. The arithmetic mean, median or geometric mean of each species is generally used for imputing values for missing measurements. Some species concentrations may be below the detection limit (BDL), in this case BDL values can be replaced with half of the detection limit value (DL/2) and corresponding uncertainties can be assigned as five sixths of the detection limit values (5/6*DL). By this way the uncertainties of BDL values are increased. If the number of samples having BDL values is higher than 95% of samples for a species, then it is advised to exclude this species from the data set.

EPA PMF has very user-friendly graphical user interface (GUI), the order of operations along with generated outputs in GUI are presented in Figure 3.5.1. In this manuscript only some outputs of PMF will be explained, all details about operations can be obtained from EPA (2008). In the Analyze Input Data screen there are four sub-screens as given in Figure 3.5.1. In the Concentration/Uncertainty screen, input data statistics (minimum, 25th percentile, 50th percentile, 75th percentile and maximum concentration values), and signal-to-noise ratio (S/N) for each species are automatically computed and presented. Signal-to-noise ratio is calculated by the below equation:

$$\left(\frac{S}{N}\right)_j = \sqrt{\frac{\sum_{i=1}^{n}\left(X_{ij} - s_{ij}\right)^2}{\sum_{i=1}^{n} s_{ij}^2}} \qquad \text{Equation 3.5.4}$$

The user should investigate these statistics and then modify the category of species as "strong", "weak" or "bad". Paatero and Hopke (2003) suggest that species with S/N ratio less than 0.2 should be assigned as "bad", species with S/N ratio equal to or higher than 2.0 should be assigned as "strong" and species with S/N ratio between 0.2 and 2.0 should be assigned as "weak". This categorization is applied so as not to overweight species with high noise than signal. Three times of the provided uncertainties are used in PMF when a species is categorized as "weak", and species is discarded if "bad" category is assigned. However, if a species is wanted to be retained in PMF, then user can provide a factor of 5-10 higher uncertainty for that particular species in the uncertainty input file (Paatero and Hopke, 2003).

The object function in PMF problem is to minimize the Q value (see Equation 3.5.3), so Q value is used as a goodness-of-fit parameter in PMF to show the model performance. The lowest Q value is chosen among different iterations and investigated if it is the global or local minima for the problem. Two Q values are generated by PMF; these are robust Q and true Q values. Robust Q value refers to Q value calculated when data points having large outliers are excluded; whilst true Q value refers to Q value calculated when all data points are used. PMF generated Q values should be equal or close to the theoretical Q value which is approximately equal to the number of data points in the input concentration file.

To accurately use the resolved factors, Fpeak run can be applied to the base solution. Selected base solution is rotated back to the real solution in the Fpeak run. Fpeak values between -5.0 to 5.0 is generally assigned as the strength of Fpeak rotation (EPA, 2008).
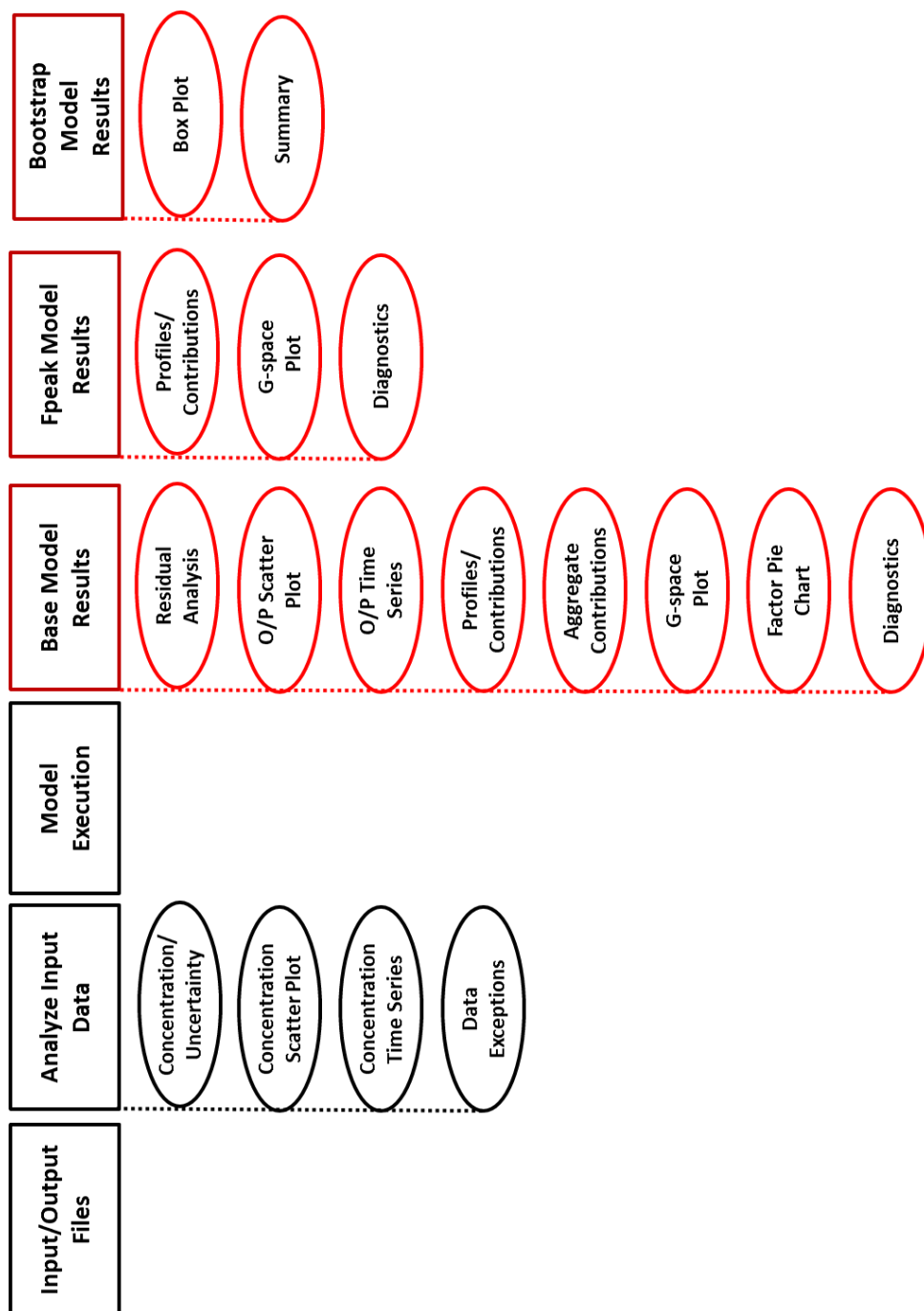
Figure 3.5.1 Flow chart of input and outputs in EPA PMF

Uncertainties in PMF can arise from the data (i.e. measurement errors and random sampling errors) and the PMF model's itself (i.e. rotational ambiguity in the solution) (Hemann et al., 2009). To estimate the uncertainties associated with these errors, bootstrap technique can be applied to the selected base solution. In general bootstrapping is a statistical method used for providing estimates hence its application is broad (Wehrens et al., 2000). In EPA PMF, block bootstrap method is used to generate new data set with the same dimensions as the original data set by randomly selecting non-overlapping blocks of samples from the original data set (EPA, 2008). The generated new data set can also be called as bootstrap data set. Then bootstrap data set is fit by the model and generated bootstrap factors are assigned to the base case factors based on the linear correlation between the factor contributions. It is advised to use coefficient of determination value of 0.6 as threshold value for assigning bootstrap factor to the base case factor. If the correlation is below the threshold value, then that bootstrap factor is not assigned to the base factor and considered as "unmapped". Discrete Difference Percentile (DDP) method is also used in EPA PMF to provide confidence intervals of the bootstrap runs (EPA, 2008).

3.5.3. **Potential Source Contribution Function (PSCF)**

Potential source contribution function (PSCF) is a conditional probability function that describes the spatial distribution of probable source locations. Species concentrations and corresponding back trajectories are used together in PSCF. Firstly the region covered by the trajectories is divided into ixj grid cells which are also called sub-regions. Trajectories are separated into hourly segments and each segment, which is also called "end point", is assigned to one of the grids, depending on its coordinates. Since 5-days back trajectories were used in this study, there were 120 segments (endpoints) available for each trajectory.

Trajectories reaching to the receptor during whole measurement period are divided into two groups, as "polluted" and "clean" trajectories. Polluted trajectories are the ones corresponding to high concentrations of the test species at the receptor. Clean trajectories, on the other hand, are the trajectories corresponding to low concentrations of the test species when they arrive to the receptor. This division between polluted and clean concentrations is tentative. In this study trajectories that correspond to the highest 40% of the measured concentrations of the test species or factor scores (i.e. contributions of sources to test species) were considered as "polluted" trajectories and remaining 60% were considered as "clean" trajectories. Then PSCF value of ij grid cell for a species is calculated using the Equation 3.5.5 in where m_{ij} is the number of polluted trajectory segments (endpoints) in ij grid cell and n_{ij} is total number of segments (polluted + clean) in the same grid.

$$PSCF_{ij} = \frac{m_{ij}}{n_{ij}}$$

Equation 3.5.5

Cells with high PSCF values refer to the potential source regions. This means that when a trajectory passes through a grid cell with high PSCF value, then it is likely that high concentration of test species will be measured at the day when this trajectory reaches to the station. PSCF values are range between 0.0 and 1.0. For a grid cell with PSCF value of 1.0 means that every trajectory passing through that particular grid cell corresponds to high concentration at the sampling point.

There are some artifacts of PSCF model. If the number of n_{ij} cells is small, then calculated PSCF for that cell will base on just one or two trajectories. If these one or two trajectories happen to be polluted, then calculated PSCF value will be very high (0.5 if only one is polluted and 1.0 if both are polluted). Such high values can be an artifact and does not necessarily mean that the region covered by that particular grid is a strong potential source region. Therefore uncertainties for these PSCF values, which bases on small number of trajectory segments will be high. There are two approaches used to overcome this problem.

One of them is to weight PSCF values with respect to the number of segments they contain (Plaisance et al., 1997, Zeng and Hopke, 1989, Polissar et al., 1999) and the other approach is to use non-parametric bootstrap techniques to test the statistical significance of each PSCF value in the study area (Hopke et al., 1995b, Lupu and Maenhaut, 2002, Gullu et al., 2005, Hopke et al., 1995a). In this study, PSCF values for the grid cells that contain few segments were weighted using the weighting functions given in Equation 3.5.6 (Zhao and Hopke, 2006). In this equation n_{avg} represents the average value of the end points in each grid cell and $W(n_{ij})$ represents the weighting function. Influence of the small values of n_{ij} is minimized by multiplication of PSCF values of that cell with corresponding $W(n_{ij})$. When $W(n_{ij})$ is multiplied with the PSCF value, the influence of the small values of n_{ij} with high uncertainties is minimized.

$$W(n_{ij}) = \begin{cases} 0.15 & n_{ij} \leq {n_{avg}}/{2} \\ 0.5 & {n_{avg}}/{2} < n_{ij} \leq n_{avg} \\ 0.75 & n_{avg} < n_{ij} \leq 2 \times n_{avg} \\ 1.0 & n_{ij} > 2 \times n_{avg} \end{cases} \qquad \text{Equation 3.5.6}$$

CHAPTER 4

RESULTS AND DISCUSSION

4.1. General Characteristics of Data Set

4.1.1. Data

In this study 350 daily TSP samples were collected in Kırklareli station between April 2006 and March 2008. Collected samples were analyzed for 50 major, minor and trace elements (from Li to U) by ICPMS, for eight ionic species (Cl^-, NO_3^- and SO_4^{2-} as anions, and Na^+, NH_4^+, K^+, Mg^{2+} and Ca^{2+} as cations) by IC and for BC by aethalometer. Particulate mass concentration (PM) was also determined by gravimetry. General features of determined aerosol composition at Kırklareli region is given in Table 4.1.1.

All species were not detected in all samples. Data completeness is important, because it gives information on the uncertainties associated with average concentrations of ions and elements. Missing data varied between 4% for NH_4^+ and 65% for Pt. Forty-eight elements and ions were detected in at least 90% of samples and 7 species were detected in between 70% and 90% of the samples. Five elements including Pt, Cr, Au, W and Bi were detected in less than 70% of samples. These elements were handled more carefully than other elements and ions in statistical tests and models, because statistical significance of results decrease as number of data points decreases. Therefore they were included in calculations for annual statistics to get an idea on levels of elements and ions but excluded from further statistical analysis.

Mean concentration of species varies from 0.0057 ng m^{-3} for Lu to 5800 ng m^{-3} for SO_4^{2-}. As can be seen in Table 4.1.1 standard deviations are comparable to the mean concentrations of species. Such high standard deviation values are typical for atmospheric pollutants and generally indicate that species fit lognormal or other skewed distributions. The Chi-square test which is a Goodness of Fit test was applied to all chemical species in order to determine whether they are lognormally or normally distributed. The Chi-square test showed that Na, Ca, V, Cu, Zn, Rb, Sr, Sn, Sb, La, Ce, Cl^-, NO_3^-, NH_4^+ followed lognormal distribution with 90% statistical significance. Lognormal and Gaussian fits to distributions of remaining elements and ions are not statistically significant at same confidence level. Frequency histograms for lognormally distributed Cl^-, Ce and neither normally nor lognormally distributed Al and Fe were given in Figure 4.1.1.

Table 4.1.1 Statistical summary of concentration (ng m^{-3}) of elements, ions, black carbon and PM mass of aerosols collected at Kırklareli station

	N[a]	Mean	STD[b]	Median	Min[c]	Max[d]
PM	334	66000	75000	49000	1100	920000
SO_4^{2-}	349	5800	2600	5600	340	16650
NO_3^-	348	2900	1800	2500	160	12000
NH_4^+	350	2000	1300	1700	242	19220
Cl^-	333	580	770	320	14	8850
BC	344	540	270	500	22	1660
Li	344	0.64	0.64	0.43	0.002	4
Be	304	0.041	0.0478	0.023	0.000098	0.3
Na	348	550	880	320	6	11450
Mg	349	650	820	290	3	5000
Al	348	920	1050	520	4	6500
P	298	37	36	24	0.6	260
K	348	460	465	335	9	5210
Ca	334	1600	3100	800	13	39300
Ti	339	67	77	35	0.5	471
V	349	3.8	2.8	2.9	0.23	16
Cr	136	33	187	3	0.02	2050
Mn	345	26	30	15	0.2	230
Fe	281	710	900	420	1	9700
Ni	328	8.6	47	2.1	0.003	780
Cu	345	9.8	25	5.8	0.1	340
Zn	323	58	250	18	0.7	3040
Ge	346	0.056	0.043	0.048	0.00014	0.4
As	338	1	0.8	0.8	0.0008	5
Se	274	0.51	0.52	0.37	0.004	4
Rb	349	2	2	1.3	0.08	13
Sr	338	4.2	6.6	2.7	0.03	100

N[a] number of samples, **STD**[b] standard deviation, **Min**[c] minimum measured value, **Max**[d] maximum measured value

Table 4.1.1cont. Statistical summary of concentration (ng m^{-3}) of elements, ions, black carbon and PM mass of aerosols collected at Kırklareli station

	N[a]	Mean	STD[b]	Median	Min[c]	Max[d]
Y	347	0.35	0.44	0.18	0.0052	3
Mo	348	1.3	5.8	0.2	0.002	70
Cd	339	0.71	1	0.37	0.0004	10
Sn	343	2.1	4.6	1	0.03	45
Sb	344	0.61	0.7	0.49	0.02	11
Cs	348	0.16	0.15	0.11	0.0065	1
La	346	0.68	0.78	0.41	0.006	7
Ce	343	1.2	1.5	0.7	0.006	13
Pr	346	0.14	0.18	0.07	0.0004	1
Nd	347	0.51	0.64	0.26	0.003	5
Eu	346	0.026	0.0326	0.0146	0.000022	0.3
Sm	346	0.11	0.13	0.06	0.00027	1
Gd	347	0.11	0.14	0.06	0.00011	1
Tb	340	0.014	0.019	0.008	0.0000012	0.2
Dy	333	0.077	0.091	0.044	0.00013	0.7
Ho	332	0.014	0.017	0.009	0.0001	0.1
Er	262	0.044	0.05	0.026	0.000002	0.3
Tm	342	0.0061	0.0083	0.0037	0.000023	0.1
Yb	342	0.037	0.0412	0.022	0.0001	0.3
Lu	301	0.0057	0.0062	0.0035	0.000017	0.04
Hf	344	0.11	0.16	0.07	0.0012	2
W	197	0.63	2.5	0.11	0.0007	25
Pt	127	0.078	0.8	0.0028	0.000095	9
Au	145	0.081	0.25	0.037	0.00016	3
Tl	349	0.083	0.077	0.068	0.0032	1
Pb	348	32	50	16	1	570
Bi	220	0.084	0.097	0.057	0.00012	0.7
Th	314	0.23	0.29	0.14	0.00033	2
U	345	0.077	0.082	0.046	0.0011	0.6

N[a] number of samples, STD[b] standard deviation, Min[c] minimum measured value, Max[d] maximum measured value
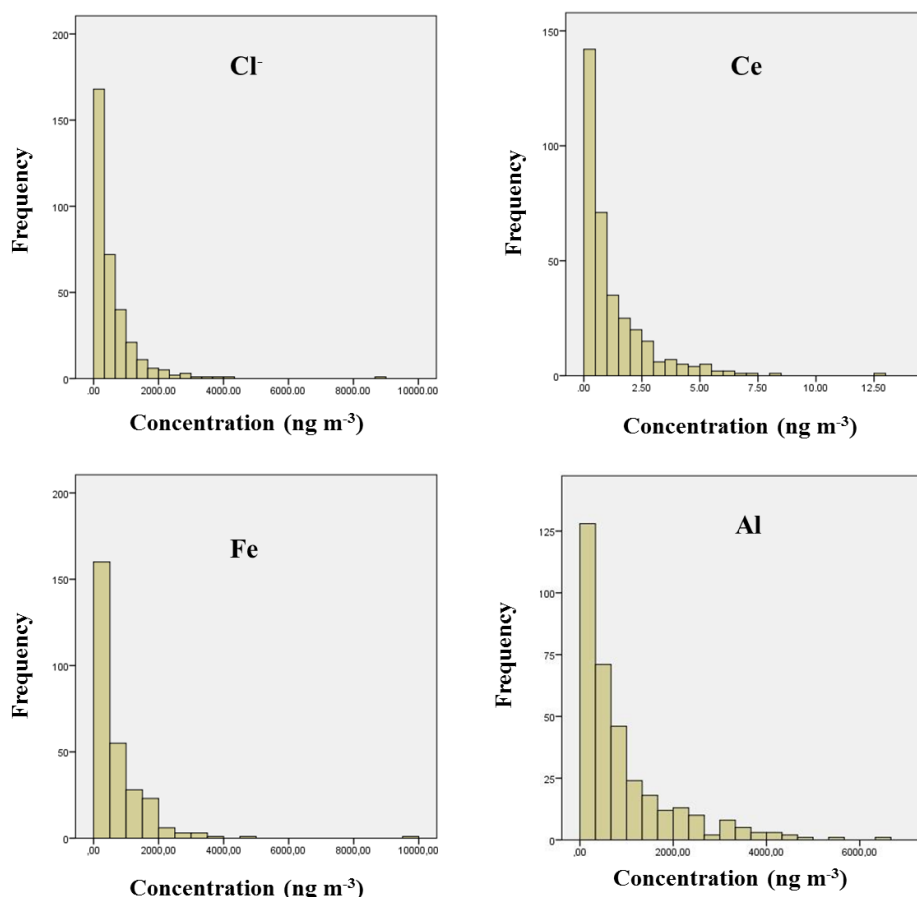
Figure 4.1.1 Frequency distribution of concentrations for selected species at Kırklareli station

Although most of the chemical species did not show normal or lognormal distribution, their frequency histograms were skewed right, as can be seen for Al and Fe in Figure 4.1.1. Skewed distributions are best represented by the median and it is well known that median is insensitive to extreme values. Therefore, median is used as a measure of central tendency for the chemical species (to show where the bulk of the data lies).

Besides trace metals and major ions, BC concentration was also determined in this study. To the best of our knowledge, BC measurements in rural parts of Turkey is few and this study one of them.

4.1.2. Comparison with Literature

To assess the pollution level at the rural site of Northwestern Turkey, concentration values of aerosol species reported for different parts of Turkey and Europe were compared with those from this study and given in Table 4.1.2. Although the number of parameters measured in this study was extensive, comparison was limited with the measured parameters in the literature. Note that arithmetic average values were used for comparison as only arithmetic average values were reported in some of the studies. Arithmetic average concentration of Cr in the current study was 33 ng m^{-3} which was a factor of eleven higher than its median concentration. There were large outliers in Cr data set, and these outliers affected the arithmetic average value and hence resulted in higher values. Large outliers were also

36

observed for Ni data set. Therefore median values of Cr and Ni were used in Table 4.1.2 for the current study. The detailed information about the studies used for comparison is given below:

1) Antalya- rural (Öztürk et al., 2012)

Antalya station was a rural station located at the Mediterranean coast of southwestern Turkey. PM10 samples were collected between 1993 and 2001, and analyzed for 48 elements, nitrate, sulfate, chloride, ammonium and BC.

2) Mersin-rural (Kocak et al., 2007b)

This station was a rural station located at the Mediterranean coast of southeastern Turkey. Fine (PM2.5) and coarse (PM10-PM2.5) fractions were collected between April 2001 and April 2002. Aerosol samples were analyzed for some trace elements and major ions. Sum of fine and coarse fraction was used as PM10 in Table 4.1.2.

3) Bursa- rural (Karakaş and Tuncel, 1997)

Bursa station was a rural station located in the southeastern part of northwestern Turkey (at Uludağ Mountain). Total suspended particulate matter samples were collected between September 1993 and April 1994. Major ions were determined.

4) Zonguldak –urban (Tecer et al., 2012)

Zonguldak station was an urban station at the Black Sea coast of the northwestern Turkey. Fine (PM2.5) and coarse (PM10-PM2.5) aerosol fractions were collected between December 2004 and October 2005. Aerosol samples were analyzed for trace elements. Sum of fine and coarse fraction was used as PM10 in Table 4.1.2.

5) İstanbul[1]- urban (Theodosi et al., 2010a)

İstanbul[1] was an urban station which was considered as representing the Greater İstanbul Area which was the most populated city of Turkey located in the northwestern part. PM10 aerosol samples were collected between November 2007 and June 2009. Collected samples were analyzed for the major ions, trace elements, water-soluble organic carbon (WSOC), organic (OC) and elemental carbon (EC).

6) İstanbul[2]- suburban (Karaca et al., 2008)

İstanbul[2] was a suburban station of the Greater İstanbul Area. Fine and coarse fractions of aerosols were collected between July 2002 and July 2003 and analyzed for trace metals. Sum of fine and coarse fraction was used as PM10 in Table 4.1.2.

7) Spain- urban (Nicolas et al., 2009)

This site was an urban background station located approximately 12 km away from the southeastern Spanish Mediterranean coast. Size segregated aerosol samples (PM2.5 and PM10) were collected between December 2004 and November 2005. Major ions were determined in both fractions. For the comparison only PM10 fraction was used in Table 4.1.2.

8) Greece[1] –suburban (Manalis et al., 2005)

In this study four stations were reported, but in Table 4.1.2 only suburban station was used; because the other stations were under the influence of high traffic activities and/or some point sources. PM10 samples were collected between June 2001 and May 2002 in Athens, Greece and analyzed for trace metals.

9) Greece[2] –rural (Glavas et al., 2008)

The sampling station was 1 km away from the shore and it was a rural station located in Patras, Greece. Ionic composition of PM2.5 samples collected between November 2004 and October 2005 were determined.

10) Italy- urban background (Perrone et al., 2011)

TSP and PM2.5 samples were collected in Lecce, Italy approximately 20 km away from the Mediterranean coast between March and December 2007. The sampling station was considered as an urban background station due to low traffic density within 50 m periphery of the station. Major ions and EC were determined in collected samples. Species concentrations of TSP were used in Table 4.1.2.

11) Romania- suburban (Arsene et al., 2011)

The sampling station was located in a suburban site of Iasi, Romania. Fine and coarse fraction of aerosols were collected between January 2007 and March 2008. Samples were analyzed only for major ionic species. Sum of fine and coarse fraction was used as PM10 in Table 4.1.2.

12) Hungary- urban (Gabor et al., 2011)

This station was under the effect of heavy traffic density in Budapest, Hungary. PM10 samples were collected between September 2004 and August 2007. Trace metal concentrations in the PM10 aerosol fraction were used in Table 4.1.2.

Concentration of water soluble Na and Cl$^-$ in the current study was lower than studies conducted near or close to the sea. As these species are markers of the sea salt, observing lower concentrations in inland stations are not surprising. Sea salt aerosols are mostly in the coarse mode therefore the probability of scavenging from the atmosphere is higher before arriving the inland stations. Also chloride may be lost due to reaction between chloride and H_2SO_4/HNO_3 vapors (see Section 4.2.1 for details of chloride loss) during the transportation of air masses. The lowest water soluble Na and Cl$^-$ concentration was reported for Greece[2] (the station was only 1 km away from the sea) because in this station only fine aerosol fraction was collected. Fairly similar concentrations of sea salt elements were also reported for Bursa, which is also not at the immediate vicinity of the sea.

Concentrations of crustal species i.e. Al, Ti, Mn and Fe in the current study were almost higher than other studies. This is expected as TSP was collected in the current study, hence contribution of crustal species were dominant and existed in higher concentrations. Surprisingly concentrations of Al, Mn and Fe in Istanbul[2] were higher than the current study. This is not expected as PM10 was collected in Istanbul[2] station. However an exceptionally dry season was reported during the sampling period of Istanbul[2] study (Karaca et al., 2008). To have dry season during the sampling period may enhance contribution of crustal species to the observed PM10 in Istanbul[2] study. Furthermore there was a cement factory only 5 km southwest of the Istanbul[2] station. This cement factory may be another reason for having high Al, Mn and Fe concentrations in Istanbul[2] station. Iron concentration in Hungary was a factor of three higher than current study. Gabor et al., 2011 also reported that Fe concentration in Hungary study was higher than comparable urban sites but they did not explain the reasons behind it.

Table 4.1.2 Comparison of current study with the other studies in the literature (µg m^{-3})

Study	Current study	1-Antalya	2-Mersin	3-Bursa	4-Zonguldak	5-Istanbul[1]	6-Istanbul[2]	7-Spain	8-Greece[1]	9-Greece[2]	10-Italy	11-Romania	12-Hungary
Station type	rural	rural	rural	rural	urban	urban	sub urban	urban	sub-urban	rural	urban backg.	sub-urban	urban
Fraction	TSP	PM10	PM10	TSP	PM10	PM10	PM10	PM10	PM10	PM2.5	TSP	PM10	PM10
Al	0.92	0.661	-	-	0.59	0.74	5.92	-	-	-	-	-	-
K	0.46	0.536	0.36	-	0.41	-	3.01	-	-	-	-	-	-
Ca	1.6	1.422	1.89	-	1.19	2.84	5.4	-	-	-	-	-	-
Ti	0.067	0.032	0.03	-	0.058	0.02	-	-	-	-	-	-	-
V	0.0038	0.00317	0.0087	-	-	0.014	0.019	-	0.0037	-	-	-	0.003
Cr	0.003	0.00677	0.0057	-	0.008	0.004	0.2	-	0.01	-	-	-	0.0069
Mn	0.026	0.00893	0.0076	-	0.02	0.02	0.037	-	0.0044	-	-	-	0.027
Fe	0.71	0.4	0.35	-	0.48	0.7	1.52	-	-	-	-	-	2.115
Ni	0.0021	0.00252	0.0037	-	0.006	0.007	0.071	-	0.0092	-	-	-	0.0027
Cu	0.0098	-	-	-	0.121	0.02	0.065	-	0.013	-	-	-	0.037
Zn	0.058	0.017	0.0097	-	0.07	0.24	0.15	-	-	-	-	-	0.053
Cd	0.00071	0.00024	-	-	-	0.001	0.003	-	0.002	-	-	-	0.0011
Pb	0.032	0.052	0.03	-	0.019	0.07	0.14	-	0.025	-	-	-	0.03
BC	0.54	0.82	-	-	-	2.92	-	-	-	-	1.9	-	-
Cl$^-$	0.58	1.88	5.49	0.47	-	1.66	-	0.6	-	0.12	0.9	0.41	-
NO$_3^-$	2.9	1.28	1.85	1	-	1.74	-	3.76	-	0.4	1.1	0.64	-
SO$_4^{2-}$	5.8	7.93	4.95	2.2	3.39	4.73	-	-	-	3.2	5.9	0.99	-
Na$^+$	0.35	-	3.43	0.67	-	2.69	-	0.99	-	-	1.1	0.18	-
NH$_4^+$	2	1.14	0.85	1	-	0.92	-	1.1	-	1.6	1.4	0.17	-
K$^+$	0.15	-	0.2	0.064	-	0.71	-	0.28	-	-	0.4	0.04	-
Mg^{2+}	0.12	-	0.49	0.12	-	0.23	-	0.16	-	-	0.4	0.13	-
Ca^{2+}	0.7	-	1.56	1.12	-	1.49	-	2.29	-	0.33	2.7	1.35	-

39

Concentrations of mixed source originated species i.e. Ca, V and Ni in the current study were comparable to those in rural stations, whilst lower than those in urban stations. As these species can be emitted both from natural sources and anthropogenic sources, higher concentrations in urban stations is not surprising. Higher concentrations of Ca in Istanbul[2] study can be explained by the influence of the nearby cement factory.

BC concentrations in urban stations were higher than the current study. There may be many BC sources in urban areas such as traffic and industrial activities, however BC sources in rural areas are few and BC is probably transported from elsewhere (i.e., long range transport and/or regional transport) to rural areas. A source receptor modeling study estimated the BC concentration in PM originated from western part of Turkey was around 0.65 μg m^{-3} (Sciare et al., 2003).

Concentrations of anthropogenic species i.e. Cu, Zn and Cd in the current study were higher than rural studies but lower than all urban studies except for Zn measured in Hungary. High water solubility of Zn in Hungary aerosol, which was reported by Gabor et al., 2011 may be the reason of having comparable Zn concentration between the current study and Hungary urban station. Chromium concentration was lowest in the current study among the all stations. Although Cr is also an anthropogenic species, higher concentrations were reported in the rural southeastern Turkey and explained by high content of Cr in the local soil mineralogy (Öztürk and Tuncel, 2009).

The use of leaded gasoline in motor vehicles was completely banned in Turkey in 2006. High Pb concentrations in rural stations of Turkey given in Table 5.1.2 are not surprising, as these studies were conducted before 2006. Current study was conducted between 2006 and 2008, but as seen in Table 2.7.1, Pb concentration was still high and comparable with those previous studies. This may be explained by re-suspension of soil which is highly enriched in Pb due to deposition of previously emitted leaded gasoline.

The most noteworthy high concentrations were observed for SO_4^{2-}, NO_3^- and NH_4^+ in the current study. The concentrations of secondary species were comparable and even higher than those reported at Eastern Mediterranean coast of Turkey and İstanbul. This is a very important finding of this study and indicates that our sampling station is under the influence of long range/regional transport of these pollutants. As stated earlier our sampling station was located in a rural area very close to Turkish-Bulgarian border and there were no anthropogenic sources in the immediate vicinity of the station.

Comparison between the current study and those reported in the literature can provide some insights about the pollution level of the station and factors controlling the chemical composition of aerosols however these comparisons cannot provide conclusive evidences for sources. Source apportionment of aerosols is discussed in detail in Section 4.6.

4.2. Temporal Variation of Pollutants

Temporal variation of pollutants can give valuable preliminary information about emission sources and fate of pollutants as well as various factors, such as, meteorological factors and air mass transport pathways, affecting pollutant transport to a receptor. In this report temporal variations of pollutants are investigated in two different temporal resolutions as daily and seasonally. Daily variation of pollutants also called as short term variation is used to identify the episodic (extreme) changes in pollutant concentrations and investigate the reasons behind these episodes. Seasonal variations are insensitive to those episodes; therefore a general pattern for each pollutant can be determined by investigating seasonal variations of pollutants. In this study aerosols are analyzed for nearly 60 different species, although temporal variations of all species are investigated, only species that are generally used as marker of specific sources are plotted to demonstrate the temporal variations.

4.2.1. **Short Term Variations**

All species show episodic changes from day to day but the magnitude of the variation may vary. Such episodic variations of elements and ions in aerosols are reported in the literature (Bergametti et al., 1989, Kocak et al., 2004, Öztürk and Tuncel, 2009). Variations in emission strength, transport pathways and local meteorological conditions are reported to cause episodes in trace element data set. The relation between local meteorology and concentrations of elements and ions are discussed later in Section 4.4. There are two meteorological parameters that can cause generation of episodes on concentration data. These two meteorological parameters are rain and wind speed. Wind speed is a local meteorological parameter that expected to cause episodic changes in concentrations. The relations between average wind speed and species concentrations are investigated in Section 4.4 and no significant relations with 95% CL are found. The relation between maximum wind speed and concentrations of elements is also investigated, because maximum wind speed, instead of average wind speed may be more representative for episodic variations. During a day wind speed can change sporadically and fast wind speeds are more effective to lift the soil into the air. When more soil is lifted into the air, concentrations of soil related species are expected to be increased, hence higher concentrations are measured. However, relatively weak and/or no relations are found between maximum wind speed and species concentrations. Obviously, wind speed does not affect measured concentrations of elements and ions, at any statistical significance level. The lack of correlation between the wind speed and episodic increases in element concentrations is due to long range transport of measured elements to the station. Wind speed is a local meteorological parameter. It is expected to be influential on concentrations of measured parameters only if these concentrations are governed by local processes, such as emissions or dispersion. Wind speed measured locally cannot affect concentrations of elements and ions transported from distant sources, because their concentrations are determined by a number of non-local parameters, such as upper atmospheric transport patterns, altitude of the air mass when it traverses source regions of pollutants, rain scavenging during transport etc. This shows that rain is the only local meteorological factor affecting concentration levels in the station. The effect of rain is found as more pronounced for crustal species than marine and anthropogenic species. The non-rainy days to rainy days ratio are around 2.0 for crustal species and less than 1.6 for marine and anthropogenic species.

Different groups of elements are affected from rain event in different ways. Because of this relation between rain and crustal marine and anthropogenic elements are discussed separately. Temporal variations in the concentrations of selected crustal elements with daily local rainfall are given in Figure 4.2.1. It is seen that concentrations of crustal species drastically decrease with rain events. There are two reasons for this: (1) Rain scavenges out most particles at the sampling point, which naturally decrease measured concentrations during and immediately after rain. (2) Soil becomes damp during rain event; therefore soil particles cannot be easily re-suspended by winds, which prevents rapid built up of concentrations of these elements to pre-rain levels. The ratio of non-rainy days to rainy days is 2.1 for Al, 2.3 for Fe and 1.7 for Li. The ratios are around 2.0 for the rest of the crustal species. Although only rain events are reported for the station, it is known that soil is covered with snow throughout the winter season. This also explains why there is less episodes during winter season.

Daily variations in concentrations of elements with marine origin, namely Na and Cl, are given in Figure 4.2.2. As can be seen in the figure, large day to day variations are common for Na and Cl^-, throughout the study period. To investigate the reasons of such variability, episodes are divided into two groups based on Na and Cl^- concentrations. First group consists of aerosols having very high Na concentrations and second group consists of aerosols having very high Cl^- concentrations. Very high Na concentrations in the first group are observed on 11 June 2006 (11 µg m^{-3}), 21 July 2006 (6.3 µg m^{-3}), 2 September 2006
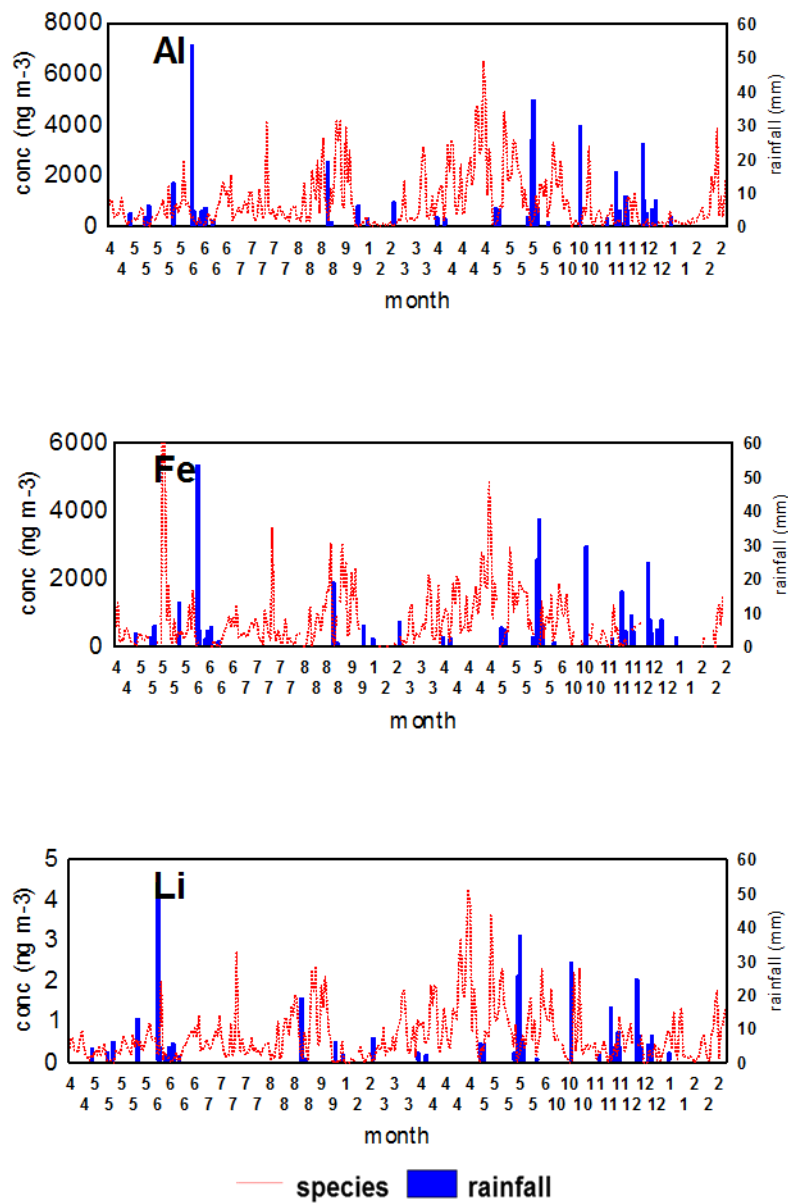
Figure 4.2.1 Time series plots of rainfall amount and concentrations of elements with known crustal sources

(3.2 μg m^{-3}) and 6 February 2008 (3.5 μg m^{-3}) with low Cl$^-$/Na mass ratios which are 0.02, 0.3, 0.05 and 0.12, respectively. Chloride to sodium mass ratio in sea water is 1.8 (Seinfeld and Pandis, 2006), this ratio tends to decrease in aerosol samples due to reaction of chloride with H$_2$SO$_4$ and HNO$_3$ vapors to form gaseous HCl. This process is known as "chloride deficit" and given in the following reactions:

$$H_2SO_4(g) + 2NaCl(s) \leftrightarrow Na_2SO_4(s) + 2HCl(g)$$ Equation 4.2.1

$$H_2SO_4(g) + NaCl(s) \leftrightarrow NaHSO_4(s) + HCl(g)$$ Equation 4.2.2

$$HNO_3(g) + NaCl(s) \leftrightarrow NaNO_3(s) + HCl(g)$$ Equation 4.2.3
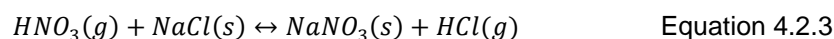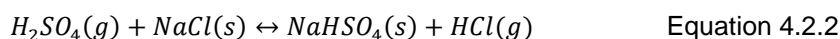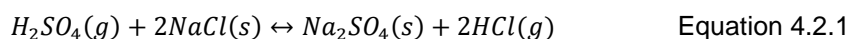
High sodium concentrations and lower Cl$^-$/Na mass ratios implies that aged sea-salt aerosols are arrived to the sampling station on episode days in the first group. When back trajectories in the first group are investigated, it is seen that air masses spent most of their time over land before arriving the sampling station (Figure 4.2.3 (a) and (b)), for this reason no fresh sea-salt aerosols reach the station.
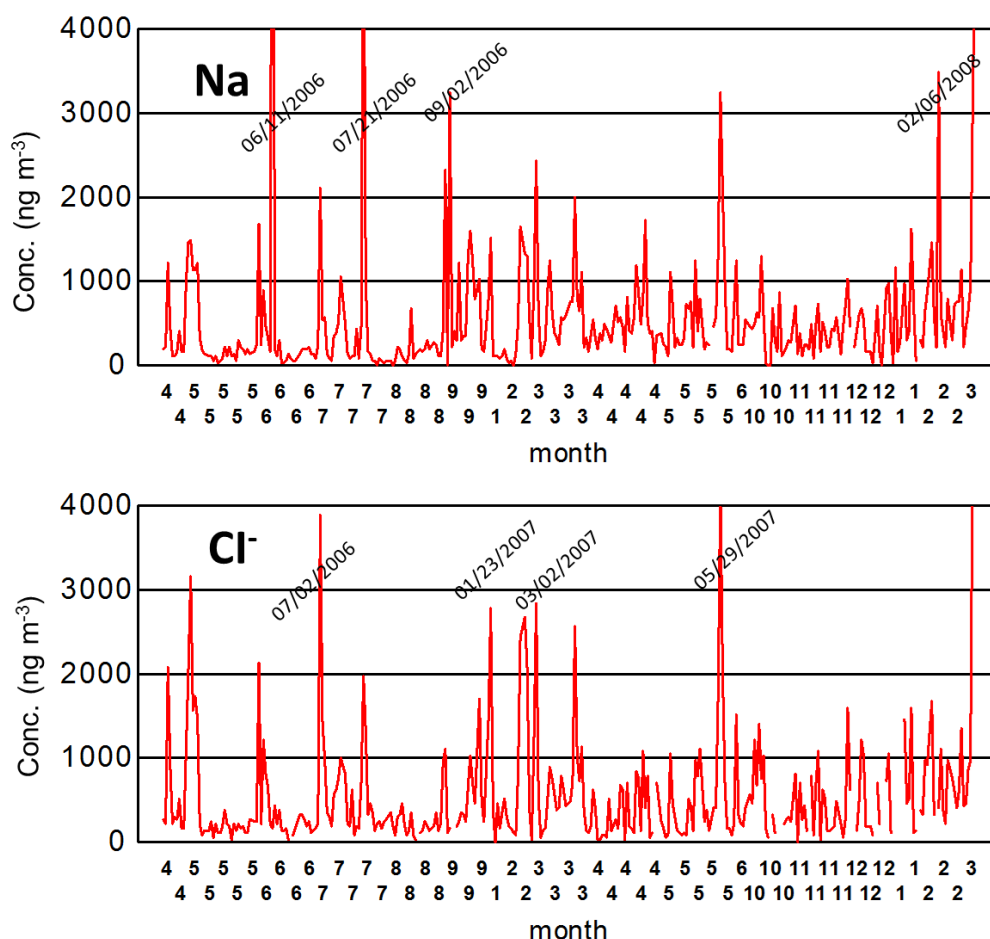
Figure 4.2.2 Time series plots of species with marine sources

02 Sep 06 (a)

06 Feb 08 (b)

02 Jul 06 (c)

23 Jan 07 (d)

100 m arrival height is red
500 m arrival height is blue
1500 m arrival height is green
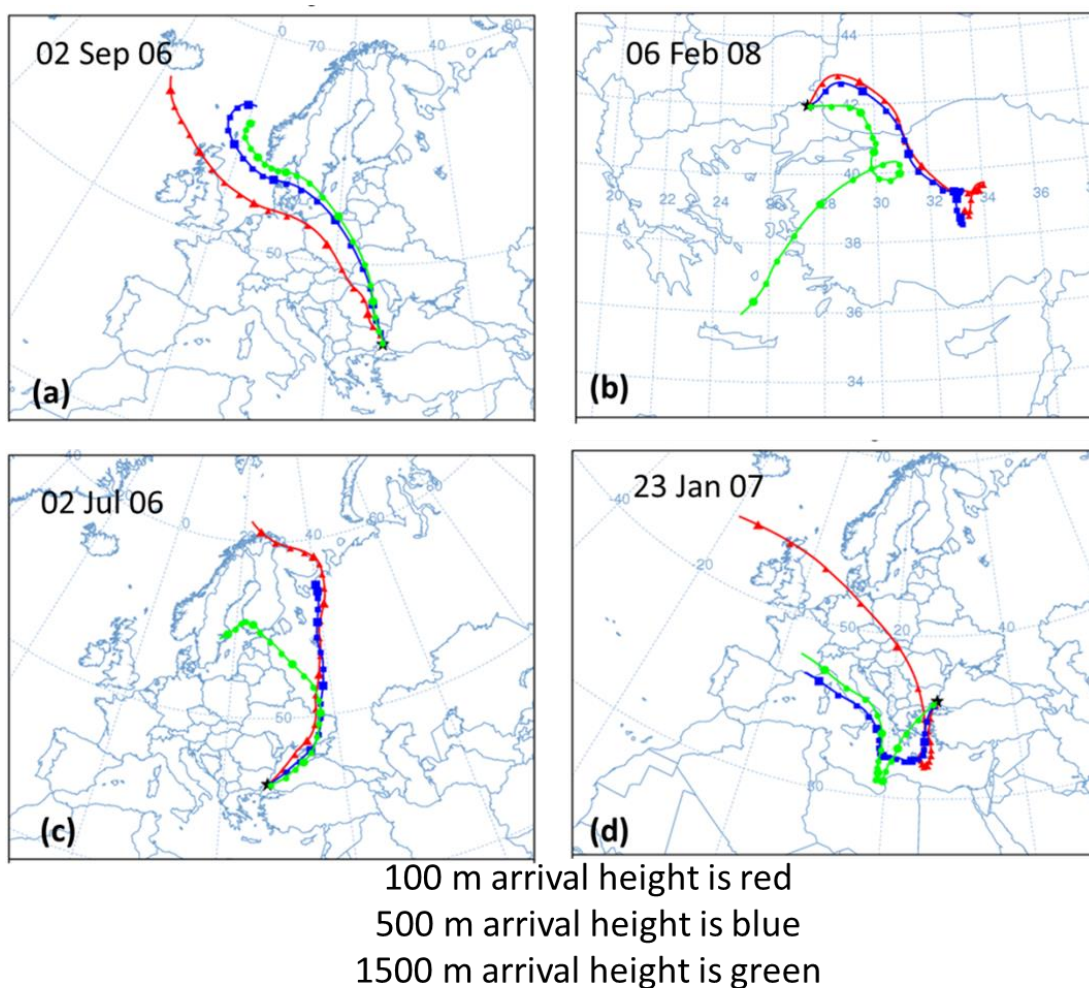
Figure 4.2.3 Back trajectories for selected episodes in the first group (a) and (b), and in the second group (c) and (d)

It should also be noted that unexpectedly high Na concentrations can also be due to episodes of crustal material, because earth's crust is also a minor source for Na. Normally soil is not important at stations that are close to the sea (like our station at Kırklareli, which is 50 km from the coast), however, during intense dust episodes, eolian material can explain a significant fraction of high Na concentrations. Aluminum concentrations in samples collected at 11 June 2006, 21 July 2006, 2 September 2006 and 6 February 2008 are 170, 4160, 900 and 750 ng m^{-3}, respectively. Considering that median Al concentration in this work is approximately 550 ng m^{-3}, these Al concentrations measured in Na episode days can be considered as "higher than general population", except for the first episode. Na-to-Al concentration ratio in the same days is 64, 1.5, 3.6 and 4.6 respectively. Typical Na-to-Al ratio in global soil compilations like Mason and Moore (1982) is 0.3 and it is not significantly different in other global soil compilations like Taylor (1964) and Wedepohl (1995). This very large difference between observed Na-to-Cl$^-$ and corresponding ratio in global compilations, demonstrate that anomalous Na concentrations measured in these days are not due to dust incursion to the study area.

Aerosols having higher Cl^- concentrations in the second group are measured on 2 July 2006 (Cl^- concentration is 3.9 $\mu g \ m^{-3}$ and Cl^-/Na mass ratios is 1.8), 23 January 2007 (Cl^- concentration is 1.8 $\mu g \ m^{-3}$ and Cl^-/Na mass ratios is 1.8), 2 March 2007 (Cl^- concentration is 1.2 $\mu g \ m^{-3}$ and Cl^-/Na mass ratios is 1.2) and 29 May 2007 (Cl^- concentration is 1.3 $\mu g \ m^{-3}$ and Cl^-/Na mass ratios is 1.3). Chloride to sodium mass ratios in the second group is in the range of sea-water mass ratio which is between 1.0 and 2.0. Lack of substantial Cl^- depletion shows that marine aerosols in the second group are due to fresh sea salt emissions. As seen in Figure 4.2.3 (c) and (d) air masses spent their time over sea before arriving the station, hence fresh sea salt emissions can be captured by air masses and transported to our station. For marine species we can conclude that regarding the distance between the Black Sea and sampling station which is 50 km, daily variability of Na and Cl^- is not due to local meteorological conditions, but mostly due to transported aged and fresh sea salt.

Above qualitative discussion indicated that short term variations in Na and Cl^- concentrations can be explained by local and distant marine sources. In that case Cl-to-Na mass ratio is expected to be inversely related with $SO_4^{2-} + NO_3^-$ concentrations. Plot of Cl^--to-Na ratio vs $SO_4^{2-} + NO_3^-$ mass concentrations is given in Figure 4.2.4. There is a slight decrease in Cl^--to-Na ratio with increasing $SO_4^{2-} + NO_3^-$ concentrations, but this decrease is significantly smaller than the decreases observed in Mediterranean (Gullu et al., 1998, Hacisalihoglu et al., 1992). There may be a variety of explanations for smaller decrease of Cl^--to-Na ratio observed in this study. Most attractive one is the lower SO_4^{2-} levels affecting the region today.
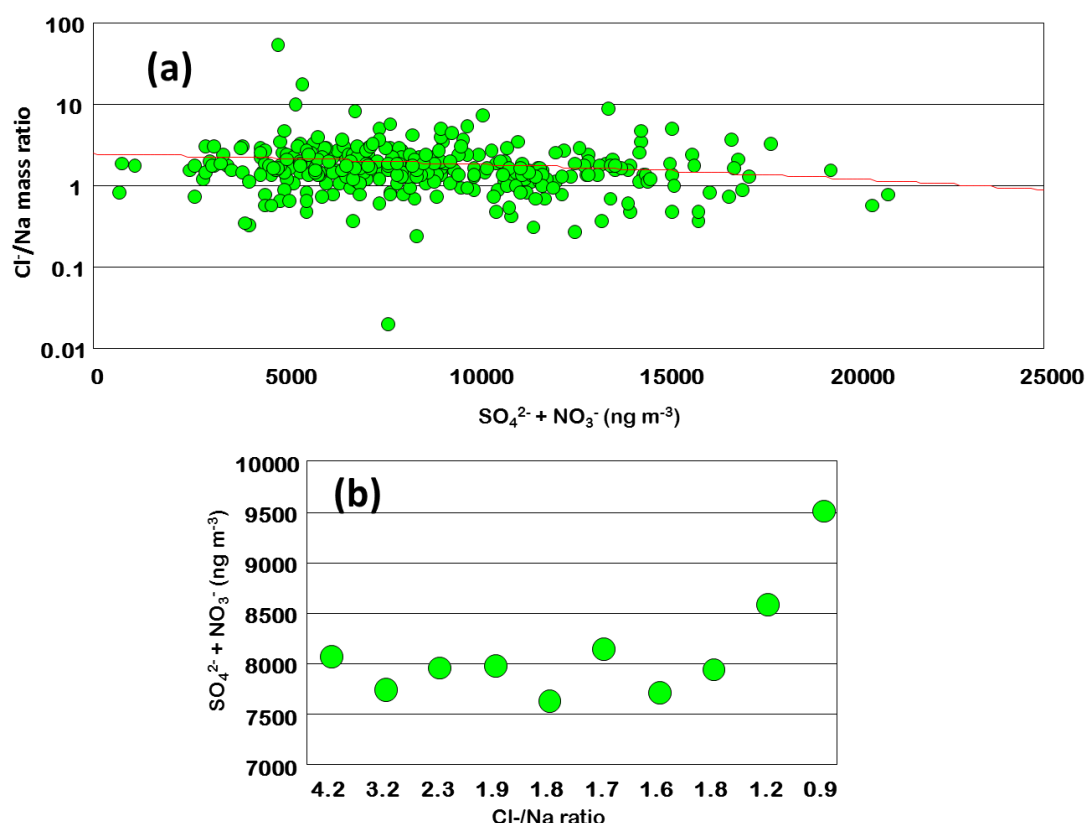
Figure 4.2.4 Plot of Cl^--to-Na mass ratio versus $SO_4^{2-} + NO_3^-$ mass concentrations

Sulfate concentrations were 8.9 ± 4.1 µg m-3 and 9.1 ± 2.6 µg m-3 in early 90s at the Mediterranean and the Black Sea, respectively. Similarly NO3- concentrations were 3.1 ± 0.8 and 2.1 ± 0.84 µg m-3 at the Black Sea and Mediterranean, respectively. In this study, on the other hand, SO42- concentration is 5.8 ± 2.6 µg m-3 and NO3- concentration is 2.9 ± 1.8 µg m-3. These averages show that SO42- concentrations decreased significantly in last 15 years in this region, whereas NO_3^- concentrations did not decrease at the same rate. This pattern is typical for the changes observed in Europe with a time gap, where SO_4^{2-} concentrations decreased by 74% but decrease in NO_3^- concentrations started later and was not as fast as the decrease observed in SO_4^{2-} concentration (Revuelta et al., 2012, Mian et al., 2010, Berglen et al., 2007, Fagerli et al., 2007). These changes occurred much earlier in Europe and SO_4^{2-} concentrations reported from EMEP stations in Western Europe is > 3 µg m^{-3}. Higher SO_4^{2-} concentrations in early 90's means more extensive interaction with sea salt aerosol and larger Cl$^-$ deficit relative to NaCl. Another possibility is that the station used in this work is downwind of Europe and air masses intercepted spend long times on the continent but not much on over the sea. Coarse sea salt particles picked up by the air masses over the Atlantic Ocean will have plenty of time to be scavenged. Because of this, our station may not be influenced from the sea, as much as the Antalya station is affected from Mediterranean. Antalya station was near the shore and was not downwind from large continental landmass. Fair number of air masses intercepted at Antalya station traveled from Gibraltar to Antalya over the Mediterranean Sea. There are no such trajectories in this work. To test this hypothesis, Cl$^-$/Na and SO_4^{2-} + NO_3^- data were sorted from high Cl$^-$/Na ratio to low and median concentrations were calculated for every 30 sample. Time series plot of Cl$^-$/Na ratio vs (SO_4^{2-} + NO_3^-) concentration for this smoothed data is given in Figure 4.2.4(b). The figure is very informative. Actually there is small number of samples in which there is Cl deficit (Cl$^-$/Na ratio <1.8). No matter what the Cl$^-$/Na ratio is average (SO_4^{2-} + NO_3^-) concentration is around 8 µg m^{-3}. But there is a clear inverse relation at Cl$^-$/Na ratio < 1.8. This pattern clearly explains why decrease in (SO_4^{2-} + NO_3^-) is so gradual with Cl$^-$/Na ratio in Figure 4.2.4(a).

Anthropogenic and natural sources such as sea salt and earth's crust can equally or comparatively contribute to concentrations of some of the elements and ions measured in this study. These species are referred to as elements with mixed origin in this manuscript. Best known examples of these elements are K, V and Ni. These species will be used as representative of mixed origin species in this manuscript. Daily variations of elements with mixed origin are given in Figure 4.2.5. Similar figures for selected anthropogenic elements are presented in Figure 4.2.6 and Figure 4.2.7. As can be seen in the figures, large day to day variations are observed. The main reason for such large variations is the changes in trajectory directions for anthropogenic component. Northerly flow in one day may bring pollution particles from Balkans and Europe, which results in rapid increase in concentrations of anthropogenic elements. Concentrations of anthropogenic elements remain high as long as upper atmospheric air flow continues to come from North. However, as soon as it turns to a clean sector, such as south, concentrations of anthropogenic elements rapidly decrease generating an episode. Anthropogenic species are not affected from variations in their source strengths, because their sources operate more or less continuously. However elements with mixed origin are influenced by variations in emission strength of crustal and/or sea spray components. As there are no anthropogenic sources in the vicinity of the station, anthropogenic elements are transported to our station by long range or regional transport. The variation in transport pattern can affect the pollution level in the station.

Another factor that may result in short-term episodic changes in concentrations of elements with mixed sources and anthropogenic elements is local rain events. Particles and elements associated with these particles can be effectively removed from atmosphere during rain, thus generating a drop in concentration time series of an element. All types of particles, including the ones containing elements with mixed sources and anthropogenic elements are affected from rain. This dependence of elemental concentrations on rainfall will be discussed in more detail in Section 4.4.
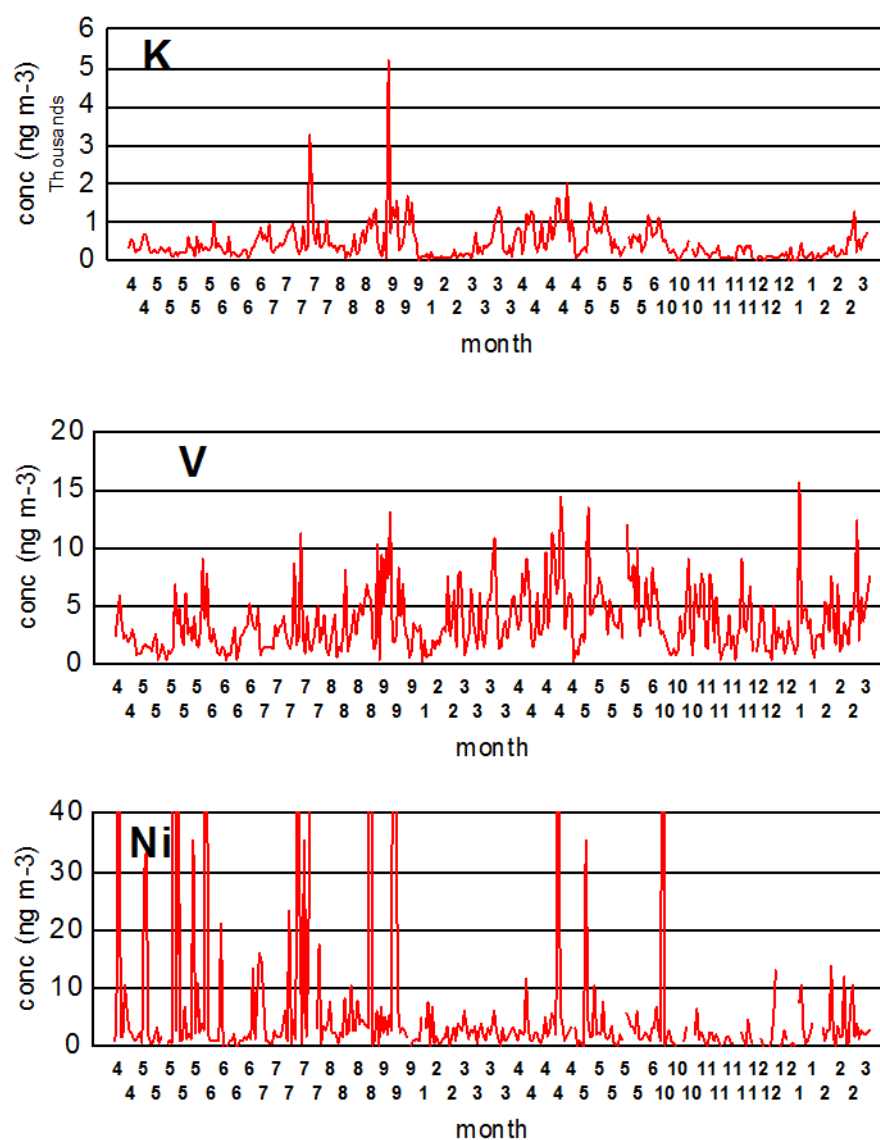
Figure 4.2.5 Time series plots of elements with known mixed sources
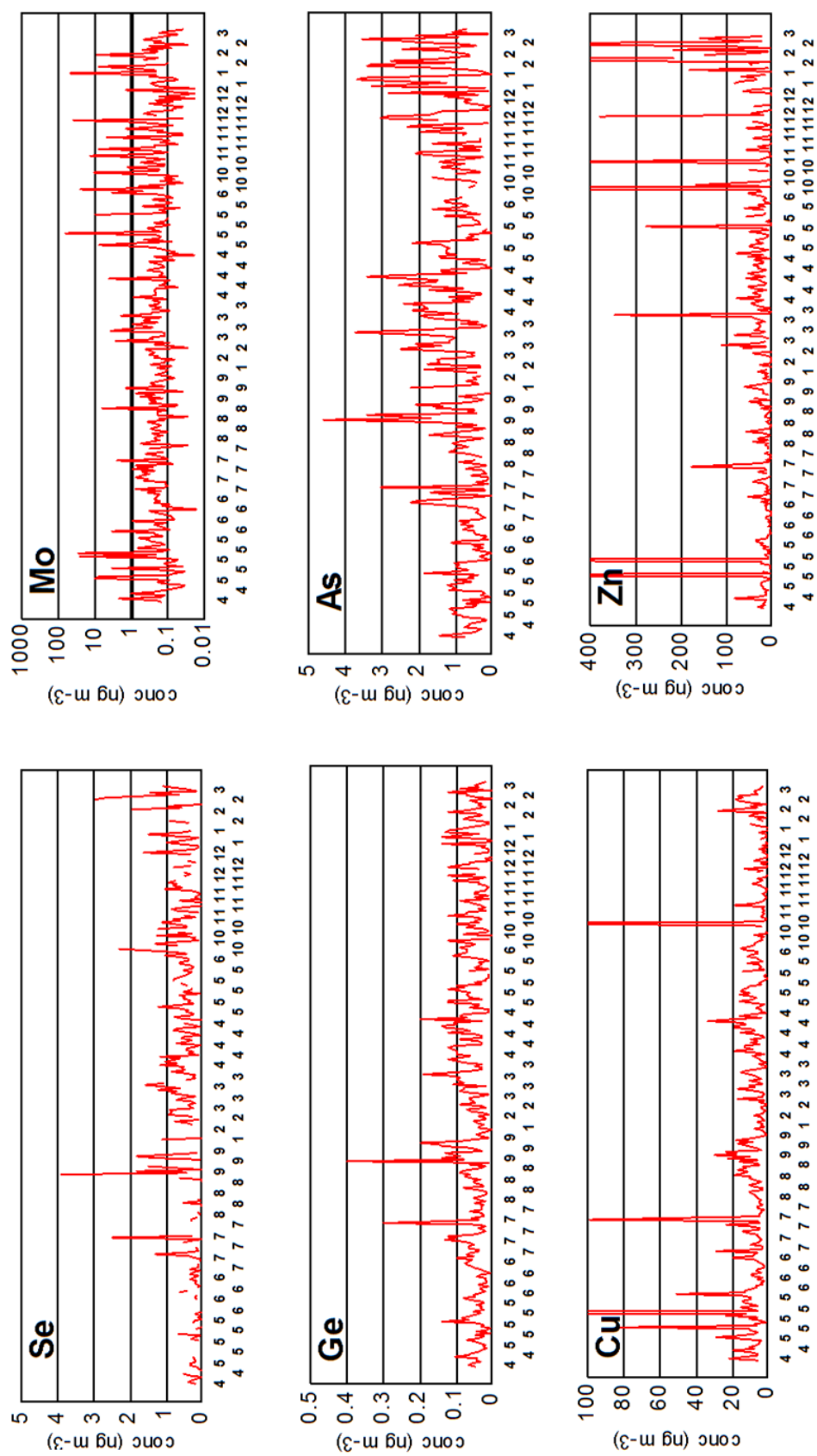
Figure 4.2.6 Time series plots of species with anthropogenic sources
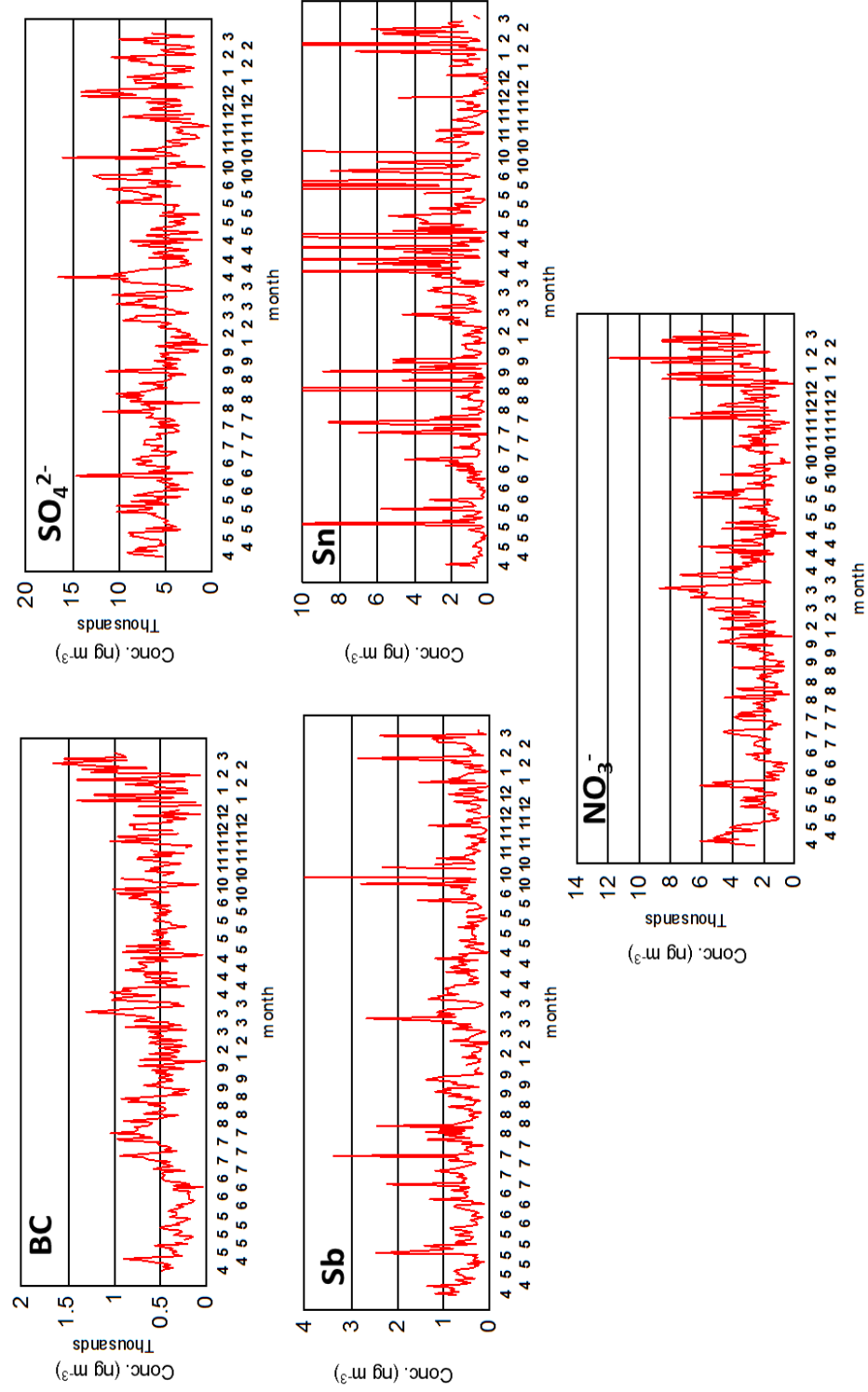
Figure 4.2.7 Time series plots of species with anthropogenic sources (continued)

49

4.2.2. **Long Term Variations**

Source strength and transport paths of pollutants can differ seasonally. Removal mechanisms of primary pollutants and especially production mechanisms of secondary pollutants show significant differences among seasons. Therefore, examining the variation of pollutants within seasons gives valuable information about their sources, transport paths and their fate in the atmosphere. Two seasons are used in this study to investigate the seasonal variations in concentrations of elements and ions. Months between November and April are selected as winter and the months between May and October are selected as summer season. This division is based on the long term seasonal distribution of precipitation because precipitation particularly rainfall has strong influence on concentrations of particle-bound species. Mann-Whitney W test is used to test the statistical significance of the difference between summer and winter median concentrations of species. Note that all species show right skewed distribution (see Section 4.1.1) hence median is chosen as a better way to represent the data set. The statistical summary of species during winter and summer season is given in Table 4.2.1 along with summer-to-winter ratios of median concentrations. For clarity, summer-to-winter (SW ratio) concentration ratios of elements are also given in Figure 4.2.8. Most species have shown significant differences between summer and winter at 95% CL, except for Be, P, V, Fe, Ni, Ge, Mo, Sn, Er, W, Bi, NH_4^+, SO_4^{2-} and PM. It is also interesting to note that when elements are sorted based on their summer-to-winter concentration ratios, crustal and anthropogenic elements are nicely grouped and separated from each other. Crustal elements have higher SW ratios than anthropogenic elements. In many cases monthly variation in concentrations of elements can be more informative than average summer and winter concentrations.

Summer to winter ratios of crustal elements vary between 3.25 for Th and 1.3 for Be and average SW for all crustal elements is 2.1 ± 0.5. Monthly variation in the concentrations of some representative crustal species is given in Figure 4.2.9 to show the general pattern which is governed by (1) rain and (2) incursion of Saharan Dust to the region. Although there are rain events, the soil is mostly dry in summer (note that other forms of precipitation usually do not occur in summer). When soil is dry, it is susceptible to wind abrasion. Hence soil particles can be easily mixed into the air. Rainfall, snow and other types of precipitation frequently occurs in winter therefore the soil is usually damp or ice covered. This prevent soil components from wind hence reduces the source strength. This general pattern results in higher concentrations of all litophilic elements in summer compared to winter. In Figure 4.2.9 it can be seen that concentrations of Al, Ca and Li are higher in summer months compared to monthly concentrations in winter season. However, concentrations of all three of elements are higher in April and September are significantly higher than concentrations measured in remaining summer months. The September peak is probably due to exceptionally dry month. Monthly rainfall data is also given in Figure 4.2.9. The rainfall in September is the lowest of all months in our sampling period. This probably results accumulation of crustal particles without rain scavenging and generated a very high September median concentration. Rainfall was not unusually low in April, on the contrary the highest rainfall was observed in May and June. Yet, concentrations of crustal elements are the highest in April, and are not particularly low in May and June, when the rainfall was the highest. This was due to incursion of desert dust to the study area, which will be discussed in detail later in Section 4.2.3. It is well documented that transport of dust from Sahara to Eastern Mediterranean is the most frequent in April and May (Alpert and Ziv, 1989, Ganor, 1991). Although rain frequency and intensity is the determining factor on monthly average or median concentrations of crustal elements, this factor is bypassed in April and May, and monthly average concentrations are determined by frequency and magnitude of dust transport.

Table 4.2.1 Summary statistics of species in winter and summer

		Winter			Summer		
	N	Mean	Median	N	Mean	Median	Sum/Win
		ng m^{-3}	ng m^{-3}		ng m^{-3}	ng m^{-3}	median ratio
Li	167	0.59 ± 0.66	0.35	177	0.68 ± 0.63	0.47	1.34
Be	138	0.04 ± 0.05	0.02	166	0.041 ± 0.044	0.026	1.33
Na	170	586 ± 612	442	178	519 ± 1070	231	0.52
Mg	171	595 ± 830	220	178	694 ± 818	395	1.8
Al	170	802 ± 1100	321	178	1037 ± 982	753	2.34
P	123	32 ± 33	22	175	40 ± 38	26	1.18
K	171	369 ± 364	233	177	547 ± 532	390	1.67
Ca	160	1551 ± 2952	683	174	1712 ± 3267	977	1.43
Ti	163	58 ± 81	20	176	76 ± 73	52	2.58
V	171	3.9 ± 2.8	3	178	3.6 ± 2.7	2.7	0.91
Cr	72	7.8 ± 41.6	2	64	61.3 ± 267.2	4.6	2.36
Mn	169	23 ± 32	9	176	29 ± 27	21	2.37
Fe	120	671 ± 775	385	161	743 ± 983	444	1.15
Ni	157	3.7 ± 9.9	2	171	13.2 ± 64.2	2.2	1.07
Cu	168	6.7 ± 6.2	4.8	177	12.8 ± 34.2	6.5	1.36
Zn	154	62 ± 251	24	169	54 ± 248	15	0.62
Ge	169	0.057 ± 0.038	0.051	177	0.055 ± 0.047	0.046	0.9
As	167	1.2 ± 0.9	1	171	0.8 ± 0.6	0.6	0.63
Se	138	0.57 ± 0.50	0.47	136	0.45 ± 0.53	0.31	0.65
Rb	171	1.7 ± 2.1	0.8	178	2.3 ± 2.0	1.7	2.2
Sr	165	3.5 ± 3.8	2.1	173	4.9 ± 8.5	3.1	1.47
Y	170	0.31 ± 0.48	0.12	177	0.39 ± 0.4	0.25	2.16
Mo	171	1.1 ± 4.9	0.2	177	1.5 ± 6.4	0.2	0.89
Cd	167	0.90 ± 0.95	0.61	172	0.53 ± 1.10	0.23	0.38
Sn	167	1.8 ± 3.1	1.1	176	2.5 ± 5.7	0.9	0.89
Sb	169	0.55 ± 0.43	0.44	175	0.68 ± 0.89	0.5	1.13
Cs	171	0.13 ± 0.14	0.07	177	0.18 ± 0.14	0.14	1.93
La	170	0.61 ± 0.85	0.27	176	0.75 ± 0.71	0.51	1.86
Ce	166	1.1 ± 1.7	0.4	177	1.4 ± 1.3	0.9	2.53
Pr	169	0.12 ± 0.18	0.04	177	0.16 ± 0.17	0.1	2.5
Nd	170	0.44 ± 0.7	0.15	177	0.58 ± 0.58	0.39	2.6
Eu	168	0.024 ± 0.034	0.012	178	0.027 ± 0.031	0.018	1.5
Sm	170	0.098 ± 0.141	0.041	176	0.117 ± 0.113	0.082	1.99
Gd	169	0.097 ± 0.151	0.035	178	0.125 ± 0.124	0.084	2.41
Tb	163	0.011 ± 0.017	0.004	177	0.016 ± 0.020	0.01	2.36
Dy	159	0.065 ± 0.098	0.025	174	0.087 ± 0.084	0.06	2.43
Ho	157	0.012 ± 0.017	0.005	175	0.016 ± 0.016	0.011	2.34
Er	104	0.043 ± 0.055	0.021	158	0.044 ± 0.045	0.029	1.35
Tm	165	0.0049 ± 0.0066	0.002	177	0.0072 ± 0.0095	0.0048	2.35
Yb	166	0.031 ± 0.043	0.013	176	0.043 ± 0.039	0.031	2.29
Lu	134	0.0049 ± 0.0066	0.0021	167	0.0063 ± 0.0058	0.0045	2.13
Hf	166	0.077 ± 0.089	0.039	178	0.151 ± 0.194	0.101	2.6
W	67	0.93 ± 3.55	0.13	130	0.48 ± 1.70	0.1	0.82

Table 4.2.1cont. Summary statistics of species in winter and summer

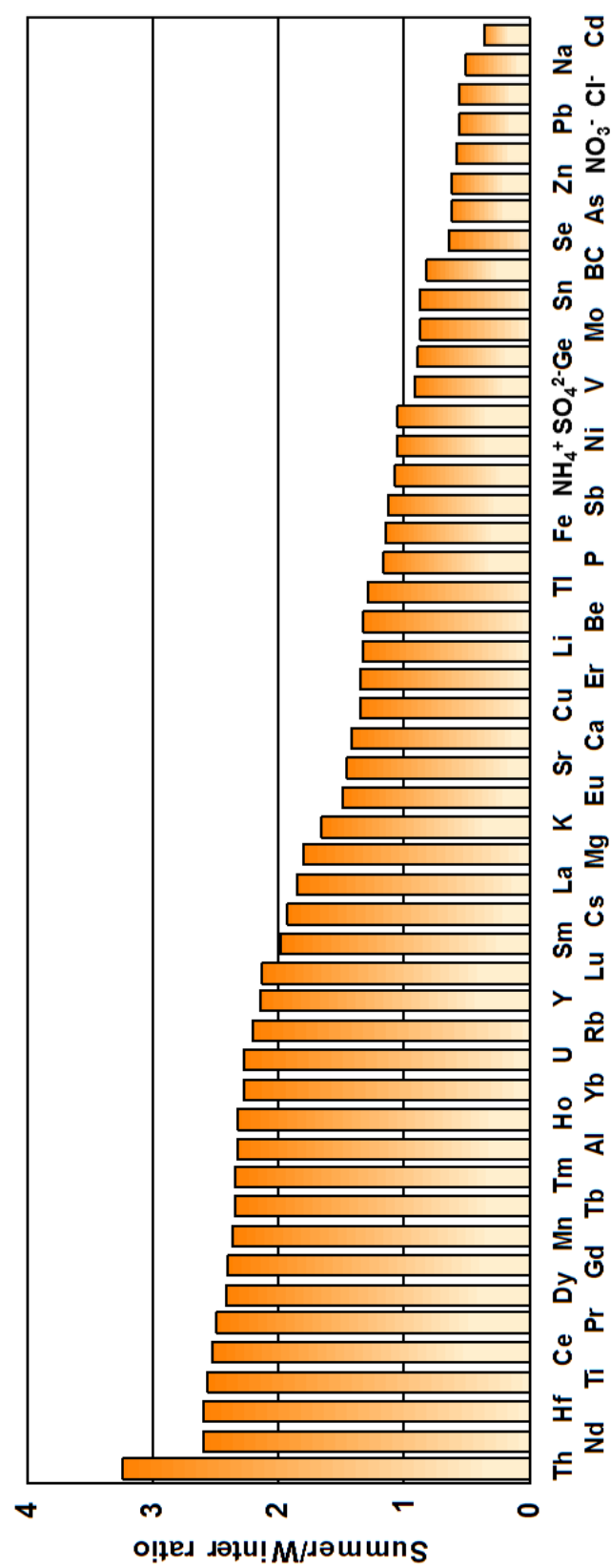|		Winter			Summer		
	N	Mean	Median	N	Mean	Median	Sum/Win
		ng m^{-3}	ng m^{-3}		ng m^{-3}	ng m^{-3}	median ratio
Pt	61	0.010 ± 0.016	0.004	66	0.141 ± 1.106	0.001	0.23
Au	38	0.032 ± 0.039	0.016	107	0.099 ± 0.293	0.049	3.01
Tl	171	0.067 ± 0.041	0.061	178	0.099 ± 0.097	0.08	1.3
Pb	171	41 ± 52	22	177	23 ± 47	13	0.57
Bi	102	0.067 ± 0.058	0.054	118	0.099 ± 0.120	0.058	1.06
Th	141	0.19 ± 0.30	0.05	173	0.27 ± 0.28	0.17	3.25
U	169	0.060 ± 0.071	0.03	176	0.093 ± 0.089	0.068	2.29
Cl$^-$	161	690 ± 917	450	171	480 ± 587	255	0.57
NO$_3^-$	171	3652 ± 2024	3385	177	2223 ± 1157	1992	0.59
SO$_4^{2-}$	171	5596 ± 2875	5320	178	6033 ± 2370	5688	1.07
NH$_4$	171	1999 ± 1671	1689	179	1947 ± 744	1824	1.08
BC	167	662± 346	623	177	527 ± 219	511	0.82

Figure 4.2.8 Summer-to-winter ratios of species at Kırklareli station
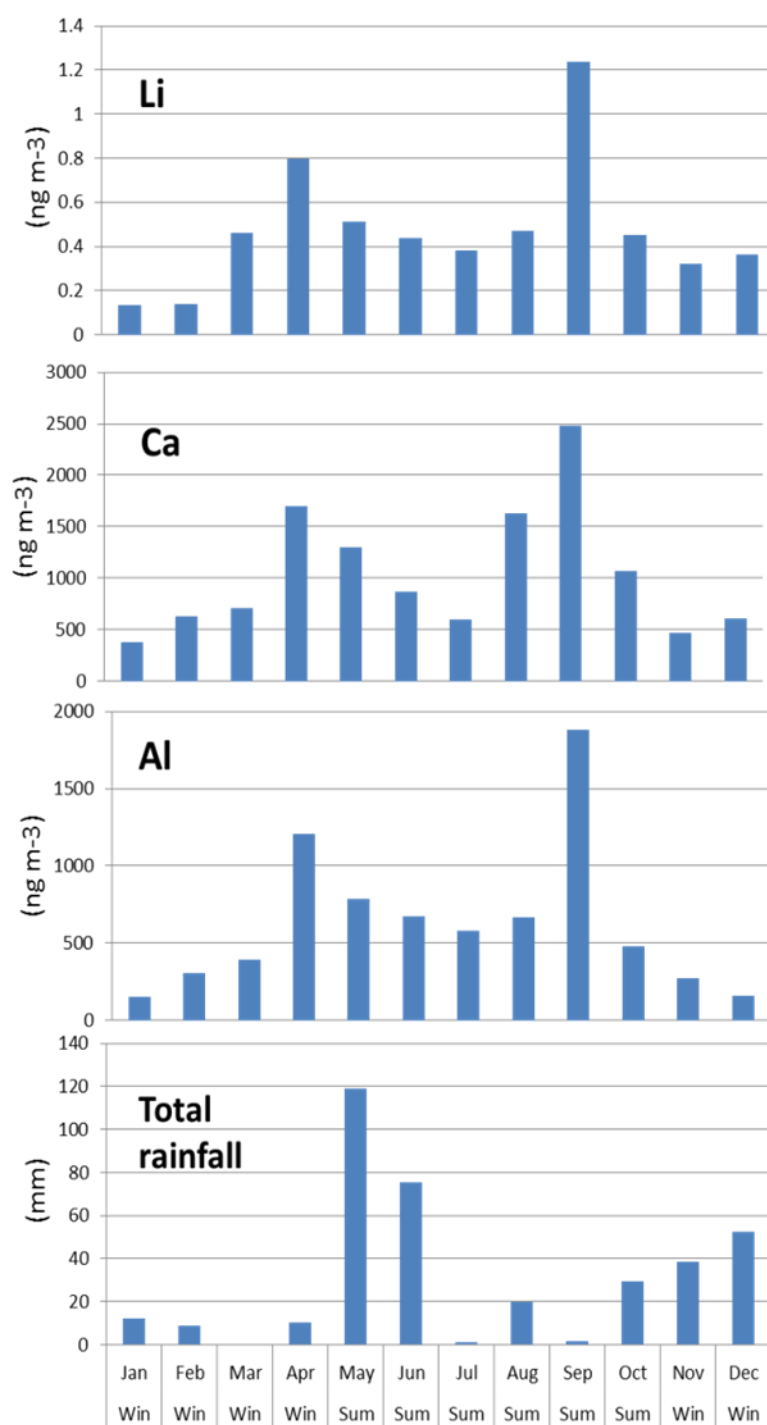
Figure 4.2.9 Monthly median concentrations of crustal species along with total monthly rainfall

Average PM mass concentration is 66 ± 88 and 67 ± 59 μg m^{-3}, while median is 49 and 47 μg m^{-3} in winter and summer, respectively. There is no statistically significant seasonal difference in PM mass concentrations. This may be explained by the variation of source strength and meteorological conditions. Although PM concentrations are fairly similar in winter and summer seasons, sources and hence types of particles may be different. Summer PM is mostly contributed by crustal and secondary inorganic particles. Approximately 29% of PM mass is due to soil components. Although contributions of crustal species decrease to approximately 15% of PM mass in winter, increase in sea salt emissions compensates this. Median Na concentration, which is a good marker for marine aerosol, increases from 239 ng m^{-3} in summer to 468 ng m^{-3} in winter. Although inorganic ions, particularly SO$_4^{2-}$, is an important component of PM mass, its contribution to seasonal variations in PM mass concentrations is not important as its summer and winter levels are similar (median SO$_4^{2-}$ concentration is 5700 ng m^{-3} in summer and 5600 ng m^{-3} in winter). In addition to seasonal variations in crustal and marine aerosol levels, lower planetary boundary levels in winter also contributes to higher PM mass concentrations measured in winter season.

Marine species Na and Cl$^-$ have the lowest SW ratios among all elements measured in this study (together with Pb and Cd). Their SW ratios are approximately 0.5, indicating that concentrations of these elements, and hence marine aerosol mass, are higher by a factor of two in winter. Seasonal variation in sea salt emission is the main reason for the significant difference between summer and winter concentrations. Monthly median concentrations of Na, Cl$^-$ and Mg are given in Figure 4.2.10 together with monthly rainfall recorded during the sampling period. Since bubble bursting process is enhanced in winter season due to stronger winds, generation of sea-salt aerosol and hence concentrations of Na and Cl$^-$ increase during winter season, which is clearly seen in Figure 4.2.10. In stations very close to the sea, large fraction of atmospheric Mg concentrations is explained by the sea salt contribution (Gullu et al., 1998). However, in this study summer concentration of Mg is approximately a factor-of-two higher than its winter concentration, thus demonstrating crustal source rather than sea salt in summer. This is also supported by the monthly variation of Mg-to-Na mass ratio, which is given in Figure 4.2.11. As seen from the figure Mg-to-Na mass ratios are enhanced in summer months due to the dominant influence of soil-related material in summer season. On the contrary, the ratios are close to the bulk sea water ratio, which is 0.18 (Seinfeld and Pandis, 2006) in winter months, hence indicating sea salt origin in winter.

The monthly variations in concentrations of anthropogenic species are illustrated in Figure 4.2.12 and Figure 4.2.13. As can be seen from the figures all anthropogenic elements do not show the same monthly pattern. Elements Zn, Ge, As, Se, Mo, Cd, Sn and NO$_3^-$ have higher concentrations in winter season. On the other hand, elements Sb, Cu, NH$_4^+$, SO$_4^{2-}$ have higher concentrations in summer. Germanium and black carbon do not show a clear seasonal variation.

In most of the studies in the Mediterranean region, it is documented that seasonal variations of elements are governed by wet scavenging during transport of air masses (Al-Momani et al., 1998, Gullu et al., 2005, Gullu et al., 1998, Kocak et al., 2004). Wet scavenging favors higher concentrations of elements in summer season. Because of this, if an element have higher concentrations in winter, then it is normal to consider that its sources should be close to our station. Again, in studies performed at the Eastern Mediterranean and Black sea there are very few elements that show higher concentrations in winter. Only As show higher concentrations in winter (Gullu et al., 1998, Karakas et al., 2004). All of the remaining elements have slightly higher concentrations in summer. It is very interesting that number of elements (Zn, Ge, As, Se, Mo, Cd, Sn and NO$_3^-$) have well-defined seasonal patterns with higher concentrations in winter. This supports earlier hypothesis that sources affecting chemical composition of particles in the Eastern Mediterranean atmosphere are located in neighboring countries, particularly Balkan countries and Ukraine (Dogan et al., 2010, Gullu et al., 2005).
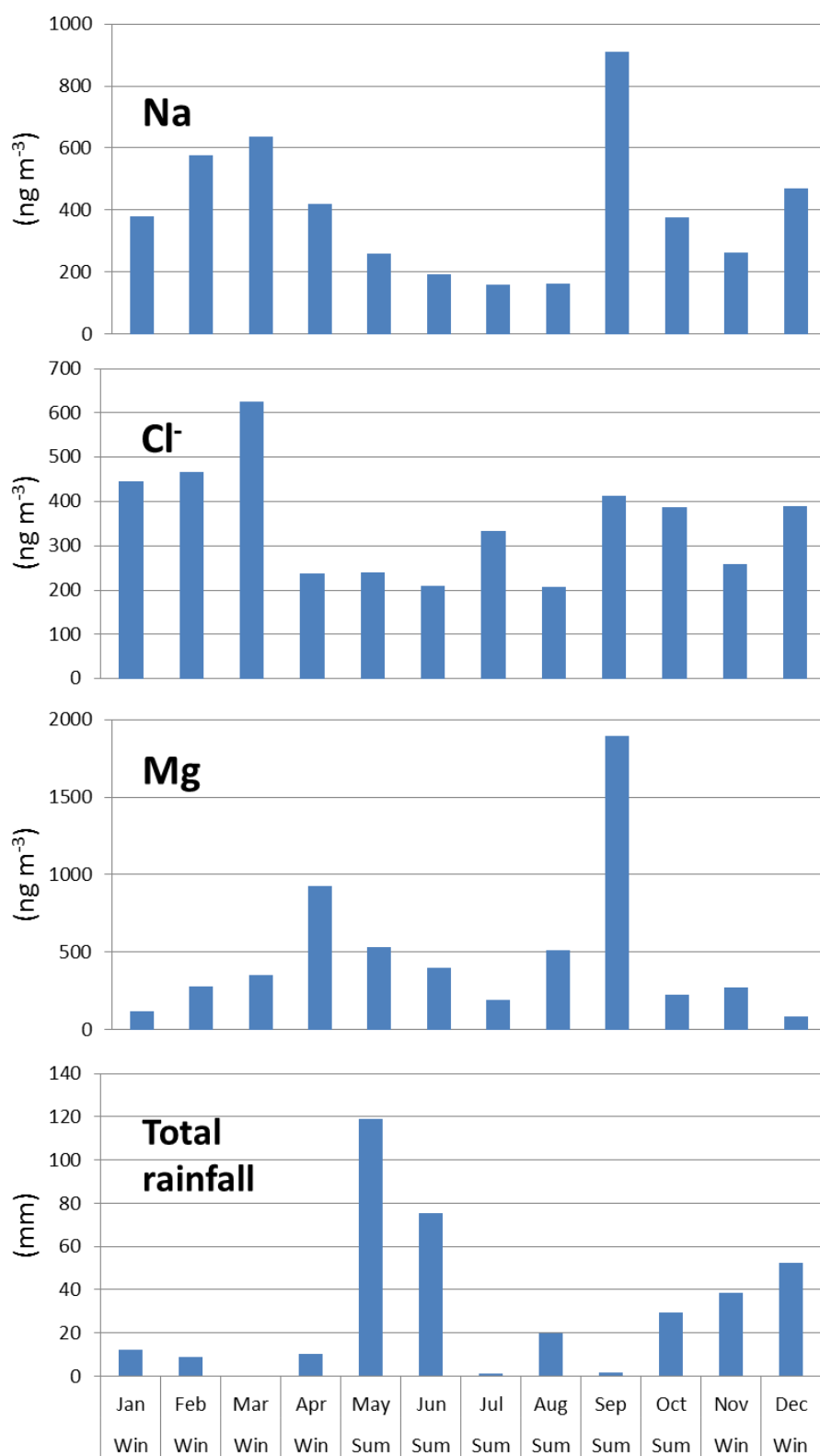
Figure 4.2.10 Monthly median concentrations of marine species along with total monthly rainfall

56
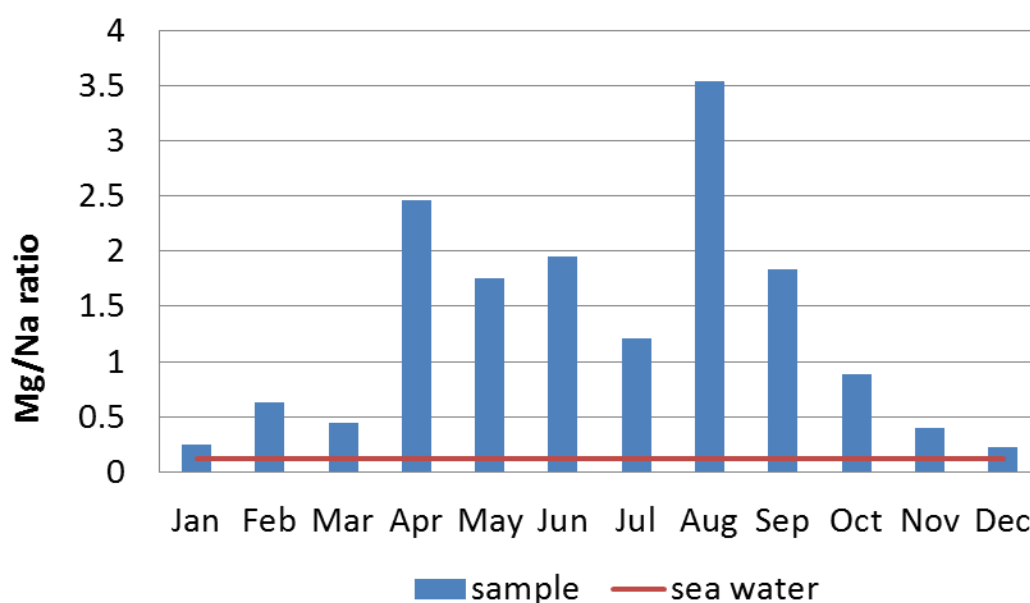
Figure 4.2.11 Monthly variation of Mg-to-Na ratio in samples along with the Mg-to-Na ratio in sea water

Copper concentration is higher in summer (Figure 4.2.12) with a Summer-to-Winter ratio of 1.4. Copper content of the local soil is high (personal communication with Necmi Kiral from MTA) therefore high concentrations of Cu during summer season is expected. This also supported by lower EFc of Cu in summer. Enrichment factor of Cu is 30 in November, December and January and approximately 10 between June and October. Concentrations of NO_3^- in winter season are approximately a factor-of-two higher than its corresponding summer concentration (Figure 4.2.13). The difference for NO_3^- is due to poor thermal stability of this compound. It is well documented that nitrogen tends to be in particulate phase as NO_3^- when ambient temperature is low as in winter months and tends to be in gas phase as NH_3 when ambient temperature is high as in summer months (Mozurkewich, 1993, Pakkanen, 1996, Zhuang et al., 1999). Consequently, high winter concentrations of NO_3^-, which is the particulate form of nitrogen in the atmosphere, can be explained by its stability in winter.
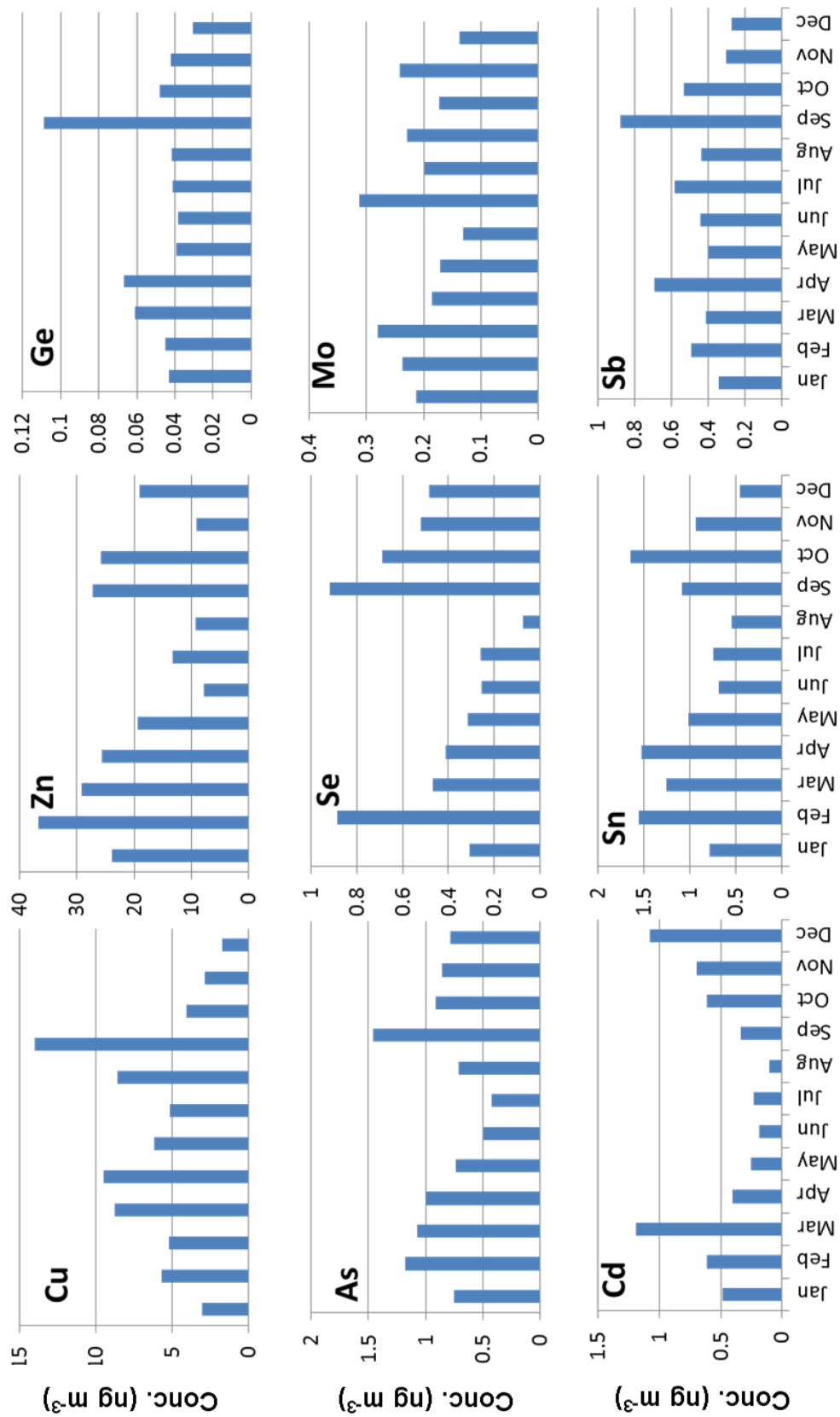
Figure 4.2.12 Monthly median concentrations of anthropogenic species

58
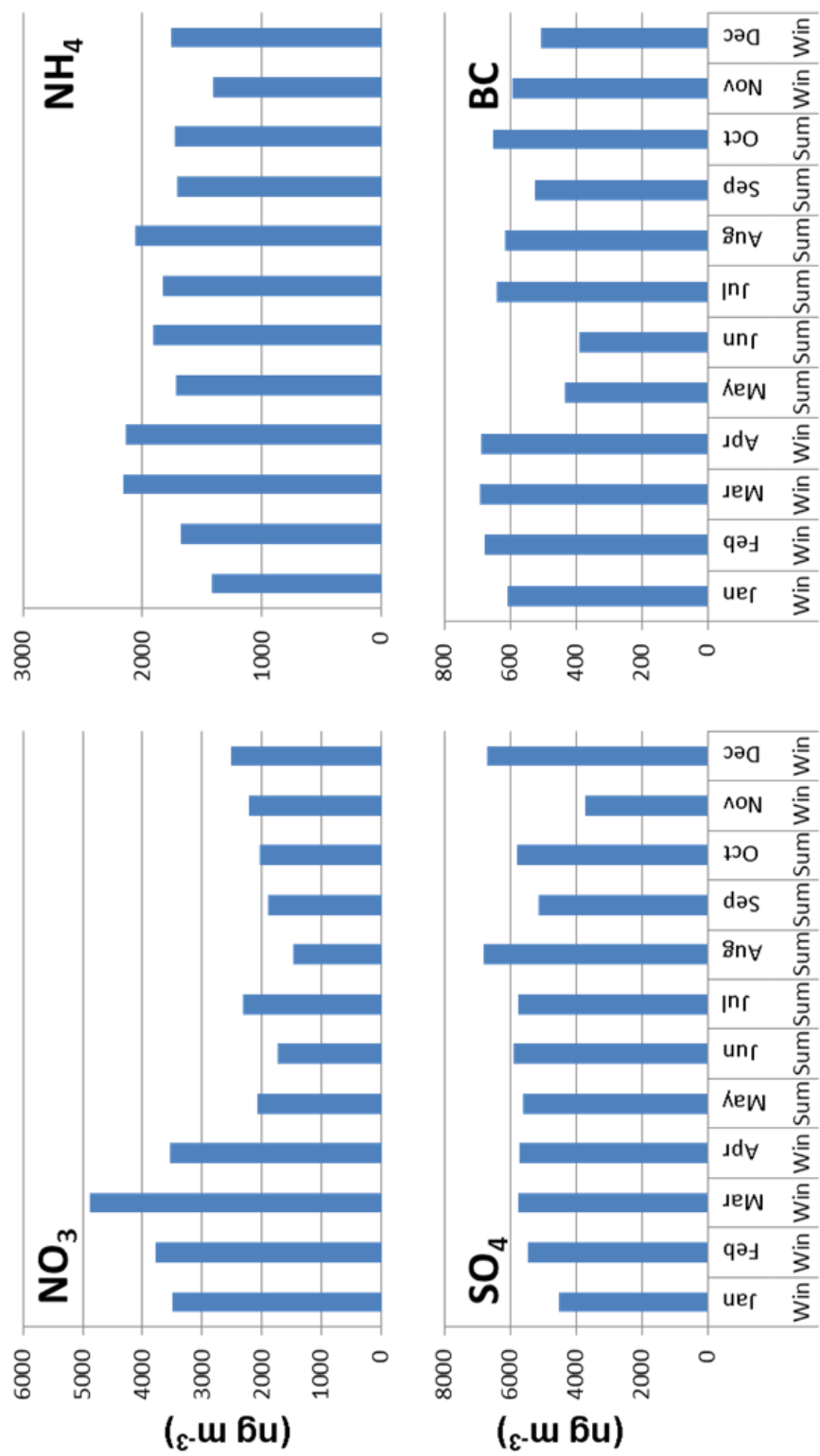
Figure 4.2.13 Monthly median concentrations of anthropogenic species (continued)

There are very weak seasonal signal in concentrations of NH_4^+ and SO_4^{2-}, with slightly higher levels in summer season. A very high correlation between NH_4^+ and SO_4^{2-} ($r=0.83$, $p<0.05$) indicates that most of the NH_4^+ is originated from the neutralization between SO_4^{2-} and NH_3. Animal farming, fertilizers and organic decomposition are the best known sources of NH_3. It should be noted that the sampling site is in rural area and there are farms around the station. In spring and summer months NH_3 is used as fertilizer in agricultural activities and in these seasons solar flux is high. At high solar flux and temperature ammonium tends to be in vapor phase (in the form of NH_3) (Nicolas et al., 2009). This may be the reason for observing similar NH_4^+ concentrations in summer and winter seasons. Median concentration of SO_4^{2-} is only slightly higher in summer as observed throughout the Eastern Mediterranean (Favez et al., 2008, Behera and Sharma, 2010, Verma et al., 2010, Arsene et al., 2011).

Elements with mixed sources frequently come up with their non-crustal and non-anthropogenic patterns in interpretation of trace element data. Behaviors of these elements with mixed sources in Kırklareli data set will be discussed in detail in this section. There are eight elements that have both crustal and non-crustal sources. This group includes Na, Mg, K, Ti, V, Mn, Cr and Ni. If sampling is performed in the close proximity of a special source, any crustal element can become an element with mixed origin. For example in the close proximity of iron and steel factories, Fe can be an element with mixed origin, in the vicinity of an aluminum plant, Al can be an element with mixed sources. However, these are special cases and can occur only in the immediate vicinity of these special sources. Otherwise, concentrations of elements Al, Fe etc are so high in alumina structure of soil that their non-crustal sources quickly become negligible as the distance between sampling point and source increase. Concentrations of Na, Mg, K, Ti, V, Mn, Cr and Ni in aluminosilicate matrix of soil, on the other hand, are high enough to make them crustal, but not high enough to make them entirely crustal in everywhere. In most of the studies their anthropogenic nature becomes apparent when sampling is relatively close to their sources or when concentration of crustal material decrease in the atmosphere.

These elements have different sources, other than crustal material. Main source of Na is the sea salt (Claeys et al., 2010, Eldering et al., 1991). In the coastal stations large fraction Na concentration in PM10 mass originate from sea salt (up to 90%), but at receptors far from the sea, salt contribution decrease and crustal contribution on Na concentration increase.

Vanadium and Ni are two well-documented markers for residual oil combustion (Cass and McRae, 1983, Jang et al., 2007). Manganese, Ti and Cr are enriched in emissions from steel industry (Choel et al., 2010, Pekey and Dogan, 2013) and metallurgical industry (SPECIATE, 2012). Crustal and non-crustal fractions of these eight species vary from one location to another depending both on the magnitude of non-crustal sources strengths and the distance between the non-crustal sources and sampling location. In rural studies non-crustal fractions can be less hence crustal fraction may dominate as in the current study.

The EFc versus Al diagrams for eight elements with mixed origin are given in Figure 4.2.14. Diagrams prepared for Na, K, Ni, V and Cr show clear indications of having anthropogenic component in their measured concentrations. Their enrichment factors decrease with increasing Al concentration, which is typical for most anthropogenic elements. However, they level off to a typical crustal pattern when Al concentration reaches to a threshold value. This threshold value changes from one element to another. For Na the threshold value is between $300 - 400$ ng m^{-3}. It is approximately 200 ng m^{-3} for K, between 600 and 800 ng m^{-3} for V and approximately 400 ng m^{-3} for Ni. Chromium data is too few (about 60% of Cr data is missing), which makes it difficult to decide on a threshold Al concentration. Unlike Na, K, V, Cr and Ni, other elements in this group, including Ti, Mg and Mn do not show anthropogenic pattern. In large number of studies in our group, anthropogenic components in Ti and Mn and sea salt component in Mg concentrations were demonstrated. In the current study their anthropogenic components are not detected. This is very likely using PM instead of PM_{10} or $PM_{2.5}$ sampling inlet in this study.
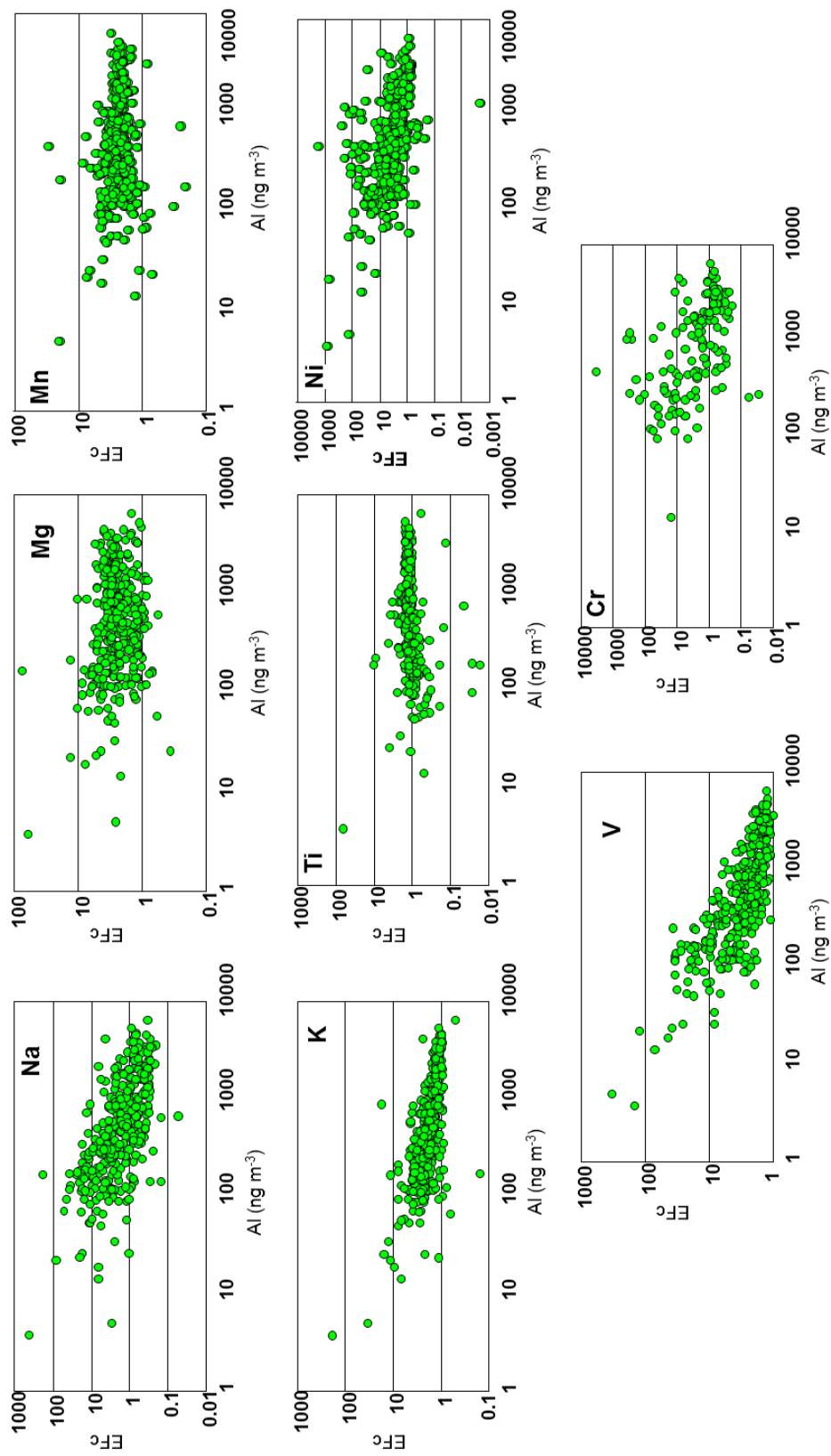
Figure 4.2.14 EFc versus Al concentration of mixed origin species

Monthly median concentrations of eight elements with mixed sources are given in Figure 4.2.15. Monthly concentration patterns do not differ significantly. All of these elements, except for Na, have higher concentrations during summer season, because crustal component in their concentrations increase in summer, due to easier resuspension of soil particles from dry surface in summer, as discussed in previous section in the manuscript. Monthly pattern depicted by Na is different, because it has strong contribution from sea salt in winter. Among these eight elements, Na is the only one, for which monthly concentration pattern gives an idea about its non-crustal source. For the remaining seven elements, their non-crustal components are not clearly visible in Figure 4.2.15. However, since concentrations of crustal material are low in winter months, as discussed in previous section, then one expects to detect their non-crustal components in winter season. This hypothesis is supported by their monthly median enrichment factors, which is given in Figure 4.2.16. Sodium, K, V, Cr and Ni are significantly more enriched in winter months relative to their enrichments in summer. This support our previous statement that enrichments of these elements may be more visible in winter season due to decrease in concentration of crustal aerosol in winter. Note that concentrations of these elements are also lower in winter season (except for Na), but yet they are more enriched in winter. Manganese, Mg and Ti are significantly enriched at any month, neither in summer, nor in winter. Titanium, showed a rather unique monthly enrichment pattern. It is more enriched in summer season than in winter. This pattern was also observed in enrichments of rare-earth elements. Although we do not have a conclusive evidence in our hands to show this, we believe that higher enrichments of rare earth elements and Ti is probably due to interception of a different soil type at the station in summer and winter seasons. More evidence is needed to corroborate this idea.

Finally we calculated non-crustal fractions of elements with mixed origin. Monthly variation of non-crustal fractions of these elements is given in Figure 4.2.17. For this calculation, firstly Element-to-Al ratios are calculated using the highest Al concentrations measured in this study. These Al concentrations are in the flat parts of the EFc – Al diagrams and in the region where these elements behave entirely as crustal. Calculated element-to-Al ratios are given in Table 4.2.2. In the table X-to-Al ratios calculated using entire data for that element and X-to-Al ratios given for Masons (1966) compilation for global composition of crustal material (Mason, 1966). It is clear from the table that element-to-Al ratios calculated using highest 20 Al concentrations is significantly different from both ratios calculated using whole data and the ratio given in Masons compilation. The difference between ratios calculated using highest 20 Al concentrations and entire data set is because in calculations using entire data also includes some anthropogenic contribution and is not realistic for the ratio of these elements in crustal material. The difference with Mason's compilation demonstrated that composition of crustal material intercepted at our station is not exactly similar to composition of crustal material given in Mason's compilation.
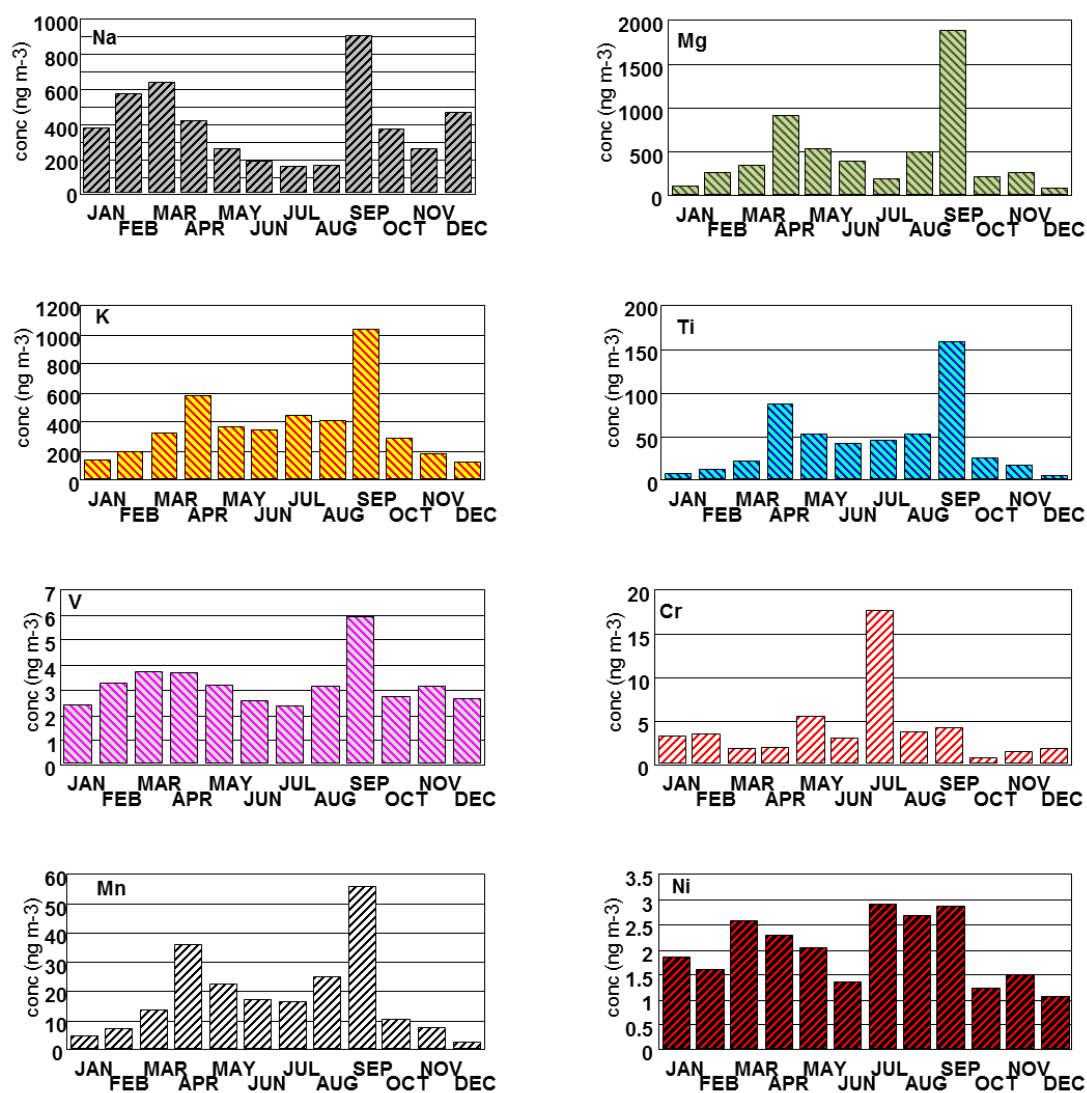
Figure 4.2.15 Monthly variation of concentrations of elements with mixed sources
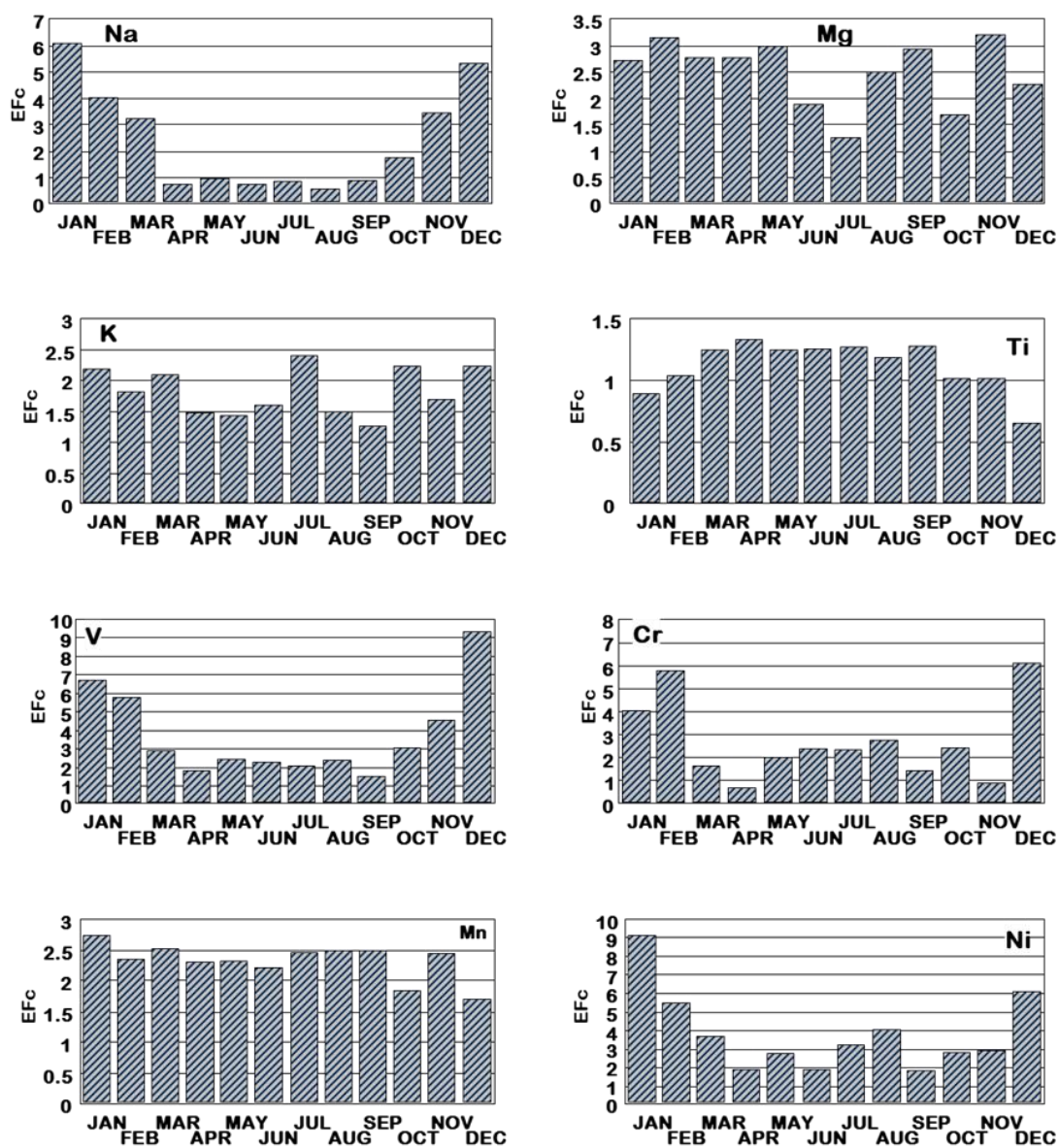
Figure 4.2.16 Monthly variation of EFc of elements with mixed sources
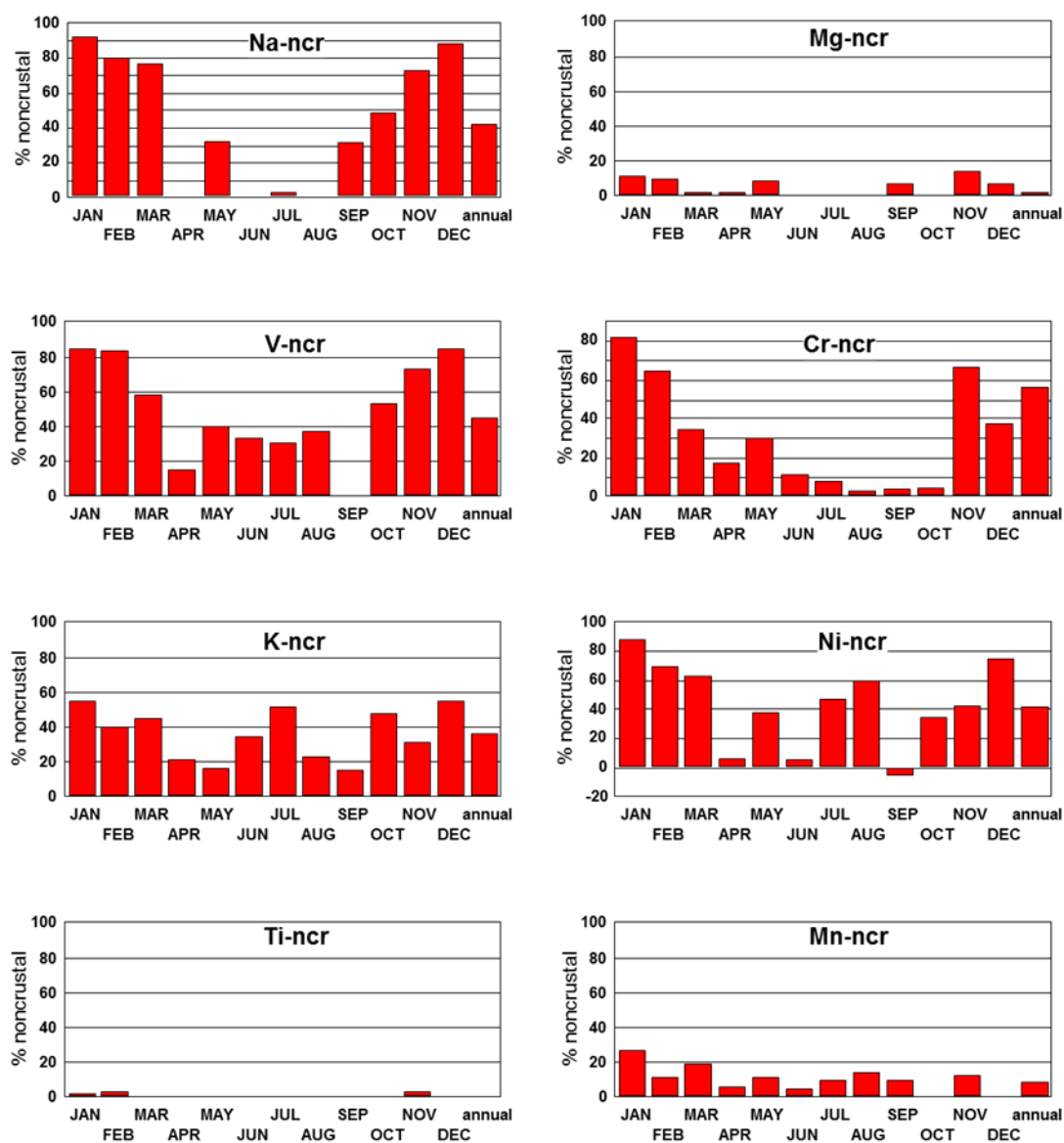
Figure 4.2.17 Monthly variation of non-crustal fractions of elements with mixed sources

Large fractions of the concentrations of Na, V, K, Cr, K and Ni, can be explain by their non-crustal sources. Their non-crustal fractions increase in winter period as suggested by the EFc calculations. Seventy-to-90% of Na concentration is non-crustal (marine) in January, February, October, November and December. Non-crustal fraction of Na in summer varies between 0 – 30%. A fairly similar contribution of anthropogenic sources is also observed for V, Ni and Cr as well.

Very high non-crustal contribution to Ni and V concentrations (up to 90%) can be explained by the presence of a nearby refinery in Bulgaria. The largest oil refinery in South-Eastern Europe, named LUKOIL Neftochim Burgas is located 60 km north north-east of the station. Trajectory analysis, which is discussed in detail in Section 4.3, shows that the frequency of air masses from north and north-east are higher in winter. Furthermore the percentage of slow moving air masses represented by cluster center originating from North east is also significantly higher in winter (see Section 4.3.1 for details). In the literature co-existence of Ni and V have been used as a tracer of fuel oil combustion (Mamane et al., 2008, Mazzei et al., 2008). Therefore transportation of oil refinery emissions to the station by the pertinent air movements may be the main reason of Ni and V in winter. Non-crustal fraction of K is lower (approximately 40% in winter). Non-crustal fractions of Mg, Ti and Mn are similar in all months.

Table 4.2.2 Element to Al ratios used in calculation of non-crustal factions of elements with mixed ratios

	All data	Max 20 Al conc	Mason
Na/Al	2.11 ± 9.72	0.26 ± 0.30	0.34
Mg/Al	0.84 ± 1.44	0.70 ± 0.35	0.25
K/Al	0.98 ± 3.67	0.37 ± 0.13	0.32
Ti/Al	0.08 ± 0.21	0.0712 ± 0.0172	0.054
V/Al	0.01 ± 0.04	0.0025 ± 0.0005	0.0016
Cr/Al	0.02 ± 0.25	0.0025 ± 0.0042	0.0012
Mn/Al	0.03 ± 0.03	0.0250 ± 0.0058	0.011
Ni/Al	0.02 ± 0.10	0.0016 ± 0.0017	0.00092

4.2.3. Effect of Saharan Dust Intrusions on Chemical Composition of Aerosols at Northwestern Turkey

Mineral dust associated with dust intrusions may be another factor causing episodic changes in crustal species. To identify a mineral dust episode combination of mineral dust tracers (Al, Fe and Ti), air mass back trajectories and satellite aerosol data and images or mineral dust forecast models have been used together (Barnaba and Gobbi, 2004, Borbely-Kiss et al., 2004, Papadimas et al., 2009, Rodriguez et al., 2001). Total Ozone Mass Spectrometer (TOMS) Aerosol Index (AI) is commonly used as an indicator of aerosols present vertically in the atmosphere. The AI is determined by comparing the intensities of back scattered radiation at 360 nm intensity measured by satellite (I_{360}^{meas}) and calculated for a Rayleigh atmosphere (I_{360}^{calc}) as $AI = 100 \log \left[\frac{I_{360}^{meas}}{I_{360}^{calc}} \right]$. Some studies have shown that aerosols below 850 hPa (below 1.5 km) cannot be detected effectively by TOMS (Herman et al., 1997, Kalivitis et al., 2007, Kubilay et al., 2005) and TOMS may not identify aerosols on the cloudy days or presence of smoke (Rivera Rivera et al., 2006, Shaw, 2008). TOMS AI value is positive for absorbing aerosols and negative for non-absorbing aerosols. Dust absorbs UV light; therefore AI value of dust is positive. There are other absorbing aerosols i.e. biomass burning aerosols (aerosols associated with black carbon) and non-absorbing aerosols i.e. SO_4^{2-} in the atmosphere.

TOMS AI cannot distinguish chemical speciation between absorbing aerosols, therefore positive AI value does not necessarily indicate dust; indeed it means that there are aerosols with absorbing properties. Moreover, in the presence of both absorbing and non-absorbing aerosols at the same time in the same volume of air, measured AI is decreased; hence TOMS underestimate the absorbing aerosols (Alpert et al., 2004, Koçak et al., 2012). As we want to focus on only dust intrusions, a mineral dust forecast model named Dust Regional Atmospheric Model (DREAM8b) is preferred to use in this study. DREAM8b is running by the Earth Sciences Division of the Barcelona Supercomputing Center in Centro National de Supercomputación (BSC-CNS). This model predicts the daily atmospheric life cycle of mineral dust by driving the NCEP/Eta regional atmospheric model and solving the Eulerian transport equations (Nickovic et al., 2001). In DREAM8b aerosols are modeled only for 8 size bins (0.15, 0.25, 0.45, 0.78, 1.3, 2.2, 3.8 and 7.1 μm). Aerosols in these size range can reside in the atmosphere for long hours (231 hours to 28 hours) hence long range transport in these size range are more probable (Tegen and Lacis, 1996). A more detailed description for DREAM8b can be found in Nickovic et al. (2001). 3-D daily dust forecasts of DREAM8b are available on http:// www.bsc.es/ projects/ earthscience/ BSC-DREAM/ web site for North Africa, Middle East, Europe, Sahara-Sahel and Spain. The forecasts are reported in 6-hour periods up to 72 hours ahead. The performance of DREAM8b is validated by comparing model results with surface measurements and satellite retrievals (Alpert et al., 2004, Carnevale et al., 2012, Mahler, 2006, Perez et al., 2006, Shaw, 2008, Yin et al., 2005, Yin et al., 2007) and found that DREAM8b shows very good agreement with them when dust transport is the main concern.

It should be noted that during the transport of air masses, mineral dust particles can be scavenged by rain events, in these cases observed concentrations of dust markers can be lower. As these cases do not represent the dust influence on aerosol composition (Borbely-Kiss et al., 2004), only cases with high concentration of mineral dust markers are used for assessing the influence of dust intrusions on aerosols. In this study 95 days out of 350 days are selected using their Al, Fe and Ti concentrations as indicators of dust episode. To identify an episode as dust event, at least one of the three back trajectory (we calculated 3 back trajectories with different starting altitudes for every sampling day) computed for that particular day must originate from North Africa or from the Middle East, and DREAM8b images must show there is dust loading over the sampling region. Among these 95 days, 16 mineral dust events with periods varying between one to four days are identified both by air mass back trajectories and DREAM8b model images. These days are 19 April, 21 May, 14

August and 19 to 22 August in 2006; 30 March, 6 to 8 May, 18 May, 28 to 31 May in 2007. Only for the episode day on 19 August 2006, Al concentration is very low (590 ng m^{-3}) compared to other dust days whilst Fe and Ti concentrations are comparable with 1080 and 123 ng m^{-3}, respectively. Satellite (TERRA and AQUA) images of 12 of these events for the years 2006 and 2007 are given in Figure 4.2.18 and Figure 4.2.19, respectively. In some of these pictures there are clouds that prevent detection of Saharan Dust at our station, but even in these images dust impact on the region are obvious. In the remaining events cloud cover was too much to detect dust under them. There is one-to-one agreement between the days identified as dust episode, based on elemental composition and DREAM8b model outputs and visual observation of dust in satellite pictures. On dust intrusion days Al concentrations vary between 1040 and 4560 ng m^{-3} (Al concentration on 19 August 2006 is not included). On the average, concentrations of Al, Fe, Ca, Mg and Ti were 670 and 3070 ng m^{-3}, 1660 and 5000 ng m^{-3}, 180 and 2525 ng m^{-3}, 80 and 310 ng m^{-3}, respectively.

Mean and median concentrations of elements on dust and non-dust days are given in Table 4.2.3. To determine the effect of dust intrusion on aerosols species, the ratio of median concentrations in dust days to non-dust days are plotted in Figure 4.2.20. The ratios are above 2.0 for all crustal species.
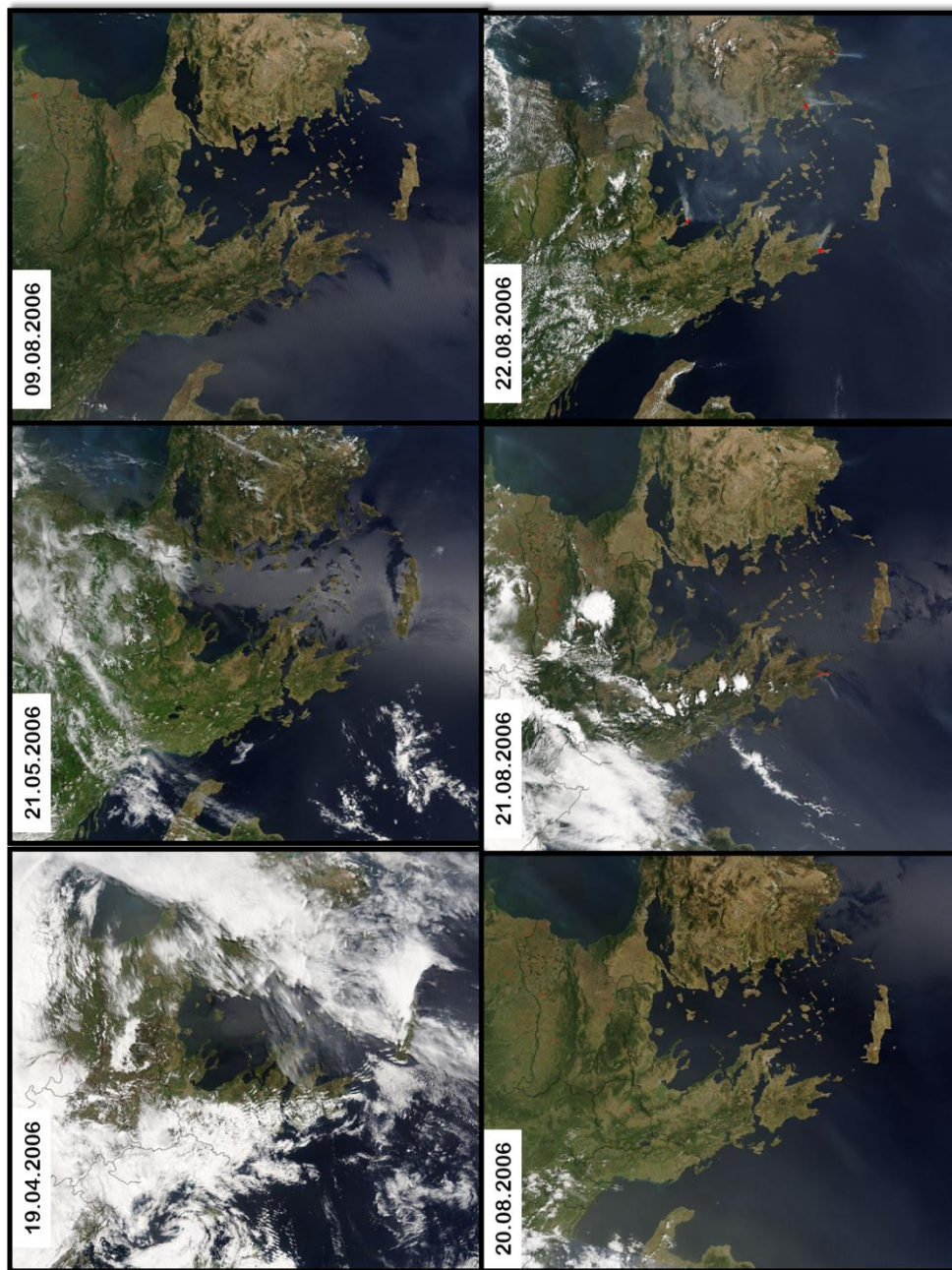
Figure 4.2.18 Sattelite pictures for the days, which are identified as dust days, based on AI concentration and Dream model results. Part 1: Episodes in 2006
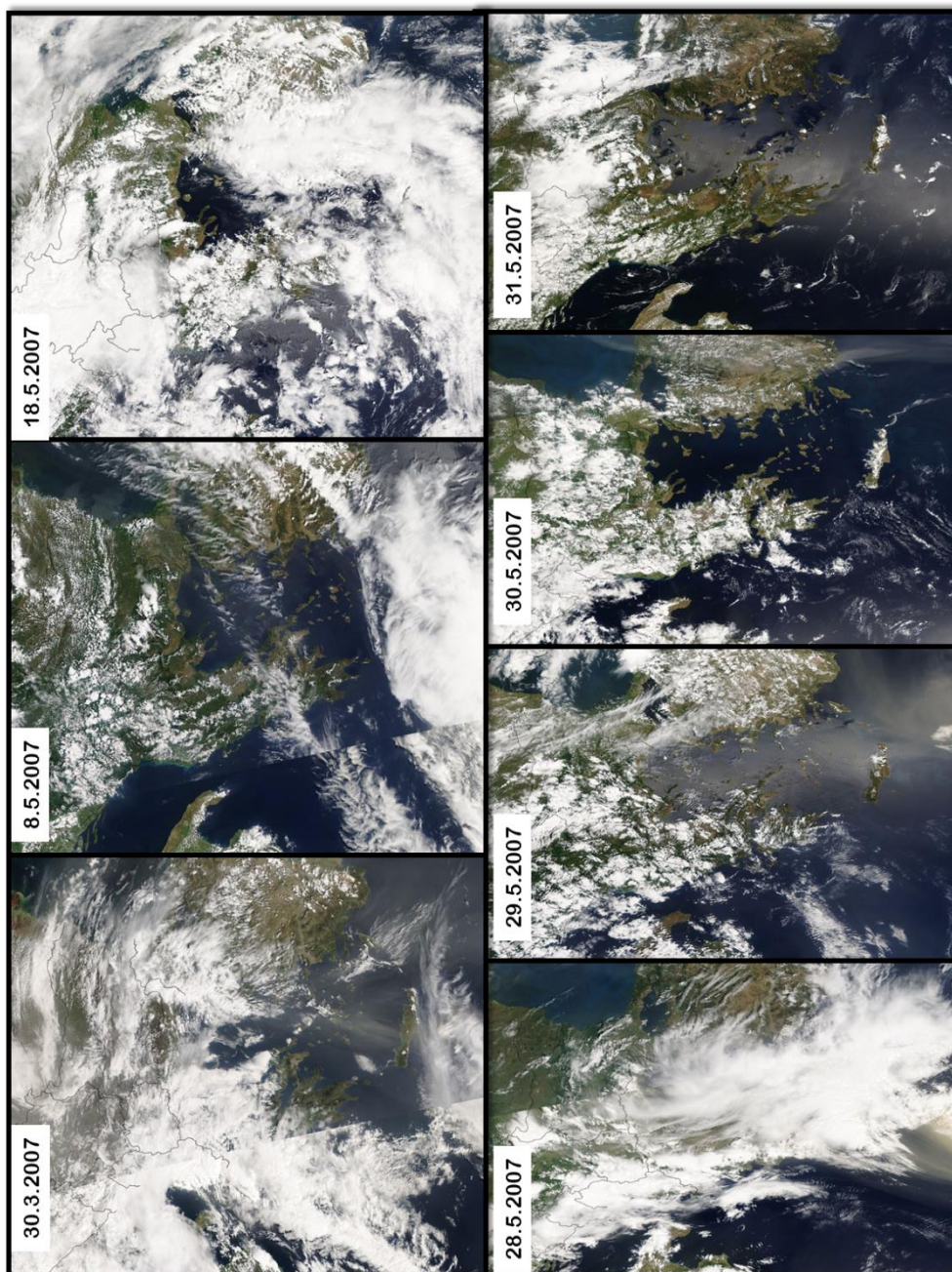
69

Figure 4.2.19 Sattelite pictures for the days, which are identified as dust days, based on AI concentration and Dream model results. Part 2: Episodes in 2007

Table 4.2.3 Mean and median concentrations of species in dust events and non-dust events days

	N	Mean ng m^{-3}	Median ng m^{-3}	N	Mean ng m^{-3}	Median ng m^{-3}	Dust/non-Dust median ratio
		Dust day			**Non-dust day**		
Li	16	1.3 ± 0.8	1.1	317	0.61 ± 0.63	0.41	2.7
Be	16	0.078 ± 0.050	0.072	278	0.039 ± 0.047	0.022	3.3
Na	16	918 ± 842	860	321	531 ± 883	313	2.7
Mg	16	1385 ± 664	1347	322	615 ± 819	274	4.9
Al	16	2012 ± 1087	1695	321	878 ± 1025	500	3.4
P	16	66 ± 53	51	273	36 ± 35	24	2.1
K	16	807 ± 337	682	321	446 ± 469	320	2.1
Ca	16	2669 ± 1067	2339	307	1604 ± 3224	791	3
Ti	16	142 ± 69	114	312	64 ± 76	33	3.5
V	16	6.6 ± 2.7	6	322	3.6 ± 2.7	2.7	2.2
Cr	11	86 ± 173	6	118	30 ± 194	3	2
Mn	16	50 ± 19	43	318	25 ± 30	14	3.1
Fe	16	1484 ± 750	1231	254	678 ± 900	392	3.1
Ni	16	24 ± 54	3	301	8 ± 47	2	1.5
Cu	16	10 ± 4	11	318	10 ± 26	6	1.8
Zn	15	23 ± 16	17	297	60 ± 260	18	0.9
Ge	16	0.062 ± 0.028	0.054	319	0.056 ± 0.044	0.046	1.2
As	16	1.00 ± 0.37	0.96	311	0.99 ± 0.82	0.78	1.2
Se	12	0.38 ± 0.15	0.38	251	0.51 ± 0.54	0.36	1.1
Rb	16	3.6 ± 1.5	3	322	2 ± 2	1.3	2.3
Sr	16	9.0 ± 5.2	7.2	311	4.0 ± 6.7	2.7	2.7
Y	16	0.66 ± 0.47	0.56	320	0.34 ± 0.44	0.18	3.1
Mo	16	1.3 ± 2.5	0.2	321	1.3 ± 6.0	0.2	1
Cd	15	0.47 ± 0.72	0.25	313	0.73 ± 1.07	0.37	0.7
Sn	16	4.6 ± 10.9	1.6	316	2.1 ± 4.2	1	1.6
Sb	16	0.43 ± 0.21	0.37	317	0.63 ± 0.73	0.49	0.8
Cs	16	0.23 ± 0.10	0.2	321	0.15 ± 0.15	0.11	1.8
La	16	1.3 ± 0.9	1.1	319	0.66 ± 0.78	0.4	2.8
Ce	16	2.6 ± 1.7	2.1	316	1.2 ± 1.5	0.7	3
Pr	16	0.27 ± 0.19	0.23	319	0.13 ± 0.18	0.07	3.3
Nd	16	1.0 ± 0.7	0.9	320	0.49 ± 0.63	0.25	3.6
Eu	16	0.047 ± 0.031	0.042	319	0.025 ± 0.033	0.015	2.8
Sm	16	0.21 ± 0.14	0.19	319	0.10 ± 0.13	0.06	3.2
Gd	16	0.23 ± 0.16	0.19	320	0.11 ± 0.14	0.06	3.2

Table 4.2.3cont. Mean and median concentrations of species in dust events and non-dust events days

	N	Dust day Mean	Median	N	Non-dust day Mean	Median	Dust/non-Dust
		$ng\ m^{-3}$	$ng\ m^{-3}$		$ng\ m^{-3}$	$ng\ m^{-3}$	median ratio
Tb	16	0.027 ± 0.019	0.024	313	0.013 ± 0.019	0.007	3.4
Dy	16	0.16 ± 0.11	0.13	306	0.074 ± 0.089	0.044	3
Ho	16	0.027 ± 0.019	0.022	305	0.014 ± 0.016	0.008	2.8
Er	15	0.084 ± 0.054	0.071	238	0.042 ± 0.048	0.025	2.8
Tm	16	0.011 ± 0.008	0.009	315	0.006 ± 0.008	0.003	3
Yb	16	0.075 ± 0.051	0.064	315	0.035 ± 0.040	0.021	3
Lu	16	0.010 ± 0.008	0.008	274	0.005 ± 0.006	0.003	2.7
Hf	16	0.25 ± 0.15	0.24	317	0.11 ± 0.16	0.07	3.4
W	14	0.38 ± 0.44	0.3	178	0.67 ± 2.61	0.11	2.7
Pt	12	0.012 ± 0.025	0.002	113	0.09 ± 0.85	0	
Au	10	0.075 ± 0.081	0.06	134	0.083 ± 0.263	0.037	1.6
Tl	16	0.086 ± 0.055	0.072	322	0.083 ± 0.079	0.069	1
Pb	16	23 ± 23	14	321	32 ± 52	16	0.9
Bi	10	0.12 ± 0.08	0.12	201	0.08 ± 0.10	0.06	2
Th	16	0.46 ± 0.40	0.33	287	0.23 ± 0.28	0.13	2.5
U	16	0.16 ± 0.09	0.13	318	0.074 ± 0.081	0.045	2.9
Cl^-	16	996 ± 1087	584	305	550 ± 738	312	1.9
NO_3^-	16	2924 ± 1443	2944	321	2903 ± 1815	2451	1.2
SO_4^{2-}	16	6028 ± 1421	6195	322	5780 ± 2685	5572	1.1
NH_4^+	16	1614 ± 595	1587	323	1995 ± 1319	1790	0.9
BC	16	611 ± 191	584	318	593 ± 301	536	1.1

Figure 4.2.20 Dust day-to-non-dust day ratios of species

High concentrations of marine elements are also measured on dust event days. The Dust-to-nondust ratio is 2.7 and 1.9 for Na and Cl, respectively. Air mass back trajectories corresponding to all dust events days reported above are from Sahara. Air masses originated from Sahara have to passes over the Mediterranean Sea before they are intercepted at the sampling station; hence they can capture sea salt particles on their way and bring them to the station.
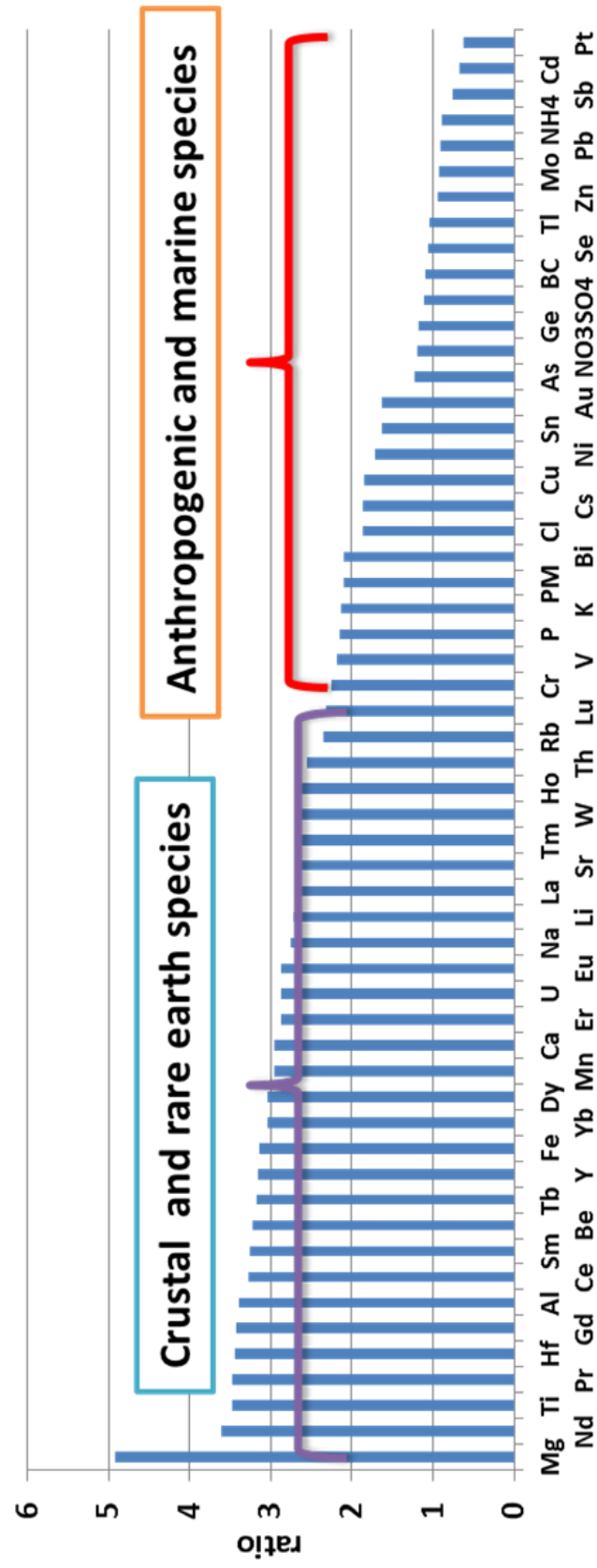
The ratio is below 2.3 and close to 1.0 for most of the elements with mixed and anthropogenic sources. High concentrations of anthropogenic species on dust event days are also reported in the literature (Koçak et al., 2012 and references therein). In these studies enrichment of mixed and anthropogenic species on dust event days is explained by high surface area of dust particles which can act as reaction surface for aerosol species (i.e. oxidation of SO_2 to SO_4^{2-}). Moreover mixing of anthropogenic species with dust particles during the transport of air masses and/or with the local sources are also reported as reasons for observing high anthropogenic species on dust days. Transport of pollution from south (North Africa) had been reported in numerous studies since 80's. There were some events that concentrations of pollution-derived species corresponding to trajectories from South are higher than the concentrations measured when air masses were coming from industrialized Europe particularly southern Europe. However, it is not clear how dust transported from most unindustrialized region of the world bring pollution. Kallos et al. (2007) explained these events by recirculation of pollutants transported from North over the North Africa. Although a number of reasons were presented to explain how south trajectories from time to time bring pollution aerosol to Mediterranean Basin, the reason is still not very clear.

In the current study when there is dust intrusion, air masses pass through Eastern Europe or Western Turkey prior the station, therefore these air masses can bring dust particles and anthropogenic species simultaneously. Lower ratios are also calculated for some anthropogenic species. These are Zn (0.95), Mo (0.92), Pb (0.90), NH_4^+ (0.89), Sb (0.75), Cd (0.68) and Pt (0.63). Lower concentrations of elements in non-dust samples means they are transported from industrialized countries to the north and northwest of the station. This is what we expect to see and anomalous behavior is to measure high concentrations of these elements in samples corresponding to trajectories from south.

Concentration ratios of mineral dust i.e. Ti/Ca, Si/Al, Al/Ca, Ti/Fe, Si/Fe and Ca/Fe have also been used for signature of dust intrusions in the literature (Borbely-Kiss et al., 2004, Borbély-Kiss et al., 1999, Marcazzan et al., 1993). On the days under the influence of mineral dust intrusions, average ratios for Ti/Ca, Al/Ca, Ti/Fe and Ca/Fe are 0.0534, 0.7655, 0.1163 and 2.2157; whilst the ratios on non-dust intrusions days are 0.0428, 0.6754, 0.1275 and 2.306, respectively. Although these ratios may vary from region to region regarding the nature of emission sources and history of the transported air masses (Borbely-Kiss et al., 2004), the ratios found in this study were not different on dust and nondust days.

Some examples of dust events will be discussed to illustrate the dust events occurred during the sampling period. The event on 19 April 2006 is illustrated in Figure 4.2.21. As can be seen from the figures, there is dust loading over the sampling location. DREM8b simulated high dust loading and TOMS-AI obtained from Ozone Monitoring Instrument (OMI) is above 1.0. The corresponding 5 days back trajectories indicates that air masses arriving our station are from south especially over the Mediterranean Sea but not from Sahara. Please note that Sofia (42.67N, 23.30E) vertical dust profile is used as the vertical dust profile forecast in our station because it is the closest city reported by DREAM8b. Vertical dust profile shows that there is very dense dust plume above 2000 m altitude, hence back trajectories arriving the station at higher altitudes are calculated and seen that these are originated from Sahara. The satellite picture also showed that there is dust under clouds, reaching to our sampling point. Therefore we can conclude that on 19 April 2006, Saharan dust is arrived over the station by scavenging of heavy dust particles into the boundary layer from the free troposphere. Contribution of air masses in the free troposphere to dust transport can be comparable to those in the lower troposphere in some regions, as reported by Kalivitis et al. (2007).
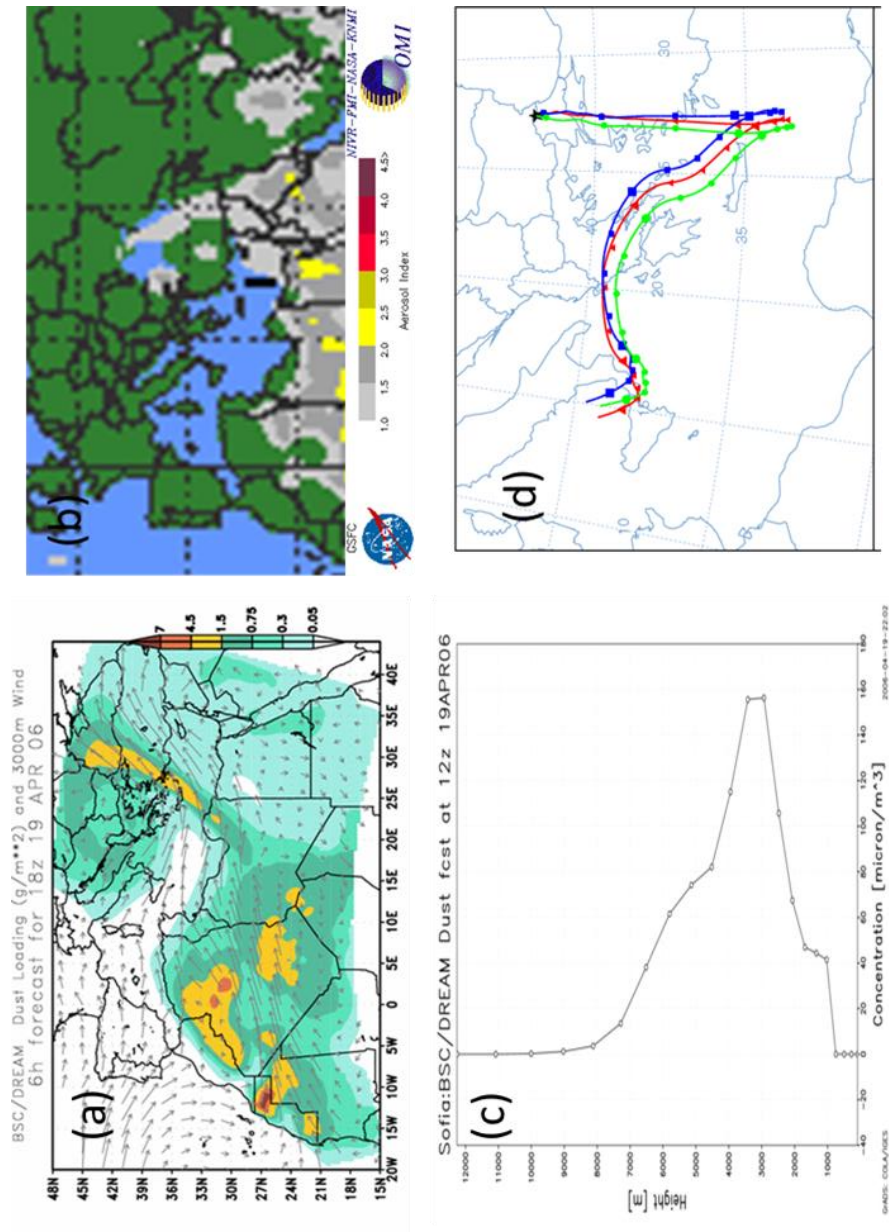
Figure 4.2.21 (a) DREAM8b dust forecast model illustrating the dust in g m^{-2}, (b) TOMS-AI, (c) DREAM8b vertical dust profile forecast, (d) 5-days back trajectories at 100(red), 500 (blue) and 1500 m (green) arrival height on 19 April 2006

Another interesting example showing the influence of Saharan dust arrived by high altitude air masses or in general terms from the free troposphere occurred on 30 March 2007 (Figure 4.2.22). Very high dust loading over the station are simulated by DREAM8b. Back trajectories arrived at 100 m and 500 m has short fetch and originated from northeast, whilst back trajectory at 1500 m has very long fetch and from Sahara. Corresponding vertical profile over Sofia also confirms that there is dust loading above 1000 m altitude. True color picture from satellite TERRA (Figure 4.2.19) clearly demonstrate the presence of Saharan dust at our station. This event was interesting, because it demonstrate that relying on trajectories for identifying dust events is risky. In this case only trajectory with starting altitude at 1500 m reaches to North Africa in 5 days long computation time. If we did not measure this particular trajectory, we would not be able to detect this very strong pulse at our site. It clearly demonstrated that trajectories should be supported by satellite pictures and model estimates, and if possible by chemical data for correct identification of episodes.

A continuous dust event occurred from 6th to 8th May 2007 is illustrated in Figure 4.2.23. Very high concentrations of Al, Fe and Ti are measured on 6th and 7th May 2007, while concentrations are relatively low on 8th May 2007. DREAM8b forecasts on these days are also in line with the observed concentrations. Corresponding back trajectories shows that Saharan dust arrived by high altitude air masses on 6th May and 8th May 2007, whilst dust is deposited by air masses inside the boundary layer on 7th May 2007. There is rain event on 8th May 2007 for 1500 m back trajectory. Relatively low concentrations of Al, Fe and Ti on this day may be explained by scavenging of dust particles by rain prior the station. This pattern can be followed in true color satellite pictures as well. Pictures demonstrate the presence of strong dust pulse on the Mediterranean extending beyond our station at 6th and 7th of May, and then dust is moved away at 8th May.
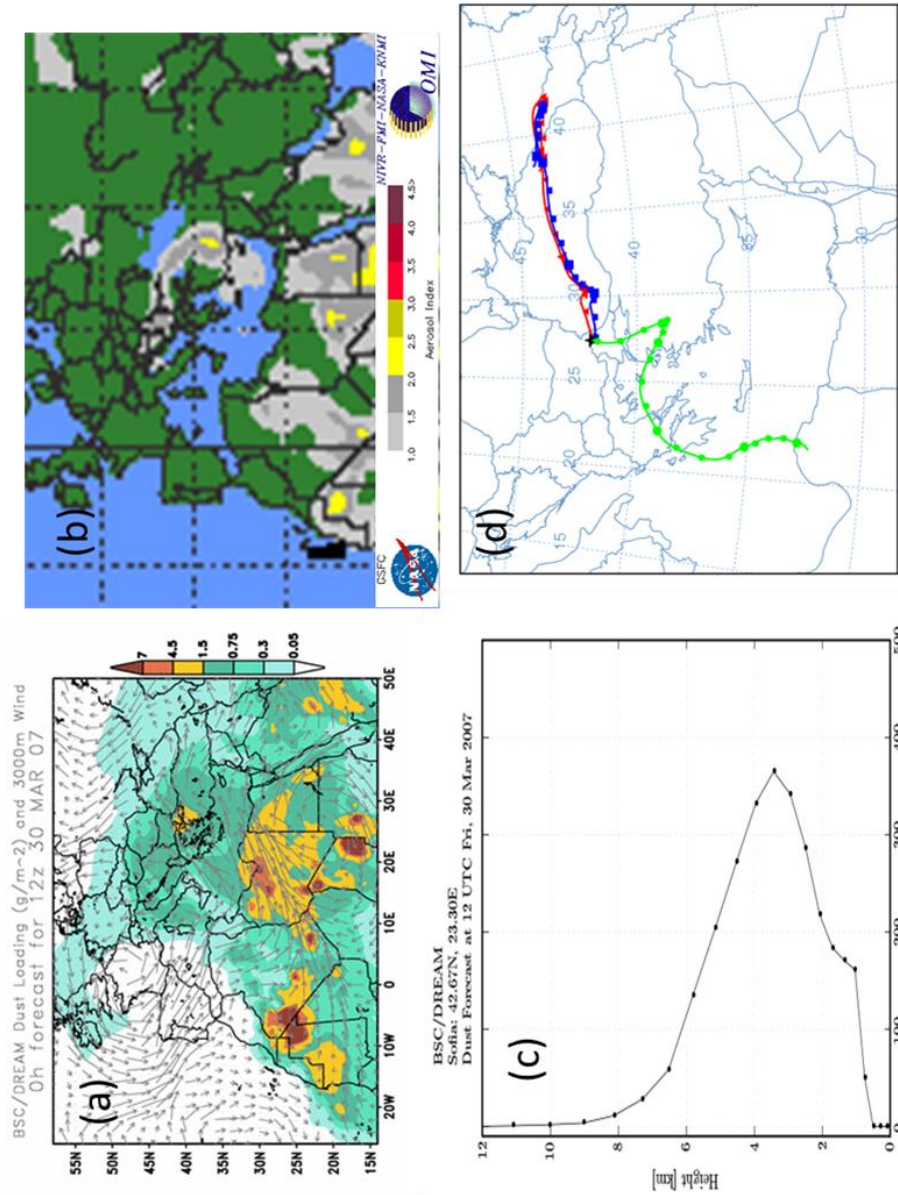
Figure 4.2.22 (a) DREAM8b dust forecast model illustrating the dust in g m^{-2}, (b) TOMS-AI, (c) DREAM8b vertical dust profile forecast, (d) 5-days back trajectories at 100(red), 500 (blue) and 1500 m (green) arrival height on 30 March 2007
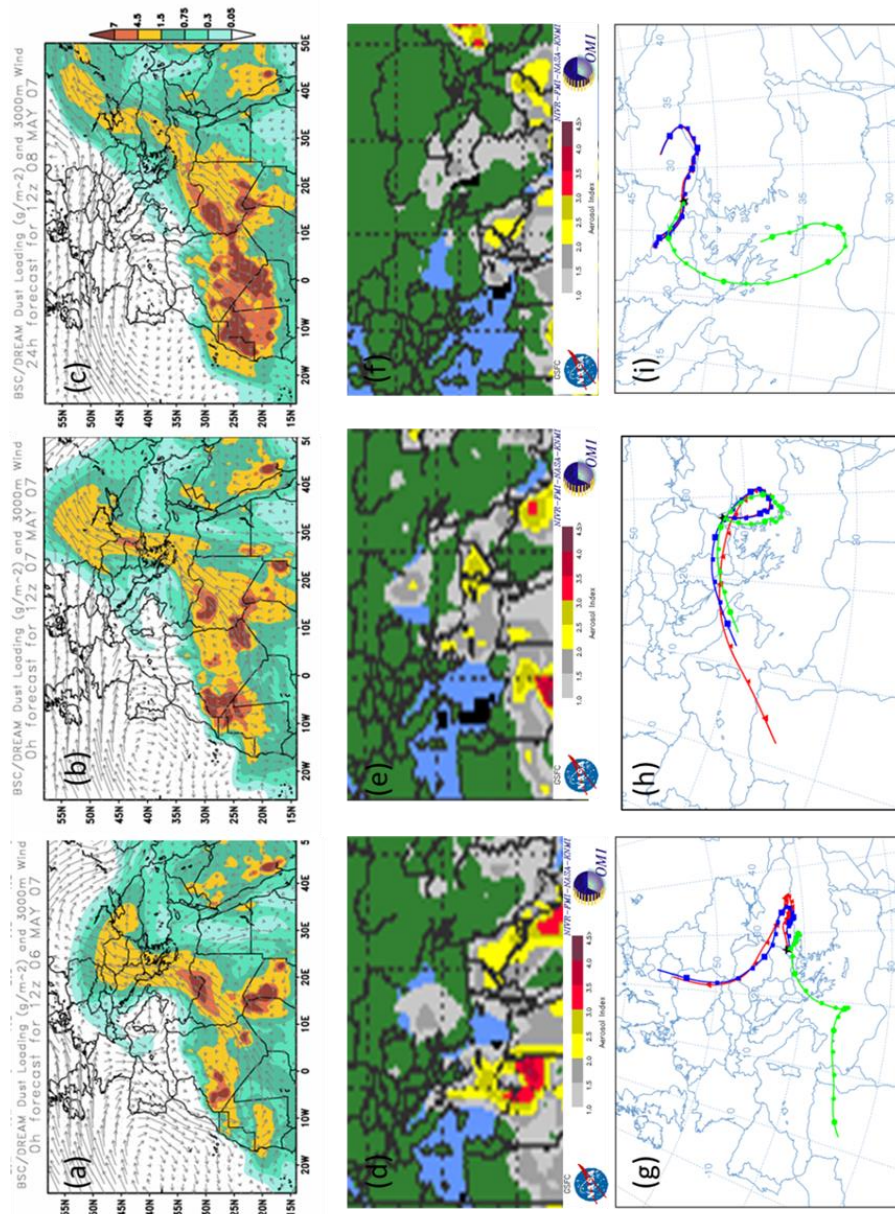
Figure 4.2.23 DREAM8b dust forecast model illustrating the dust in g m^{-2} (a,b,c), TOMS-AI (d,e,f), 5-days back trajectories at 100 (red), 500 (blue) and 1500 m (green) arrival height on 6,7 and 8 May 2007, respectively

4.3. Flow Climatology

Five-day back trajectories starting at the sampling point at 19:00 UTC, at altitudes of 100 m, 500 m and 1500 m were calculated for the years 2006, 2007 and 2008. Assuming all trajectories ending within and below the boundary layer may influence the air quality, a new trajectory group was defined. This trajectory group is called as combined back trajectory and defined as the sum of 100, 500 and 1500 m trajectories. The number of back trajectories calculated for 100, 500 and 1500 m arrival height and combined back trajectories were 1090, 1090, 1089 and 3269, respectively.

MapInfo, a GIS software, was used to determine the frequency of synoptic scale air flow patterns or directions affecting our station. Firstly study domain which extends from Siberia to Middle of Africa in North-South direction (74°N - 14°N) and from West of UK to middle of Asia in East – West direction (20°W - 60°E) is divided into 1°x1° grids, using the MapInfo software. Then the study domain was divided into 8 directional sectors as follows: North (N), North East (NE), East (E), South East (SE), South (S), South West (SW), West (W) and North West (NW). The grid system and sectors that imbedded to the grid system to calculate residence times of trajectories in each wind sector are given in Figure 4.3.1. While N and NW sectors cover nearly all Eastern and Northern European countries, W sector covers Western and Southern European countries. Africa is in between SW and S sector, Asia and Middle East are located between SE and E sector. Russian Federation and half of Ukraine reside in NE sector. The contribution of N and NW sectors to anthropogenic content of aerosols intercepted at the sampling station is expected to be high, because there are numerous anthropogenic sources e.g., power plants and industries within these sectors. Contribution of northern sectors on anthropogenic elements in the Mediterranean basin is well documented (Herut et al., 2001, Lelieveld et al., 2002, Sciare et al., 2003). The probability of anthropogenic contribution is expected to be low for southern sectors as there are few anthropogenic sources. However there are Saharan dust intrusion from southern sectors, especially in spring and autumn months.

Hourly position of a trajectory as longitude, latitude and pressure is called as a "segment". A five-day back trajectory consists of 121 segments. Note that each segment is a 1-hour-long part of the trajectory. The segments residing in each sector was counted and then divided by the total segments in the whole domain during the study period using MapInfo software. This method is called as Residence Time Analysis (RTA) and estimates probability of the overall residence time of air parcels over a given geographic region as they travel toward a receptor (Ashbaugh et al., 1985). This analysis provides information on how much time trajectories spent in each sector before they are intercepted at the station. This means that as the residence time of air parcels in a particular sector increases, the probability of being pollution source for this sector increases because air parcels have enough time to pick up pollution from this sector. This, of course depends also on the availability of pollution sources in that sector. Residence times of air masses in each wind sector are calculated both for different trajectory starting altitudes separately and for combined trajectories. Results are presented in Table 4.3.1 and Figure 4.3.2. Total number of segments during the study period for 100, 500, 1500 m starting altitudes and combined back trajectories are 129848, 128972, 125340 and 384160, respectively. Although the general frequency patterns are the same at all starting altitudes, there are some minor differences, which may be important for pollutant transport to the station. The general patterns that is observed for all trajectory starting altitudes is higher contribution of W, NW, N and NE sectors and particularly low contributions of SE, S and SW sectors. Total contribution of W+NW+N+NE sectors are 74%, 73%, 74% and 74% for 100m, 500 m, 1500 m and combined trajectories, respectively. Total contributions of SE + S + SW sectors, on the other hand, are 16%, 17%, 17%, and 17% for 100, 500, 1500 m starting altitudes and combined trajectories, respectively. The most important difference between starting altitudes is lower contribution of N and NE sectors to trajectories with 1500 m starting altitude and higher contributions of NW and particularly W sectors to this trajectory group. This has significant implications in terms of pollution
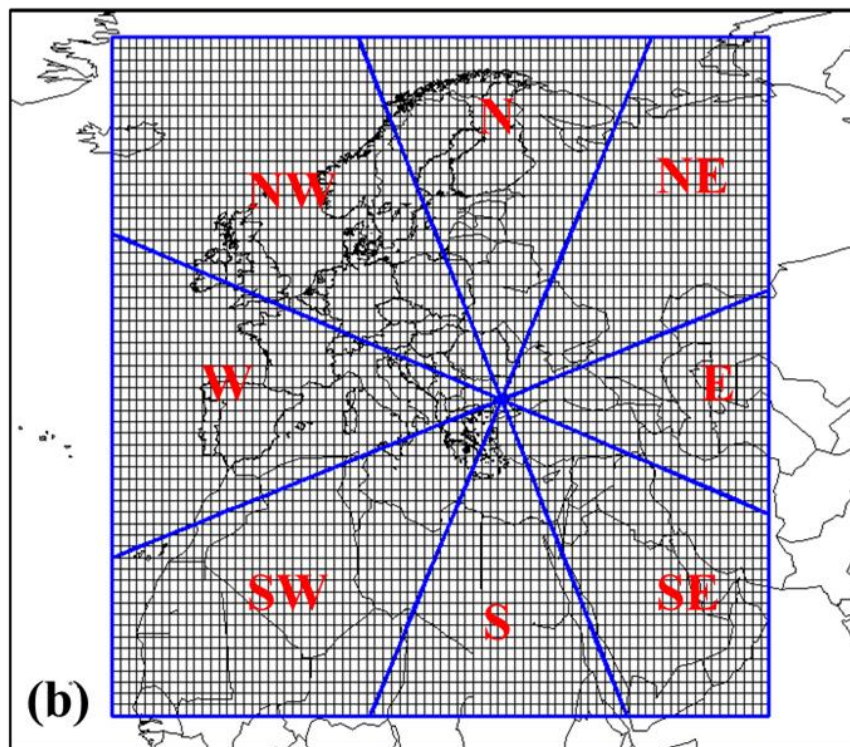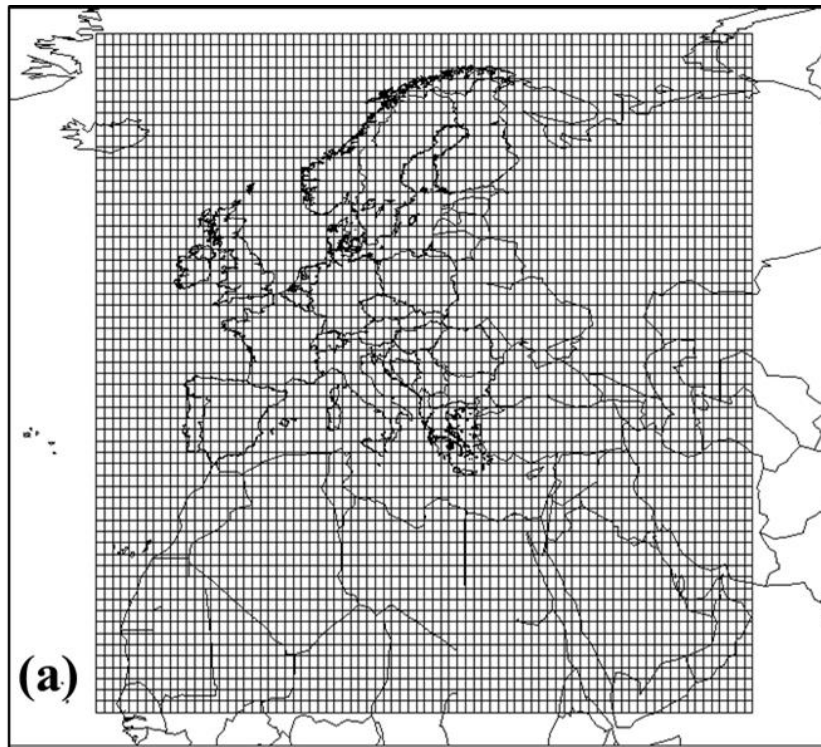
Figure 4.3.1 1°×1° gridded domain (a), assigned sectors for flow climatology (b)

transport to our station and to Turkey in general. Trajectories with 1500 m starting altitude are the ones that travel the longest distance in 5 days. Since W sectors includes Spain, Italy, France, Albania, Croatia and part of Greece, aerosol transport from countries like Spain and France are more likely than aerosol transport from Germany and other European countries, which are equally far from our station. East sector accounts nearly 10% of total air flows for all starting heights. Although the frequency of flows from E sector is low compared to northern sectors (nearly 50%), İstanbul, Kocaeli and Bursa which are the most industrialized Turkish cities are located in E sector. Air parcels from these cities travel short distance to arrive sampling station, therefore they have enough time to pick up pollutants and they may bring pollutants without scavenging mechanism. Episodic increases in concentrations of pollution derived elements are expected when trajectories come from E sector.

Table 4.3.1 Annual frequency of flow from each wind sector for 100, 500, 1500 m arrival height back trajectories and combined back trajectories*

wind sector	100 m	500 m	1500 m	Combined
N	19	18	15	17
NE	22	21	14	19
E	11	11	10	10
SE	3	4	3	3
S	7	6	4	6
SW	6	7	10	8
W	15	15	24	18
NW	18	19	21	19

*Numbers in the table are percent contribution of each sector to total residence time of air masses arriving to sampling point in the course of this study
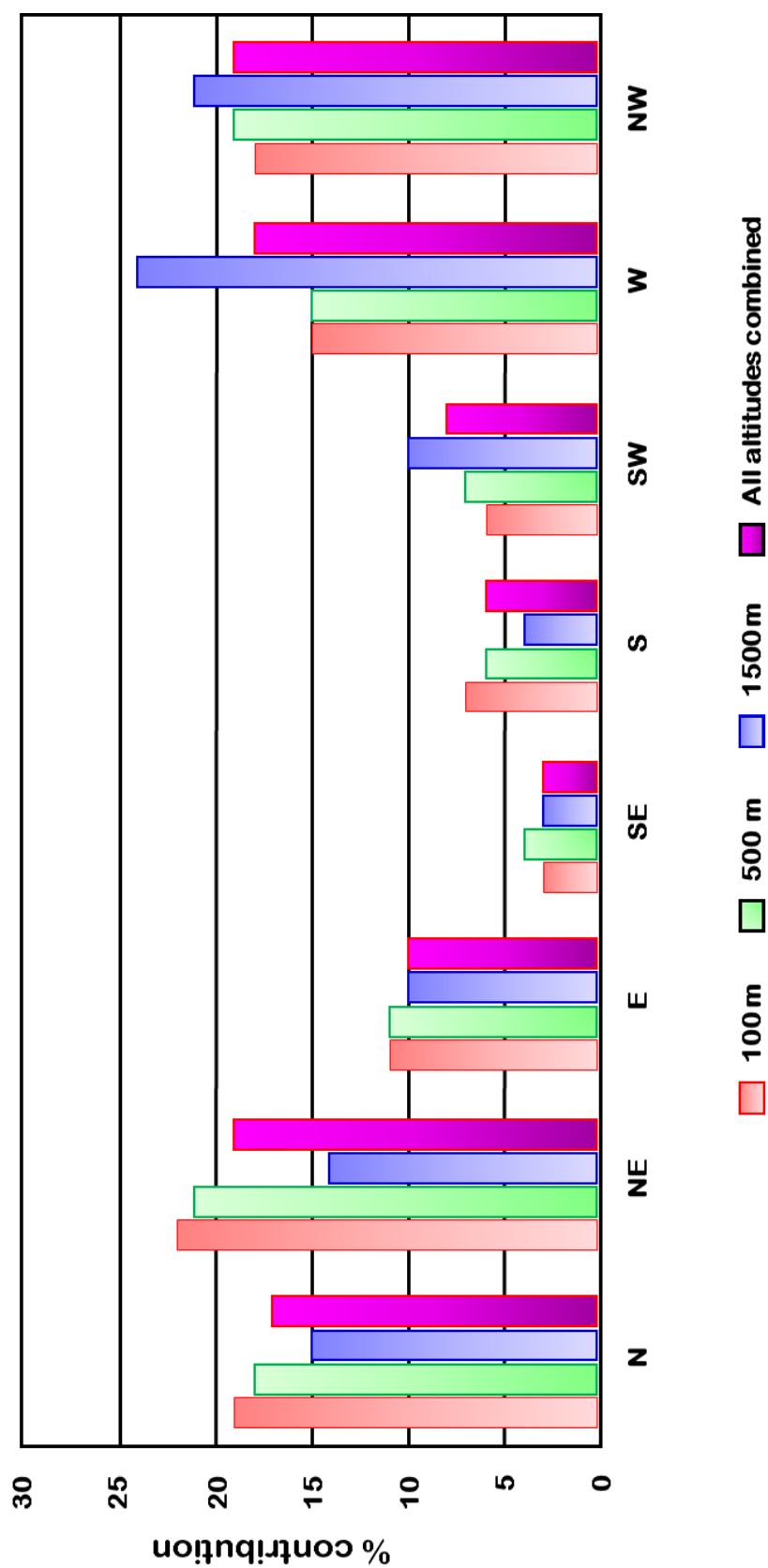
Figure 4.3.2 Contribution of wind sectors to residence time of trajectories arriwing to the station

Air flow may change seasonally, with the change of upper atmospheric meteorology, such as relocation of high and low pressure systems in summer and winter seasons. Therefore seasonal variation of directional frequencies is also investigated and flow patterns calculated for summer and winter seasons are presented in Figure 4.3.3. In summer season air parcels arriving at the sampling station spent 80% of its total time in W, NW, N and NE sectors, while this percentage decreased to 65% in winter due to increase of air flows in southerly sectors. The difference between summer and winter air flows is illustrated in Figure 4.3.4. To create this thematic map, total number of segments in each grid cell is calculated for summer and winter season, and then the difference between them is calculated for each grid cell. It is clearly seen in Figure 4.3.4 that emissions from Eastern Europe countries, especially Central Russia, Ukraine, Bulgaria and Romania, reach to the sampling site more frequently in summer. However air flows are more frequent in West and NW sectors in winter season, therefore the likelihood of emissions from Southern and Western Europe countries reaching to the sampling station is high in winter season. Furthermore Turkey's own emissions especially from Marmara Region, Aegean Region and Central Anatolia reach more frequently in winter.

Upper atmospheric flow patterns discussed in previous paragraphs are similar to previous studies (Doğan and Tuncel, 2005, Munzur and Tuncel, 2008, Öztürk and Tuncel, 2009, Yıkmaz and Tuncel, 2010) performed at the Eastern Mediterranean basin. A similar pattern observed in good number of widely dispersed locations show that this is a regionally representative flow pattern and suggest transport of pollutants from North of the basin and Europe for the whole region including Eastern Mediterranean basin, Middle East, Black Sea and Aegean regions.
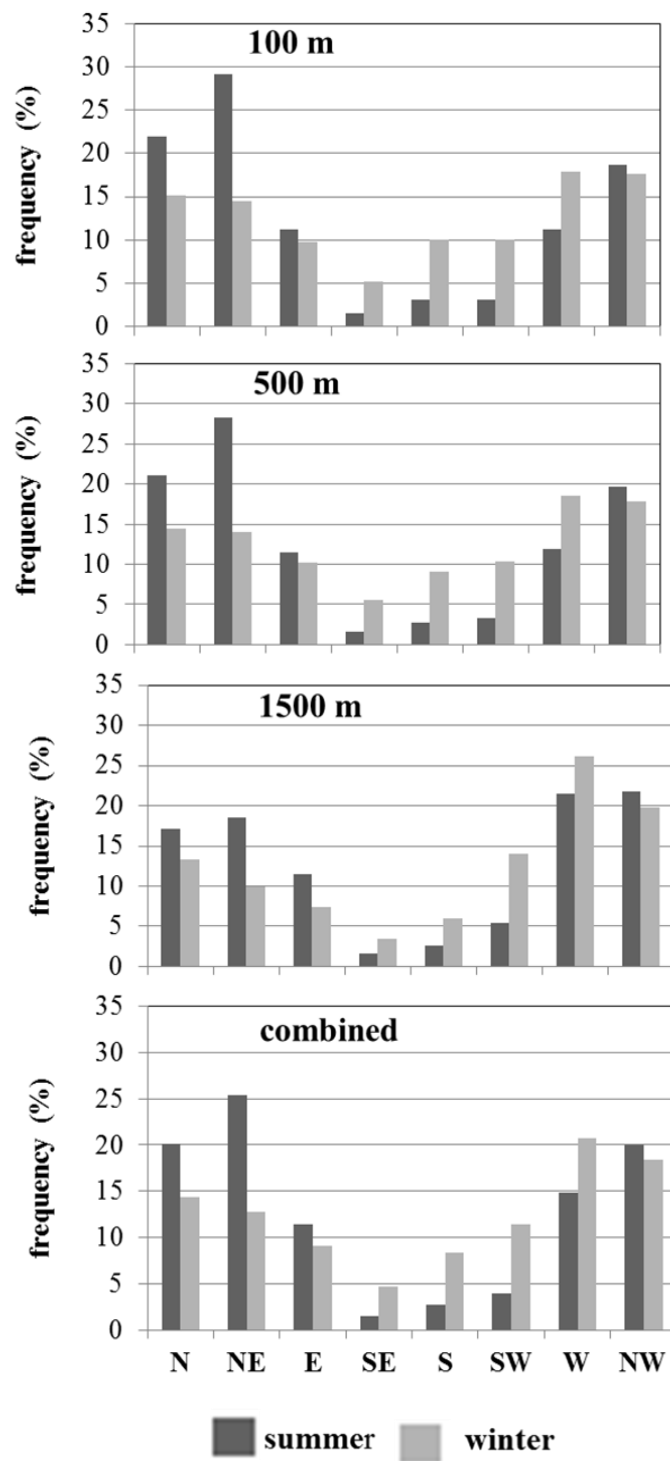
Figure 4.3.3 Seasonal variation of directional frequencies
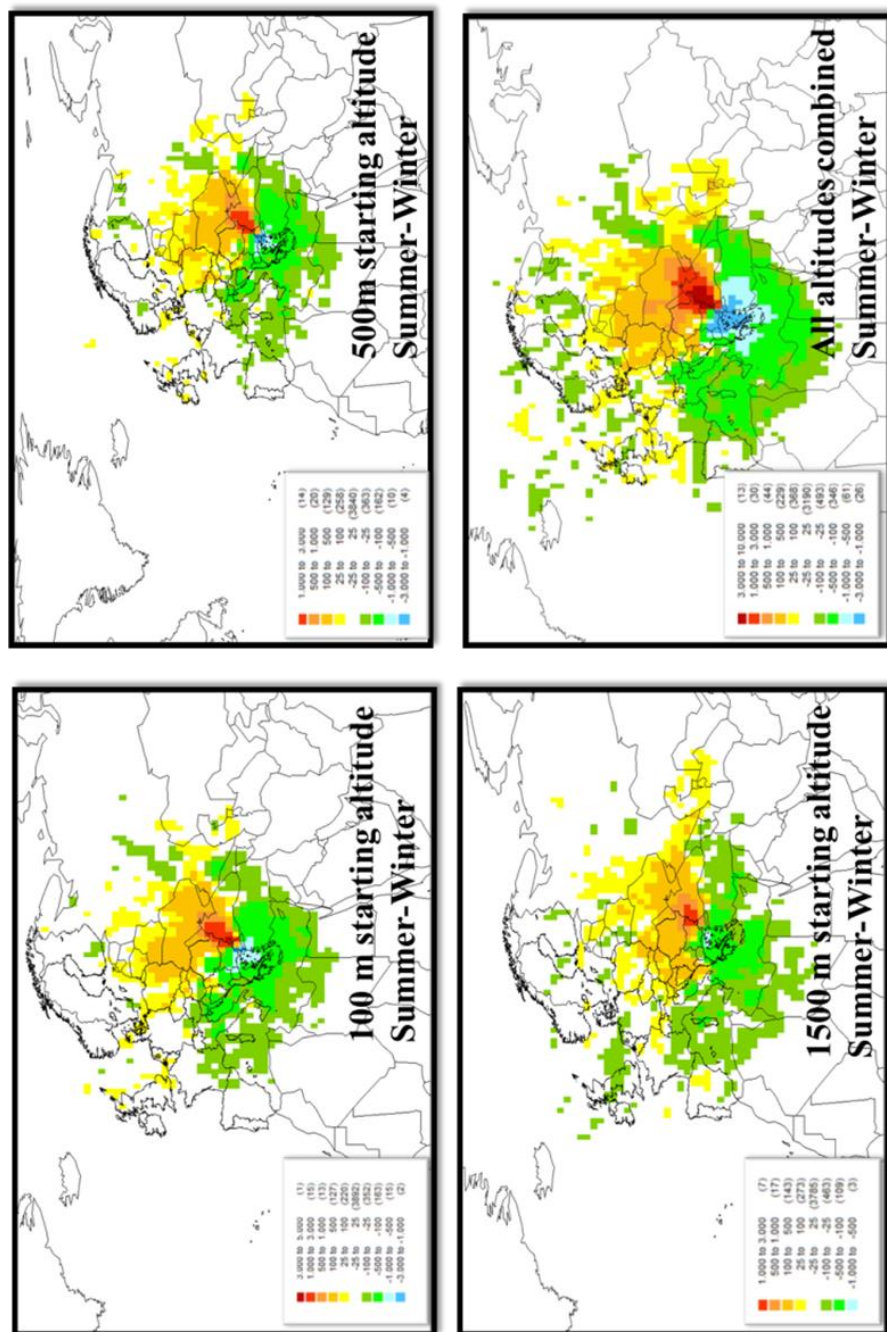
Figure 4.3.4 Differences between summer and winter residence times of air masses arriving at the sampling point (a) air masses with starting altitude of 100 m, (b) air masses with 500 m starting altitude, (c) air masses with 1500 m starting altitude and (d) all trajectory segments

4.3.1. **Cluster Analysis**

Cluster Analysis (CA) is a multivariate statistical technique that "combines the flow climatology and pollutant transport pathways with particle or gas measurements at a sampling station" (Wang et al., 2009). Cluster analysis is used to determine the atmospheric transport pattern and to examine the influence of different atmospheric transport pattern on observed chemical composition at the receptor. Many researchers have used CA to examine the relation between synoptic scale transport patterns and atmospheric pollution (Cape et al., 2000, Borge et al., 2007). The criterion used in CA is to split a large trajectory data set into a number of groups based on trajectory transport speed and direction, simultaneously (Abdalmogith and Harrison, 2005, Brankov et al., 1998). The produced groups in CA are called clusters. Members of each cluster have similar trajectory length and curvature, while distinct clusters represent different synoptic regimes. When coupled with aerosol chemical composition, CA can be a good tool to examine the effect of synoptic scale atmospheric patterns on observed chemical composition; hence will aid to establish source-receptor relationship. The uncertainty in individual trajectory is high and increases with the total travel distance (Stohl and Koffi, 1998). In CA large sets of trajectories are used, therefore the accuracy of trajectory analysis is improved.

In this study TrajStat software (Wang et al., 2009) is used for CA. Although there are several algorithms for CA, Ward's hierarchical method (Ward, 1963) and 2D Euclidean distance are used in TrajStat. Two dimensional Euclidean distance using longitude and latitude coordinates between trajectories are calculated, and then nearest trajectories are combined to form clusters. In some studies 3D Euclidean distance between trajectories were calculated by including pressure or elevation of trajectories (Cape et al., 2000, Taubman et al., 2006). However Owen (2003) indicated that adding pressure or elevation coordinate have little impact in produced clusters and do not change the result and increase the computation time and cost.

Residence Time Analysis, which was discussed in previous section, showed that flow climatology of the region is affected by seasonal variation of meteorology (see Section 4.3); because of this season dependent variability, clusters were calculated for each season. Total number of back trajectories in CA data sets is given in Table 4.3.2 and these trajectories are plotted separately for each starting altitude in Figure 4.3.5. In winter season air flow paths are longer than summer for all arrival height trajectories and air flows paths become longer as the arriving altitude increases. Trajectories at higher altitudes have high speed, therefore have long flow path, because they are less influenced from the friction of earth. Another point that worth noting is that air flows from westerly direction is more frequent for 1500 m arrival height trajectories in both seasons.

Table 4.3.2 Trajectory data set used for CA

Back trajectory	Summer[*]	Winter[*]
100 m	549	541
500 m	541	541
1500 m	549	540
Combined	1642	1622

[*]number of back trajectories
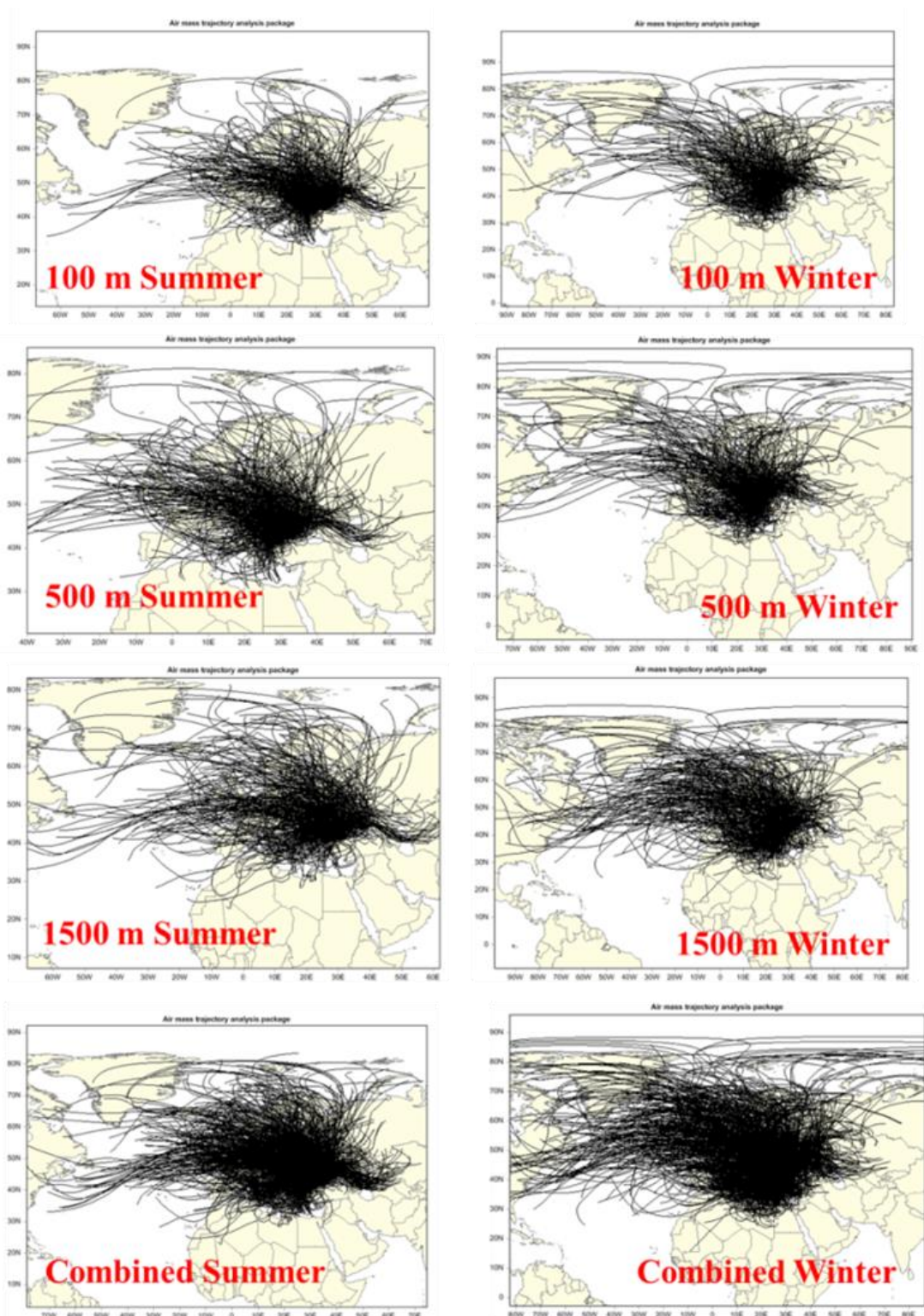
Figure 4.3.5 Compilation of trajectories for each starting altitude

Different number of clusters (maximum 20) were calculated and inspected. Unfortunately there is no accepted criterion to select optimum number of clusters. Therefore a procedure developed by Dorling et al. (1992) was adopted to determine optimal number of clusters. According to this procedure percent change in total root-mean-square-deviation (TRMSD) between clusters is used. A threshold value of 5% change in TRMSD is assumed to be significantly large and constituted the criterion for merging of different clusters (Dorling et al., 1992).

Total root-mean-square-deviation for different number of clusters was calculated using SPSS software. The plot of percent change in TRMSD against number of clusters is depicted in Figure 4.3.6. This figure shows that when decreasing cluster number from 6 to 5, percent change in TRMSD exceeds 5% threshold value (green line) for 1500 m arrival height trajectory data set. This indicates that if cluster number is decreased from n to n-1, trajectories having different speed and/or curvature is classified in the same group as if they were similar. Therefore when examining the clusters, we kept this criterion in mind and finally 6 clusters were selected as the optimum cluster number for all analyses. It should also be noted that as the number of clusters increase number of data points associated with each cluster decrease, which in turn increase the uncertainty of conclusions reached. Investigation of clusters at different runs demonstrated that after six clusters, increasing number of clusters splits clusters based on length only, which does not add much to information value. Based on all these arguments we decided to use 6 clusters to explain transport-related variations in data set. Clusters formed at 100 m and 500 m starting altitudes were identical, that is why only runs performed with 500 and 1500 m starting altitudes are shown in Figure 4.3.6.
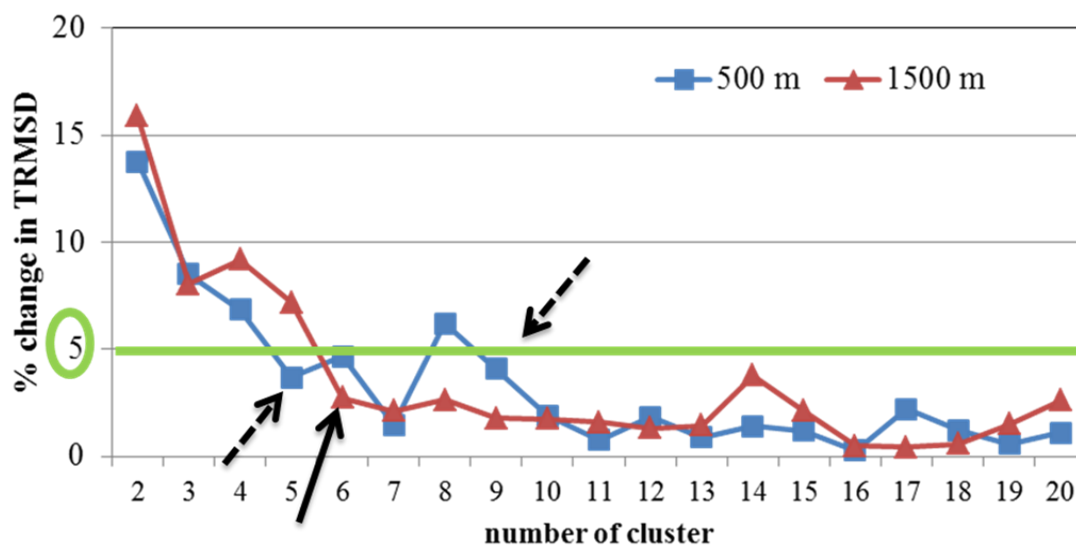
Figure 4.3.6 Selection of optimum number of clusters for 500 and 1500 m arrival height trajectories

Cluster centroids generated for 500 m and 1500 m arrival height back trajectories are given in Figure 4.3.7(a) and (b), respectively. As can be seen from the figures, calculated cluster centroids for all starting altitudes are quite similar in direction and curvature. A receptor site can be influenced from all trajectories arriving at within the boundary layer. Boundary layer can change from season to season and even hour to hour, i.e. day and night. The boundary layer height for our sampling site varies from 1800 m to 80 m. Therefore, combined trajectories (sum of 100, 500 and 1500 m trajectories) could be more representative for this study. That is why we used combined trajectories and 5 clusters calculated for them in interpretation of transport of elements to the region.

CA is applied for combined trajectory data set and 5 clusters are generated (Figure 4.3.7(c)). Back trajectories corresponding to cluster centroids for the combined data set is given in Figure 4.3.8. Cluster 1, accounted for 37% of all trajectories. It has the highest percentage and shows the shortest length among the clusters. Air flows from Eastern Europe especially from Bulgaria and Romania and from Western Turkey are represented in Cluster 1. Consequently, this group of trajectories represents slow moving (SM) air masses from all directions and is important as the samples corresponding to these trajectories represent contribution of relatively local sources on measured concentrations of pollutants at the Northwestern Turkey.

Trajectories that are associated with Cluster 2 and Cluster 4 comes nearly from the same direction (same travel path) but having different speeds, and hence different lengths. These trajectories are from Atlantic Ocean which then passes through north-western Europe and then Balkans and accounts 31% of total flow between the years 2006 and 2008. Cluster 4 (12%), represents the fastest air movements (FM) hence longest fetch from Canada and Atlantic Ocean then pass over UK (northern Europe), Germany (Western Europe) and Balkans. Cluster 2 (20%) shows medium fetch (MM) mainly from Atlantic Ocean and crossed over northern Europe and Balkans. Although similar to Clusters 2 and 4, Cluster 3, which accounts for approximately 14% of all trajectories exhibits moderate fetch and represents the back trajectories mainly from northern Europe countries.

Cluster 5 represents 18% of all trajectories and exhibits a long and medium fetch from Russia and passing over Ukraine and then the Black Sea. Trajectories from Eastern Turkey and from Asia are also retained in Cluster 5. Therefore Cluster 5 indicates long fetch from Eastern Europe passing over the Black Sea, and from Asia and flow through the Black Sea, and from Asia and crossed over Turkey, before they all are intercepted at our station.

In the previous studies cyclones in the Northwestern Turkey were classified according to back trajectories. Akkoyunlu and Tayanc (2003) classified cyclonic air flows into two groups. First group was represented by air movements from Eastern Europe, especially from Russia, and passing over the Black Sea which is similar to Cluster 5 in the current study. Second group was represented by air flows from Mediterranean Sea passing over Italy, Germany and Aegean Sea which corresponds to Cluster 1 in the current study.

Okay et al. (2002) classified cyclones into four groups. In his study air movements from Mediterranean and Northern Africa was separated into two groups, which are combined in Cluster 1 in the current study. Air flows from northwestern and central parts of Europe and Balkans were classified into a single group. In the current study clusters were based on not only trajectory direction, but also on the air mass speed. This allowed us to separate trajectories from northwestern Europe, central Europe and Balkans into 3 different clusters (Cluster 2, 3 and 4) with each having similar direction but different length.

Calculating clusters is informative as they provide information on transport patterns of atmospheric constituents to the station. What is more important is to relate these clusters to concentration data, because differences in concentrations or enrichments of elements between different clusters can be very informative on how these elements are arriving to our sampling point. Median concentrations of elements in different clusters are presented in Table 4.3.3. Cluster-to-cluster variations of median concentrations of selected elements with crustal, anthropogenic and mixed sources are also plotted in Figure 4.3.9.
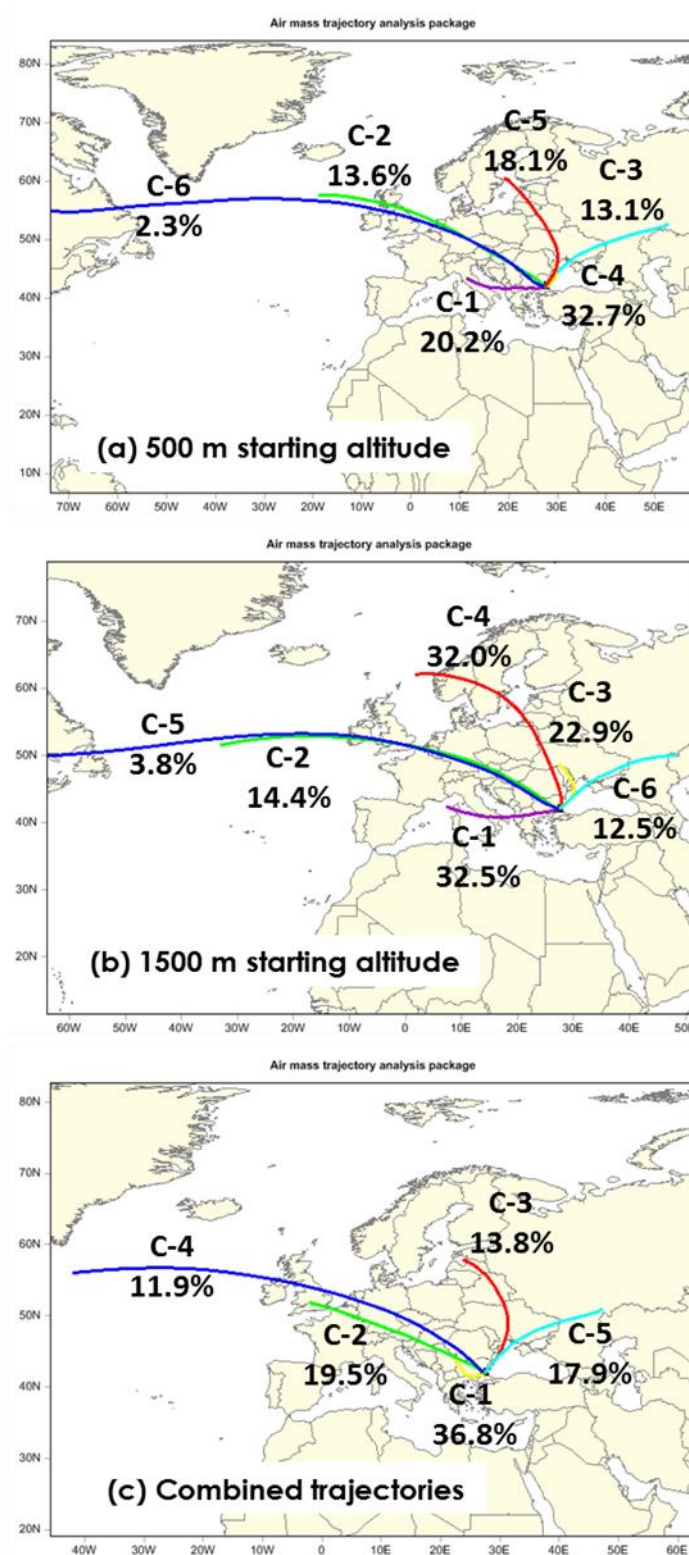
Figure 4.3.7 Cluster centroids calculated for trajectories with 500 m (a) and 1500 m (b) starting altitudes and for combined trajectories (c) between years 2006-2008
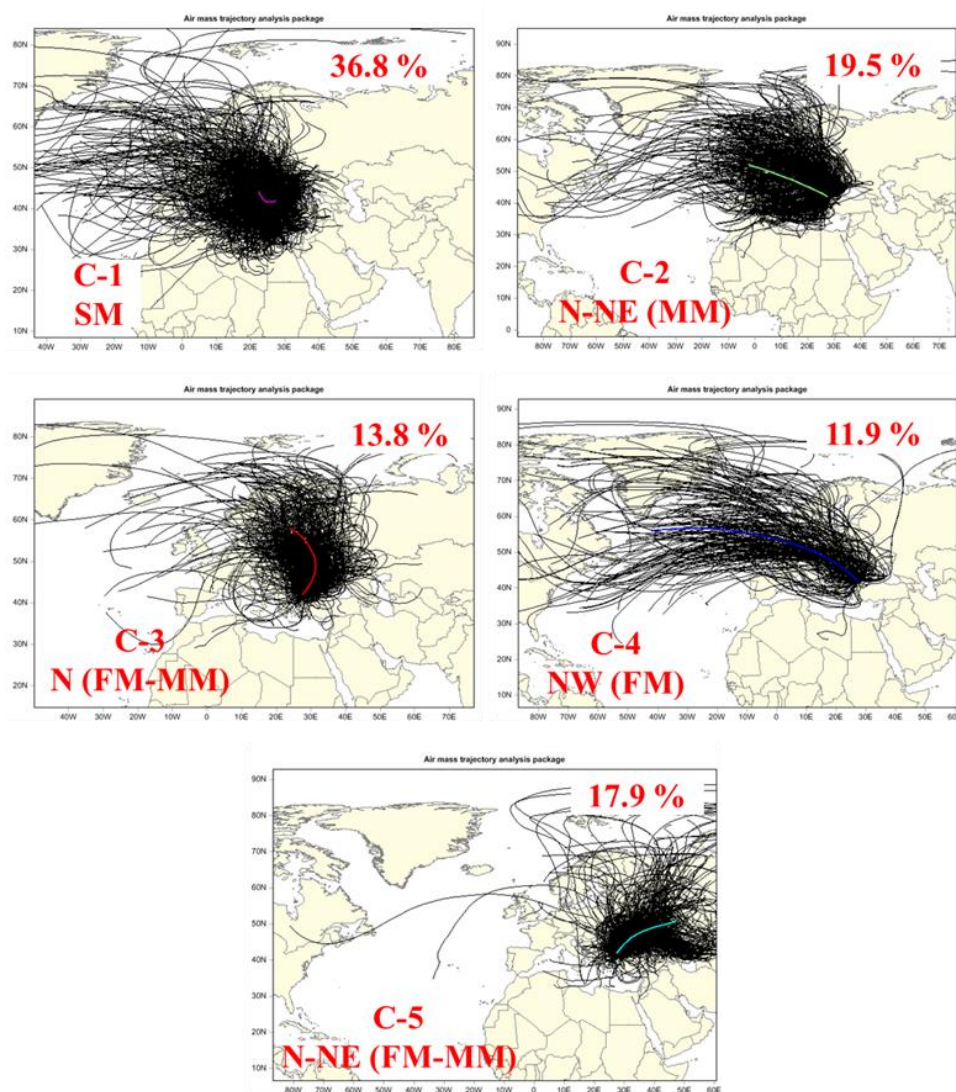
Figure 4.3.8 Corresponding back trajectories for each cluster center of combined data set

Table 4.3.3 Median concentrations of measured species (ng m^{-3}) and K-W test result

	C-1	C-2	C-3	C-4	C-5	K_W test
PM	56615	46856	44005	68545	49307	rejected
SO_4^{2-}	6461	5180	5145	3761	5622	rejected
NO_3^-	2687	2360	2203	2617	2410	rejected
NH_4^+	1994	1689	1747	1342	1848	rejected
Cl^-	295	285	255	393	327	retained
BC	551	544	559	571	526	retained
Na	289	303	262	493	343	rejected
Li	0.41	0.42	0.39	0.61	0.5	rejected
Be	0.02	0.03	0.02	0.04	0.02	rejected
Mg	313	461	244	772	250	rejected
Al	501	621	471	878	580	rejected
P	25	22	19	46	22	rejected
K	301	318	355	396	372	rejected
Ca	930	993	689	1801	737	rejected
Ti	32	50	35	79	44	rejected
V	3.25	2.93	2.59	3.53	2.62	rejected
Mn	14	17	16	24	19	rejected
Fe	384	375	422	668	404	rejected
Ni	2.3	2.2	1.6	2.2	1.8	retained
Cu	5.8	5.6	5.9	8.2	5.8	retained
Zn	19	15	16	20	19	retained
Ge	0.04	0.05	0.04	0.06	0.05	rejected
As	0.85	0.78	0.52	0.97	0.76	rejected
Se	0.38	0.37	0.32	0.46	0.32	rejected
Rb	1.08	1.44	1.38	2.05	1.75	rejected
Sr	2.8	2.44	2.44	4.24	2.9	rejected
Y	0.19	0.2	0.18	0.35	0.18	rejected
Mo	0.19	0.16	0.2	0.18	0.24	rejected
Cd	0.37	0.24	0.35	0.42	0.43	rejected
Sn	1.1	1.2	0.71	1.15	0.74	rejected
Sb	0.49	0.44	0.5	0.39	0.53	rejected
Cs	0.1	0.1	0.13	0.15	0.13	rejected
La	0.4	0.48	0.38	0.57	0.47	rejected
Ce	0.65	0.74	0.63	1.17	0.69	rejected
Pr	0.07	0.09	0.07	0.13	0.07	rejected

Table 4.3.3cont. Median concentrations of measured species (ng m^{-3}) and K-W test result

	C-1	C-2	C-3	C-4	C-5	K_W test
Nd	0.25	0.32	0.25	0.48	0.26	rejected
Sm	0.06	0.07	0.06	0.11	0.06	retained
Eu	0.01	0.02	0.01	0.02	0.02	retained
Gd	0.06	0.07	0.05	0.12	0.06	rejected
Tb	0.01	0.01	0.008	0.012	0.008	rejected
Dy	0.04	0.05	0.04	0.07	0.05	retained
Ho	0.01	0.01	0.009	0.013	0.009	rejected
Er	0.02	0.03	0.02	0.06	0.03	rejected
Tm	0.002	0.002	0.002	0.006	0.002	rejected
Yb	0.02	0.03	0.02	0.04	0.02	retained
Lu	0.002	0.003	0.003	0.008	0.003	rejected
Hf	0.07	0.08	0.08	0.1	0.09	retained
Tl	0.06	0.06	0.08	0.07	0.08	rejected
Pb	18	12	14	18	16	rejected
Th	0.15	0.16	0.12	0.23	0.11	rejected
U	0.05	0.05	0.05	0.08	0.05	rejected

Kruskal Wallis (K-W) test at 95% confidence level (criteria is $\alpha < 0.05$ indicates that median concentrations of that element in different clusters are different) was used to examine if median concentrations of elements are different between different cluster pairs. Kruskal Wallis test is a non-parametric tool for testing the equality of medians among groups, in this case median concentrations of elements in different clusters. The null hypothesis that observed element or ion has been drawn from the same clusters was tested. If the null hypothesis was rejected ($\alpha < 0.05$), that means there is a statistically significant difference between concentration of that element between clusters. Results of the K-W test are included in Table 4.3.3. Data in the Table 4.3.3 points that there are statistically significant differences between median concentrations of elements and ions in clusters with few exceptions.

All crustal elements except for Hf ($\alpha=0.460$), Eu ($\alpha=0.051$), Dy ($\alpha=0.059$), Yb ($\alpha=0.061$) and Sm ($\alpha=0.093$) showed significant differences between clusters. The highest concentrations of crustal elements were observed in Cluster 4. In fact this is not an expected result, because Cluster 4 represents the fastest air movements from north west. Crustal species are expected to be highest in Cluster 1 as trajectories reside in Cluster 1 are slow moving and from all directions. Furthermore there are no trajectories in Cluster 4 that can be associated with direct Saharan dust transport. However corresponding back trajectories in Cluster 4 can be linked to the transport from arid regions in the Mediterranean basin, such as Spain and Northern parts of Italy. Therefore back trajectories originated from and/or passing over these regions may bring dust, but not necessarily Saharan dust to our station.

Enrichment factors of representative crustal species are depicted in Figure 4.3.10(a). These elements are not enriched in any of the clusters as expected. Their enrichment factors vary between 1 and 2, but more or less the same in all clusters. This is not surprising, because although concentrations of these elements are high in Cluster 4, since concentrations of all crustal elements are high in that cluster, enrichment factors, which bases on ratio of these elements to Al do not change.
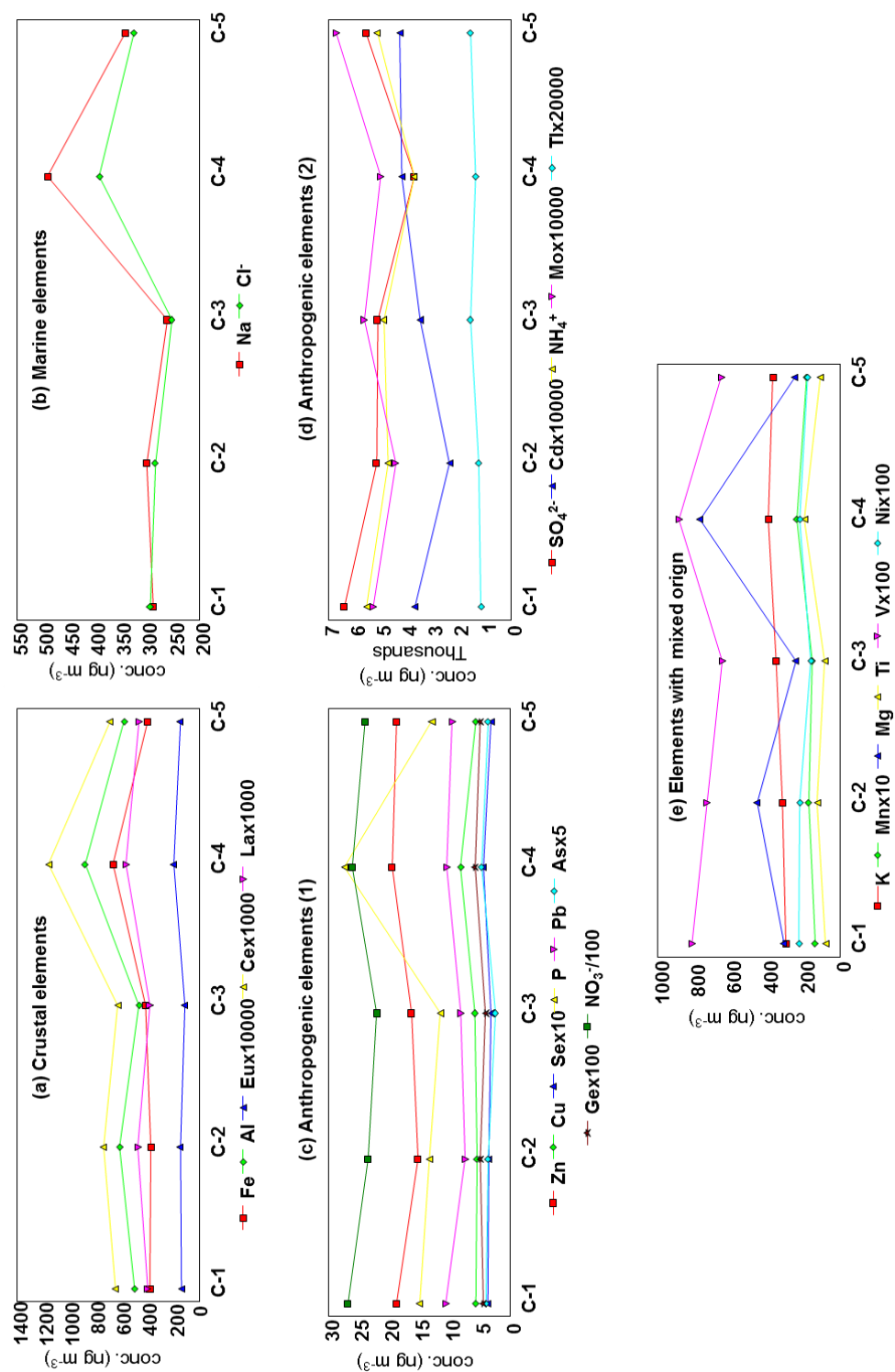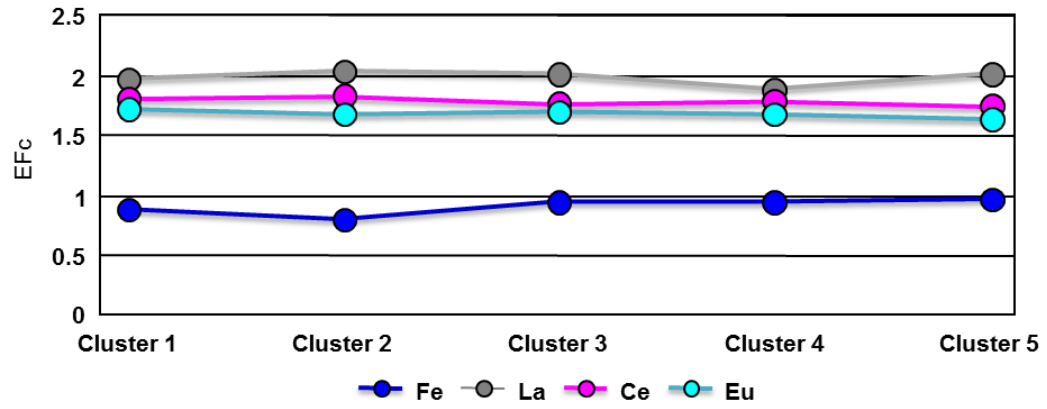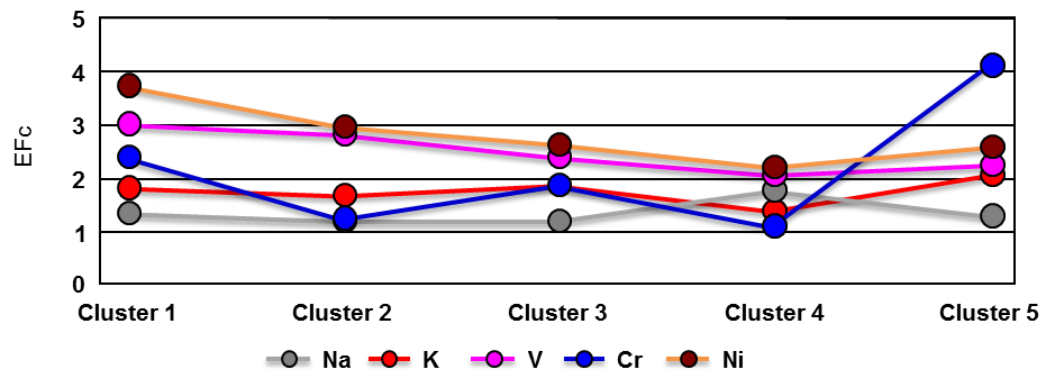
Figure 4.3.9 Median concentrations of elements with crustal (a), marine (b), anthropogenic (c-d) and mixed sources (e) in Clusters

(a) Crustal elements

(b) Elements with mixed sources
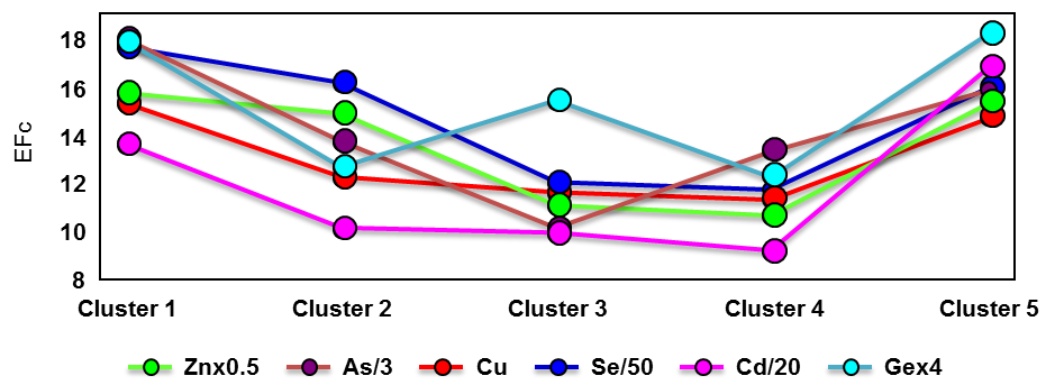
(c) Anthropogenic elements

Figure 4.3.10 Crustal enrichment factors of elements in Clusters

Concentrations of Na and Cl$^-$, which are the elements associated with sea salt are shown in Figure 4.3.9(b). Cluster-to-cluster variations in concentrations of these two elements are very similar to the variations observed in crustal elements, with higher concentrations in Cluster 4. For Na, at least some of this pattern can be attributed to crustal contribution on measured Na concentrations. However, Cl$^-$ concentrations are not affected significantly from the presence of soil aerosols in the atmosphere. Similarity in patterns shown by Na and Cl$^-$ implies that observed pattern, with higher concentrations of these elements in Cluster 4 is not due to soil contribution on their concentrations, but shows that samples included in this cluster group are affected from marine aerosol. Crustal enrichment factor of Na is depicted in Figure 4.3.10(b), together with enrichment factor of elements with mixed sources. Enrichment factor of Cl$^-$ is not shown in the figure, because it was exactly the same with that of Na. Sodium is not enriched in any cluster. It is slightly more enriched in Cluster 4, but the difference is very small and not statistically significant.

Variation in median concentrations of pollution-derived elements from one cluster to another is given in Figure 4.3.9 (c) and (d). Two different figures were prepared for anthropogenic elements, because they portrayed two different behaviors. Cluster-to-cluster variation in median concentrations of some of the anthropogenic elements, including Zn, Cu, Se, P, Pb, As and Ge were very similar to the pattern observed in crustal and marine elements. These elements have higher concentrations in Cluster 4 and observed differences are statistically significant as can be seen in column of the Table 4.3.3. They all have higher concentrations in Cluster 4. Concentrations of Zn and Se are also high in Cluster 1, but other elements in this group (Cu, Se, Ge and P) do not have high concentrations in Cluster 1. Observing high concentrations of these elements in Cluster 4 and also in Cluster 1 are not as surprising as measuring high concentrations of crustal and marine elements in these clusters. Both Cluster 1 and Cluster 4 include trajectories originating and/or passing through from high emission areas in Eastern and Western Europe. These clusters are expected to bring anthropogenic elements and ions to Northwestern Turkey. However, there is one important difference between Cluster 1 and 4 in terms of pollution transport. Cluster 4 includes the longest trajectories in our database and thus represents pollutants, including anthropogenic elements transported from distant sources. Cluster 1, on the other hand, includes the shortest trajectories and represents slow moving air masses that stagger around the station. Elements that have high concentrations in Cluster 1 can be suspected to originate from more local sources. If we look at Figure 4.3.9 (c) with this perspective, we can conclude that, elements Zn and As which have high median concentrations in Cluster 1 and Cluster 4, probably have both local and distant sources. Other pollution-derived elements that have high median concentrations in only Cluster 4 are probably transported to the sampling point from distant sources. The second group of anthropogenic elements and ions, including NH$_4^+$, SO$_4^{2-}$, Cd, Mo and Tl, showed different variations between clusters. Cluster-to-cluster variations in their median concentrations are given in Figure 4.3.9(d). These elements and ions have higher concentrations in Cluster 1 and Cluster 5. The only exception to this is Cd, which has fairly low concentration in Cluster 1. Cluster 5 represent upper air flow from Northeast, high median concentrations in Cluster 5 may imply that they are being transported from countries located to the northeast of our sampling point. Candidate countries are obviously Ukraine and Russian Federation. Crustal enrichment factors of these elements with well-defined anthropogenic sources are given in Figure 4.3.10(c). Unlike in concentrations, EFc patterns of all anthropogenic species were very similar. This pattern was also observed for elements that are not included in the figure. General feature is that all anthropogenic species are more enriched in Clusters 1 and 5, which are clusters that are associated with high concentrations of different groups of anthropogenic species. The difference between different anthropogenic species is the high median concentrations of some of them in Cluster 4. However, since concentration of crustal elements and Al is also high in Cluster 4, those anthropogenic species do not have higher EFc values in Cluster 4.

Concentrations and enrichment factors of elements with mixed sources are given in Figure 4.3.9 and Figure 4.3.10. Their concentration pattern, with higher median concentrations in Cluster 4, is generally similar to those with crustal origin. However, V and Ni also have high

concentrations in Cluster 1, like anthropogenic elements. The same statement is also true for EFc of these elements.

Calculation of clusters can be a tedious and difficult task, but provided valuable information when clusters were associated with concentrations of elements. Since trajectories are separated into clusters based on their direction and speed, an element having high concentration in one of the clusters can be related to the speed and direction of that cluster. Based on this logic, pollution derived elements are separated into different groups, depending their concentrations in different clusters. An element can be associated with more than one of these groups, because it can have high concentrations in more than one cluster.

The first group consists of elements that has distant sources and reach to the station through long range transport. This group includes Zn, Cu, Ni, V, Se, P, Pb, As and Ge, which have high median concentrations in Cluster 4. The second group includes elements that have relatively local sources around the station. Relatively local means sources in Balkans, and at Northwestern parts of Turkey. This group includes Zn, Ge, SO_4^{2-}, NH_4^+, Cd and Tl, which have high median concentration in Cluster 1, because Cluster 1 consists of short trajectories representing slow moving air masses that are influenced from local emissions. Finally the third group includes elements that can have sources located at NW of our station. Ukraine and Russian Federation are two candidate for these sources. Elements included in this group are NH_4^+, SO_4^{2-}, Cd, Mo and Tl.

4.3.2. Contribution of Forest Fires on Aerosol Composition at Northwestern Turkey

In this study K-W test showed that there were significant differences between the clusters in terms of soluble K concentrations (Figure 4.3.11). As soluble K has been reported as a good marker of biomass burning in various studies (Andreae and Merlet, 2001, Watson et al., 2001, Watson et al., 2002, Duncan et al., 2003, Watson and Chow, 2007, Sciare et al., 2008, Viana et al., 2008b, Alves et al., 2010), the main source of soluble K in our station is speculated to be biomass burning i.e., agricultural waste burning and forest fires. Bonferroni test which is a post-hoc tests for multiple comparisons was applied to determine which clusters are significantly different from the others for soluble K. Cluster 5 and Cluster 3 were found to be significantly higher than others and similar to each other. Cluster 5 (18%) represents the air masses from Russia and Ukraine, whilst Cluster 3 (14%) represents the air masses from northern Europe countries that passes over Balkans prior the station. Trajectories reside in Cluster 5 and Cluster 3 are fast and medium moving hence can be suspected regional and/or long-range transport of soluble K. High biomass burning activities have been reported for countries surrounding the Black Sea (Sciare et al., 2008). Trajectories in Cluster 5 and Cluster 3 cover the Black Sea coast, so they can bring pollution from these regions to our station if there were biomass burning activities around.

Episode days for soluble K were selected based on two criteria 1) soluble K concentration >220 ng m^{-3} (corresponds to upper 20th percentile) 2) must last at least 2 days. Based on these criteria 11 cases were determined. These are 22 to 26 April, 3 to 4 May, 24 to 26 June, 4 to 15 July, 21 July to 2 August, 18 to 21 August and 14 to 16 September in 2006; 11 to 20 March, 2 to 3 April, 6 to 7 October and 10 to 12 October in 2007. For the sake of brevity, only four cases out of 11 cases will be discussed here. These cases are Case 1: 24 April to 26 April, Case 2: 8 to 14 July, Case 3: 21 July to 1 August and Case 4: 18 August to 21 August in 2006. Fire maps showing the fire hot spots as orange dots were downloaded from the NASA's Fire Information for Resource Management System (FIRMS) web page. Note that fires occurred five days ago was assumed to influence observed PM data in our station. Back trajectories and locations of forest fires provided by satellites for these days are given in Figure 4.3.12 and Figure 4.3.13.
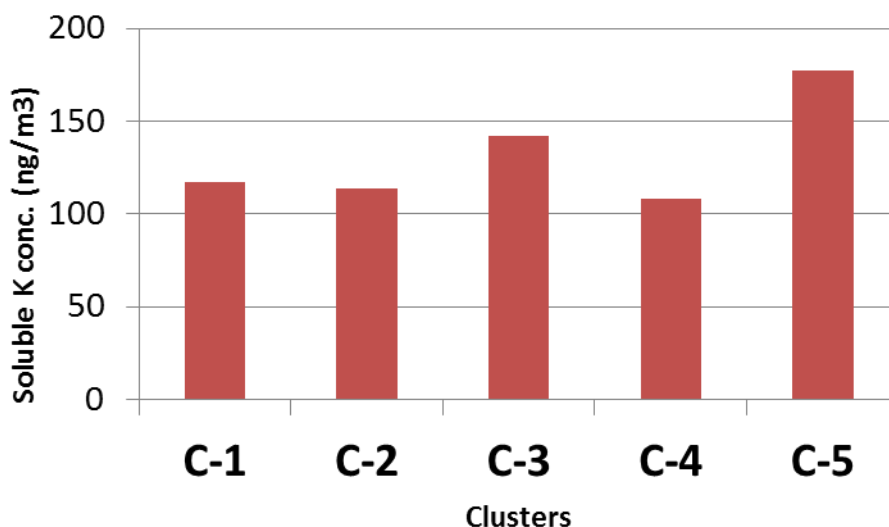
Figure 4.3.11 Soluble K concentrations (median values) of clusters

Average soluble K concentrations for Case 1, Case 2, Case 3 and Case 4 are 376, 420, 397 and 344 ng m^{-3}, respectively. As clearly seen from in Figure 4.3.12 and Figure 4.3.13, back trajectories' paths in all cases coincided well with the hot spots on fire maps. This indicates that our station is influenced by long-range transport of fire activities. As fires are more frequent in Russia, Ukraine, Belarus, Bulgaria and Romania, soluble K concentrations are found significantly higher in Cluster 3 and Cluster 5. It is worth to note that there are some cases with low soluble K concentrations in these two clusters. For example average soluble K concentration is 73 ng m^{-3} on 7-8 May 2006. Fires that may affect the measurements on these days are given in Figure 4.3.14. As seen from the figure, there were fires over Russia, Ukraine and Belarus but back trajectories' paths did not coincide with the fire hot spots. Because fire hot spots were located further North, which is away from the path of trajectories, which were along the Black Sea coast. For this reason fire emissions could not be transported to our station and low concentration of soluble K was measured.

Such forest fires are frequent in Russian Federation and Ukraine, when air masses comes from N and NE they have potential to bring particles emitted from those fires. The relation between soluble K and trajectory direction indicate that the station is influenced from these forest fires at least in certain time of the year and soluble K is a good tracer to track forest fires. The effect of Forest fires in Ukraine end Russian Federation on chemical composition of Eastern Mediterranean was noted previously (Amiridis et al., 2009, Balis et al., 2003, Gerasopoulos et al., 2011) through analysis of organic carbon, in this study we did not measure organic carbon and demonstrated that forest fires can also be identified by measuring soluble fraction of K.
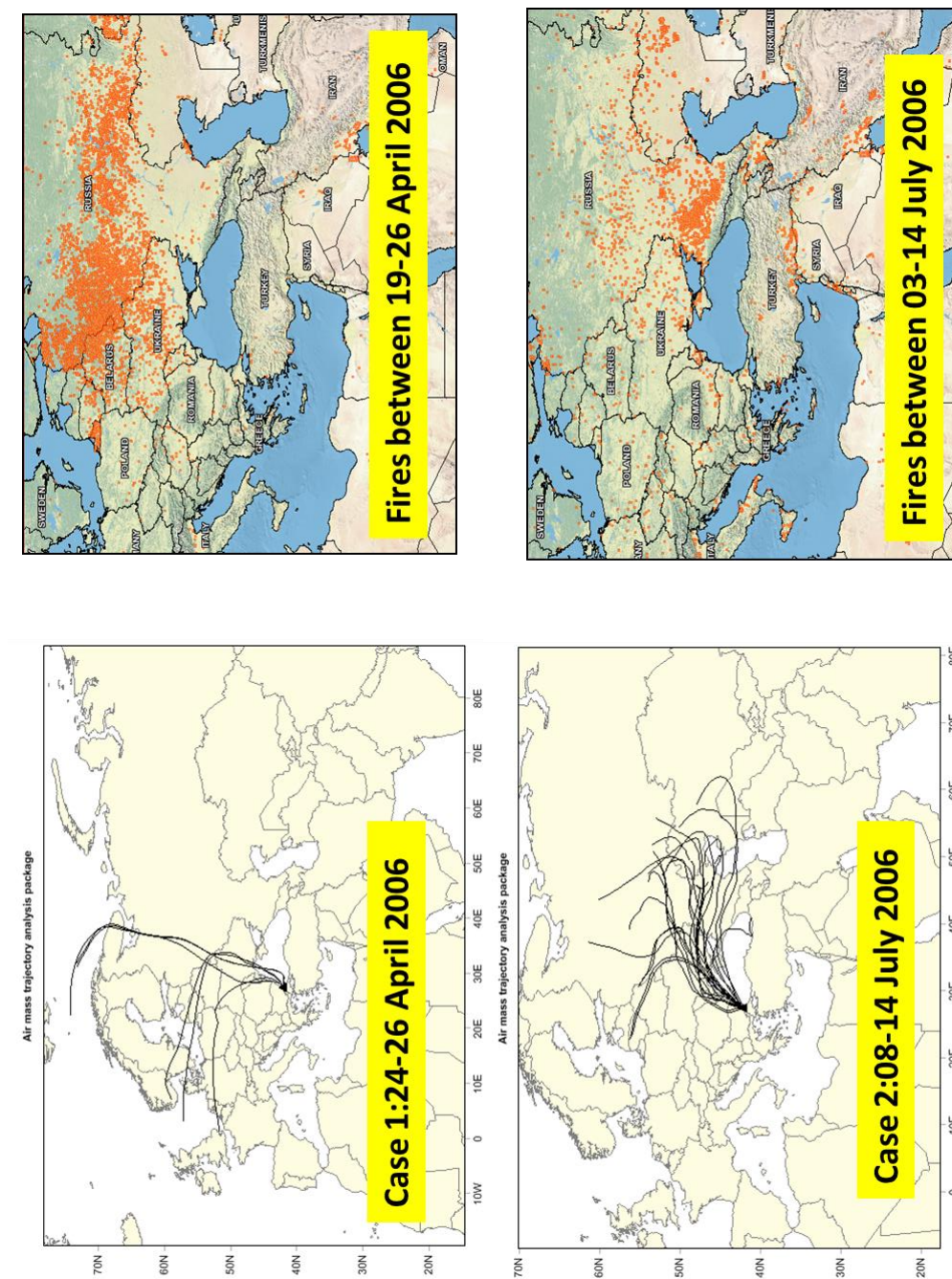
Figure 4.3.12 Back trajectories and fire maps for Case 1 and Case 2
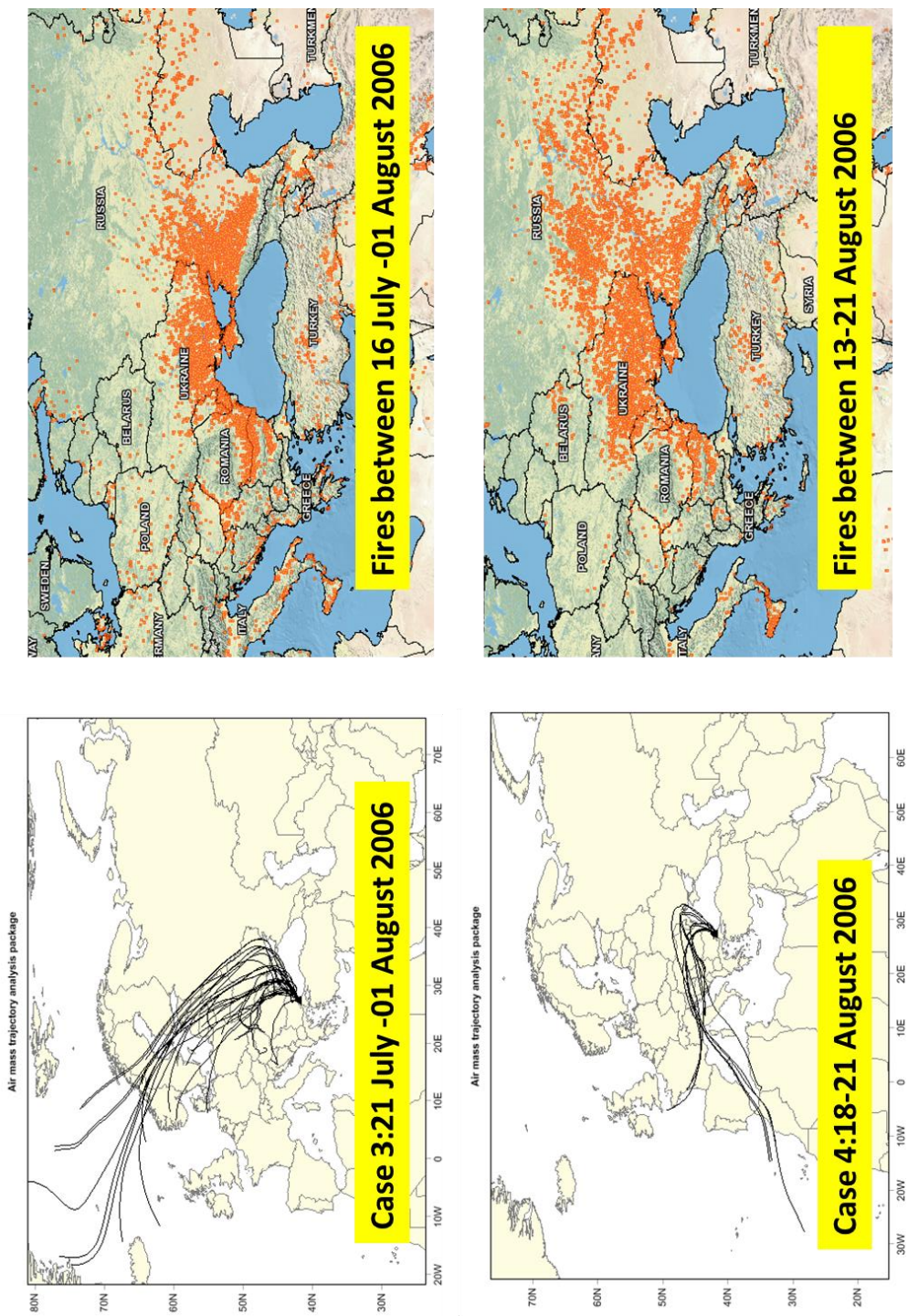
Figure 4.3.13 Back trajectories and fire maps for Case 3 and Case 4

Fires between 01-07 May 2006

06-07 May 2006
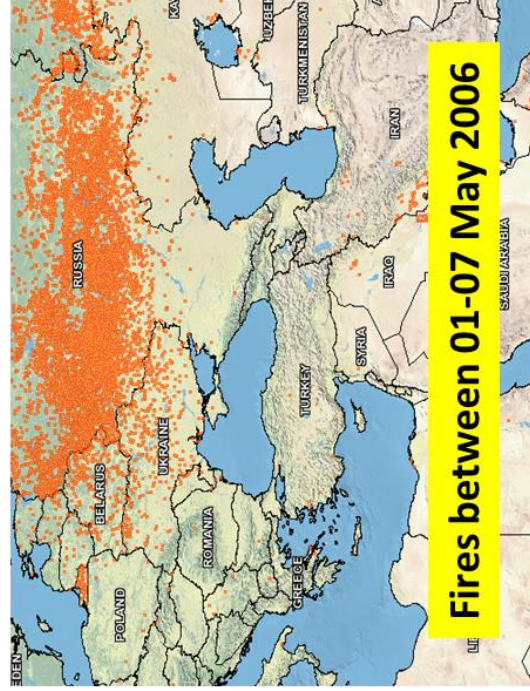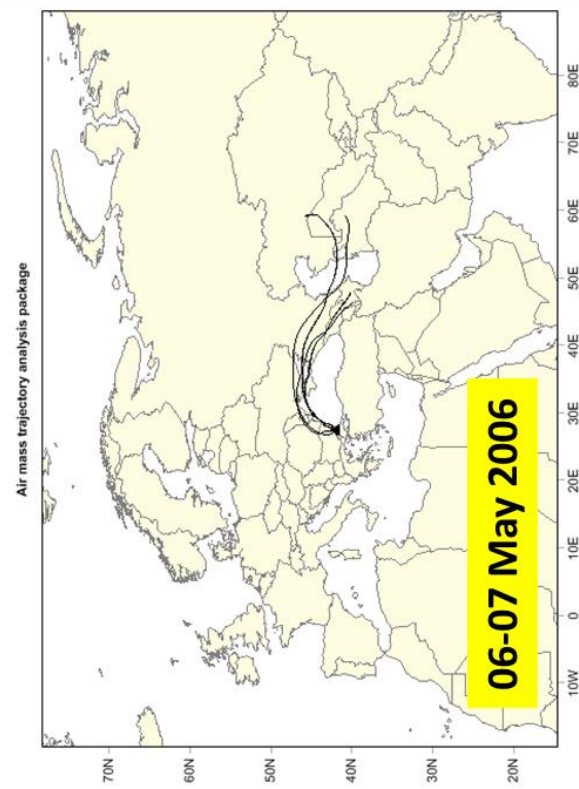
Figure 4.3.14 Back trajectories and fire maps on low soluble K days

4.4. Relation Between Elemental Concentrations and Local Meteorology

Local meteorology, in general terms surface meteorology plays an important role in air quality studies. If there were local sources around the vicinity of the station, they may affect the air quality. To determine the contribution of local sources on air quality of the station, surface meteorological parameters, especially wind speed and wind direction are used. A general discussion on the surface meteorology of the region and its relation with pollution is investigated in this section.

The climate of the Kırklareli varies regarding to the closeness to the sea. The regions bordering the Black Sea experience Oceanic climate having precipitation both in summers and winters. The regions far away from the Black Sea as our sampling station have continental (inland) climate. In continental climate summer is hot and winter is cold and relatively wet. The summary of the meteorological parameters recorded at Kırklareli meteorological station which represents surface meteorology of our station during the 30-year period (1975-2006) are given in Table 4.4.1. The mean temperature in winter is $6^{o}C$ and $20^{o}C$ during the summer. January is the coldest month while July is the warmest. The annual mean rainfall is about 540 mm, which is smaller than rainfall in the Black Sea coast (2200 mm) and higher than rainfall amount in Center Anatolia (250-300 mm). The mean rainfall in winter is 315 mm (58% of the annual mean) and 225 mm (42% of the annual) in summer. The annual mean relative humidity is 69%. Wind speeds are below 2 m s^{-1} in both seasons.

The annual and seasonal variations in wind direction are illustrated in Figure 4.4.1. It is clearly seen that the dominant surface wind direction is NE (about 20%) irregardless of the season. The seasonal differences are more prominent for winds from ENE and Southerly (ESE to WSW) directions. Frequency of wind directions for ENE is 20% in summer and 14% in winter. Summer frequency of winds from Southerly directions is 30%, while its frequency decreases to 19% in winter.

Table 4.4.1 Long term (1975-2006 years) average temperature, relative humidity, total rainfall and wind speed at Kırklareli meteorological station

Season	Month	Temperature (°C)	Relative Humidity (%)	Rainfall (mm)	Wind Speed (m s^{-1})
winter	January	3	77.5	50.9	1.7
winter	February	3.7	74.3	38.7	1.8
winter	March	6.8	71.7	45	1.7
winter	April	11.9	67.2	44	1.5
summer	May	17	65	49.8	1.3
summer	June	21.4	62	51.1	1.2
summer	July	23.7	59.1	27.3	1.2
summer	August	23	61.5	23.1	1.2
summer	September	19	64.6	26.7	1.3
summer	October	13.8	71.7	47.1	1.4
winter	November	8.5	76.5	72.3	1.4
winter	December	4.7	78.6	64.1	1.6

Figure 4.4.1 Annual and seasonal wind roses at Kırklareli station

The relations between pollutant concentrations and wind speed are investigated using daily and monthly average values. There are no statistically significant relations between daily average wind speed and daily concentrations at 95% CL. The scatter plots given in Figure 4.4.2 clearly show this lack of relation between wind speed and concentrations on daily basis. The relations between pollutant concentrations and wind speed on monthly basis are given in Figure 4.4.3 for some representative crustal, marine and anthropogenic species. The concentrations of crustal originated species e.g. Al and Fe are high in summer when wind speed is slower and their concentrations are low when wind blows faster as seen in Figure 4.4.3(a). Remember that no relations were found between daily average wind speed and daily concentrations at 95% CL. Although here it seems as if there were relation between concentrations and wind speed, it is not a direct relation. The main reason for observing such an indirect relation between them is precipitation. Precipitation is less in summer hence soil is dry. When soil is dry, it is lifted into the atmosphere even by mild winds. Soil is damp during winter due to frequent precipitation events; therefore soil cannot resuspend easily.

Yıldız Mountain Massif (also called Istranca Mountains) surrounds the Black Sea coastline by running parallel to the Black Sea. When considering the distance between the station and the Black Sea, which is 50 km, and the altitude difference between the sea level and the Yıldız Mountains (Figure 4.4.4), the transport of sea salt particles to the station by surface winds seems infeasible. Therefore wind speed is indirectly related with concentration of marine originated species (Figure 4.4.3(b)). This indirect relation can be explained by bubble bursting which is the mechanism for formation of sea spray droplets to form sea-salt aerosols (Andreas et al., 1995). Higher winter wind speeds observed in the Black Sea efficiently break waves. This enhances bubble bursting mechanism therefore increases sea-salt aerosols formation. Slow winds cannot break waves as efficient as fast winds, so formation of sea-salt aerosols diminishes in summer when wind speeds are slow.
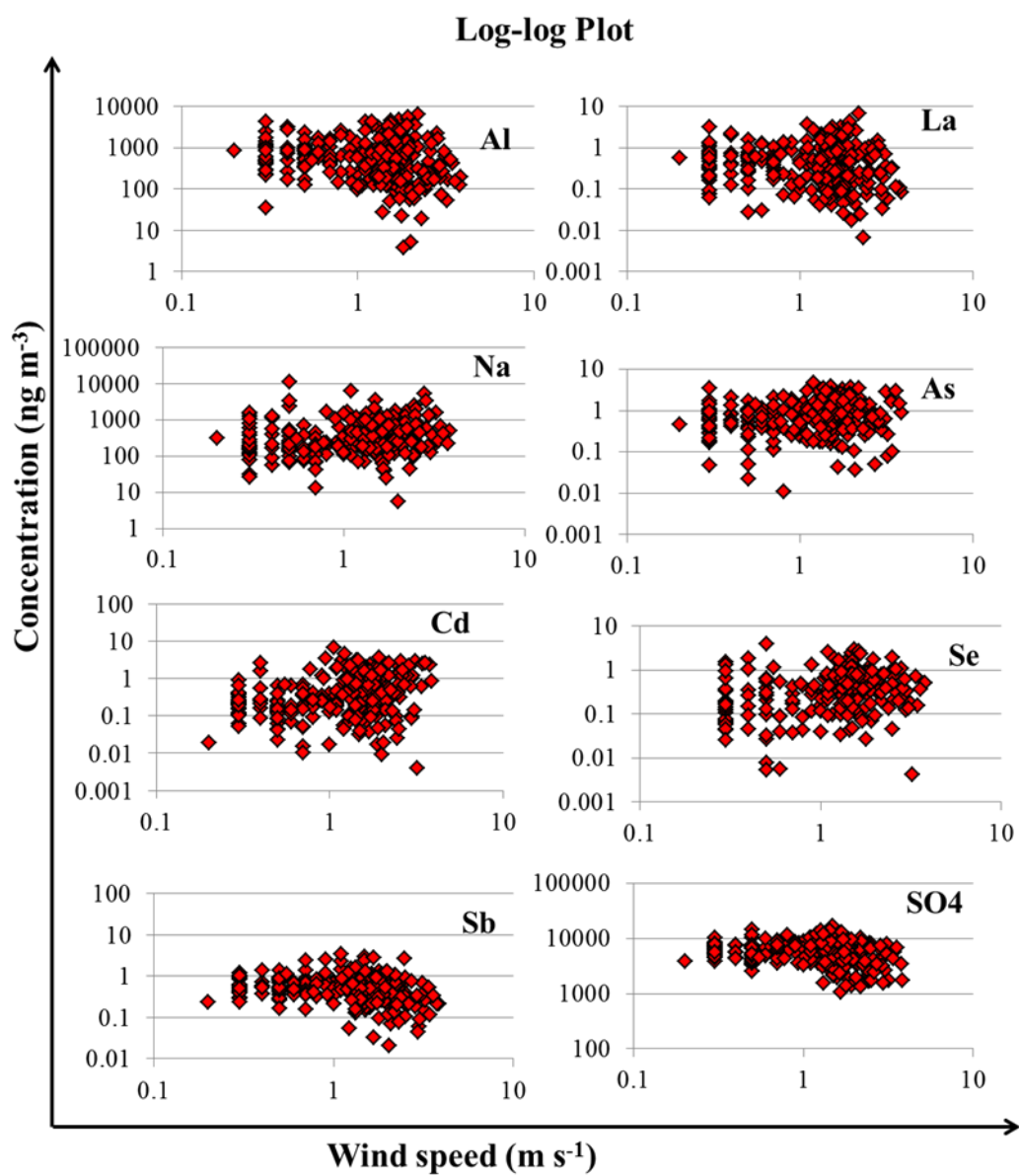
Log-log Plot

Figure 4.4.2 Log-log scatter plots of crustal, marine and anthropogenic species against wind speed
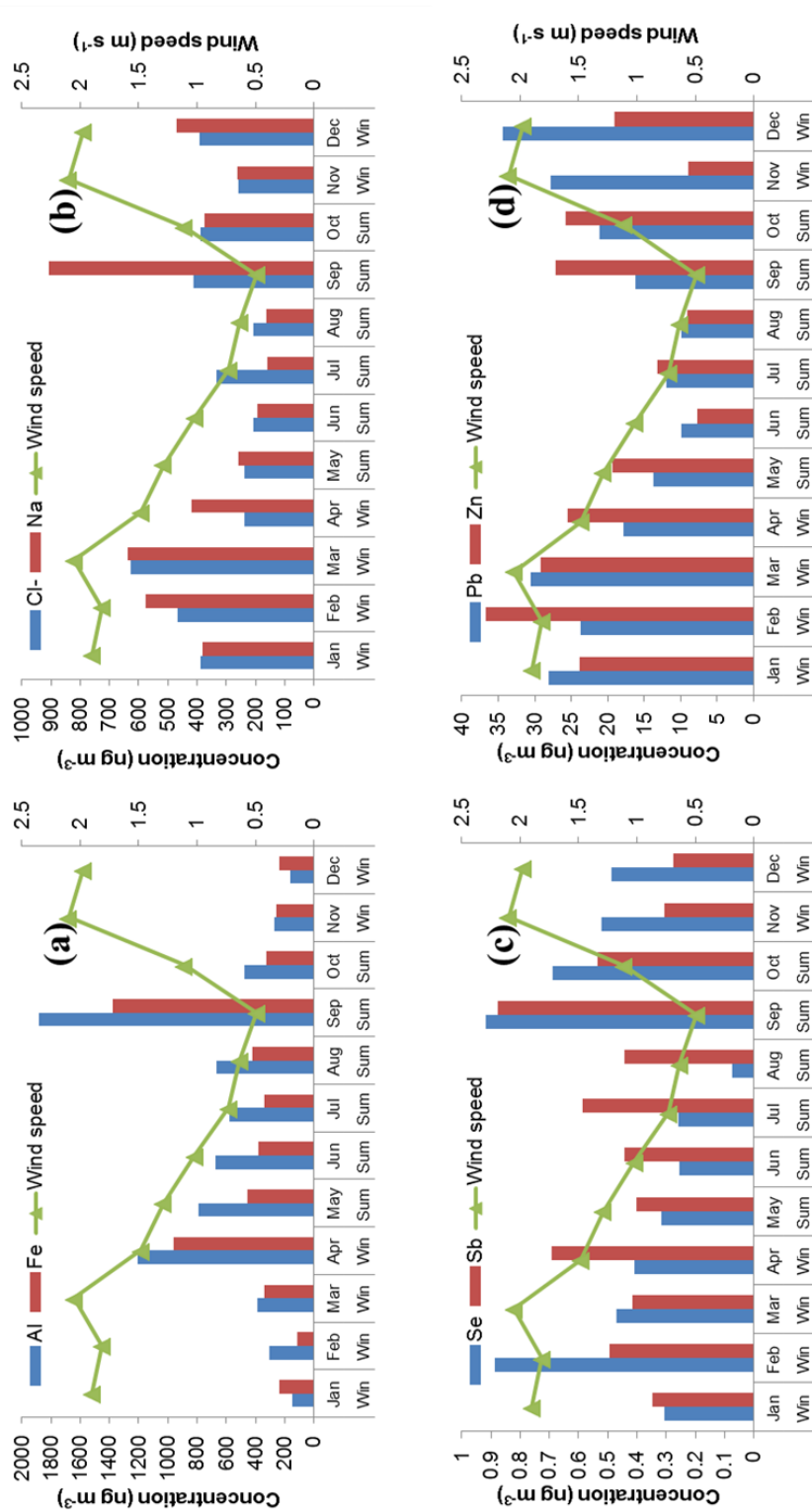
Figure 4.4.3 Relation between monthly average concentrations of (a) crustal, (b) marine and (c and d) anthropogenic elements with wind speed
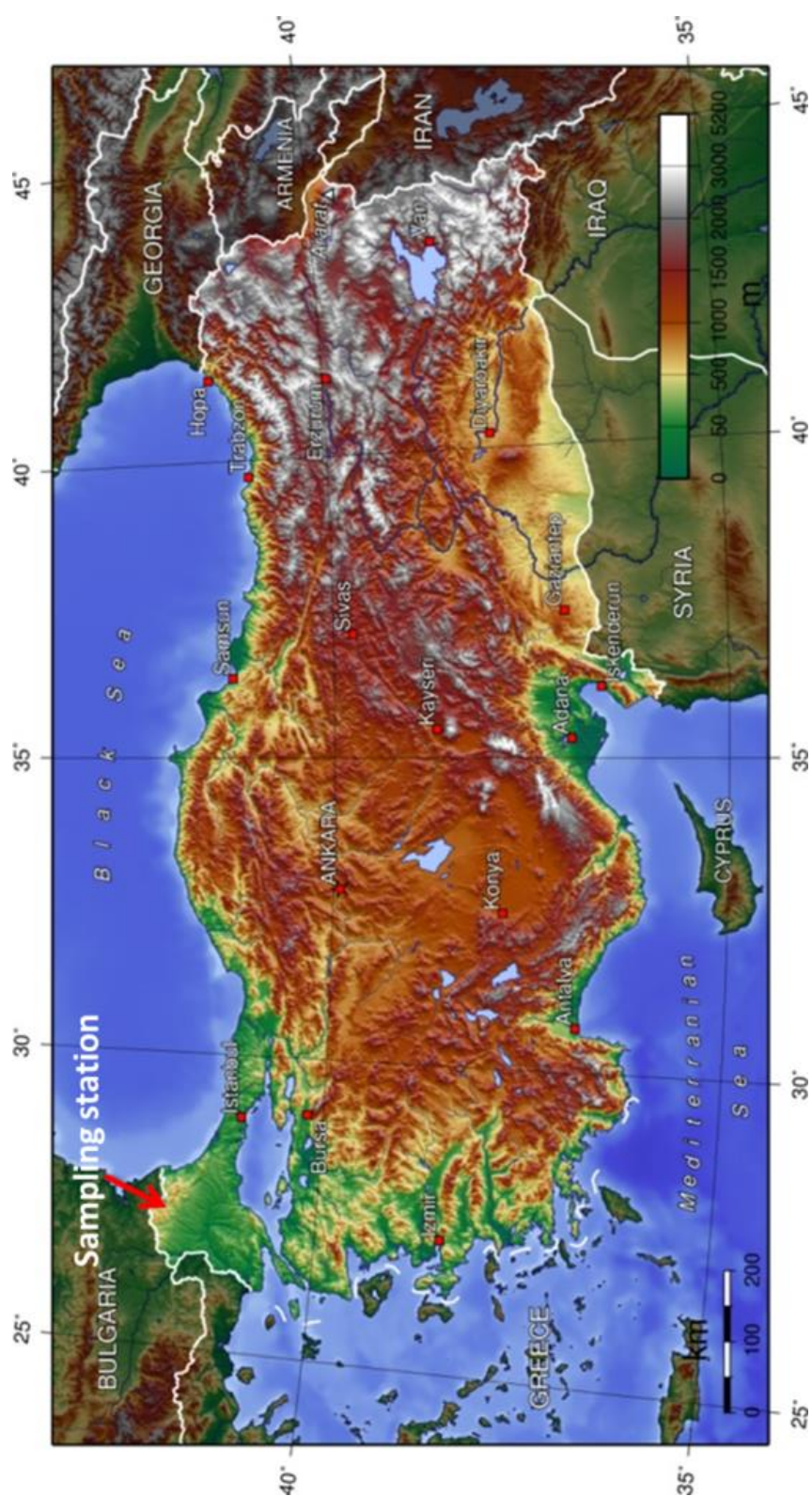
Figure 4.4.4 Topographical map of Turkey

Daily and monthly average values are used to assess the relations between pollutant concentrations and temperature as given in Figure 4.4.5 and Figure 4.4.6, respectively. No statistically significant relations are found between daily average temperature and daily concentrations at 95% CL. Like the relation between wind speed and concentrations, the relation between temperature and concentrations are indirect. Remember that our sampling station has continental climate with hot summer and cold and relatively wet winters. The inverse relation between temperature and crustal species is mainly due to having less precipitation in summer whose temperature is higher than winter and vice versa. The decrease in the concentration of sea-salt species with increasing temperature is explained by the decrease of sea-salt aerosols formation caused by frequent slow winds in summer, not high temperature in summer. Anthropogenic species show different seasonal variations that mostly depend on their formation and removal mechanisms in the atmosphere. The sampling station in this study is a rural station having no anthropogenic activities around. Hence measured anthropogenic species are mainly due to transported pollution. Boundary layer is one of the most important factors determining the level of ambient pollution. If boundary layer is high, transported pollutants can mix with air and are diluted. Short boundary layer means less air mixes with pollutants, so concentrations do not decrease as much as decrease observed in high boundary layer case. Observed indirect relation between temperature and anthropogenic species are because of the relation between boundary layer and temperature. At high temperatures as in summer boundary layer becomes deep; however boundary layer is shorter in winter at low temperature.

Rain is one of the most efficient scavenging mechanisms for aerosols. Existing aerosols in ambient air can be swept out by rain droplets. Summary statistics of species concentrations on rainy days and non-rainy days are given in Table 4.4.2. To determine the effect of rain on aerosols species, the ratio of median concentrations on non-rainy days to rainy days are calculated and reported in Table 4.4.2. The ratios are above 1.0 almost for all species (except Pt and Cr), ranging from 2.4 as in Ti and 1.1 as in P. This indicates that all aerosol species are scavenged by rain but the magnitude of the effect vary from species to species. The ratios are sorted in descending order and then plotted as bar diagram in Figure 4.4.7. It is seen that species having high ratios are all crust originated but comparatively lower ratios belong to anthropogenic and marine species as marked in Figure 4.4.7. The source strength of crustal originated species is high on non-rainy days because of the dry soil. During the rain events no more crustal species from the ground can enter into the air because rain droplets cause soil particles to stick into the ground. This process explains the reason of having high non-rainy days to rainy days ratio for crustal species.

Rainy days usually accompanied by stronger winds. These stronger winds increase sea salt aerosols formation by enhancing bubble bursting mechanism. As sea-salt aerosols are water soluble and in the coarse fraction, they are scavenged easily by rain droplets. So we can say that both formation and removal processes efficiently occur at the same time for sea-salt aerosols during rain events. The ratio for total Na, soluble Na and Cl⁻ is 1.5, 1.2 and 1.6, respectively.

The non-rainy days to rainy days ratio are in the range of 1.6 (Cd) to 1.1 (P) for anthropogenic species. Relatively low ratios for anthropogenic species indicate that anthropogenic species are not affected by rain like crustal species do. A study conducted in our group demonstrated that scavenging efficiency of aerosols by rain depends on the particle size. As particle size increases scavenging by rain increases, however as particle size decreases scavenging reduces (Figure 4.4.8; Yosunçığır, unpublished data). Another study conducted by Galloway et al. (1993) has shown that although the scavenging efficiency differs from species to species, species associated with fine fraction scavenges less efficiently than species associated with coarse fraction. This also proves that anthropogenic species in our study is due to fine fraction of collected aerosols.
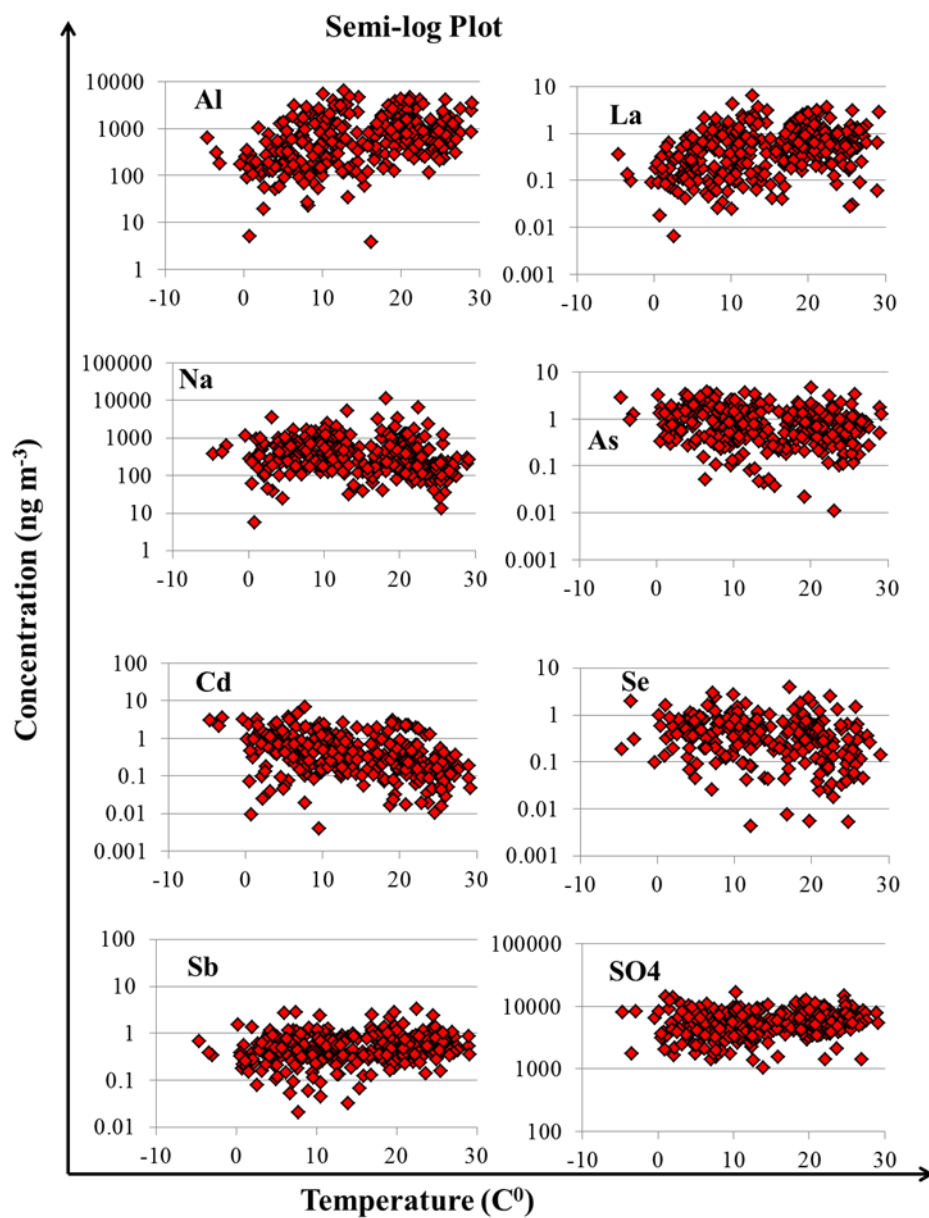
Figure 4.4.5 Binary correlations between concentrations of selected elements and temperature
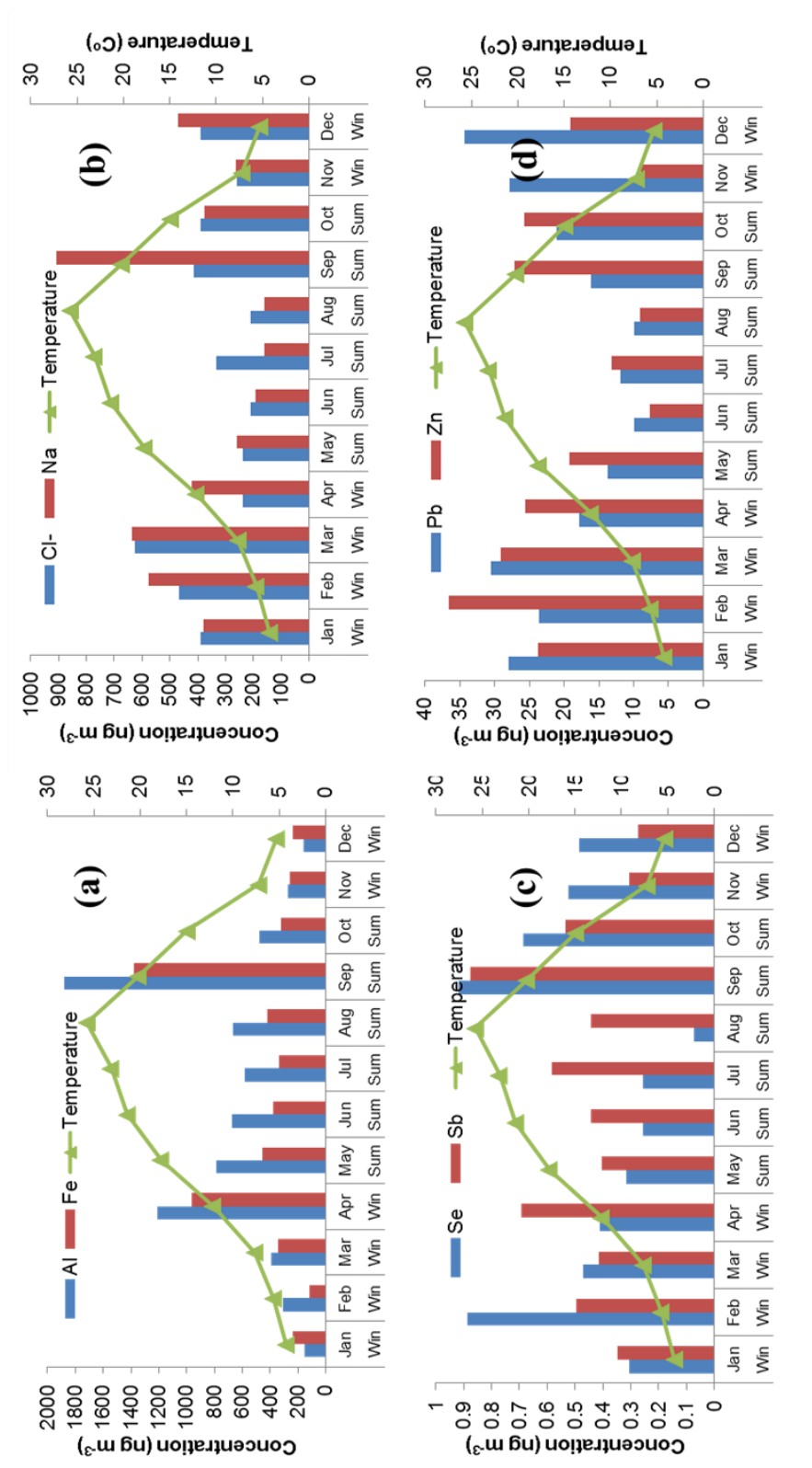
Figure 4.4.6 Relation between monthly average concentrations of (a) crustal, (b) marine and (c) and (d) anthropogenic elements with temperature

Table 4.4.2 Mean and median concentrations of elements in rainy and non-rainy days

		Rain day			Non-rainy day		Non-rainy/rainy
	N	Mean	Median	N	Mean	Median	median ratio
		ng m^{-3}	ng m^{-3}		ng m^{-3}	ng m^{-3}	
Li	68	0.38 ± 0.31	0.3	245	0.73 ± 0.71	0.51	1.7
Be	59	0.02 ± 0.02	0.01	217	0.05 ± 0.05	0.03	1.9
Na	70	342 ± 361	236	245	615 ± 981	376	1.6
Mg	70	328 ± 360	208	246	765 ± 915	370	1.8
Al	70	468 ± 451	323	245	1092 ± 1150	669	2.1
P	58	36 ± 36	23	216	38 ± 38	25	1.1
K	70	268 ± 184	237	245	535 ± 518	380	1.6
Ca	65	877 ± 919	531	237	1933 ± 3604	1010	1.9
Ti	66	34 ± 36	21	241	79 ± 84	50	2.4
V	70	2.8 ± 2.5	2.1	246	4.1 ± 2.8	3.3	1.6
Cr	17	38 ± 119	5.1	105	36 ± 207	2.8	0.5
Mn	70	13 ± 13	9	242	31 ± 33	20	2.2
Fe	51	390 ± 512	215	206	819 ± 986	493	2.3
Ni	62	6 ± 26	1.1	236	10 ± 54	2.3	2.0
Cu	70	6 ± 10	4.1	243	11 ± 29	6.3	1.5
Zn	63	45 ± 152	12	229	65 ± 286	19	1.6
Ge	69	0.04 ± 0.03	0.03	245	0.06 ± 0.05	0.05	1.9
As	68	0.76 ± 0.67	0.55	239	1.07 ± 0.82	0.84	1.5
Se	50	0.41 ± 0.32	0.34	197	0.54 ± 0.58	0.37	1.1
Rb	70	1.04 ± 0.85	0.76	246	2.38 ± 2.22	1.69	2.2
Sr	65	2.31 ± 2.00	1.75	241	4.94 ± 7.60	3.21	1.8
Y	70	0.17 ± 0.17	0.11	244	0.42 ± 0.49	0.24	2.1
Mo	70	1.4 ± 5.0	0.17	245	1.3 ± 6.0	0.2	1.2
Cd	68	0.68 ± 0.88	0.23	241	0.74 ± 1.13	0.37	1.6
Sn	69	1.13 ± 1.15	0.67	242	2.42 ± 4.96	1.06	1.6
Sb	69	0.41 ± 0.31	0.34	243	0.70 ± 0.80	0.53	1.6
Cs	70	0.08 ± 0.07	0.07	245	0.18 ± 0.16	0.13	2.1
La	70	0.37 ± 0.32	0.32	243	0.80 ± 0.87	0.5	1.7
Ce	69	0.63 ± 0.62	0.42	242	1.48 ± 1.71	0.85	2.0
Pr	70	0.07 ± 0.06	0.04	243	0.16 ± 0.20	0.09	2.0

Table 4.4.2cont. Mean and median concentrations of elements in rainy and non-rainy days

	N	Rain day Mean ng m^{-3}	Median ng m^{-3}	N	Non-rainy day Mean ng m^{-3}	Median ng m^{-3}	Non-rainy/rainy median ratio
Nd	70	0.25 ± 0.25	0.17	244	0.60 ± 0.71	0.34	2.0
Eu	69	0.014 ± 0.012	0.01	244	0.030 ± 0.037	0.02	1.6
Sm	70	0.057 ± 0.052	0.04	243	0.13 ± 0.14	0.07	1.7
Gd	70	0.055 ± 0.053	0.04	245	0.132 ± 0.154	0.07	1.9
Tb	66	0.007 ± 0.007	0.01	242	0.016 ± 0.021	0.01	1.8
Dy	68	0.04 ± 0.04	0.03	235	0.091 ± 0.101	0.056	1.9
Ho	68	0.007 ± 0.007	0.001	233	0.017 ± 0.018	0.01	2.0
Er	46	0.023 ± 0.023	0.02	193	0.051 ± 0.053	0.032	1.9
Tm	68	0.003 ± 0.003	0.002	241	0.007 ± 0.009	0.004	2.0
Yb	69	0.020 ± 0.017	0.017	241	0.043 ± 0.046	0.03	1.7
Lu	58	0.003 ± 0.003	0.002	214	0.006 ± 0.007	0.004	1.8
Hf	69	0.065 ± 0.068	0.04	243	0.14 ± 0.18	0.09	2.1
W	31	0.64 ± 2.57	0.07	152	0.49 ± 1.64	0.12	1.6
Pt	24	0.010 ± 0.022	0.004	94	0.10 ± 0.93	0.002	0.7
Au	29	0.074 ± 0.113	0.03	107	0.09 ± 0.30	0.046	1.5
Tl	70	0.065 ± 0.056	0.05	246	0.090 ± 0.084	0.07	1.6
Pb	70	29 ± 41	11	245	34 ± 55	17	1.5
Bi	43	0.073 ± 0.096	0.03	156	0.088 ± 0.100	0.06	1.9
Th	61	0.14 ± 0.20	0.09	224	0.27 ± 0.32	0.17	1.9
U	69	0.040 ± 0.036	0.03	243	0.092 ± 0.090	0.09	2.0
Cl$^-$	69	406 ± 472	239	233	613 ± 819	348	1.5
NO$_3^-$	70	2360 ± 1594	1796	244	3116 ± 1802	2674	1.5
SO$_4^{2-}$	70	5326 ± 2519	4916	245	6032 ± 2609	5758	1.2
NH$_4^+$	70	1783 ± 769	1689	246	2075 ± 1423	1811	1.1
BC	69	430 ± 240	378	243	580 ± 262	519	1.4
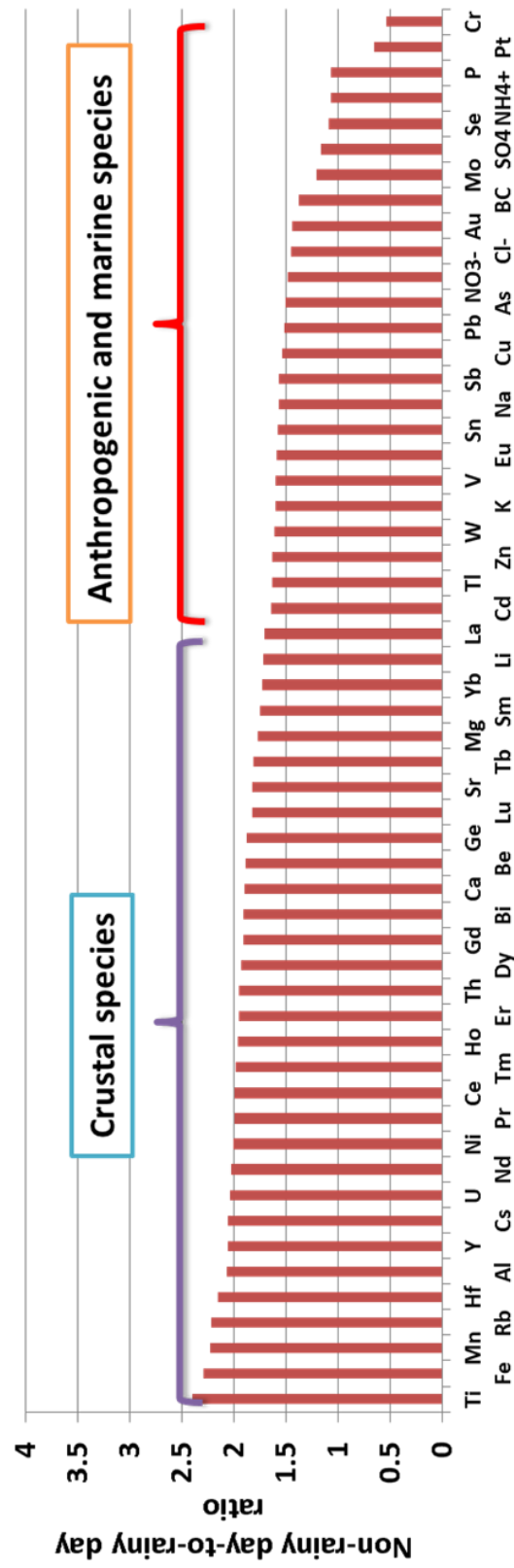
Figure 4.4.7 Non-rainy day-to-rainy day ratios of elements
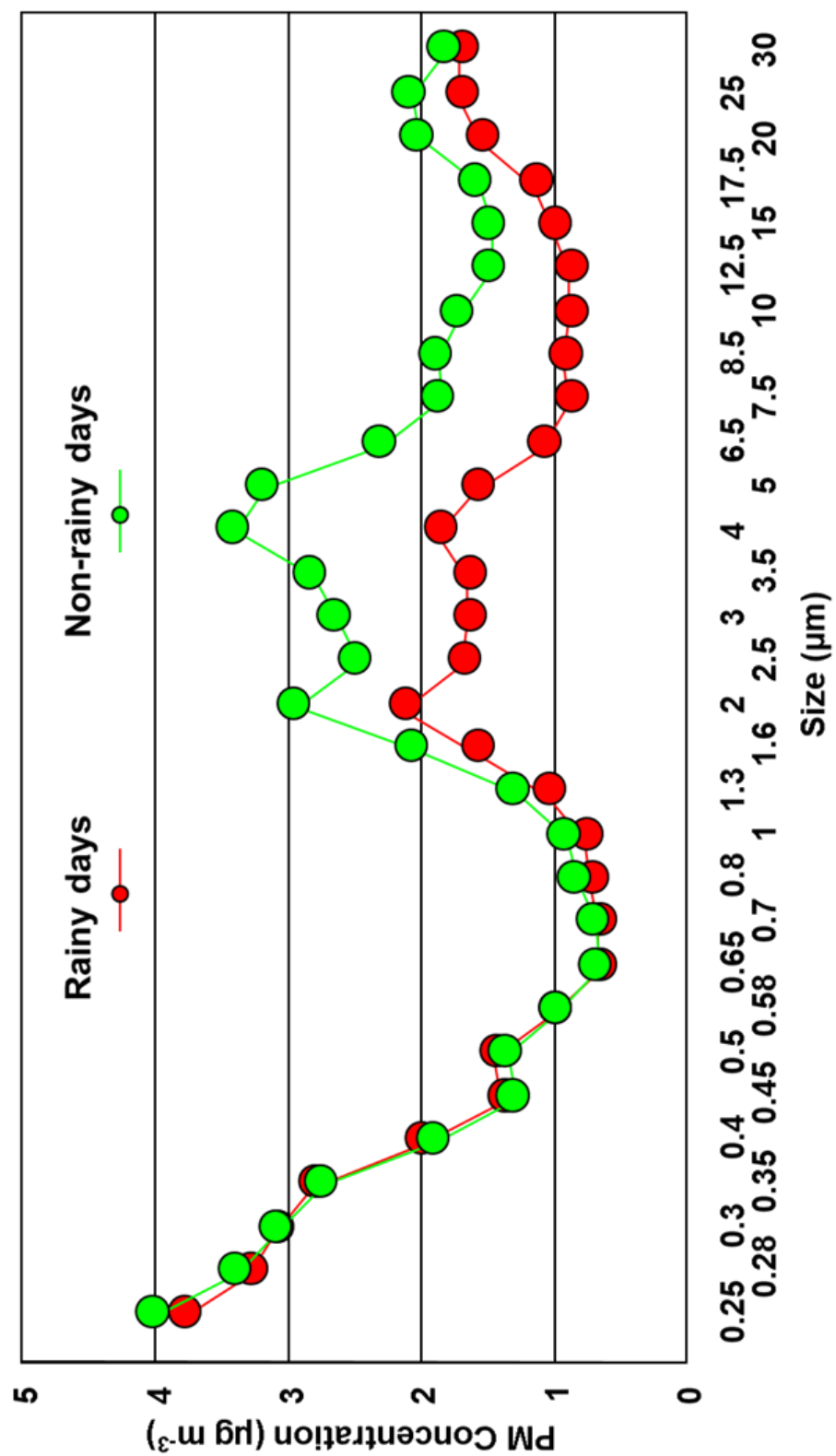
Figure 4.4.8 Comparison of rainy and non-rainy days average size distributions (Yosunçığır unpublished data)

4.5. Contribution of Local Sources

There are no point sources around the sampling station. Kırklareli city is 30 km away from and located in the south of the station. As winds blowing from south are not frequent (see Figure 4.4.1), the probability of pollution from Kırklareli that is affecting the sampling station is less. In the NE and ENE direction of the sampling station, which is the prevailing wind direction, there is a Bulgarian town named Malko Tarnovo whose population was 2500 in 2009 census. The distance between the town and the station is 10 km. Although average wind speed is 2 ms^{-1}, there are cases in which wind blows at higher wind speeds (as much as 9 ms^{-1}). In such cases winds may carry pollution from Malko Tarnovo in where residential heating and farming are the only known sources. However Malko Tarnovo is surrounded by mounts which prevent transport of the pollution to the sampling station by surface winds.

The effects of local meteorology on aerosols concentrations are discussed in the previous section (Section 4.4). Rainfall is found as the only local meteorological parameter affecting aerosols concentrations. Aerosols concentrations indirectly related with surface wind speed and temperature. This lack of direct relations between local meteorology and aerosols indicates that local sources around the station are not significant factors controlling the aerosols concentrations. Comparing the concentrations at weekends and on weekdays may be used as another way to proof this conclusion. Anthropogenic activities are generally reduced at weekends, especially on Sundays, e.g. no school, no office therefore less traffic. If there are anthropogenic sources around the station, at weekends lower concentrations of anthropogenic species are expected. Therefore concentrations at weekends and on weekdays are compared and no significant differences are found at 95% CL. Weekend to weekday ratio of median aerosols concentrations are around 1.0 i.e. varied between 1.3 for Ho and 0.7 for Cr as seen in Figure 4.5.1. Similar concentrations at weekends and on weekdays and lack of relation between concentrations and local meteorology show that our station is not under the influence of local sources. The main and dominant factor controlling the aerosols is long-range transport.

115

Figure 4.5.1 Weekend-to-weekday ratio of elements

4.6. Source Apportionment

4.6.1. Enrichment Factors

The definition of EF is given in Section 3.5.1 therefore it will not be repeated here. Mason's soil composition (Mason and Moore, 1982) was used as the reference crustal source to calculate 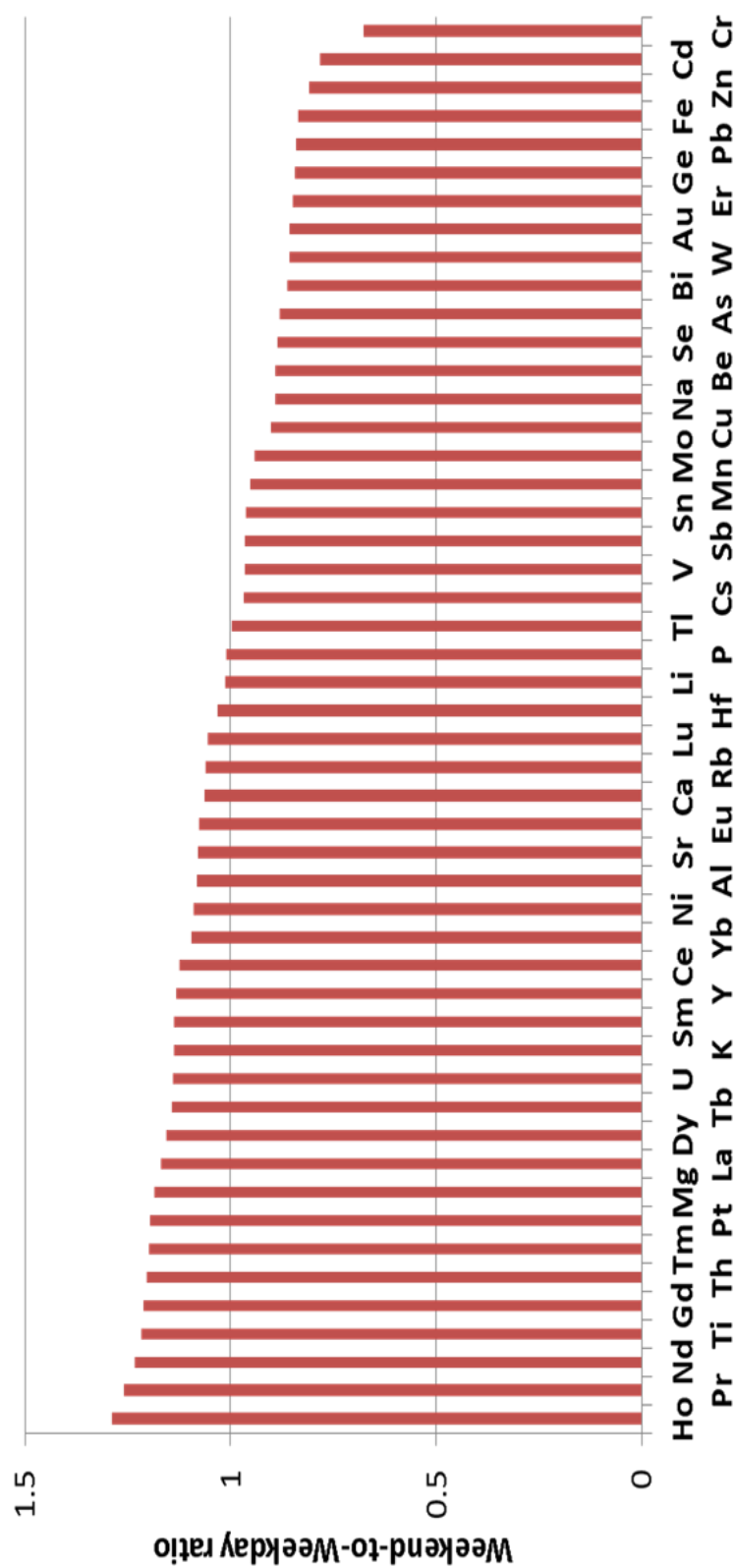EFc in this study. Aluminum is used as the reference soil element. Although there are other options for soil reference element, i.e. Fe, Li, Sc, Zr, Mn and Ti, Al is the best, because it can be easily measured with a variety of analytical techniques that are frequently used in environmental studies and soil is it's only source. Although there are Al plants or smelters that can modify Al content of particles in the atmosphere, their influence is very local. Aluminum is used as a reference element in many studies, both in Turkey and elsewhere (Gullu et al., 2005, Öztürk et al., 2012, Lin et al., 2008, Furuta et al., 2005, Gao et al., 2002) Al was used as the reference element in EFc.

In general EFc values around unity indicate that target element comes primarily from soil and contribution of other sources is negligible. However, it should be noted that composition of local soil can be different from the global compilations of soil composition, which are generally used in EFc calculations. Therefore one should be careful when interpreting the EF values as the variability of local soil composition and degree of human interferences on local soil cannot be taken into account in EF calculation (Guieu et al., 2002, Reimann and de Caritat, 2005).In this study an arbitrary threshold value of 3.0 was used to account these uncertainties. Elements with average EFc values <3.0 were considered as non-enriched because they are solely originated from crustal sources. In contrast, elements with EFc >30 were regarded as highly enriched as these elements are associated with non-crustal sources. Elements with EFc values between 3.0 and 30 were considered as moderately enriched. These moderately enriched elements are called as elements with mixed origin due to comparative contributions of crustal and non-crustal sources to their observed concentrations. Elements, like V, Cr, Na, and Mg are good examples of such elements with dual sources. These elements are all enriched in soil matrix, but they also have well documented non-crustal sources. Vanadium and Ni are good marker elements for residual oil combustion. Sodium and Mg have substantial contribution from marine aerosol.

Average crustal and marine enrichment factors of elements and ions measured in this study are presented in Figure 4.6.1. Lutetium, Al, Y, Yb, Fe, Be, Tb, Ti, Sr, Nd, Sm, Gd, Ce, Dy, Mn, La, Th, Eu and Rb are considered as crustal originated elements, because they all have EFc values smaller than 3.0. Copper, Cr, W, As, Mo, Zn, Sn, Pb, Sb, Cd, SO_4^{2-} as S, Se and Au are highly enriched elements, with EFc values ranging between 30 and >1000. These elements will be referred to as enriched elements throughout the discussions. Potassium, Mg, Li, Hf, U, Na, V, Ge, Cs, Ca and Ni are moderately enriched, with EFc values varying between 3 and 30 and will be referred to as elements with mixed origin.

Among elements with mixed origin, enrichment of Mg, K, Li, Cl and Ca is probably due to contribution of sea salt aerosol. This point can be clearly seen in Figure 4.6.1(b), where marine enrichment factors of elements are plotted. Chloride has EFm value close to unity, indicating that sea salt aerosol is the main source of Cl at our station. Marine enrichment factors of Mg, and Sr is approximately 100. This implies that there is significant contribution from sea salt aerosol to concentrations of Mg and Sr, but sea salt is not their main source (their main source is crustal material). There is one point worth noting about marine enrichment factors of elements. Sea salt aerosol consisted of large particles, which are quickly scavenged out from atmosphere. Because of this rapid removal process, marine contribution on concentrations of elements like Mg, Sr, K, Ca, S varies substantially from one place to another depending on the distance between sampling point and the coast. For example, Mg can be 100% marine at the coast, but 50% of can be crustal at a sampling site located approximately 50 km from the sea (as in our Kırklareli station). Average EFm values are around 1000 for K, Li, S and Ca. Sea salt has only minor contributions to concentrations
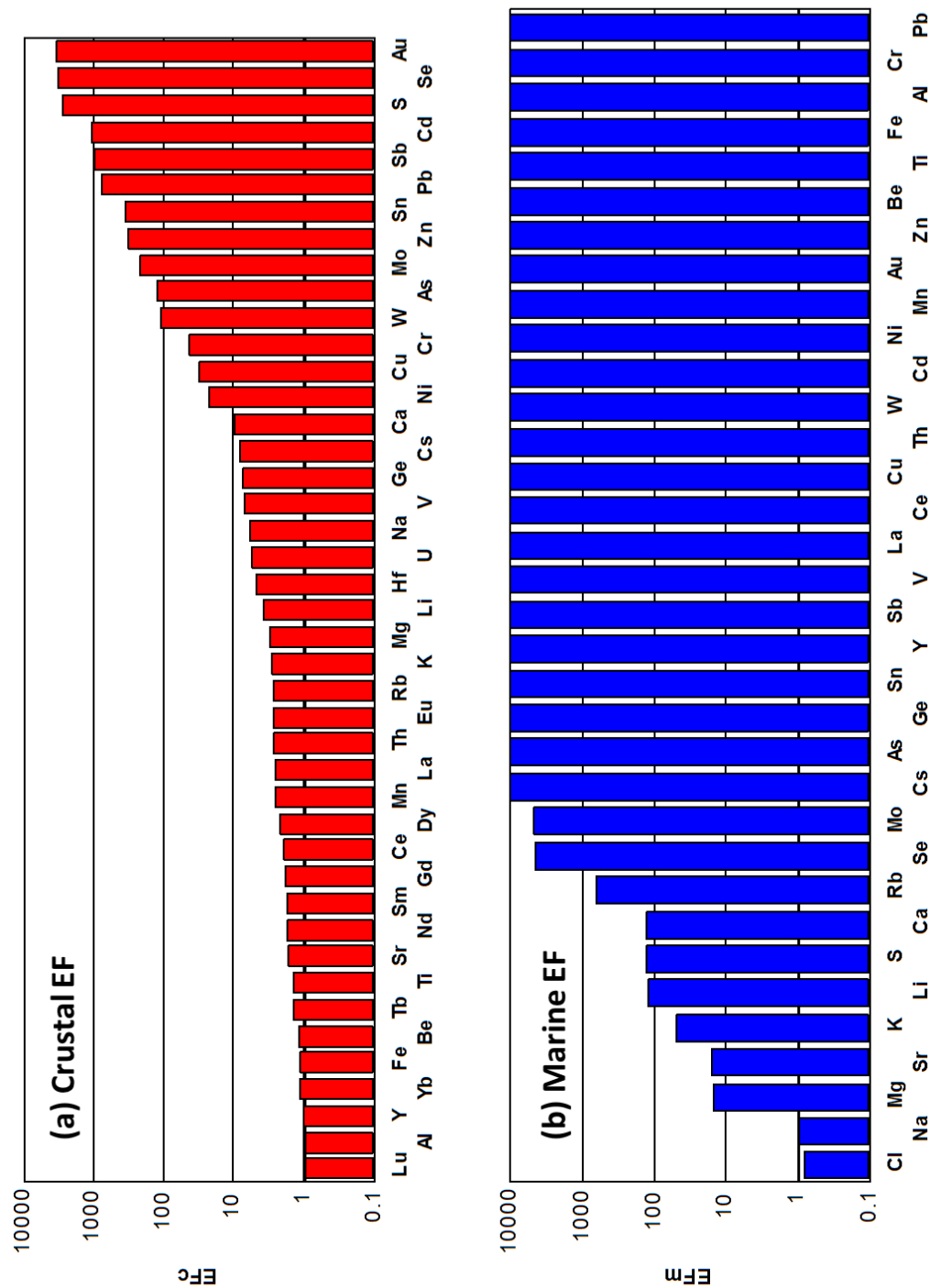
Figure 4.6.1 Average (a) EFc values of elements (b) EFm values of elements

of these elements at Kırklareli area. But this small marine contribution should be kept in mind in source apportionment studies. Elements V, Ge and Ni have well documented anthropogenic sources and contributed by these sources in addition to soil.

EFc of target element versus Al concentration plots can also be used to assess the possible sources and behavior of the target element in the atmosphere. This approach is particularly useful for elements with mixed sources. It provides qualitative information on relative significance of crustal and non-crustal sources on measured concentrations of these elements. For all elements EFc values against the corresponding Al concentrations are plotted and investigated carefully. Three different patterns were observed. First one was a typical pattern for crustal elements and shown in Figure 4.6.2 for Ce, Fe, La and Sm. Concentrations of these elements, for which the only source in the atmosphere, are independent of Al concentration. Normally, enrichments of these elements should be constant at EFc = 1.0. If the EFc is constant at a different value than 1.0, this means that concentration of these element in global soil composition used in EFc calculations is different from the composition of soil actually collected on filters, The EFc versus Al concentration plots for all remaining crustal elements were showed similar patterns as shown in Figure 4.6.2.

The EFc versus Al plots of selected moderately enriched elements are given in Figure 4.6.3. These patterns are fairly characteristic for elements with mixed crustal and anthropogenic sources in the atmosphere. Concentrations of these elements decrease with increasing Al concentration, which is typical for elements with anthropogenic sources. However, after a certain Al concentration, EFc values levels off and becomes independent of Al concentration. This part of the graph represents typical patterns observed in entirely crustal elements. Al concentration at which anthropogenic pattern changes into a crustal pattern can vary from element to element. For example, EFc values of K level off at Al concentrations slightly higher than 100, whereas EFc values of V levels off when Al concentrations is between 500 and 1000 ng m^{-3}. The EFc values of Ni levels off even at higher Al concentrations. These all shows the magnitude of crustal contributions on observed concentrations of these elements. Potassium enrichment factors levels off at lower Al concentrations, because contribution of crustal particles on measured K concentrations are high and crustal nature dominates even at moderate Al concentrations, on the other hand, concentrations of V and Ni are much lower than K concentration in soil and because of this they become crustal at higher Al concentrations.

Enrichment versus Al concentration plot for K is a good example to explain why these graphs are so useful. Potassium is moderately enriched in Figure 4.6.1, which can be easily attributed to different composition of soil collected on filters from global soil composition used in EFc calculations. However, EFc versus Al concentration plot for this element demonstrated that moderate enrichment observed in EFc of K is not due to difference in soil compositions, but because of contribution of a non-crustal source, which becomes apparent only at low Al concentration (low crustal contribution).

EFc versus Al concentration diagrams for selected highly enriched elements are given in Figure 4.6.4. The EFc values of highly enriched elements show an inverse relation with Al concentration. The difference between these patterns and those observed in moderately enriched elements is continuous decrease of EFc with increasing Al concentration. For highly enriched elements EFc values don't level off at any Al concentration and even minimum EFc values at very high Al concentration are higher than 10.

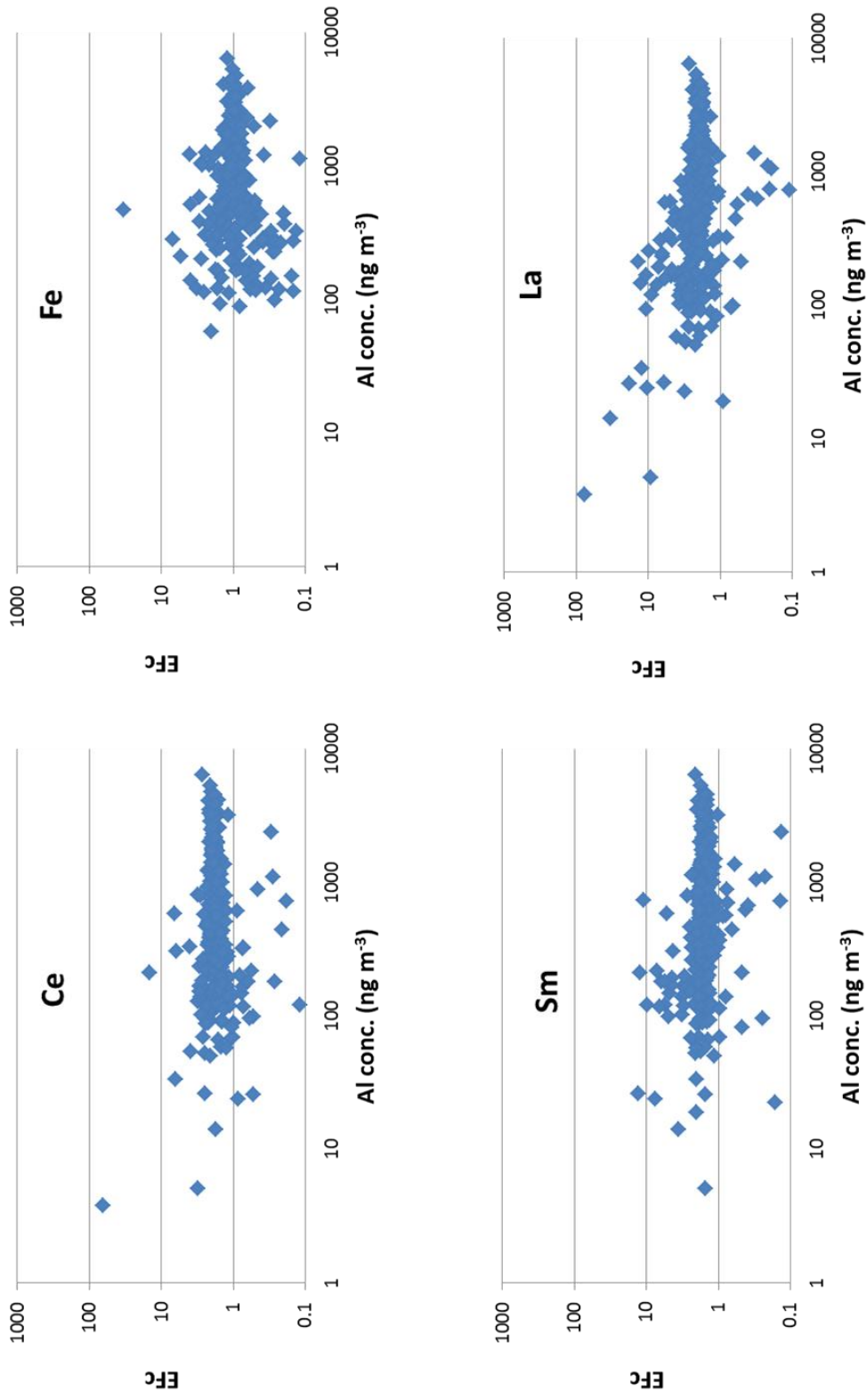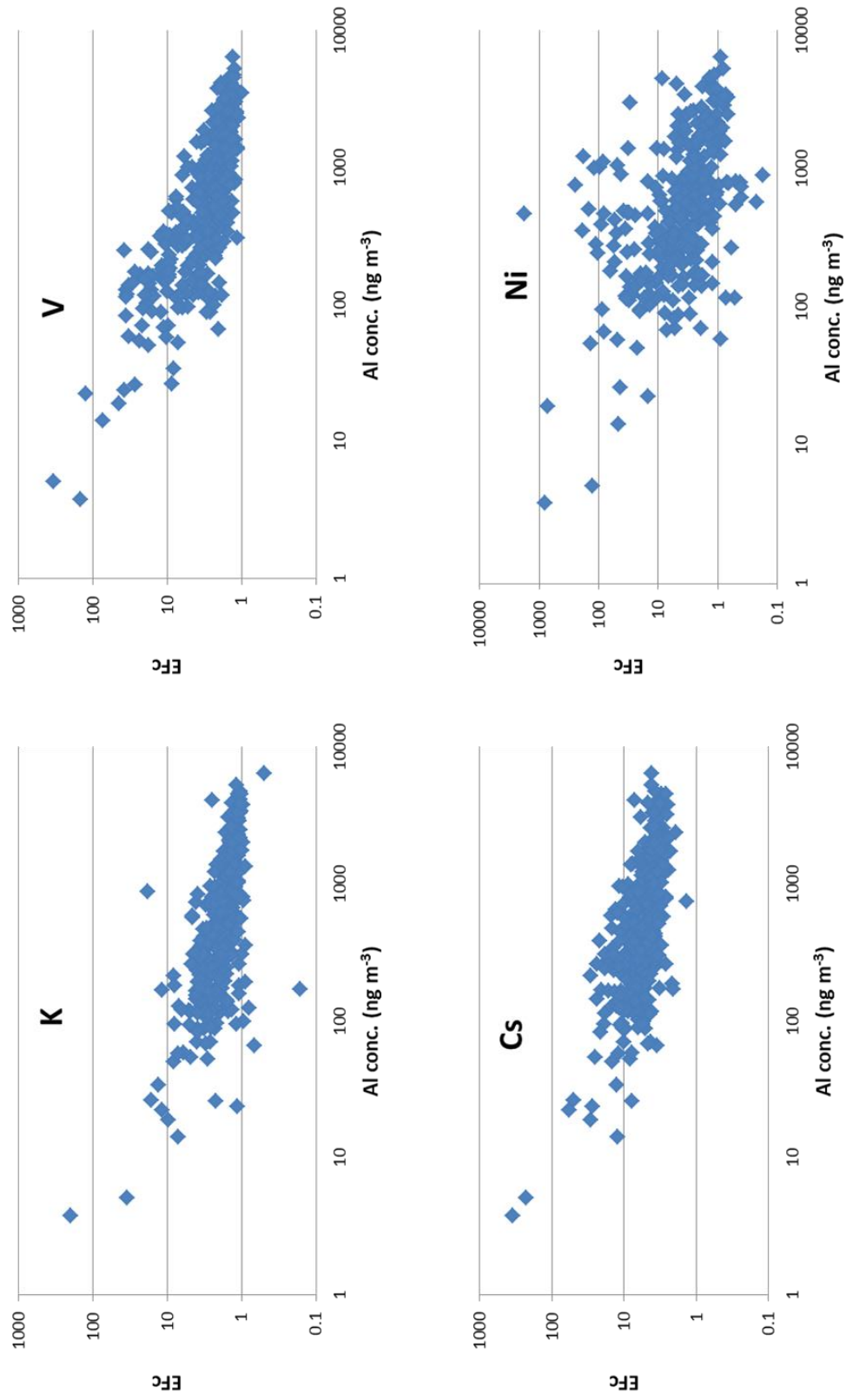Figure 4.6.2 EFc versus Al concentration of representative crustal elements

120

Figure 4.6.3 EFc versus Al concentration of representative mixed origin elements
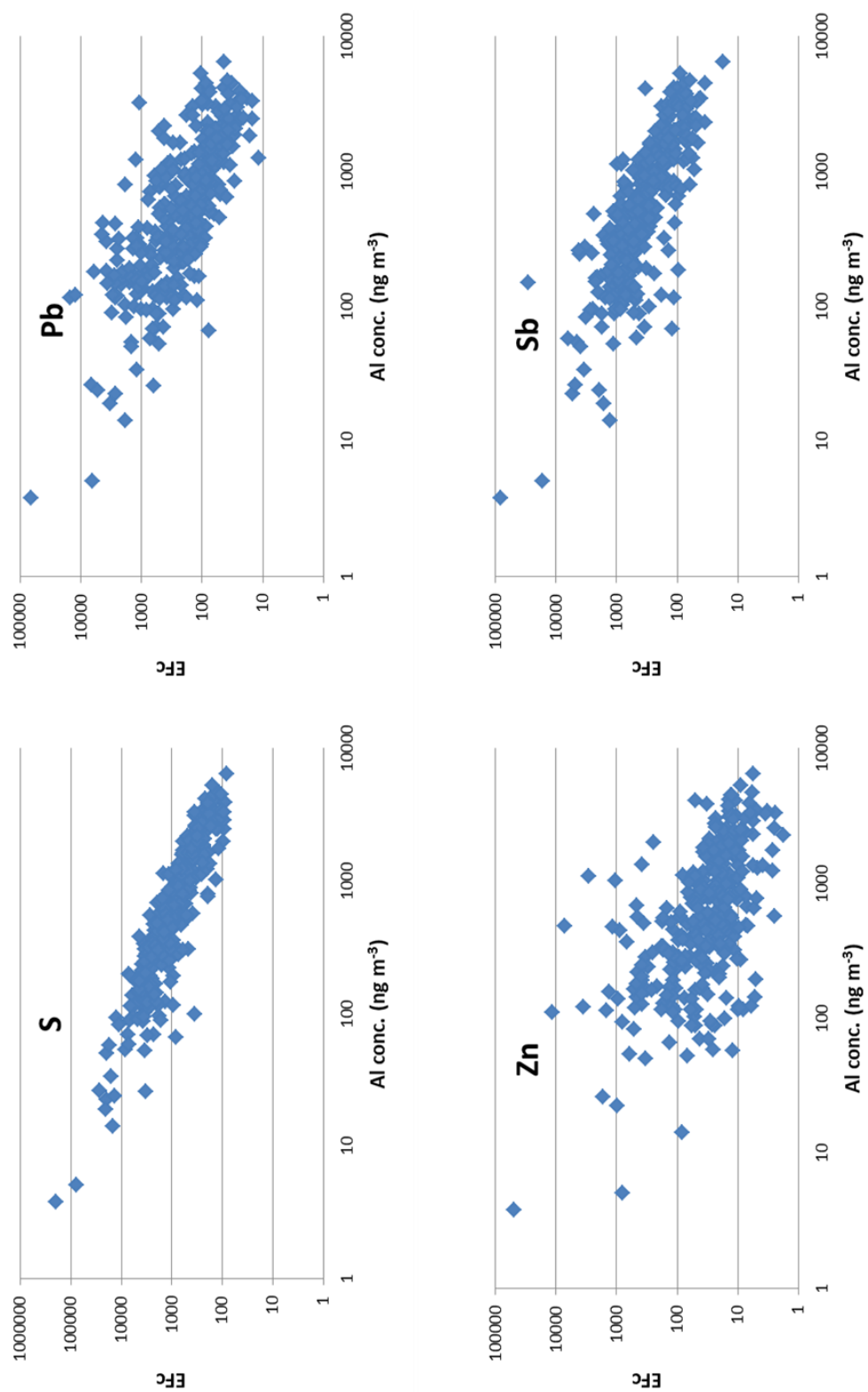
Figure 4.6.4 EFc versus Al concentration of representative anthropogenic elements

Crustal enrichment factor values of elements in summer and winter season are given in Figure 4.6.5. As seen from the figure anthropogenic elements have higher EFc in winter season. This pattern is followed by all anthropogenic originated elements with exception of W, Au and Cr. Some of the elements with mixed origin also depicted a similar pattern. Elements that have more than one source in the atmosphere measured in this study are V, Cr, Ni, Mn, Na and Mg. Among these V and Ni have high concentration in soil, but they are also good markers for residual oil combustion. Chromium and Mn are enriched in soil, but they are also enriched in emissions from steel industry. Na is marker for marine component in aerosol. Monthly median EFc of typical elements with anthropogenic and mixed origin are given in Figure 4.6.6.

Monthly variations of EFc of other pollution-derived elements are similar to those shown for Cu, Pb, Se and As in Figure 4.6.6(a), (b), (c) and (d), respectively. For this group of elements median EFc values are clearly higher in November, December, January and February. All elements that are known to have dominant man-made sources, namely Cu, Zn, Ge, As, Se, Mo, Cd, Sn, Sb and Pb have this unique, monthly EFc pattern. Higher winter enrichments of these elements are due to decrease in concentrations of crustal material and hence Al concentration in winter, which in turn is owing to more difficult resuspension of crustal aerosol from muddy or ice-covered surface soil. This feature provided a method to detect anthropogenic contribution to some other unexpected elements, which will be discussed later in the manuscript.

Different patterns are observed in monthly variation of EFc of elements with mixed origin. Since most of these elements also have anthropogenic sources, we expected to see an anthropogenic pattern, which is discussed in previous paragraph, but with a smaller difference in monthly median EFc between summer and winter months. Vanadium, Ni, Cr and Na showed this expected pattern, with higher monthly median EFc in winter months. However, Mn followed a totally different pattern. Monthly median EFc of Mn did not show any systematic variation form one month to another. This is the expected pattern for soil related elements and suggests that contribution of non-crustal sources on Mn concentrations is not significant at Kırklareli area. This is supported by the EFc – Al diagram prepared for Mn, which is depicted in Figure 4.6.6(g). The EFc of Mn is independent of Al concentration at all concentration levels, indicating that Mn is crustal in nature even at very low Al concentrations. However, Mn/Al ratio in crustal material intercepted at our station is 2.7 times higher than the Mn/Al ratio in Mason's global compilation. Since the Mn/Al ratio in Mason compilation is 0.0012, actual Mn/Al ratio in our samples should be 0.0032.

Figure 4.6.5 Summer and winter EFc of elements

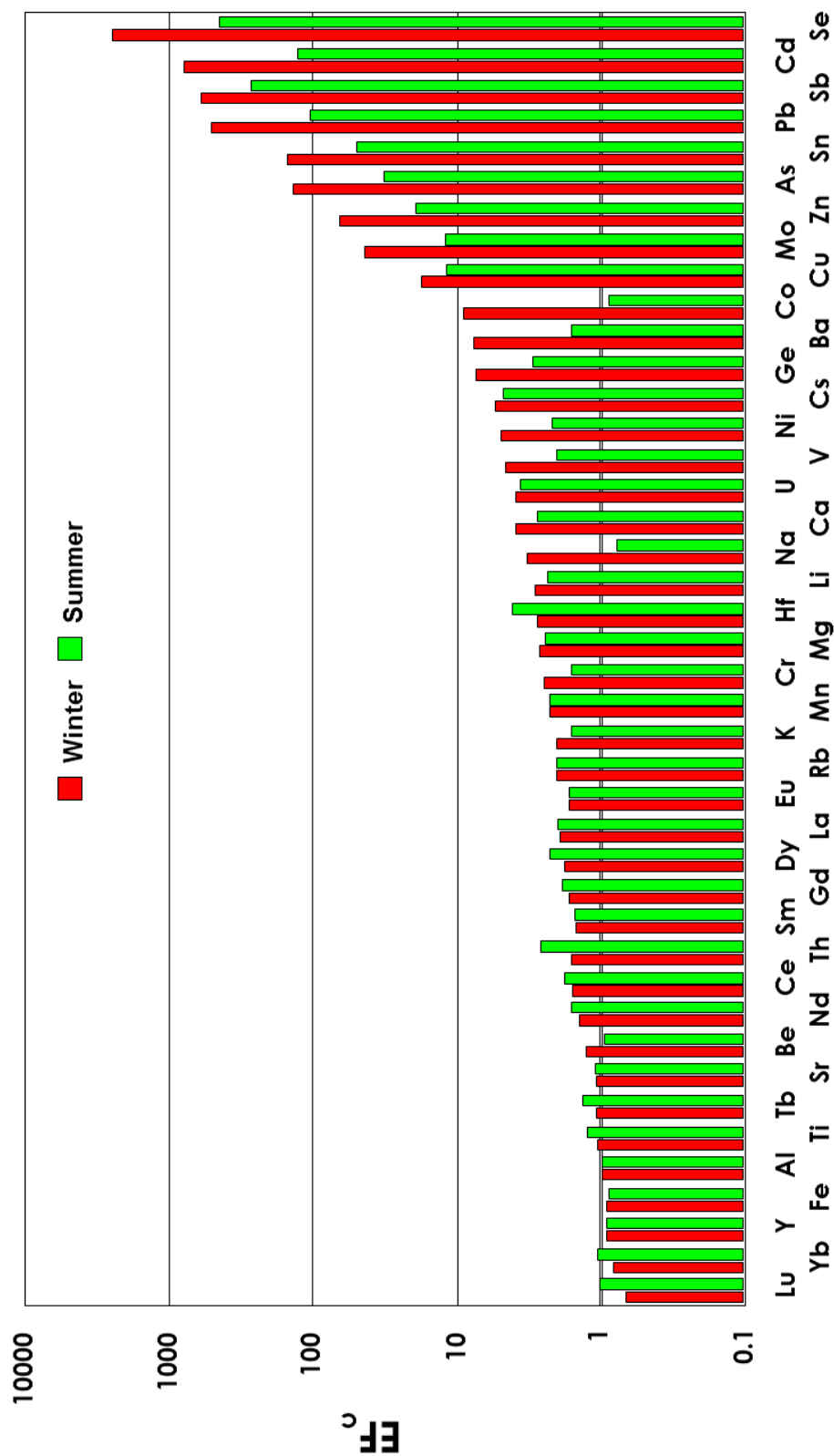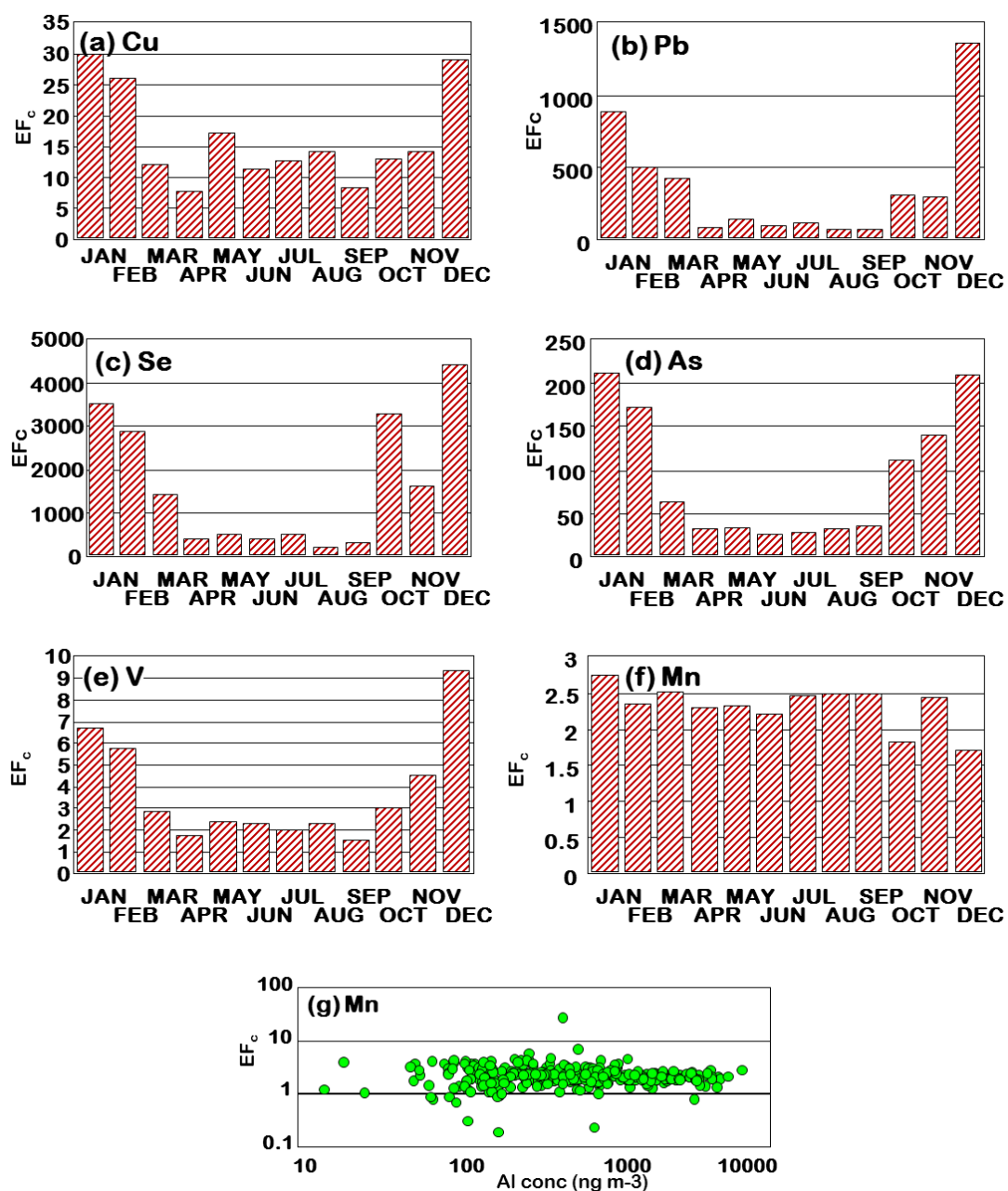Figure 4.6.6 Monthly median EFc values of elements with anthropogenic and mixed origins (a - f) and EFc –Al diagram for Mn (g)

Twenty-seven of the elements measured in this study are litophilic elements which are abundant in earth's crust. This makes soil as the most important source for them. These elements included Li, Be, Mg, Al, K, Ca, Fe, Rb, Sr, Y, Cs, La, Ce, Nd, Eu, Sm, Gd, Tb, Dy, Yb, Lu, Hf, Ta, Th and U. Average EFc for these elements varied between 0.8 for Lu and Ta and 5.1 for Cs. These elements make up non-enriched element group in our data set. Summer and winter season median EFc are comparable for most of them. However, monthly median EFc provided valuable information on the non-crustal sources of some of these crustal elements. Monthly median EFc of selected crustal elements are given in Figure 4.6.7.

Twenty-seven crustal elements showed three different monthly patterns. Monthly median enrichments of Li, Mg, Ca, K, Fe and Y, Rb, Sr, Cs, Eu, Sm, La do not change significantly throughout the year. This pattern is shown in Figure 4.6.7(a) and (b) for Fe and Rb, respectively.

However Be showed anthropogenic-like pattern, with higher EFc values in winter as seen in Figure 4.6.7(c). Beryllium is known as crustal in most of the rural studies. It probably has some anthropogenic contribution to atmospheric levels at Northwestern Turkey. This is confirmed by its EFc – Al diagram, which is shown in Figure 4.6.7(e). In this EFc -Al diagram of Be, there are two groups of EFc values. The first group decreases with increasing Al concentrations, which is typical behavior of anthropogenic elements. The second group varies independently from Al concentrations, which is typical behavior of crustal elements. The two curves merge to crustal pattern when Al concentration reaches to 200 – 400 ng m^{-3}. These clearly demonstrate that Be has non-crustal contribution to its measured concentrations. Beryllium can be emitted into the atmosphere by coal combustion or as a result of open-pit coal mining activities (Bezacinsky et al., 1984, Kram et al., 1998). These anthropogenic sources seem to affect concentrations of Be at Northwestern Turkey.

The third group of crustal elements, which consists of Ti, Ce, Nd, Gd, Tb, Dy, Yb, Lu, Hf and Th, show a very different monthly EFc pattern. These elements have slightly higher EFc medians in summer season. Examples of this pattern is given in Figure 4.6.7(d) and (f) for Ce and Nd, respectively. Summer-time enrichments of these elements are slightly higher but consistent. Such pattern can be either due to contribution of non-crustal sources, which are significant in summer only, or due to different soil types affecting our station only in summer season.

There are anthropogenic rare-earth sources. Olmez and Gordon (1985) demonstrated that rare earth elements and ratios between them can be used as markers for oil combustion and refinery emissions. The source of rare earth emissions from refineries was zeolite catalyst used in the process. Later rare earth elements were used to differentiate refinery and oil combustion emissions in a number of ambient aerosol measurements (Pandolfi et al., 2011, Moreno et al., 2010, Kitto et al., 1992). In this study average La/Sm ratio was very close to crustal ratio which is 6.3 (Olmez and Gordon, 1985), indicating that on the average crustal component is the main source of REEs. However, there are 16 REE episodes in the data set, where La/Sm ratio increase up to 20 which is the ratio measured in refinery emissions. Some, but not all of them also corresponds to V episodes, which is a good marker for oil combustions. Some of the REE anomaly in our data set is probably due to existence of refinery emissions and oil combustion. However, timing and frequency of these anthropogenic REE episodes cannot explain higher REE EFc observed in summer.

Slight summer enrichment of REEs in our data set probably indicates different crustal component affecting our sampling site in summer and winter seasons. Tuncel et al. (1989) used REE composition of atmospheric particles to identify different types of crustal material affecting Amudsen Scott station in Antarctica. Vieira et al. (2012) demonstrated different REE composition of Saharan dust sampled at their Azores station at Atlantic Ocean.
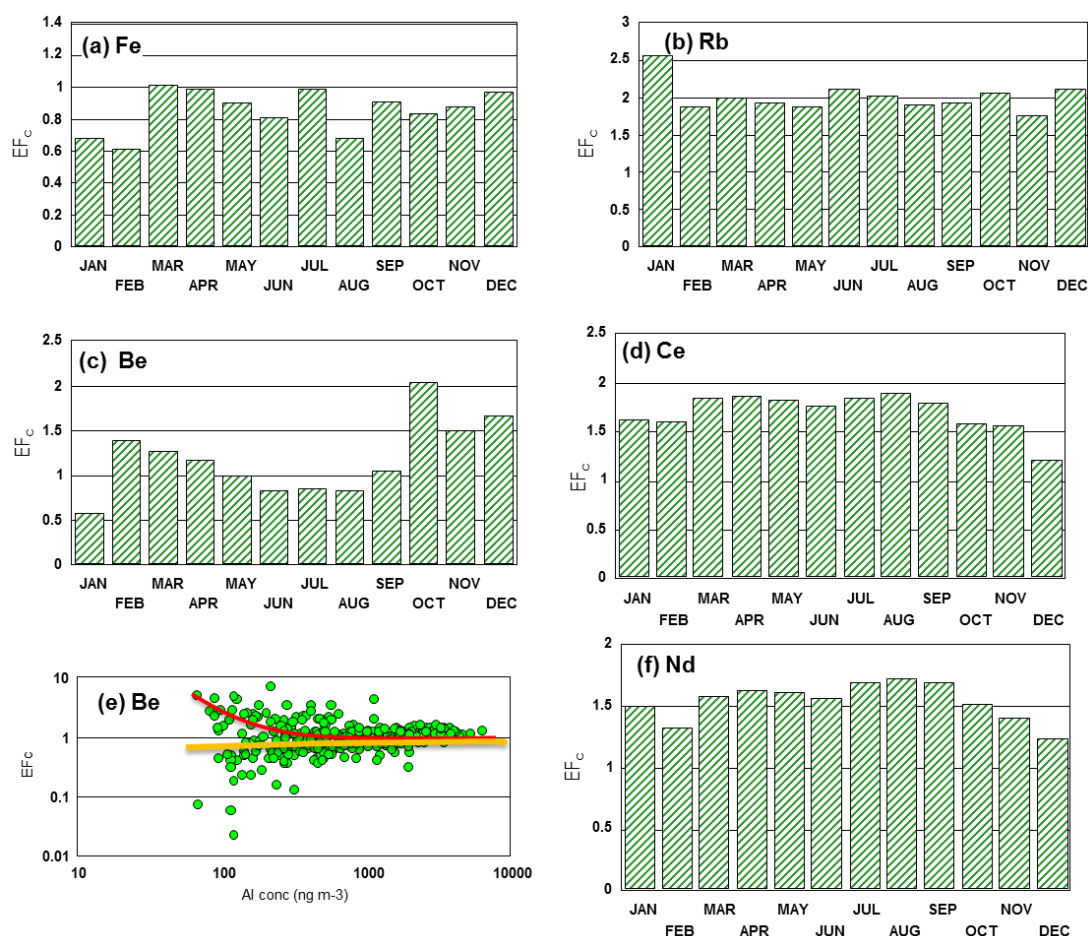
Figure 4.6.7 Monthly median EFc values of crustal elements

Similarly Trapp et al. (2010) also showed different REE composition of Saharan Dust sampled at North America. Rare earth element composition of environmental samples were used to differentiate different types of crustal material in other studies as well (Aubert et al., 2006, Li et al., 2009).

Slight enrichment of REEs in summer season is probably due to more frequent arrival of Saharan dust to Northwestern Turkey in April and May which is included in our summer season. Differences between summer and winter EFc of REEs is very small, which makes isolation of different soils a difficult task. Positive matrix factorization, which will be discussed extensively in Section 4.6.2, attempted to isolate two crustal factors, one of which explained most of the variances of REES. Although we believe that this component probably represent Saharan dust intrusions to our sampling location, factor scores were strongly correlated with the scores of the other crustal factor, indicating that PMF is not able to isolate the two crustal factors. Uncertainties of REEs are increased and the factors were pushed into one.

4.6.2. **Positive Matrix Factorization**

Since the PMF, how it is executed and how data and uncertainty files are prepared is explained in Section 3.5.2, it will not be repeated here. Bismuth, Er, and Se were excluded from the analysis by assigning their category as "bad" because these species were missing in more than 25% of samples. Species with missing values less than 25% were replaced with geometric mean value and 4 times the geometric mean was used as corresponding uncertainty value for that datum. BDL values were treated by replacing with DL/2 and assigning uncertainty as 5/6xDL. Note that the number of samples with BDL is less than 20%, so no species were excluded due to BDL value. The summary of the data used in PMF model is given in Table 4.6.1. Some species were measured by both ICPMS and IC, i.e Na, K, Mg and Ca. Concentrations of these species measured by ICPMS were used in PMF analysis. Water soluble forms of Na, K, Mg and Ca were assigned as "bad" and hence excluded from the analysis.

In the beginning 345 samples were included in PMF, however in the data set there were large outliers that could not be modeled. These outliers were excluded and finally 313 samples were retained in PMF. Tin, Sb, P, Ni and Mo were also excluded as these species were not modeled well (coefficient of determination was below 0.30 for observed to predicted regression analysis) within acceptable performance limits. Forty-four elements and ions were included in PMF. Twenty-two of these elements and ions were assigned as "strong" and other half were assigned as "weak" (see Section 3.5.2).

Different numbers of factors (from 3 to 9 factors) were tested in PMF model. Solution with 5-factors was selected as optimum based on the closeness to the performance criteria in PMF analysis. Unlike in factor analysis, the approach that can be used to select optimum number of factors in PMF is not well defined and not easy. The approach commonly used is to compare the model outputs against some predefined performance criteria. These criteria includes closeness of theoretical Q values and model generated Q values, number of observations that are beyond the 0 ± 3.0 limit in distribution of scaled residuals, closeness of the observed and predicted concentrations of elements and particle mass, investigation of correlations between factor scores (or G-scores) and the proven robustness of generated factors in bootstrapping test.

Bootstrapping is rather new tool to test the stability of factors generated in PMF. In this study, stability of the PMF solution was tested by bootstrapping with 100 iterations. The threshold value of 0.6 was used as coefficient of determination value for assigning bootstrap factor to base run factor (see Section 3.5.2 for bootstrapping). As seen in Table 4.6.2, only for Factor 2 and Factor 3, 2 out of 100 bootstrap factors were not mapped to the base solution. The variability of bootstrap factors is plotted as box and whisker plot in Figure 4.6.8. As seen from the figure the variability in the bootstrap runs is less, note that 25th to 75th percentile of data is close to 1 (here 1 refers to the base run).

Table 4.6.1 Percentage of missing and BDL values and S/N ratio for the variables used in PMF analysis

Species	Category	S/N ratio	Min	Median	Max	% of Missing Values	% of BDL Values
Li	Strong	3.9	0.015	0.423	4.263	2	2
Be	Weak	1.9	0.001	0.021	0.302	14	4
Na	Strong	4	42	300	3489	0	10
Mg	Weak	8	8	278	4980	0	1
Al	Strong	6.7	7	519	6524	0	1
P	Bad	1.2	3	23	261	17	8
K	Strong	6.8	10	339	2009	0	1
Ca	Weak	2	108	792	7809	5	11
Ti	Weak	3.9	0.57	35	471	3	2
V	Weak	8.1	0.23	2.9	16	0	0
Mn	Weak	5.8	0.099	15	232	1	0
Fe	Weak	1.4	17.5	362	4859	24	5
Ni	Bad	5.9	0.379	2	206	6	18
Cu	Weak	3.3	0.06	5.6	51	1	1
Zn	Weak	1.6	0.903	16	148	8	4
Ge	Strong	3.8	0.001	0.047	0.198	1	1
As	Strong	2.5	0.003	0.741	4.6	3	0
Se	Bad	1.1	0.012	0.298	1.8	28	3
Rb	Weak	8.6	0.075	1.3	12	0	0
Sr	Weak	2.7	0.023	2.5	23	3	0
Y	Strong	6.1	0.004	0.178	3.4	1	1
Mo	Bad	8.8	0.015	0.193	70	0	2
Cd	Strong	3.9	0.006	0.338	7.9	3	1
Sn	Bad	6.4	0.041	0.95	45	2	1
Sb	Bad	3.5	0.011	0.475	11	1	0
Cs	Weak	8.2	0.006	0.114	1.01	0	0
La	Weak	5.5	0.009	0.404	6.5	1	1
Ce	Strong	4.7	0.016	0.651	13	2	2
Pr	Strong	5.7	0.002	0.068	1.4	1	2
Nd	Strong	6.2	0.006	0.253	5.3	1	2
Eu	Strong	3.2	0.003	0.015	0.28	1	18
Sm	Strong	5.7	0.001	0.06	0.99	1	1
Gd	Strong	6.2	0.001	0.058	1.17	1	0
Tb	Strong	4	0.0002	0.007	0.126	3	2
Dy	Strong	3.1	0.0002	0.043	0.704	5	0
Ho	Strong	2.8	0.0002	0.008	0.115	5	4
Er	Bad	1.4	0.0002	0.022	0.312	34	2
Tm	Strong	3.7	0.0001	0.003	0.043	2	2
Yb	Strong	3.9	0.0003	0.022	0.261	2	2

Table 4.6.1cont. Percentage of missing and BDL values and S/N ratio for the variables used in PMF analysis

Species	Category	S/N ratio	Min	Median	Max	% of Missing Values	% of BDL Values
Lu	Weak	1.8	0.0001	0.003	0.035	15	2
Hf	Weak	3.7	0.004	0.071	0.639	2	5
Tl	Weak	7.8	0.003	0.069	0.39	0	0
Pb	Strong	6.1	0.829	15.4	287	0	0
Bi	Bad	1.1	0.005	0.046	0.654	57	11
Th	Weak	2.5	0.003	0.11	2	11	3
U	Strong	2.8	0.008	0.045	0.348	1	17
Cl	Strong	2.4	11.5	334	4193	5	1
NO3	Weak	4.6	160	2362	8715	0	0
SO4	Weak	4.4	337	5583	16635	0	0
sol_Na	Bad	6.4	2.8	172	2468	0	1
NH4	Weak	8	242	1759	5958	0	0
sol_K	Bad	6.8	17	125	639	0	0
sol_Mg	Bad	4	2.5	92	493	2	0
sol_Ca	Bad	4.6	39	521	2601	0	0
BC	Weak	2.6	23	530	1547	1	0
PM	Weak	1.5	2500	45233	256392	5	3

Table 4.6.2 Bootstrap factors mapped to base factors

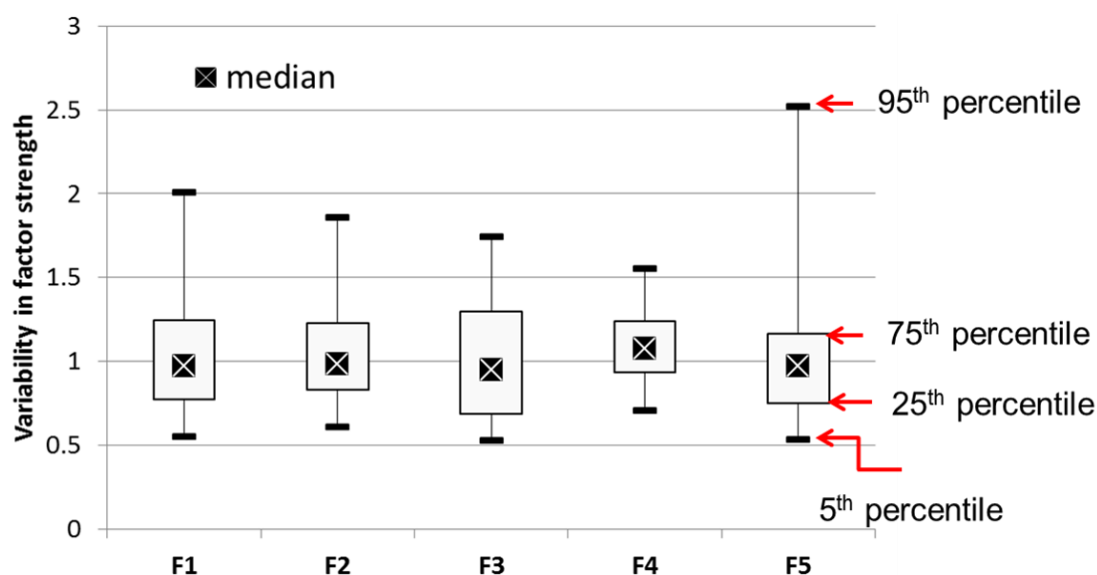|	Base F1	Base F2	Base F3	Base F4	Base F5	Unmapped
Boot. F1	100	0	0	0	0	0
Boot. F2	1	95	2	0	0	2
Boot. F3	1	0	97	0	0	2
Boot. F4	0	0	0	100	0	0
Boot. F5	1	0	0	0	99	0

Figure 4.6.8 Variability in the factor strengths of PMF resolved factors from 100 bootstrap runs

The theoretical Q value ($Q_{theoretical}$) of 11987 were very close to the true Q value obtained via model, which was 15519.2, (see Section 3.5.2 for definition of Q values). Residuals were in the range of -3 to +3 for most of the species. This spacing of residuals were found acceptable in most PMF applications (EPA, 2008). Observed to predicted plots of each species were examined and given for some representative species in Figure 4.6.9, Figure 4.6.10 and Figure 4.6.11. The agreement between measured and calculated concentrations of elements is close, which implies that 5 factor solution is adequate. Scatter plots of G-scores between factors which is called as G-space plots were also examined. These plots are presented in Figure 4.6.12. G-space plots demonstrate the presence or absence of autocorrelation between factors. If two factors are auto-correlated, then there may be a chance for these two factors to represent one single source. When the PMF was run with 6 factors, the sixth factor turned out to be a crustal factor which explained most of the variances of rare-earth elements. This factor was very exciting, because if this was a valid factor it was demonstrating that rare earth elements are good tracers for Saharan Dust. Since people have been trying to find elemental signatures of Saharan dust, without success, for a long time, the rare-earth factor would be a very significant finding. Unfortunately, factor scores of the rare-earth element factor was highly correlated with the other crustal factor. Then we increased the uncertainties of rare earth elements and pushed the rare-earth factor to merge with the other crustal factor. The crustal factor, which will be discussed below is generated by the merging of the crustal factors. The correlation of scores of the two crustal factors does not necessarily mean that rare-earth elements are not good tracers of Saharan dust, it simply shows that PMF cannot separate it from other crustal sources. G-space plots given in Figure 4.6.12 clearly demonstrate that these five factors are not auto-correlated.
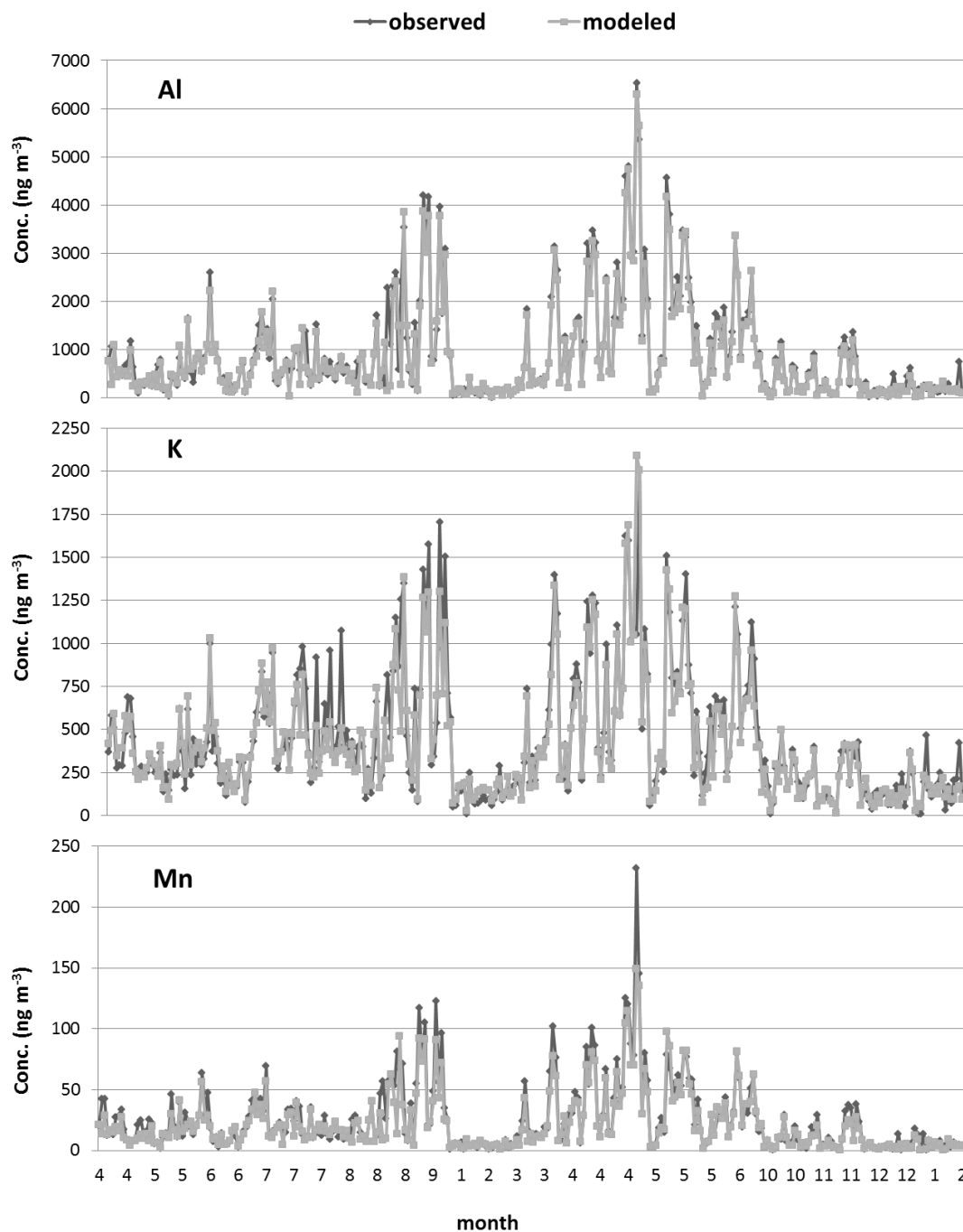
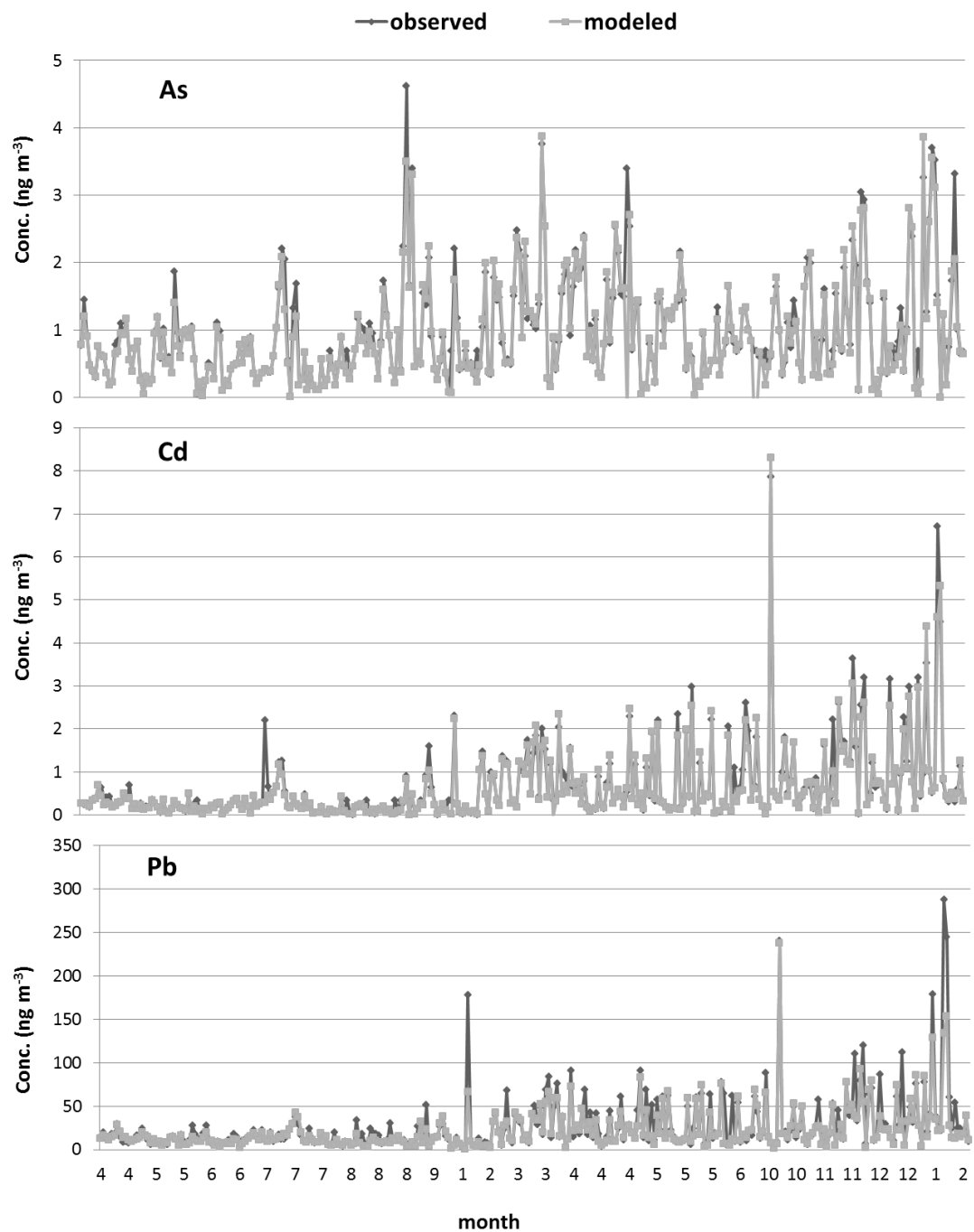Figure 4.6.9 Measured and modeled concentrations of selected species

132

Figure 4.6.10 Measured and modeled concentrations of selected species (continued)
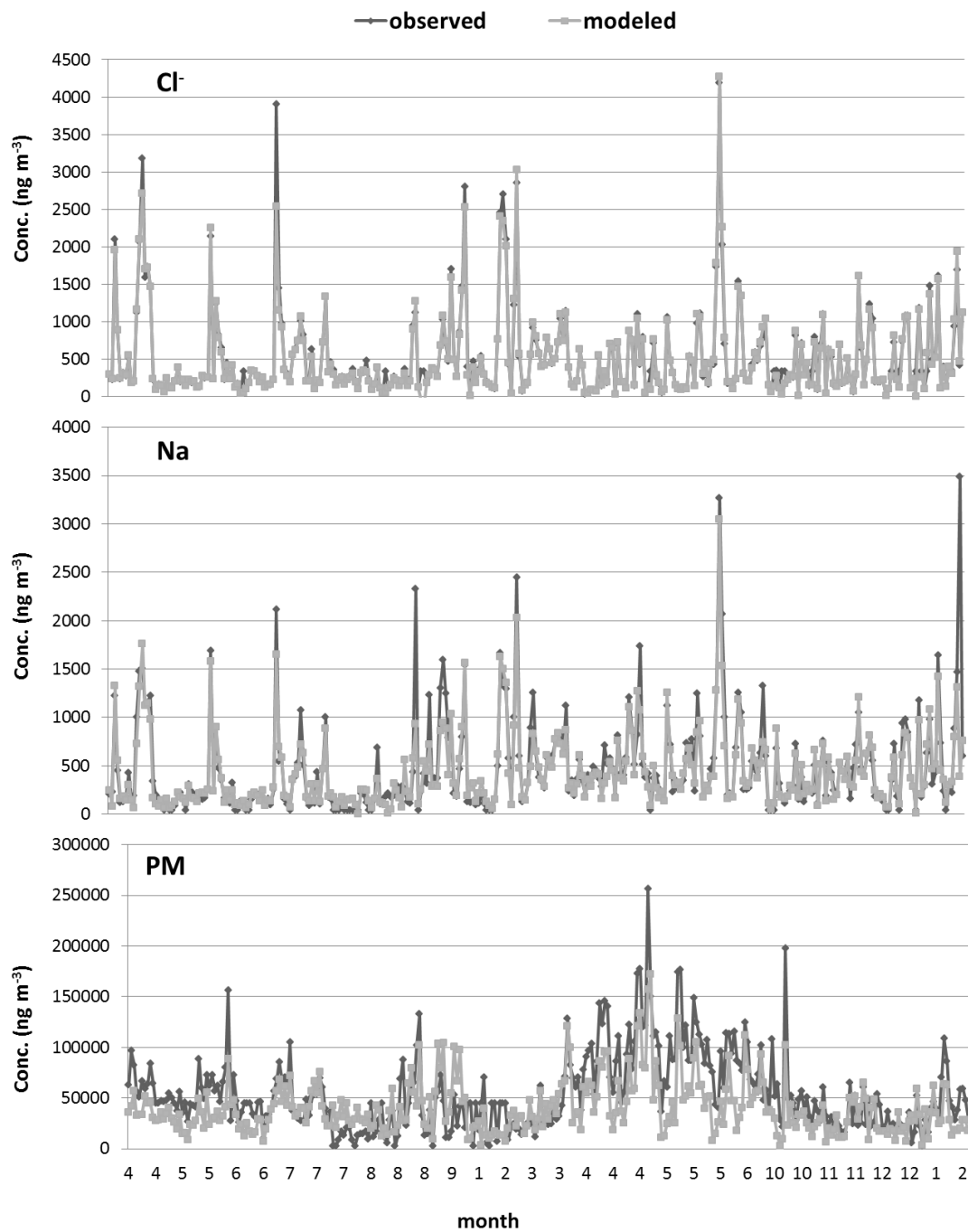
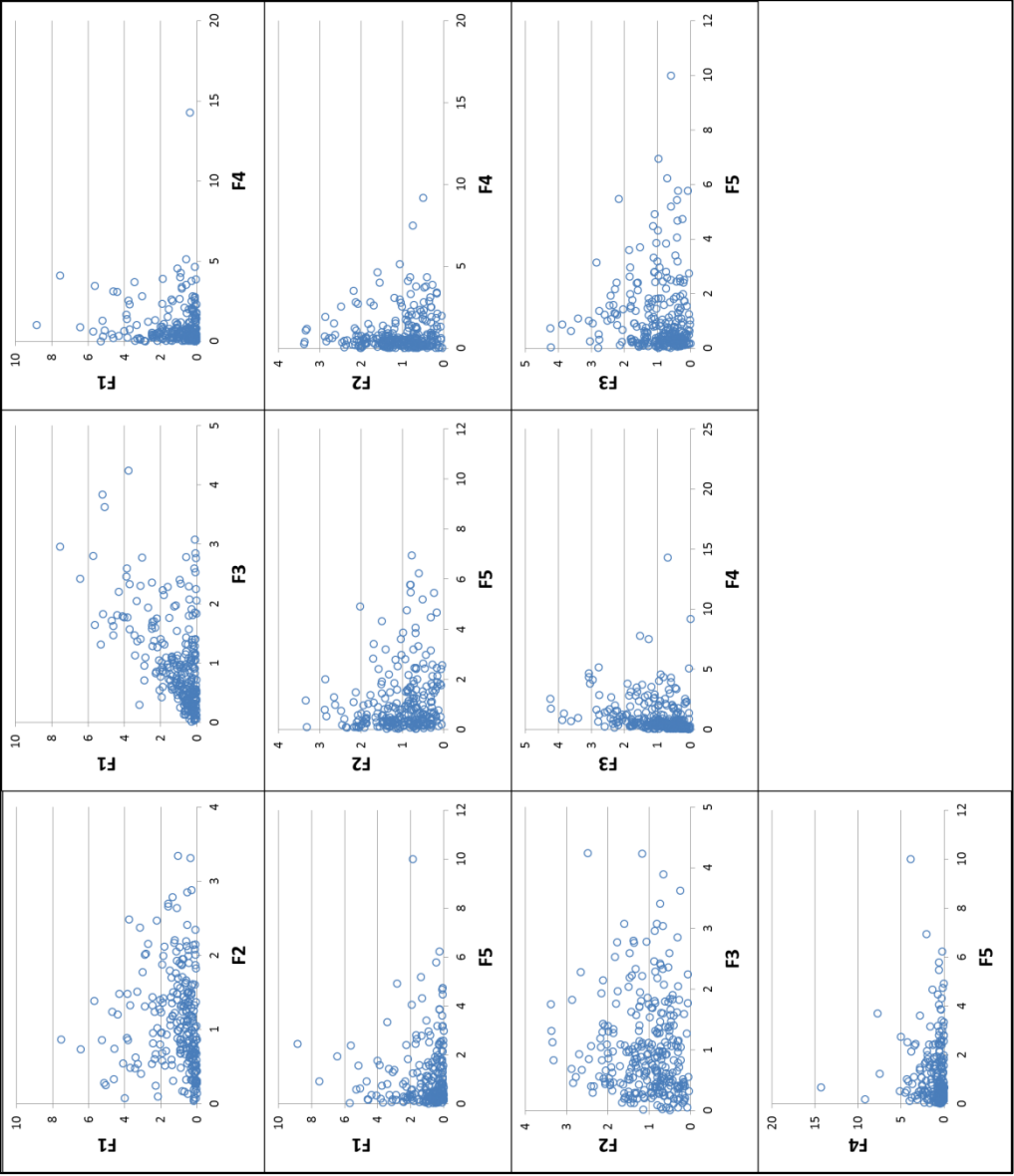Figure 4.6.11 Measured and modeled concentrations of selected species (continued)

134

Figure 4.6.12 G-space plots

135

One important step in PMF model is identification of physical meaning of factors. There is no well-established method for that. Identification of some of the factors is relatively simple. For example a factor containing high concentrations of litophilic elements can be easily identified as crustal or soil, because there is not many sources that can emit all litophiles in high concentrations. A factor primarily consists of Na and Cl⁻ can also be easily identified as marine source. However, identification of factors representing anthropogenic sources is not as straightforward, because many of the pollution-derived elements are emitted from more than one source. Mixing of particles emitted from different sources during their transport to sampling point is another complicating factor.

In this study, concentrations of elements in factors (also called factor loadings), fractions of variances of elements explained by each factor (or fractions of elements accounted for by factors), enrichment factors (EFc) of elements in factors, monthly variations of G-factor scores and trajectories that correspond to the highest values of G-scores for each factor are investigated to assign a physical meaning for the five factors generated by PMF.

Fractions of elements accounted by each factor is given in Figure 4.6.13. The first factor explains > 80% of the variances of crustal elements including, Ti, Be, Al, Fe, Mg and rare earth elements. It is obvious that this factor represents the crustal material. More than 75% of Mn, 60% of Ca, 55% of K are also accounted by this factor. These are crustal elements to see them in this factor is not surprising. As discussed in Section 4.2.1, Al, Ti, Fe and rare earth elements can be used as signatures of dust intrusion, considering that high percentages of these markers are explained in the soil factor, we may conclude that Factor 1 represents the mixed soil dust which is a mixture of local dust and long range transported dust (Öztürk et al., 2012). This factor will be referred to as "crustal" factor in the remainder of the manuscript.

Small fractions of pollution-derived elements are also accounted for by Factor 1. The percentages of anthropogenic elements accounted for by Factor 1 are: V (40%), Ge (15%), BC (10%), Tl (9%), Zn (9%), Pb (4%) and SO_4^{2-} (2%). This contribution is expected for two reasons. First these so called anthropogenic elements also occur in small concentrations in soil as well. Normally, their crustal fractions are not significant when PM10 or PM2.5 particles are collected, because crustal mass is not very much in fine fraction samples. However, PM samples were collected in this work, which means there is very large contribution of crustal material in our samples. Because of this, crustal fractions of pollution-derived elements may become important. Secondly, there is always a mixing of anthropogenic particle during transport of soil particles to the station. Naturally, the opposite is also true (crustal particles mix with anthropogenic aerosol during transport). Because of this there is always some anthropogenic fraction in crustal factors and some crustal elements in anthropogenic factors. This mixing is also reported for Mediterranean aerosol (Koçak et al., 2012 and references therein).

Crustal Enrichment factors of elements in Factor 1 are given in Figure 4.6.14(a). As can be seen in the figure, none of the elements are significantly enriched in Factor 1 (Crustal). Species concentrations in Factor 1 are given in Figure 4.6.15. Note that for species concentration and enrichment factor (EF) plots, semi-log scale is used due to large variation between the species concentrations and EF values. EF values were calculated by Mason soil composition (Mason and Moore, 1982) considering Al as reference crustal element. Please note that for some species (e.g., NH_4^+, NO_3^-, BC and Tl) EF values could not calculated as crustal abundance are highly variable. The monthly variations of Factor 1 scores (or G-scores of Factor 1) (averaged to 1) are given in Figure 4.6.16 is a typical pattern for soil related sources.

The second factor explains more than 50% of NH_4^+, SO_4^{2-} and NO_3^- (Figure 4.6.13). This indicates that this factor is an anthropogenic factor, which is dominated by secondary pollutants. The factor also accounts for 64% of Tl, 44% of BC, 37% of Cu, 33% of K and 15% of Ge. Crustal Enrichment factors of elements in Factor 2 are given in Figure 4.6.14. Sulfate, Pb, Zn, Cu, Cs, U, Ge, Hf and K are moderately-to-highly enriched in Factor 2. Monthly variation of Factor 2 scores is given in Figure 4.6.16. Factor 2 scores are profoundly high in summer months compared to winter. As pointed out earlier in the manuscript, long range transport is more favored in summer, because it is limited in winter season owing to enhanced wet scavenging of aerosol from atmosphere by frequent rain events. This suggests that Factor 2 represents transport from distant anthropogenic sources rather than local ones. Since aerosols emitted from local sources are not affected from scavenging as much as the ones emitted from distant sources and spent long days in the air before they reach to sampling point, their summer and winter concentrations are expected to be fairly similar. Higher summer concentrations are attributed to distant sources in many studies performed in the Mediterranean atmosphere (Gullu et al., 1998, Karakas et al., 2004, Öztürk et al., 2012).
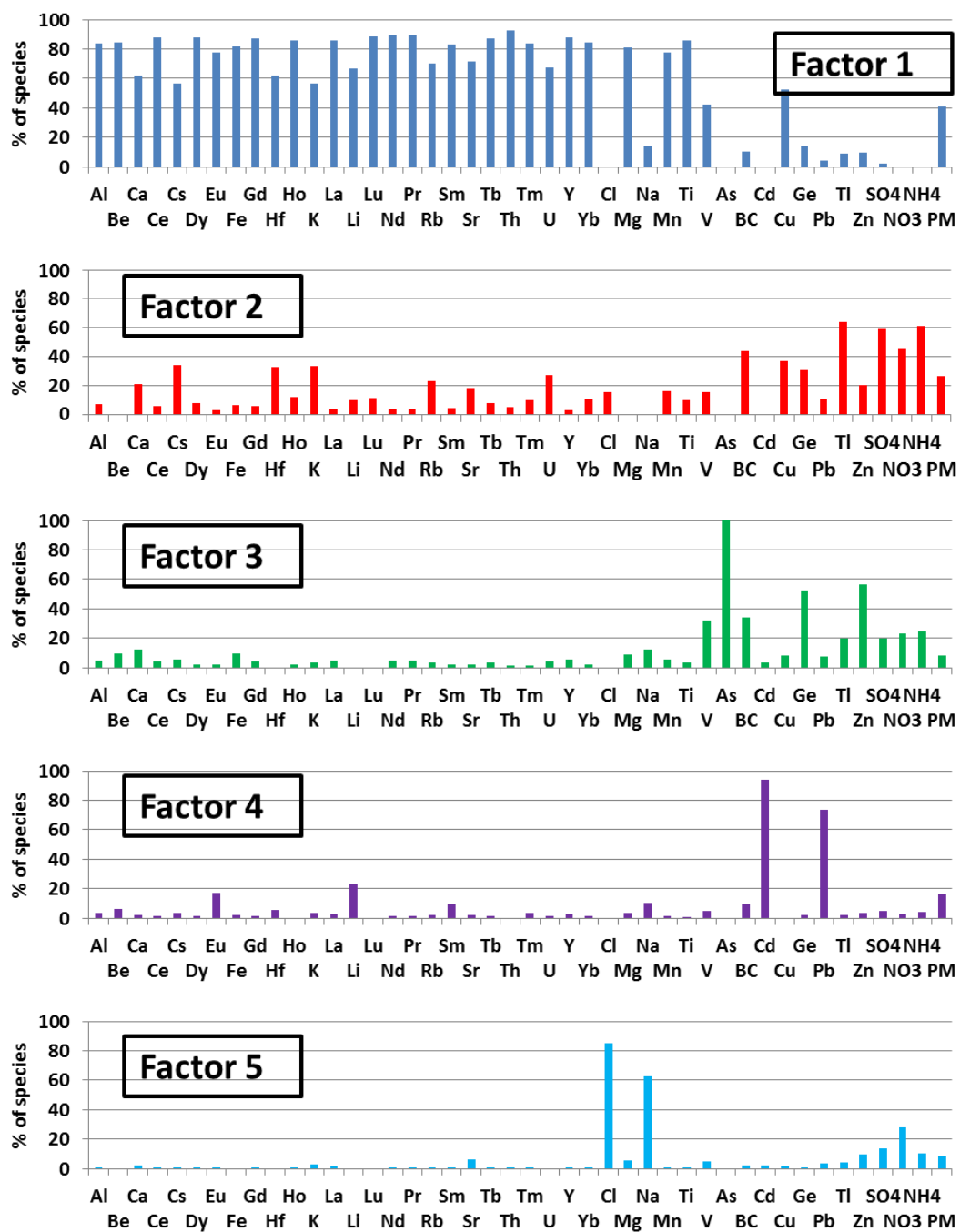
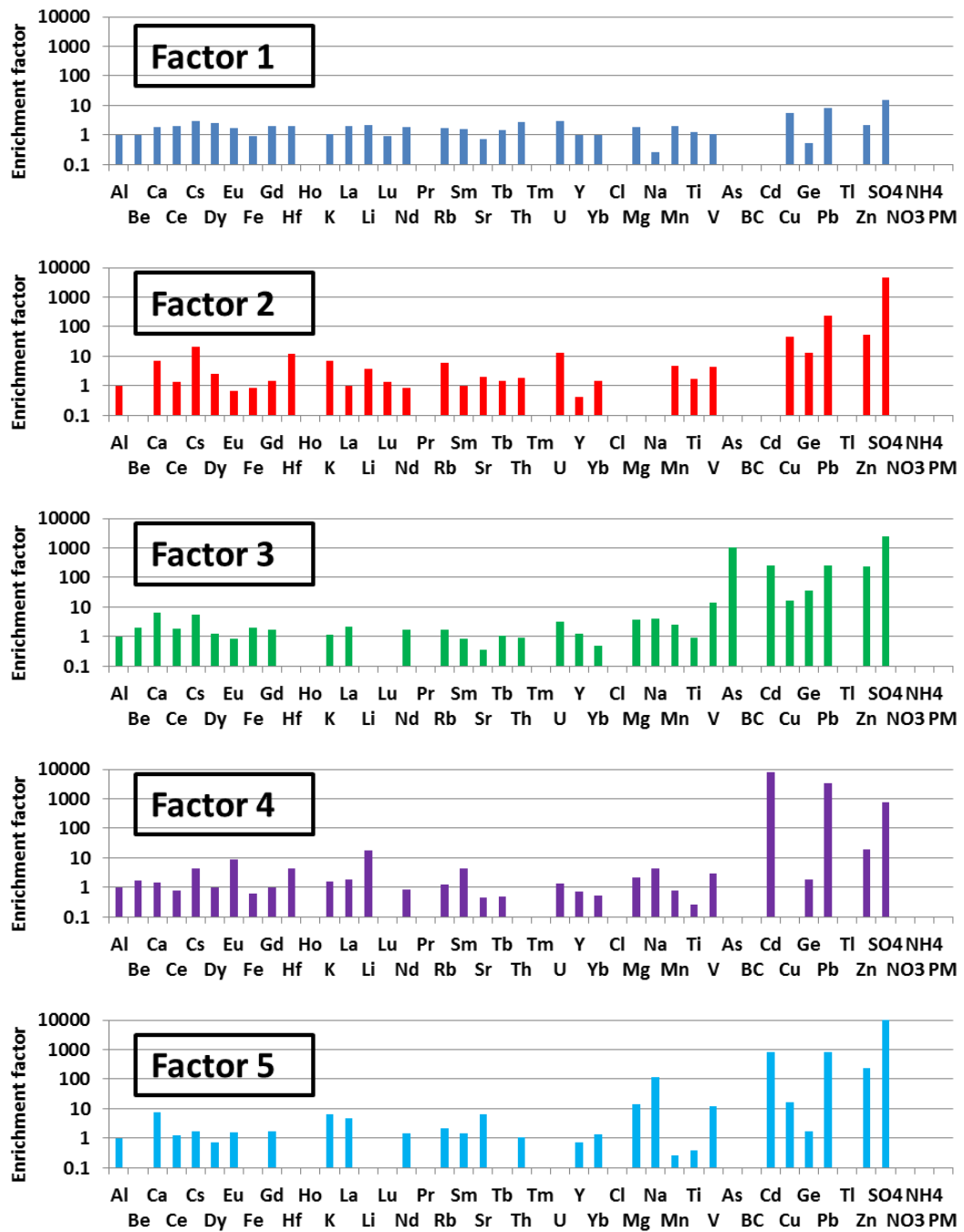Figure 4.6.13 Fractions of elements explianed by each factor

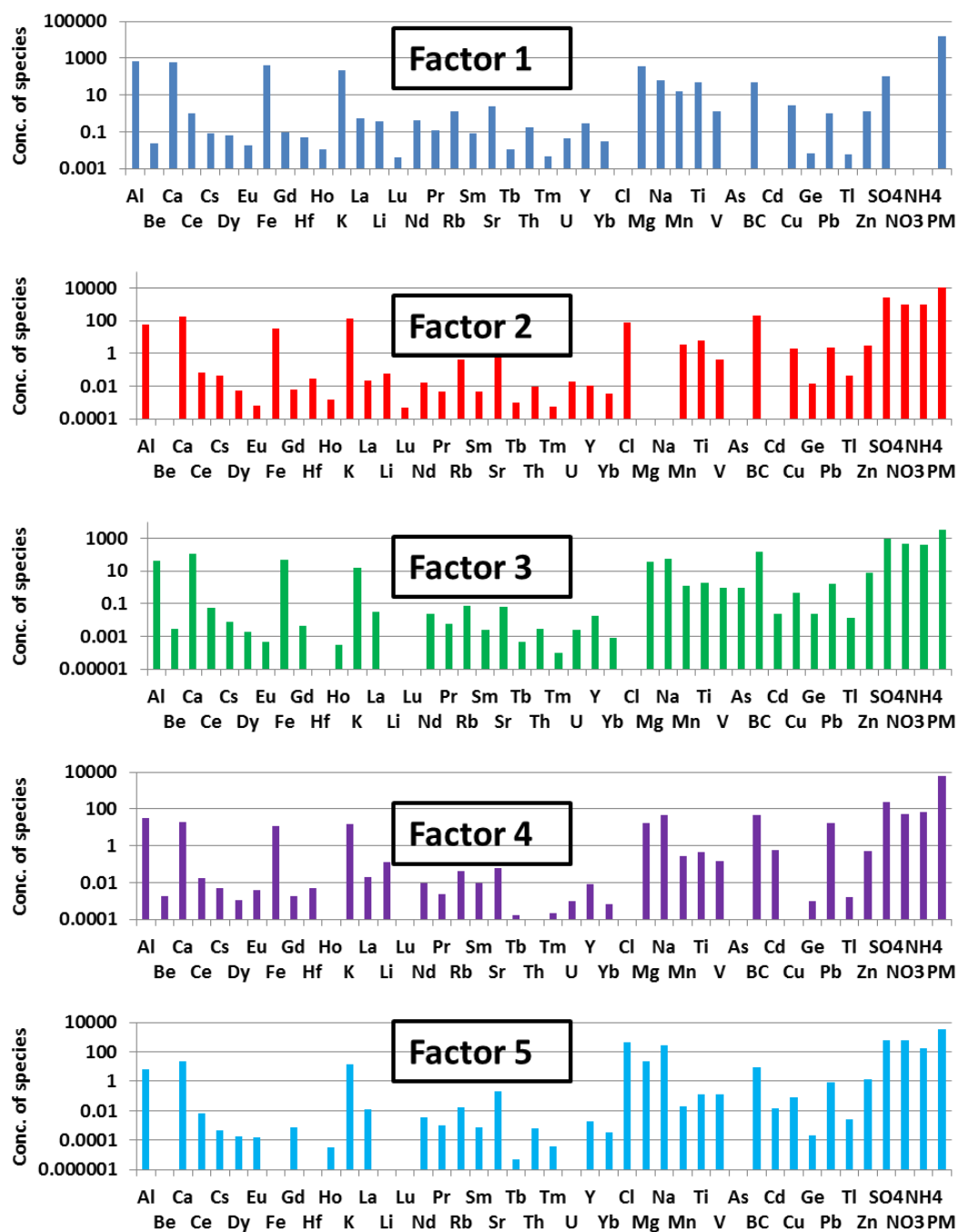Figure 4.6.14 Crustal enrichment factors of elements in each factor

Figure 4.6.15 Composition of five factors found in PMF
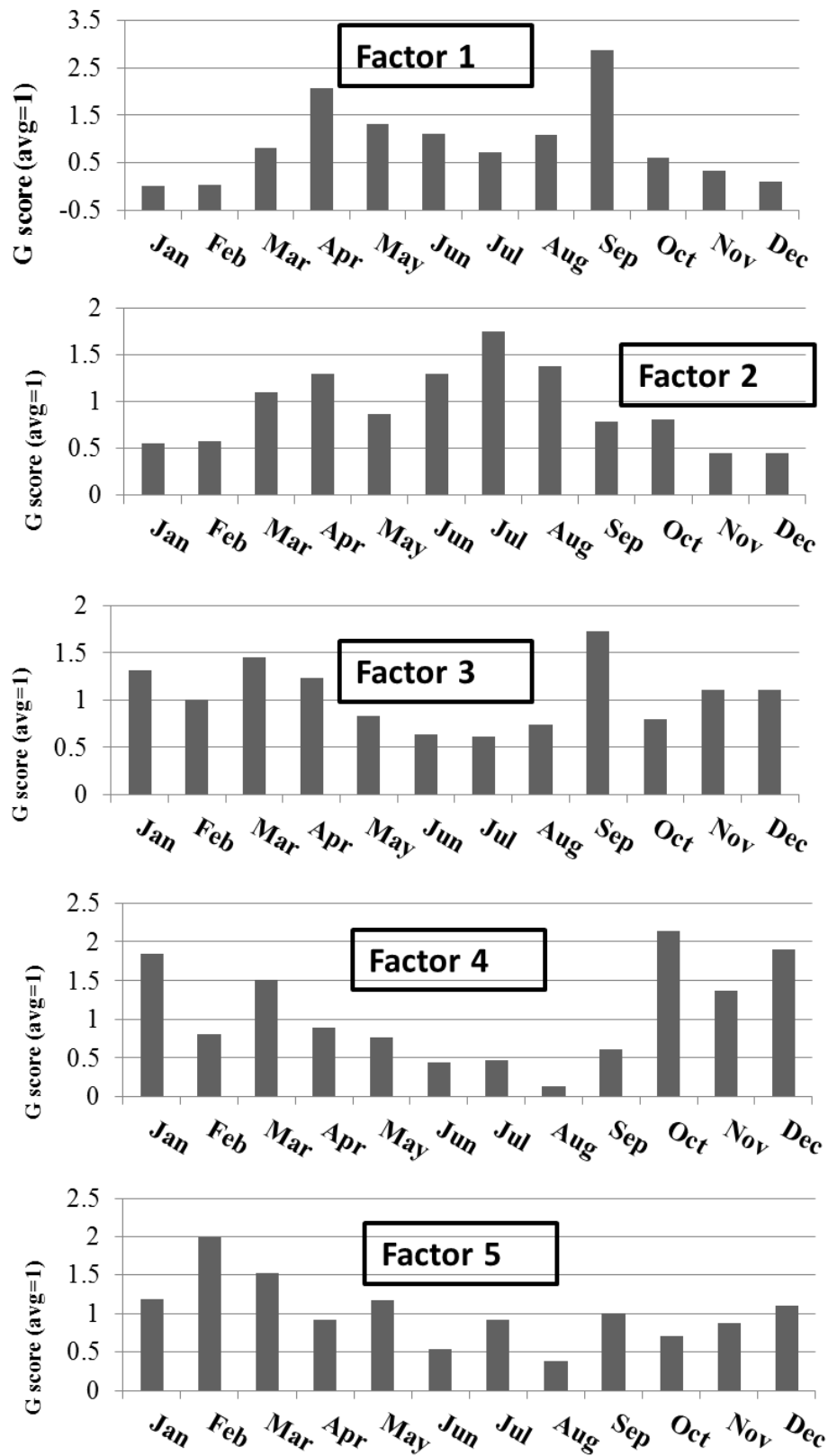(concentrations are in ng m^{-3})

Figure 4.6.16 Monthly variation of G-scores

Fractions of elements accounted for by Factor 3 are depicted in Figure 4.6.13. Factor 3 explains about 100% of As and more than 50% of Zn and Ge. The other major species contribution to Factor 3 in the descending order is: BC (34%), V (32%), NH_4^+ (25%), NO_3^- (24%), Tl and SO_4^{2-} (20%). Enrichment factors of elements in Factor 3 are given in Figure 4.6.14. Arsenic, SO_4^{2-}, Cd, Pb, Zn, Ge and Cu are highly enriched in Factor 3. In the literature As, Ge and Zn is reported as the primary markers of coal combustion with contributions of Tl, Cd, Cu, Mn and Pb whilst V is reported as the marker of oil combustion (Pacyna and Pacyna, 2001). Higher G-scores values in winter indicates that Factor 3 is a "local" source rather than distant. Please note that here "local" does not necessarily mean immediate vicinity of the station. Back trajectories corresponding to the highest 25th percent G-scores of Factor 3 (see Figure 4.6.17) clearly show that air masses were from all directions but highlighting the air masses from western part of Turkey and Balkan countries which are referred as "local" in this discussion. Based on these discussions Factor 3 is identified as local anthropogenic sources mainly related with stationary combustion sources, e.g. power plants, boilers, stoves and furnaces.

Fractions of elements explained by Factor 4 is given in Figure 4.6.13. Factor 4 explains high fractions of two important elements, namely, Cd (94%) and Pb (74%). Soil related species also contributes to Factor 4 but their contributions are moderately less. Enrichment factor plots shows that Cd, Pb, and Zn are highly enriched. Higher winter G-scores values (Figure 4.6.16) and non-directional back trajectories (Figure 4.6.17) indicates "local" anthropogenic sources for Factor 4. Simultaneous enrichments of Pb, Zn and Cd is attributed to traffic emissions in a number of studies (Hjortenkrans et al., 2007, Minguillon et al., 2012, Nazir et al., 2011). Enrichment of these elements in traffic emissions is explained by particle generation in brake linings (Hjortenkrans et al., 2007, Minguillon et al., 2012), tires (Councell et al., 2004, Hjortenkrans et al., 2007, Rhodes et al., 2012) or combustion of lubricating oil (Pakkanen et al., 2003, Thorpe and Harrison, 2008, Pulles et al., 2012). Since these emissions accumulate onto dust after they are emitted very close to the surface, their presence in the atmosphere is also linked to the presence of road dust in the atmosphere (Amato et al., 2009, Sternbeck et al., 2002, Thorpe and Harrison, 2008). In this study two lines of evidence suggest that Factor 4 represent true traffic emissions, rather than road-dust. One of these evidences is the lack of crustal component in Factor 4. Only very small fractions of litophilic elements are accounted for by Factor 4. If the factor 4 was a road dust factor, it is expected to contain higher fractions of crustal elements. The second evidence is the monthly median values of Factor 4 scores. Road dust has to become airborne (resuspended) before it is intercepted at our station. In that sense road dust is like soil and hence its concentration is expected to be higher during dry summer season. Monthly variations in Factor 4 scores are shown in Figure 4.6.16. As can be seen from the figure, Factor 4 scores are higher in winter and lower in summer. These two pieces of information suggest that Factor 4 represent emissions from motor vehicles rather than resuspended road dust.

Fractions of elements accounted for by Factor 5 is depicted in Figure 4.6.13. The fifth factor is dominated by Cl (85%) and Na (63%). Furthermore the monthly variation of G-scores shows high values in winter, therefore it is clear that Factor 5 represents sea salt. This factor explains 6% of Mg and Sr which may be also used as markers of sea salt. About 28% of NO_3^-, 14% of SO_4^{2-} and 10% of NH_4^+ also explained in Factor 5. One interesting point in this factor is the presence of crustal and anthropogenic elements associated with it. Concentrations of elements and ions in Factor 5 are given in Figure 4.6.15. As can be seen from the figure, concentrations of crustal and anthropogenic elements like Cd, Cu, Pb, As, Se etc are not zero in Factor 5. Fraction of these litophilic and chalcophilic elements explained by Factor 5 is negligibly small. This implies that Factor 5 is not a factor that contributes significantly to measured concentrations of these elements. However, they are detected in this aerosol component. This is typical in PMF and can be seen in other factors, in this study as well. Presence of litophilic and chalchophilic aerosols in Sea salt component is a typical example of mixing of aerosol components during transport. Air masses that bring sea salt to our station are not originally generated over the seas. Probably air masses come

from Russian Federation or Ukraine and picks up sea salt over the sea, if there is storm activity, which generates sea salt in large quantities when the air mass was passing over that area, or if the air mass advects below the boundary layer, where it picks up sea salt more effectively. In either the case, the same air mass passes over non-sea areas and pick up other aerosol types as well. That is why, we can see all elements in all factors, when we look at the factor loadings given in Figure 4.6.13, but fractions of elements explained by a particular factor will not be high if they are there only due to mixing and if that particular factor does not represent their main source affecting their concentrations measured at the receptor.

Contribution of factors to PM mass concentrations resolved by PMF is given in Figure 4.6.18. The dominant source is soil dust, which accounts for 41% of PM mass concentration at Northwestern Turkey. Such high contribution of crustal material to total particle mass was due to collection of PM samples. Contribution of crustal material would be smaller if PM10 or PM2.5 samples were collected. Distant anthropogenic source (Factor 2) is the second major contributor of PM. Secondary pollutants (NO_3^-, SO_4^{2-} and NH_4^+) are the major species that accounted 26% of PM. Secondary inorganic particles are reported to be the highest contributor to PM10 and PM2.5 mass in many studies performed in the Eastern Mediterranean basin (Querol et al., 2009, Luria et al., 1996, Gullu et al., 1998). Traffic (Factor 4) accounts for 16% of PM mass concentration. Other sources, namely sea salt and stationary combustion contributes 9% and 8% of PM, respectively.
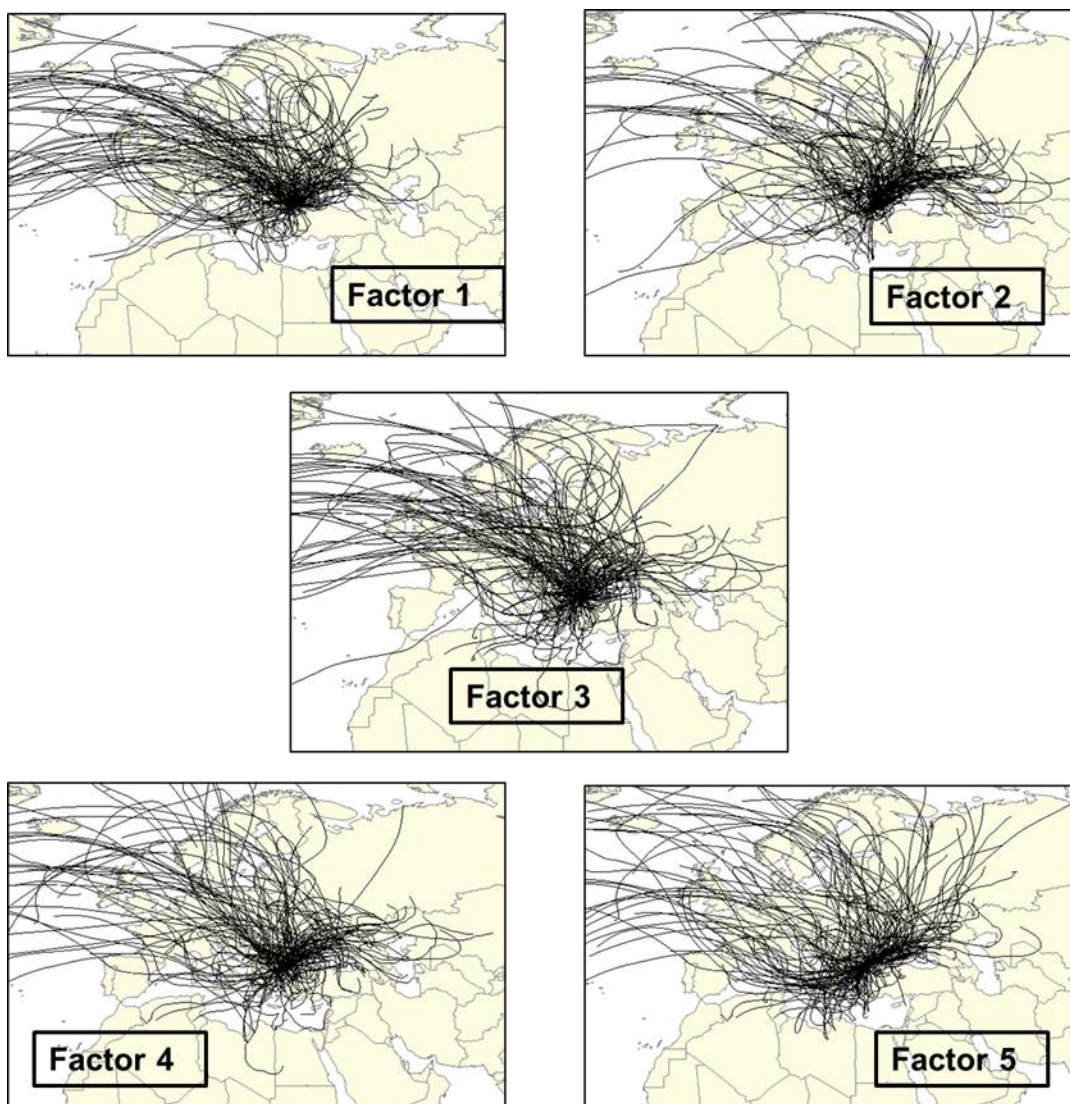
Figure 4.6.17 Back trajectories corresponding to the highest 25th percent G-score
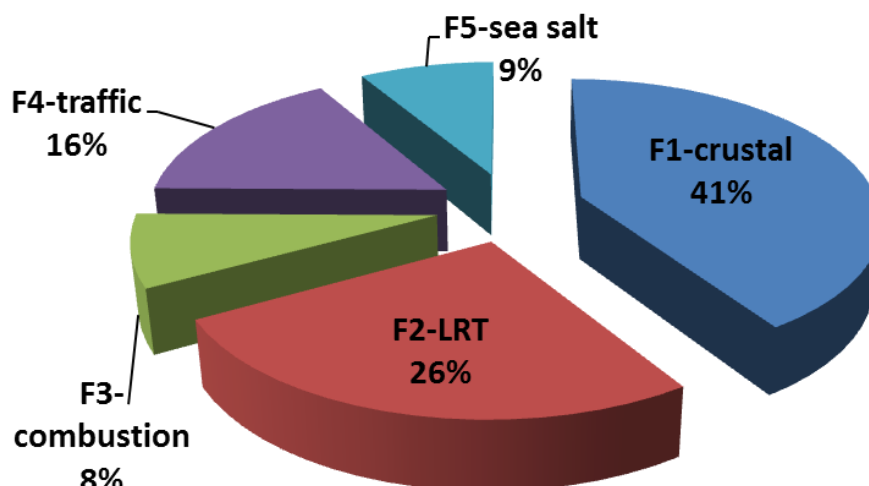
Figure 4.6.18 Contributions of resolved factors to PM

4.6.3. **Potential Source Regions**

We have used PMF model to determine the potential sources and their contributions. The spatial distribution of probable source locations cannot be determined by PMF alone. To determine the probable geographic locations of sources, PMF resolved factors were combined with back trajectories and PSCF approach was applied. In this PSCF analysis, the highest 40th percentiles of G-scores values were used as threshold value of pollution.

The study domain used in PSCF analysis extends from west of UK (20°W) to Center of Asia (60ºE) in North East direction and from Siberia (75ºN) to middle of Africa (15ºN). The study area is divided into 1°×1° grids. Total number of cells (grids) in the study domain is 4800. Grid cells and study domain is presented in Figure 4.6.19, where the location of sampling station is shown with a dark circle.

Back trajectories arriving at 100 m and 500 m heights were found very similar in direction, as discussed previously in Section 4.3. Therefore only trajectories with 500 and 1500 m starting altitude were used in PSCF analysis. To determine the weighting function, the average end points in each grid cell (n_{avg}) was calculated (which was 13) for the used combined trajectory data set. Then the weighting factors were calculated as discussed in Section 3.5.3 and given in Table 4.6.3.
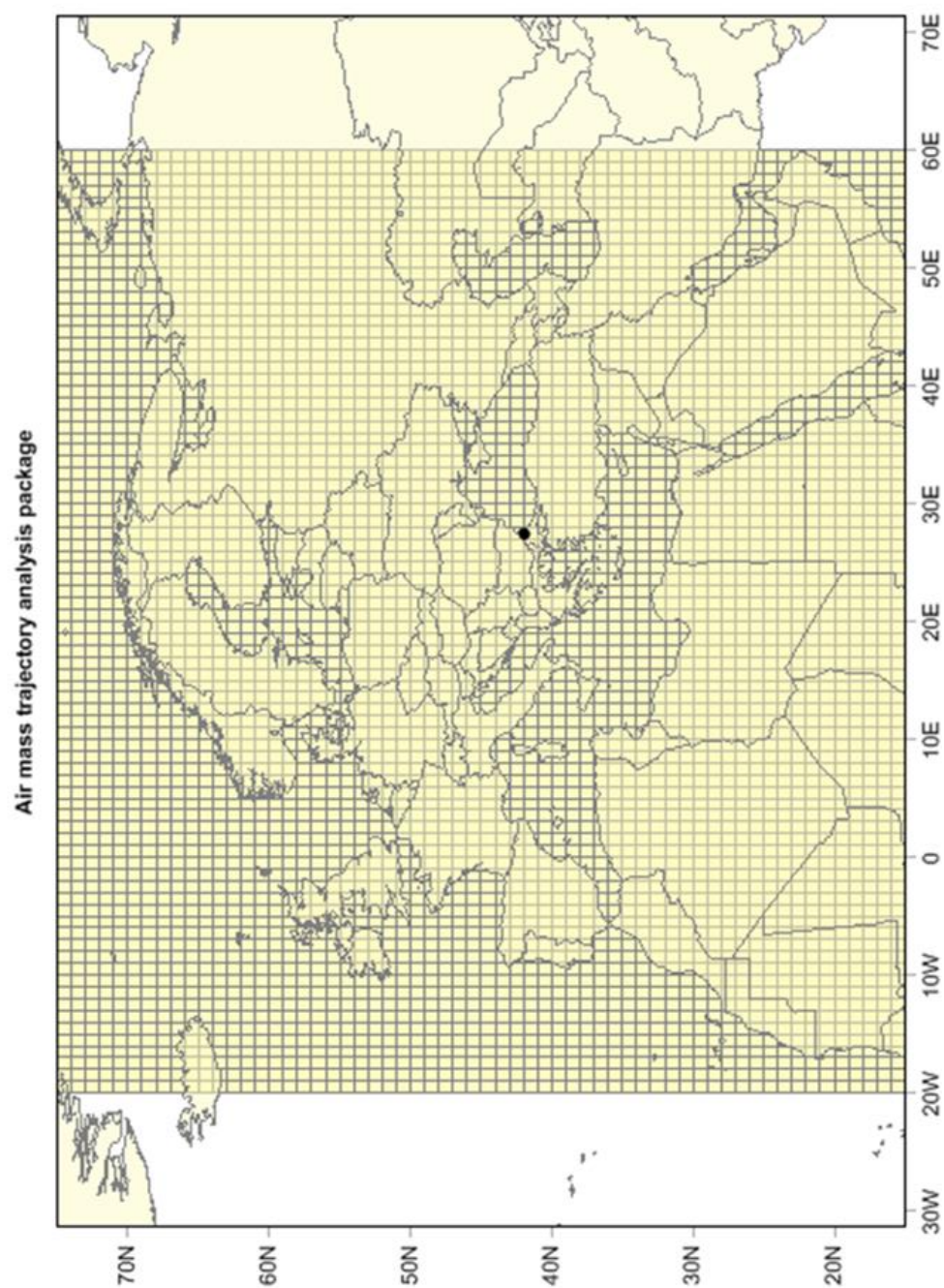
Figure 4.6.19 The grid layer used in PSCF analysis

Table 4.6.3 The weighting function used in PSCF

Weighting factor	Constraint
1	$n_{ij} > 26$
0.75	$13 < n_{ij} < 26$
0.50	$6 < n_{ij} < 13$
0.15	$n_{ij} \leq 6$

The potential regions found as the source locations of Factor 2 are plotted in Figure 4.6.20. Factor 2 was defined as the distant anthropogenic sources dominated by secondary pollutants. As clearly seen from the figure, Eastern European countries are major source regions affecting the northwestern Turkey. Especially Moldova, Ukraine, Russia and Azerbaijan are highlighted as the hot spots for Factor 2. Large point sources (LPS) reported to EMEP-CEIP (the EMEP Centre on Emission Inventories and Projections) can be visualized through http://www.ceip.at/webdab-emission-database/ web page. The LPS for SO_x (as SO_2) are downloaded for Ukraine and Russia and given in Figure 4.6.21. Coincidence of LPS and the PSCF maps shows that sources in Eastern Europe countries influence the northwestern part of Turkey by long range transport. Eastern Europe countries have also been reported as the source regions affecting Turkey in other studies (Kindap et al., 2006, Karaca et al., 2009, Kocak et al., 2009, Dogan et al., 2010, Karaca and Camci, 2010, Uygur et al., 2010, Kocak et al., 2011, Öztürk et al., 2012).

Distribution of weighted PSCF values of Factor 3 is illustrated in Figure 4.6.22. Factor 3 was defined as stationary combustion sources and based on its seasonality it was "local" rather than distant. The PSCF analysis showed that "local" potential source regions for Factor 3 is Bulgaria, Romania, Hungary, Greece and western part of Turkey, while the distant source regions are Check Republic, Austria, Slovakia, Germany, Poland, Ukraine and Russia. High temperature fossil fuel combustion, especially coal combustion may be the major source in Factor 3. The largest thermal power plant complex, namely Maritsa Iztok Complex in South Eastern Europe is located in Bulgaria. As our knowledge there are several thermal power plants in Bulgaria and Romania, most of them are coal-fired. We have found (see Section 4.3.1 for detail) that 41% of air flows were short therefore slow moving and from all directions in winter. When we combined these two findings, we may speculate Bulgaria and Romania as the major source regions for Factor 3. The locations of LPS of SO_x (as SO_2) for Turkey (Figure 4.6.23) coincide well with the PSCF hot spots. So northwestern Turkey is also under the influence of Turkey's own emissions especially in winter.

Factor 4 was identified as traffic emissions because of the high enrichment of Pb, Zn and Cd. The distribution of weighted PSCF is given in Figure 4.6.24. The source regions for Factor 4 are Russia, Ukraine, Eastern Black Sea coast, western and central Anatolia, Thrace, Bulgaria, Romania and Greece. Gridded emission data of Turkey for road transport sector in 2006 is plotted in Figure 4.6.25. The hot spots on emission map coincided well with the PSCF map. This information distribution of PSCF values support our identification of Factor 4 as traffic emissions.

PSCF map generated for Factor 5 (Figure 4.6.26) clearly indicates the Mediterranean and Black Sea as the source locations. The regions on the way of air masses between the sea and receptor site is also highlighted as the source regions.
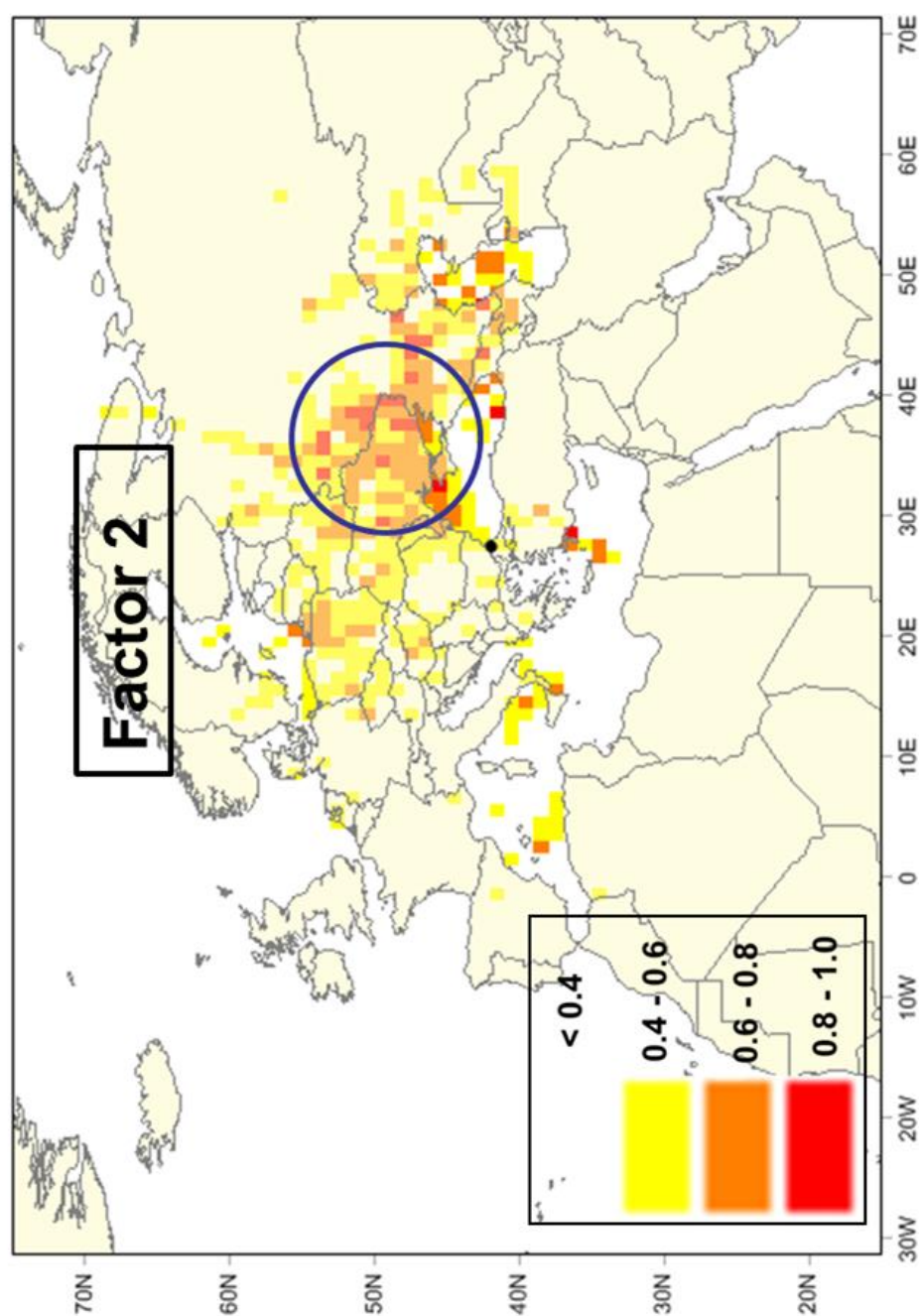
Figure 4.6.20 Weighted PSCF distribution of Factor 2

148
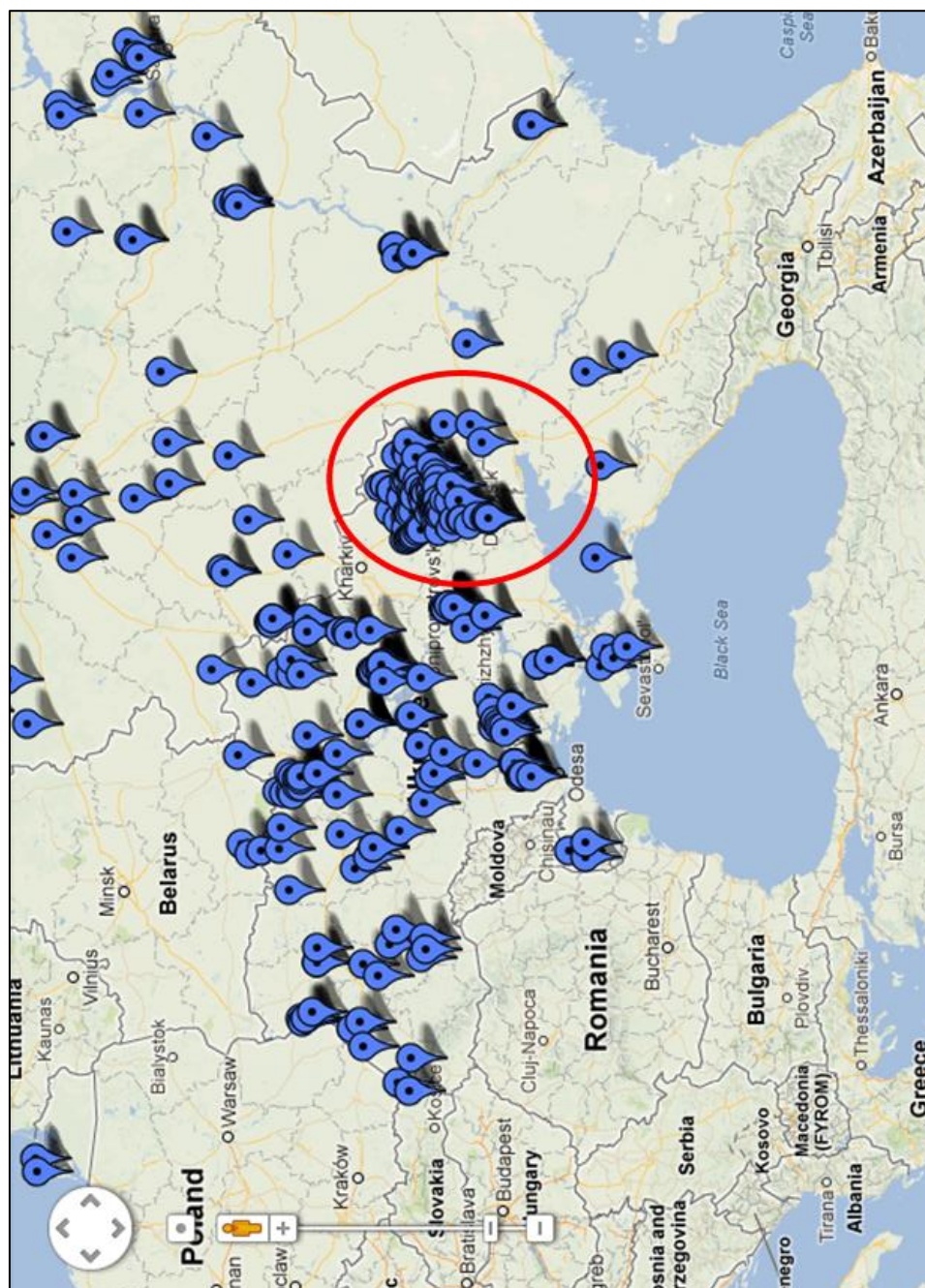
Figure 4.6.21 LPS of SO_x (as SO_2) for Ukraine and Russia

(downloaded from http://www.ceip.at/webdab-emission-database/lps-emissions-in-google-maps/)

149

Air mass trajectory analysis package

Factor 3

< 0.4

0.4 - 0.6

0.6 - 0.8

0.8 - 1.0
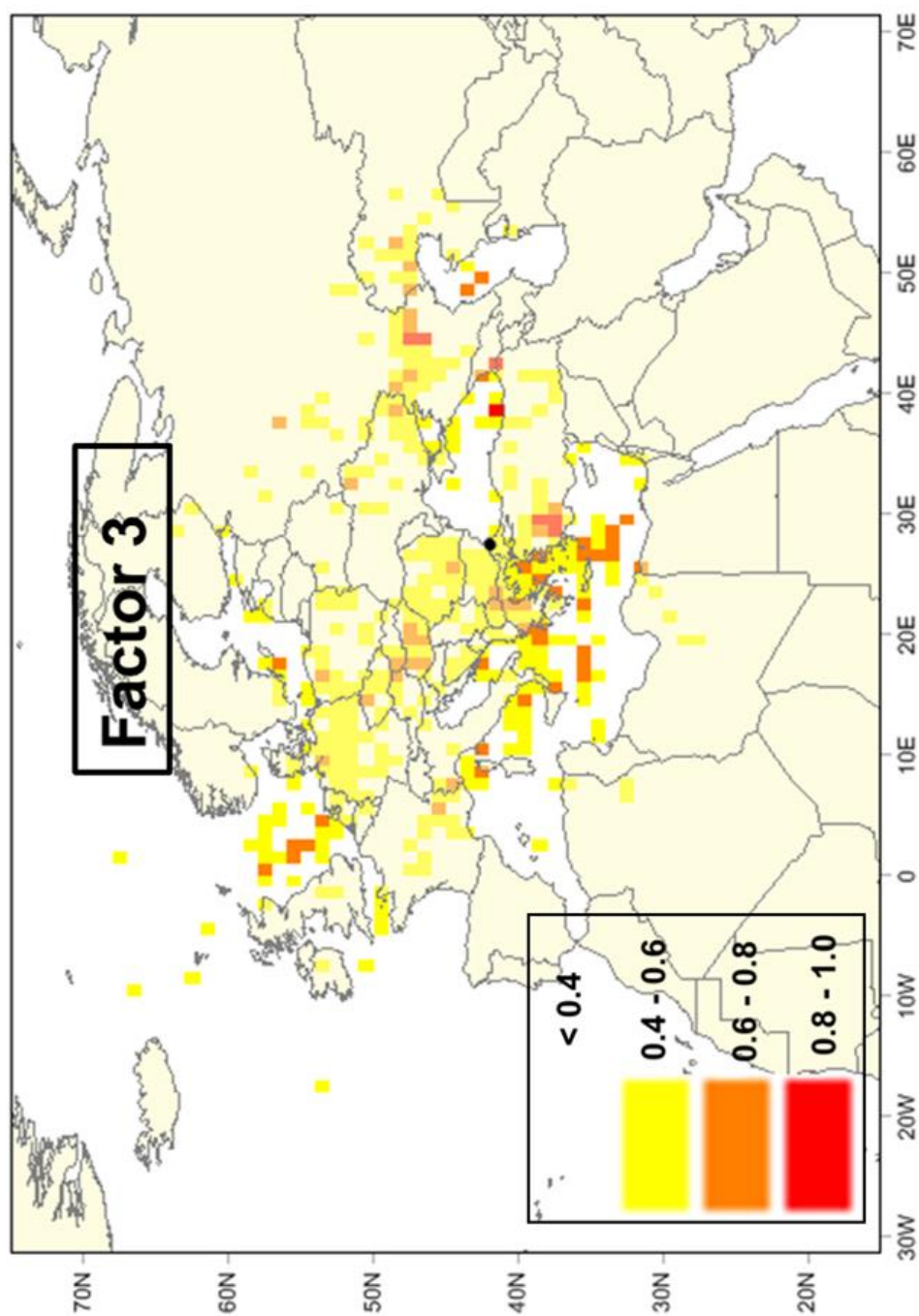
Figure 4.6.22 Weighted PSCF distribution of Factor 3

150
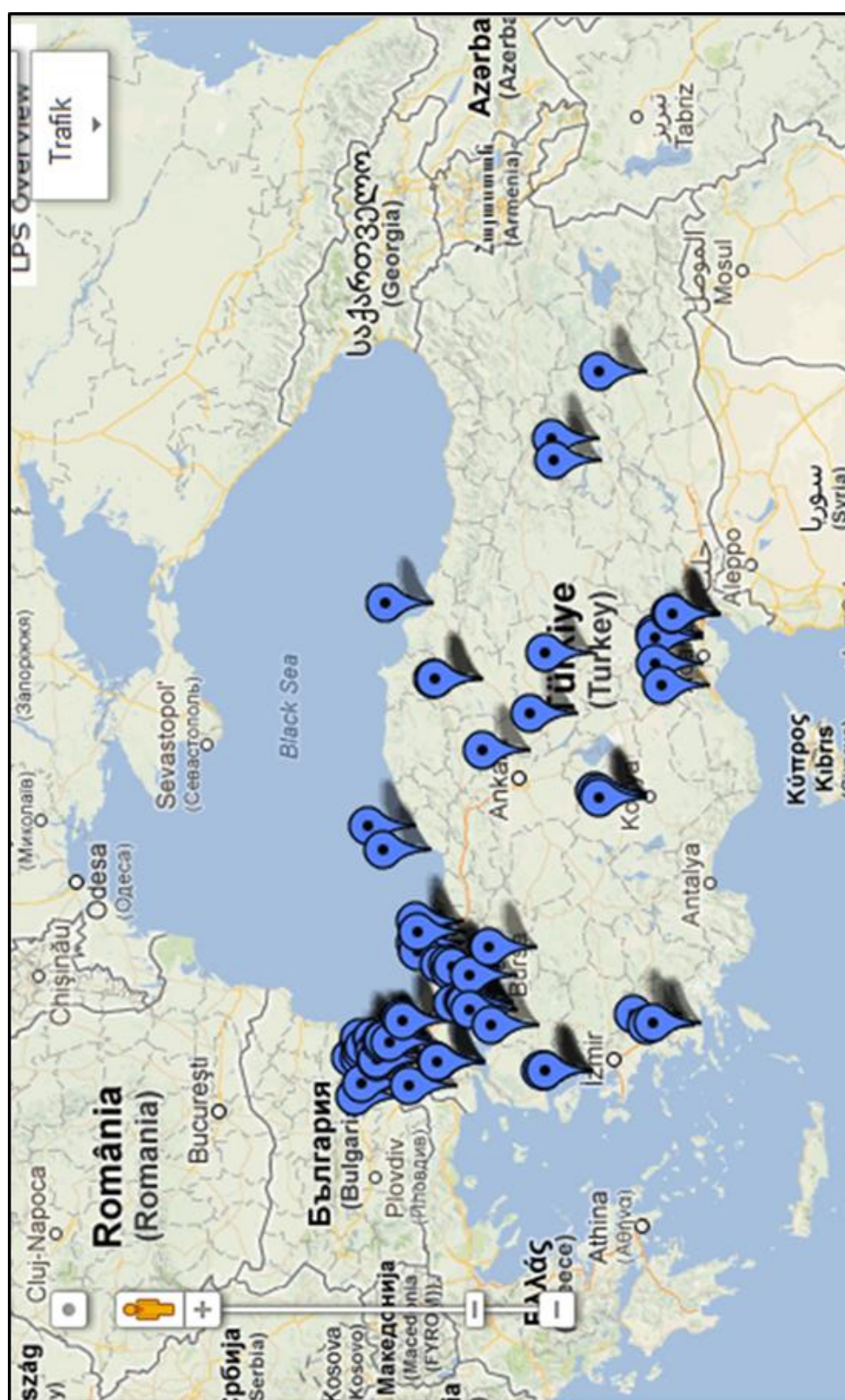
Figure 4.6.23 LPS of SO$_x$ (as SO$_2$) for Turkey
(downloaded from http://www.ceip.at/webdab-emission-database/lps-emissions-in-google-maps/)

151
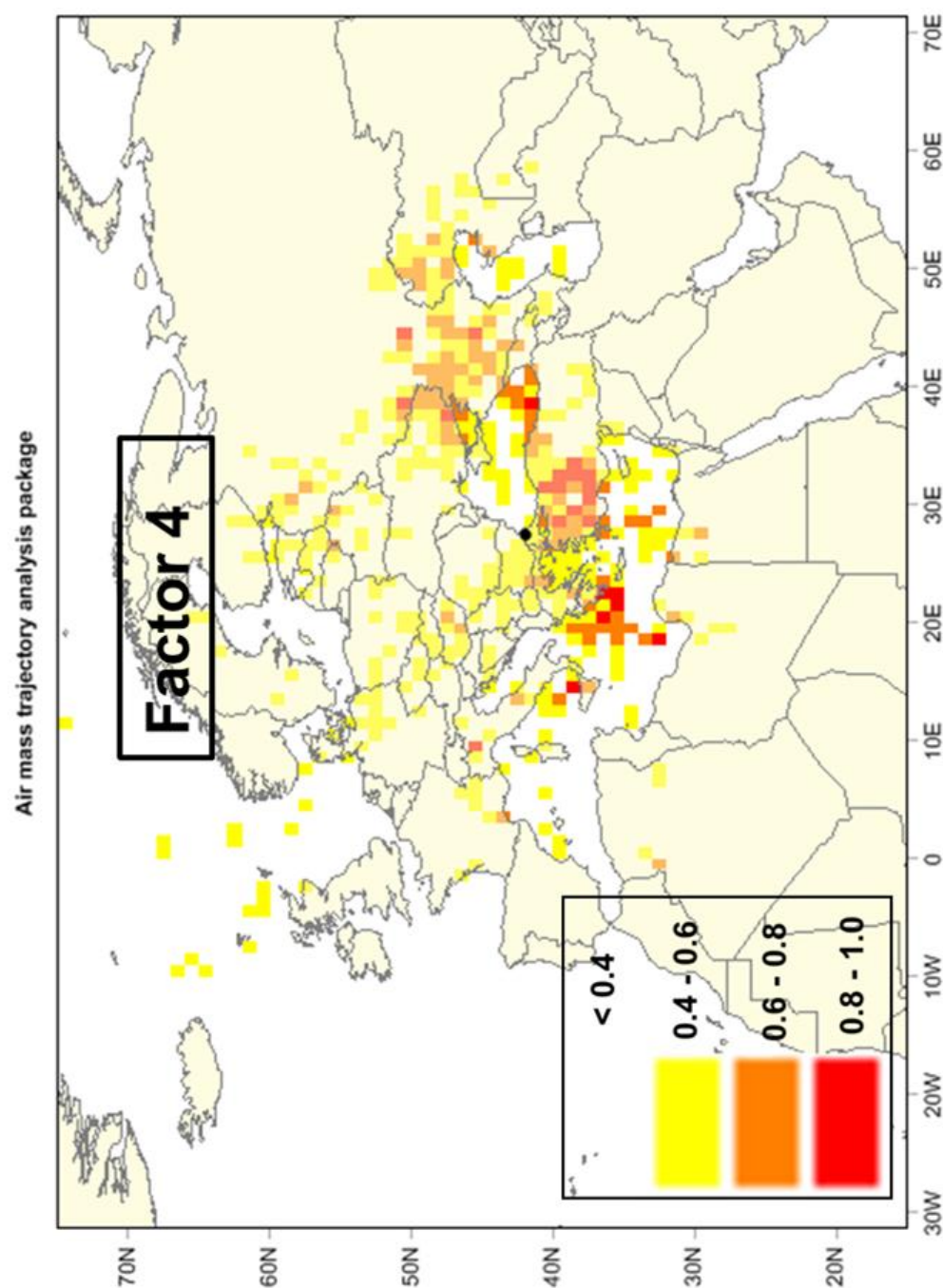
Figure 4.6.24 Weighted PSCF distribution of Factor 4

PM2.5 emissions of Turkey for road transport sector

(http://www.ceip.at/webdab-emission-database)
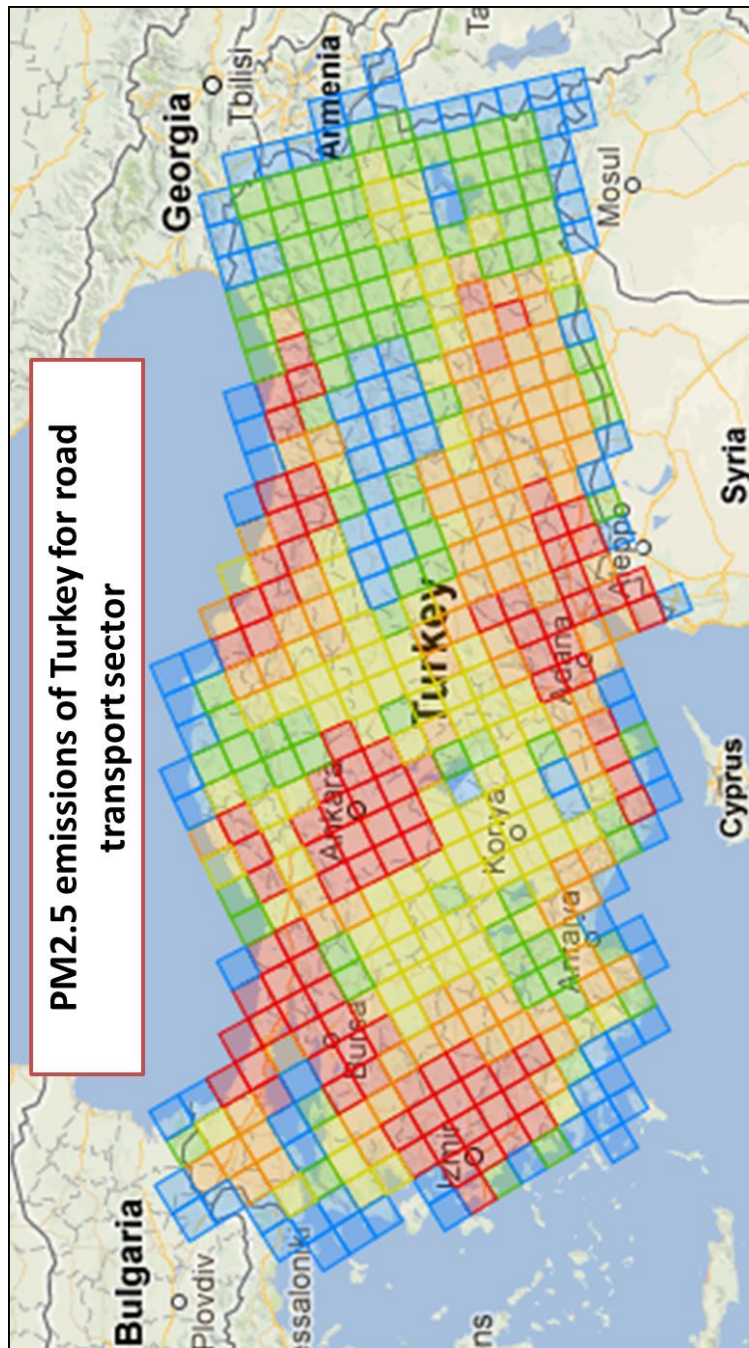
P_{20} : Value range where the first (lowest) 20% of the values can be found
P_{40} : Value range where the second 20% of the values can be found
P_{60} : Value range where the third 20% of the values can be found
P_{80} : Value range where the fourth 20% of the values can be found
P_{100} : Value range where the last (highest) 20% of the values can be found

Figure 4.6.25 Gridded emission data of Turkey for road transport sector in 2006
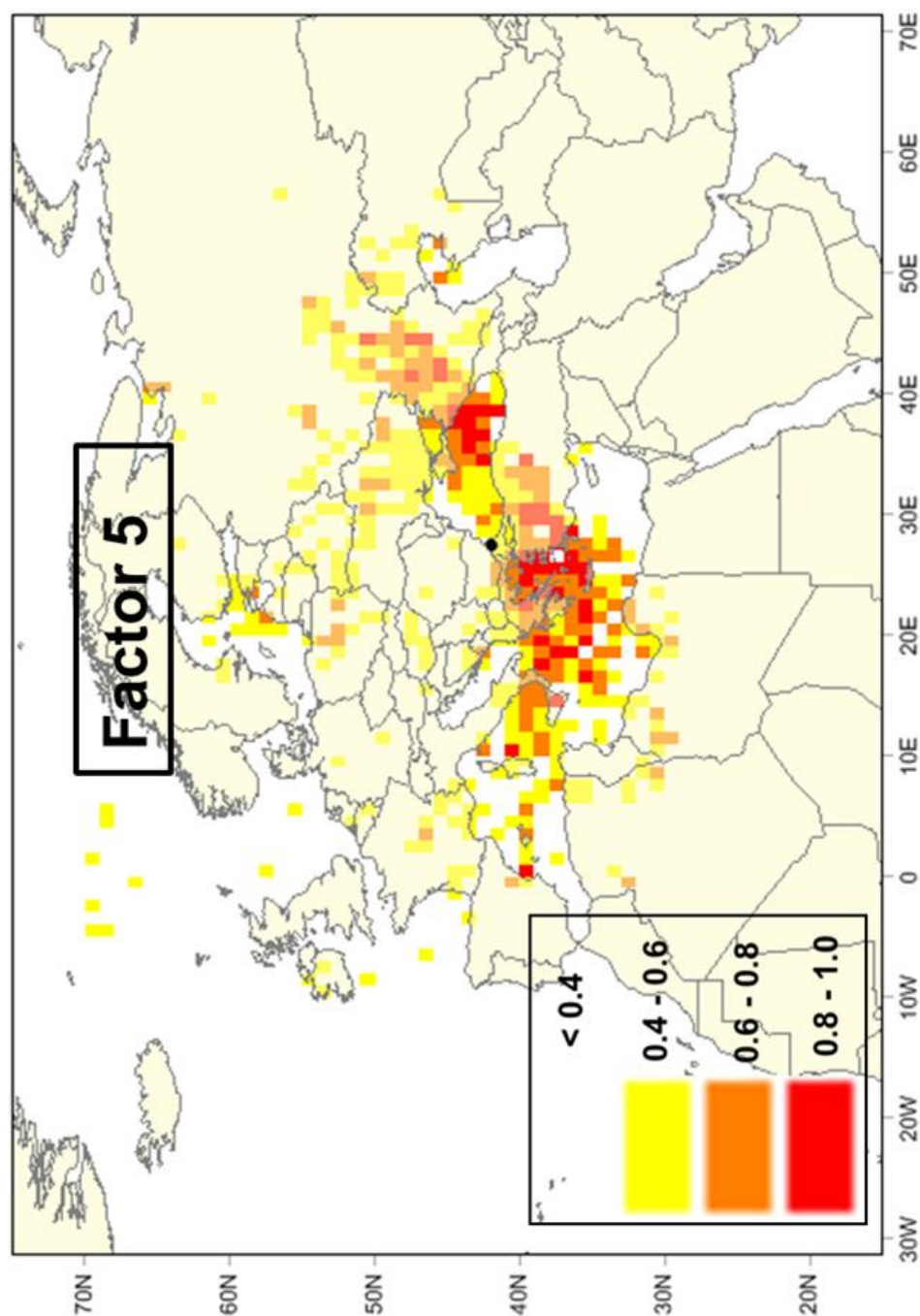
Figure 4.6.26 Weighted PSCF distribution of Factor 5

CHAPTER 5

CONCLUSIONS AND RECOMMENDATIONS

5.1. Summary of Significant Results and Conclusion

The main outcomes of this study can be summarized as:

- ✓ A comprehensive data set including inorganic ions and trace elements is generated for the Northwestern Turkey, which is the entry point of particles and gases from Europe.

- ✓ Aerosols reaching Northwestern Turkey already contain high concentrations of pollution-derived parameters. Its composition is only slightly modified during its transport over Turkey.

- ✓ Variations in upper atmospheric flow patterns, rain events, dust transport to the region and photochemistry are identified as factors affecting short and long-term temporal variations in concentrations of measured parameters.

- ✓ A clear relation was observed between Cl^- deficit on particles and concentrations of acidic species.

- ✓ Main upper atmospheric flow climatology for Northwestern Turkey was established by clustering back trajectories.

- ✓ Contribution of forest fires on chemical composition of particles at the Northwestern Turkey is demonstrated.

- ✓ Components of aerosol population at Northwestern Turkey were resolved using positive matrix factorization.

- ✓ Potential source regions of aerosol components found in PMF analysis were identified using instruments of trajectory statistics.

These major findings of the study are further elaborated in following paragraphs. Generation of the data set reflecting chemical composition of atmosphere at the Northwestern border of the country is important, because this is the port from where air masses enter to Turkey in 70% of the time. A complete data set will reflect the composition of air parcels when they first enter the country. This data can be used as reference composition that can be compared with data generated in different parts of Turkey.

Even a very brief preliminary study of such comparison gave us an outcome. Air masses arriving Turkey have relatively high particulate pollutant levels. For example, concentration of SO_4^{2-} ion measured in this work is 5600 ng m^{-3}. Sulfate concentrations measured at the Mediterranean and Black Sea coasts of Turkey are 5300 and 4100 ng m^{-3}, respectively. This indicates that aerosols reaching to Turkey from NW sector are already polluted. Compositions of air masses are modified only slightly during their transport over the country. This is not only true for SO_4^{2-} ion, but is also observed in other major particulate pollutants.

Average concentration of aerosol species varied between 0.0057 ng m^{-3} for Lu and 5800 ng m^{-3} for SO_4^{2-} (Section 4.1.1). There were no significant differences between weekdays and weekends concentrations of species (Section 4.5). Furthermore species concentrations were not directly related with local wind speed. This indicated that aerosol chemical composition was controlled by transported aerosols rather than local point sources (Section 4.4). High concentrations of secondary aerosols namely SO_4^{2-}, NO_3^- and NH_4^+ also corroborate this finding (Section 4.1.2).

Temporal variations of species were investigated in two different temporal time-scales as daily and seasonally. All elements and ions, except Be, P, V, Fe, Ni, Ge, Mo, Sn, Er, W, Bi, NH_4^+, SO_4^{2-} and PM showed episodic and seasonal variations (Section 4.2). Rain and long range transport of particles were identified as major factors determining these variations. Effect of rain was more pronounced for crustal species than marine and anthropogenic species. The non-rainy days to rainy days ratio were around 2.0 for crustal species and less than 1.6 for marine and anthropogenic species (Section 4.4). The relation between Cl^--to-Na mass ratio and $(SO_4^{2-} + NO_3^-)$ concentrations indicated that chloride deficit was more pronounced when average $(SO_4^{2-} + NO_3^-)$ concentration was higher than 8 µg m^{-3} (Section 4.2.1). Seasonal variation in sea-salt emissions i.e. higher emissions in winter and lower in summer was found as the major factor determining the seasonal differences in marine species (Section 4.2.2). Seasonal differences for crustal species were mostly controlled by the variation in source strength, while episodic variations were caused by rain events and Saharan dust intrusions (Section 4.2). Episodic and seasonal variations in concentrations of anthropogenic species were caused by the variations in transport paths of air masses. Indeed, seasonal variations in atmospheric transformation mechanisms also played significant role in seasonal variations or lack of seasonal variation observed in secondary aerosols. The absence of seasonal variation in SO_4^{2-} and NH_4^+ and higher concentrations of NO_3^- in winter was explained by their reactions in the atmosphere (Section 4.2.2).

Mineral dust tracers (Al, Fe and Ti), air mass back trajectories, satellite images and mineral dust forecast models were used to identify aerosol samples affected from Saharan dust intrusions. Sixteen dust events with periods varying between one to four days were identified with this approach. The ratios of Ti/Ca, Al/Ca, Ti/Fe and Ca/Fe on dust days and non-dust days were calculated to examine if these ratios could be used for Saharan dust markers, but no significant differences was found between the ratios corresponding to dust and non-dust samples (Section 4.2.3).

Residence time analysis of back trajectories showed that emissions from Eastern Europe countries, especially Central Russia, Ukraine, Bulgaria and Romania, could reach to the sampling site more frequently in summer. However air flows were more frequent in West and NW sectors in winter season, indicating that emissions in Southern and Western Europe were more influential on aerosol composition at the Northwestern Turkey during winter months (Section 4.3).

Back trajectories were classified into five clusters depending on their direction and speed. Each of these groups represented main atmospheric transport pattern of air masses arriving the region. Relation between chemical composition of aerosols and clusters were investigated. Cluster 2 and 4 together represented moderate and fast moving back trajectories originated from Atlantic Ocean and then passed over Europe before the station within 5 days. Thus, these clusters represent long range transported anthropogenic elements at our station. Cluster 3 represented back trajectories with medium wind speeds. These trajectories generally originated from northern Europe. Slow moving back trajectories were represented by Cluster 1, therefore species having higher concentrations in Cluster 1 was assumed to be relatively local and have emission sources at northwestern Turkey and Balkan countries. Fast and moderately fast moving, which bring anthropogenic particles from Russia and Ukraine to the station was represented in Cluster 5 (Section 4.3.1).

Crustal enrichment factors (EFc) of elements were calculated, using Al as crustal reference element and Mason's compilation of crustal composition, for the preliminary source identification of elements. Elements with average EFc values <3.0 were considered as non-enriched. In contrast, elements with EFc >30 were considered as highly enriched and were associated with non-crustal sources. Elements with EFc values between 3.0 and 30 were considered as moderately enriched (Section 4.6.1).

The influence of forest fires in Ukraine and Russian Federation on aerosol composition at Northwestern Turkey was identified by cluster analysis, satellite pictures and using soluble K as tracer for forest fire emissions. Forest fires were frequent in Russian Federation and Ukraine and air masses carry emissions from these forest-fires when they come from N and NE sectors. The relation between soluble K and Cluster 5 and 3 indicated that the station was influenced from those forest fires especially in summer months and soluble K is a good marker for tracking forest fires (Section 4.3.2).

Source apportionment of PM was carried out by EPA PMF model. PMF resolved aerosols sampled at our station into five components. These components include (1) Crustal emissions which accounted for 41% of PM and accounted for approximately 80% of concentrations of crustal elements including, Ti, Be, Al, Fe, Mg and rare earth elements; (2) Particles emitted from distant anthropogenic sources and carried to our station via long range transport accounted for 26% of PM and explained more than 50% of NH_4^+, SO_4^{2-} and NO_3^- concentrations; (3) Particles emitted from stationary combustion sources particularly in Balkan countries and Thrace part of Turkey. This factor accounted for 8% of PM and 100% of As and more than 50% of Zn and Ge; (4) Particles emitted from traffic activities, which accounted for 16% of PM mass and explained 94% of Cd and 74% of Pb concentrations; (5) Sea salt particles emitted from the sea. Marine emissions accounted for 9% of PM mass and explained 85% and 63% of Cl and Na concentrations, respectively (Section 4.6.2).

Potential source regions for sources resolved by PMF were identified using weighted potential source contribution function (PSCF) approach. Eastern European countries particularly Moldova, Ukraine, Russia and Azerbaijan were highlighted as the major source areas for distant anthropogenic source factor. Distant and relatively local source regions were found for stationary combustion emissions factor. Bulgaria, Romania, Hungary, Greece and western part of Turkey's contribution was considered as local, while contributions from Check Republic, Austria, Slovakia, Germany, Poland, Ukraine and Russia were considered as distant source regions. The potential source regions for traffic emission factor were Russia, Ukraine, Eastern Black Sea coast, western and central Anatolia, Thrace, Bulgaria, Romania and Greece. For marine emissions the Mediterranean and Black Sea was highlighted as the source regions (Section 4.6.3).

5.2. Recommendations for Future Research

This study indicated that Turkey is influenced from long range and regionally transported aerosols. To highlight contribution of anthropogenic sources, size segregated PM sampling can be more informative as the contribution of natural crustal matter greatly diminishes in PM10 particularly in PM2.5. Organic carbon content of aerosols can also be determined as organic matter is expected to make up a significant fraction of aerosol mass. Measurement of Persistent Organic Pollutants (POPs) is highly recommended due to its impact on health and ecosystem and lack of data in Turkey. For comparison and source apportionment studies, simultaneous measurements of chemical aerosol data in different parts of Turkey and in eastern European countries like Bulgaria and Romania can be performed using the same measuring and analyzing techniques. In the current study, receptor model was used for source apportionment of PM. Source oriented models for example EPA's Models-3 air quality model can also be used along with receptor model. As these two models have conceptually different approaches, they complement each other. Furthermore comparison of the results can give valuable information for the limitations and strength of models. Unfortunately there is no emission inventory for Turkey to be used in source models. Therefore there is a need to prepare emission inventory for Turkey.

REFERENCES

ABDALMOGITH, S. S. & HARRISON, R. M. 2005. The use of trajectory cluster analysis to examine the long-range transport of secondary inorganic aerosol in the UK. *Atmospheric Environment,* 39**,** 6686-6695.

ADLER, K. B., FISCHER, B. M., WRIGHT, D. T., COHN, L. A. & BECKER, S. 1994. Interactions between respiratory epithelial-cells and cytokines - relationships to lung inflammation. *In:* CHIGNARD, M., PRETOLANI, M., RENESTO, P. & VARGAFTIG, B. B. (eds.) *Cells and Cytokines in Lung Inflammation.*

AHMED, T., DUTKIEWICZ, V. A., SHAREEF, A., TUNCEL, G., TUNCEL, S. & HUSAIN, L. 2009. Measurement of black carbon (BC) by an optical method and a thermal-optical method: Intercomparison for four sites. *Atmospheric Environment,* 43**,** 6305-6311.

AKKOYUNLU, B. O. & TAYANC, M. 2003. Analyses of wet and bulk deposition in four different regions of Istanbul, Turkey. *Atmospheric Environment,* 37**,** 3571-3579.

AL-MOMANI, I. F., AYGUN, S. & TUNCEL, G. 1998. Wet deposition of major ions and trace elements in the eastern Mediterranean basin. *Journal of Geophysical Research-Atmospheres,* 103**,** 8287-8299.

ALMOMANI, I. F., GULLU, G., OLMEZ, I., ELER, U., ORTEL, E., SIRIN, G. & TUNCEL, G. 1997. Chemical composition of Eastern Mediterranean aerosol and precipitation: Indications of long-range transport. *Pure and Applied Chemistry,* 69**,** 41-46.

ALP, K. & KOMURCU, M. 2009. Characterisation of pollutant sources in Istanbul with PM10 and EU directives. *International Journal of Environment and Pollution,* 39**,** 204-212.

ALPERT, P., KISHCHA, P., SHTIVELMAN, A., KRICHAK, S. O. & JOSEPH, J. H. 2004. Vertical distribution of Saharan dust based on 2.5-year model predictions. *Atmospheric Research,* 70**,** 109-130.

ALPERT, P. & ZIV, B. 1989. The Sharav Cyclone: Observations and some theoretical considerations. *Journal of Geophysical Research-Atmospheres,* 94**,** 18495-18514.

ALVES, C. A., GONCALVES, C., PIO, C. A., MIRANTE, F., CASEIRO, A., TARELHO, L., FREITAS, M. C. & VIEGAS, D. X. 2010. Smoke emissions from biomass burning in a Mediterranean shrubland. *Atmospheric Environment,* 44**,** 3024-3033.

AMATO, F., PANDOLFI, M., VIANA, M., QUEROL, X., ALASTUEY, A. & MORENO, T. 2009. Spatial and chemical patterns of PM10 in road dust deposited in urban environment. *Atmospheric Environment,* 43**,** 1650-1659.

AMIRIDIS, V., BALIS, D. S., GIANNAKAKI, E., STOHL, A., KAZADZIS, S., KOUKOULI, M. E. & ZANIS, P. 2009. Optical characteristics of biomass burning aerosols over Southeastern Europe determined from UV-Raman lidar measurements. *Atmospheric Chemistry and Physics,* 9**,** 2431-2440.

ANDERSON, H. R. 2009. Air pollution and mortality: A history. *Atmospheric Environment,* 43**,** 142-152.

ANDREAE, M. O. & CRUTZEN, P. J. 1997. Atmospheric aerosols: Biogeochemical sources and role in atmospheric chemistry. *Science,* 276**,** 1052-1058.

ANDREAE, M. O. & MERLET, P. 2001. Emission of trace gases and aerosols from biomass burning. *Global Biogeochemical Cycles,* 15**,** 955-966.

ANDREAS, E. L., EDSON, J. B., MONAHAN, E. C., ROUAULT, M. P. & SMITH, S. D. 1995. The spray contribution to net evaporation from the sea - a review of recent progress. *Boundary-Layer Meteorology*, 72**,** 3-52.

ANDRES, R. J. & KASGNOC, A. D. 1998. A time-averaged inventory of subaerial volcanic sulfur emissions. *Journal of Geophysical Research-Atmospheres,* 103**,** 25251-25261.

ANIL, I., KARACA, F. & ALAGHA, O. 2009. Investigation of Long-range Atmospheric Transport Effects on Istanbul: "Inhalable Particulate Matter Episodes". *Ekoloji,* 19**,** 86-97.

ARSENE, C., OLARIU, R. I., ZARMPAS, P., KANAKIDOU, M. & MIHALOPOULOS, N. 2011. Ion composition of coarse and fine particles in Iasi, north-eastern Romania: Implications for aerosols chemistry in the area. *Atmospheric Environment,* 45**,** 906-916.

ASHBAUGH, L. L., MALM, W. C. & SADEH, W. Z. 1985. A Residence Time Probability Analysis of Sulfur Concentrations at Grand-Canyon-National-Park. *Atmospheric Environment,* 19**,** 1263-1270.

AUBERT, D., LE ROUX, G., KRACHLER, M., CHEBURKIN, A., KOBER, B., SHOTYK, W. & STILLE, P. 2006. Origin and fluxes of atmospheric REE entering an ombrotrophic peat bog in Black Forest (SW Germany): Evidence from snow, lichens and mosses. *Geochimica Et Cosmochimica Acta,* 70**,** 2815-2826.

BALIS, D. S., AMIRIDIS, V., ZEREFOS, C., GERASOPOULOS, E., ANDREAE, M., ZANIS, P., KAZANTZIDIS, A., KAZADZIS, S. & PAPAYANNIS, A. 2003. Raman lidar and sunphotometric measurements of aerosol optical properties over Thessaloniki, Greece during a biomass burning episode. *Atmospheric Environment,* 37**,** 4529-4538.

BARDOUKI, H., LIAKAKOU, H., ECONOMOU, C., SCIARE, J., SMOLIK, J., ZDIMAL, V., ELEFTHERIADIS, K., LAZARIDIS, M., DYE, C. & MIHALOPOULOS, N. 2003. Chemical composition of size-resolved atmospheric aerosols in the eastern Mediterranean during summer and winter. *Atmospheric Environment,* 37**,** 195-208.

BARNABA, F. & GOBBI, G. P. 2004. Aerosol seasonal variability over the Mediterranean region and relative impact of maritime, continental and Saharan dust particles over the basin from MODIS data in the year 2001. *Atmospheric Chemistry and Physics,* 4**,** 2367-2391.

BEHERA, S. N. & SHARMA, M. 2010. Reconstructing Primary and Secondary Components of PM2.5 Composition for an Urban Atmosphere. *Aerosol Science and Technology,* 44**,** 983-992.

BERGAMETTI, G., DUTOT, A.-L., BUAT-MENARD, P., LOSNO, R. & REMOUDAKI, E. 1989. Seasonal variability of the elemental composition of atmospheric areosol particles over the northwestern mediterranean. *Tellus Series B-Chemical and Physical Meteorology,* 41**,** 353-361.

BERGIN, M. H., GREENWALD, R., XU, J., BERTA, Y. & CHAMEIDES, W. L. 2001. Influence of aerosol dry deposition on photosynthetically active radiation available to plants: A case study in the Yangtze delta region of China. *Geophysical Research Letters,* 28**,** 3605-3608.

BERGLEN, T. F., MYHRE, G., ISAKSEN, I. S. A., VESTRENG, V. & SMITH, S. J. 2007. Sulphate trends in Europe: are we able to model the recent observed decrease ? *Tellus Series B-Chemical and Physical Meteorology,* 59**,** 773-786.

BERRESHEIM, H. & JAESCHKE, W. 1983. The contribution of volcanoes to the global atmospheric sulfur budget. *Journal of Geophysical Research-Oceans and Atmospheres,* 88**,** 3732-3740.

BEZACINSKY, M., PILATOVA, B., JIRELE, V. & BENCKO, V. 1984. To the problem of trace elements and hydrocarbons emissions from combustion of coal. *Journal of Hygiene Epidemiology Microbiology and Immunology* 28**,** 129-138.

BORBELY-KISS, I., KISS, A. Z., KOLTAY, E., SZABO, G. & BOZO, L. 2004. Saharan dust episodes in Hungarian aerosol: elemental signatures and transport trajectories. *Journal of Aerosol Science,* 35**,** 1205-1224.

BORBÉLY-KISS, I., KOLTAY, E., SZABÓ, G. Y., BOZÓ, L. & TAR, K. 1999. Composition and Sources of Urban and Rural Atmospheric Aerosol in Eastern Hungary. *Journal of Aerosol Science,* 30**,** 369-391.

BORGE, R., LUMBRERAS, J., VARDOULAKIS, S., KASSOMENOS, P. & RODRIGUEZ, E. 2007. Analysis of long-range transport influences on urban PM10 using two-stage atmospheric trajectory clusters. *Atmospheric Environment,* 41**,** 4434-4450.

BRANKOV, E., RAO, S. T. & PORTER, P. S. 1998. A trajectory-clustering-correlation methodology for examining the long-range transport of air pollutants. *Atmospheric Environment,* 32**,** 1525-1534.

CAPE, J. N., METHVEN, J. & HUDSON, L. E. 2000. The use of trajectory cluster analysis to interpret trace gas measurements at Mace Head, Ireland. *Atmospheric Environment,* 34**,** 3651-3663.

CARNEVALE, C., FINZI, G., PISONI, E., VOLTA, M., KISHCHA, P. & ALPERT, P. 2012. Integrating Saharan dust forecasts into a regional chemical transport model: A case study over Northern Italy. *Science of the Total Environment,* 417–418**,** 224-231.

CARSLAW, N., CARPENTER, L. J., PLANE, J. M. C., ALLAN, B. J., BURGESS, R. A., CLEMITSHAW, K. C., COE, H. & PENKETT, S. A. 1997. Simultaneous observations of nitrate and peroxy radicals in the marine boundary layer. *Journal of Geophysical Research-Atmospheres,* 102**,** 18917-18933.

CASS, G. R. & MCRAE, G. J. 1983. Source-receptor reconciliation of routine air monitoring data for trace metals: an emission inventory assisted approach. *Environmental Science & Technology,* 17**,** 129-139.

CHEN, S. H., DUDHIA, J., KAIN, J. S., KINDAP, T. & TAN, E. 2008. Development of the online MM5 tracer model and its applications to air pollution episodes in Istanbul, Turkey and Sahara dust transport. *Journal of Geophysical Research-Atmospheres,* 113.

CHESTER, R. & STONER, J. H. 1973. Pb in particulates from the lower atmosphere of the eastern Atlantic. *Nature* 245**,** 27–28.

CHOEL, M., DEBOUDT, K. & FLAMENT, P. 2010. Development of Time-Resolved Description of Aerosol Properties at the Particle Scale During an Episode of Industrial Pollution Plume. *Water Air and Soil Pollution,* 209**,** 93-107.

CHUEINTA, W., HOPKE, P. K. & PAATERO, P. 2000. Investigation of sources of atmospheric aerosol at urban and suburban residential areas in Thailand by positive matrix factorization. *Atmospheric Environment,* 34**,** 3319-3329.

CLAEYS, M., WANG, W., VERMEYLEN, R., KOURTCHEV, I., CHI, X. G., FARHAT, Y., SURRATT, J. D., GOMEZ-GONZALEZ, Y., SCIARE, J. & MAENHAUT, W. 2010. Chemical characterisation of marine aerosol at Amsterdam Island during the austral summer of 2006-2007. *Journal of Aerosol Science,* 41**,** 13-22.

COUNCELL, T. B., DUCKENFIELD, K. U., LANDA, E. R. & CALLENDER, E. 2004. Tire-wear particles as a source of zinc to the environment. *Environmental Science & Technology,* 38**,** 4206-4214.

ÇELIK, M. B. & KADI, İ. 2007. The Relation Between Meteorological Factors and Pollutants Concentrations in Karabük City. *G.U. Journal of Science,* 20**,** 87-95.

DENTENER, F. J., CARMICHAEL, G. R., ZHANG, Y., LELIEVELD, J. & CRUTZEN, P. J. 1996. Role of mineral aerosol as a reactive surface in the global troposphere. *Journal of Geophysical Research-Atmospheres,* 101**,** 22869-22889.

DOCKERY, D. W., POPE, C. A., XU, X., SPENGLER, J. D., WARE, J. H., FAY, M. E., RERRIS, B. G. & SPEIZER, F. E. 1993. An association between air pollution and mortality in six US cities. *New England Journal of Medicine,* 329**,** 1753–1759.

DOGAN, G., GULLU, G., KARAKAS, D. & TUNCEL, G. 2010. Comparison of Source Regions Affecting SO42- and NO3- Concentrations at the Eastern Mediterranean and Black Sea Atmospheres. *Current Analytical Chemistry,* 6**,** 66-71.

DOĞAN, G. & TUNCEL, G. 2005. Comparison of the rural atmosphere aerosol compositions at different parts of Turkey. *M.S. Thesis, Department of Environmental Engineering, Middle East Technical University, Ankara*.

DORLING, S. R., DAVIES, T. D. & PIERCE, C. E. 1992. Cluster- Analysis- A Technique for Estimating The Synoptic Meteorological Controls on Air and Precipitation Chemistry - Method and Applications. *Atmospheric Environment Part a-General Topics,* 26**,** 2575-2581.

DRAXIER, R. R. & HESS, G. D. 1998. An overview of the HYSPLIT_4 modelling system for trajectories, dispersion and deposition. *Australian Meteorological Magazine,* 47**,** 295-308.

DRAXLER, R. R. 1991. The accuracy of trajectories during ANATEX calculated using dynamic-model analyses versus rawinsonde observations. *Journal of Applied Meteorology,* 30**,** 1446-1467.

DUCE, R. A., HOFFMAN, G. L. & ZOLLER, W. H. 1975. Atmospheric trace-metals at remote northern and southern-hemisphere sites - Pollution or natural. *Science,* 187**,** 59-61.

DUNCAN, B. N., MARTIN, R. V., STAUDT, A. C., YEVICH, R. & LOGAN, J. A. 2003. Interannual and seasonal variability of biomass burning emissions constrained by satellite observations. *Journal of Geophysical Research-Atmospheres,* 108.

ELBIR, T., MANGIR, N., KARA, M., SIMSIR, S., EREN, T. & OZDEMIR, S. 2010. Development of a GIS-based decision support system for urban air quality management in the city of Istanbul. *Atmospheric Environment,* 44**,** 441-454.

ELDERING, A., SOLOMON, P. A., SALMON, L. G., FALL, T. & CASS, G. R. 1991. HYDROCHLORIC-ACID - A REGIONAL PERSPECTIVE ON CONCENTRATIONS AND FORMATION IN THE ATMOSPHERE OF SOUTHERN CALIFORNIA. *Atmospheric Environment Part a-General Topics,* 25**,** 2091-2102.

ENGLERT, N. 2004. Fine particles and human health - a review of epidemiological studies. *Toxicology Letters,* 149**,** 235-242.

EPA 1983. 40 CFR 50, Appendix B to Part 50:Reference Method for the Determination of Suspended Particulate Matter in the Atmosphere (High-Volume Method). *47 FR 54912, Dec. 6, 1982; 48 FR 17355, Apr. 22, 1983*.

EPA 2008. EPA Positive Matrix Factorization (PMF) 3.0 Fundamentals & User Guide. *U.S. Environmental Protection Agency Office of Research and Development Washington, DC 20460,* EPA 600/R-08/108.

FAGERLI, H., LEGRAND, M., PREUNKERT, S., VESTRENG, V., SIMPSON, D. & CERQUEIRA, M. 2007. Modeling historical long-term trends of sulfate, ammonium, and elemental carbon over Europe: A comparison with ice core records in the Alps. *Journal of Geophysical Research-Atmospheres,* 112.

FAST, J. D. & BERKOWITZ, C. M. 1997. Evaluation of back trajectories associated with ozone transport during the 1993 North Atlantic regional experiment. *Atmospheric Environment,* 31**,** 825-837.

FAVEZ, O., CACHLER, H., SCIARE, J., ALFARO, S. C., EL-ARABY, T. M., HARHASH, M. A. & ABDELWAHAB, M. M. 2008. Seasonality of major aerosol species and their transformations in Cairo megacity. *Atmospheric Environment,* 42**,** 1503-1516.

FURUTA, N., IIJIMA, A., KAMBE, A., SAKAI, K. & SATO, K. 2005. Concentrations, enrichment and predominant sources of Sb and other trace elements in size classified airborne particulate matter collected in Tokyo from 1995 to 2004. *Journal of Environmental Monitoring,* 7**,** 1155-1161.

GABOR, M., MIHALY, O., ISTVAN, V., PETER, C., ROLAND, D. & GYULA, Z. 2011. Chemical characterization of PM10 fractions of urban aerosol. *Microchemical Journal,* 98**,** 1-10.

GALLOWAY, J. N., SAVOIE, D. L., KEENE, W. C. & PROSPERO, J. M. 1993. The temporal and spatial variability of scavenging ratios for nss sulfate, nitrate, methanesulfonate and sodium in the atmosphere over the north-atlantic ocean. *Atmospheric Environment Part a-General Topics,* 27**,** 235-250.

GANOR, E. 1991. The composition of clay minerals transported to Israel as indicators of Saharan dust emission. *Atmospheric Environment Part a-General Topics,* 25**,** 2657-2664.

GAO, Y., NELSON, E. D., FIELD, M. P., DING, Q., LI, H., SHERRELL, R. M., GIGLIOTTI, C. L., VAN RY, D. A., GLENN, T. R. & EISENREICH, S. J. 2002. Characterization of atmospheric trace elements on PM(2.5) particulate matter over the New York-New Jersey harbor estuary. *Atmospheric Environment,* 36**,** 1077-1086.

GERASOPOULOS, E., AMIRIDIS, V., KAZADZIS, S., KOKKALIS, P., ELEFTHERATOS, K., ANDREAE, M. O., ANDREAE, T. W., EL-ASKARY, H. & ZEREFOS, C. S. 2011. Three-year ground based measurements of aerosol optical depth over the Eastern Mediterranean: the urban environment of Athens. *Atmospheric Chemistry and Physics,* 11**,** 2145-2159.

GHIO, A. J., STONEHUERNER, J., DAILEY, L. A. & CARTER, J. D. 1999. Metals associated with both the water-soluble and insoluble fractions of an ambient air pollution particle catalyze an oxidative stress. *Inhalation Toxicology,* 11**,** 37-49.

GILDEMEISTER, A. E., HOPKE, P. K. & KIM, E. 2007. Sources of fine urban particulate matter in Detroit, MI. *Chemosphere,* 69**,** 1064-1074.

GLAVAS, S. D., NIKOLAKIS, P., AMBATZOGLOU, D. & MIHALOPOULOS, N. 2008. Factors affecting the seasonal variation of mass and ionic composition of PM2.5 at a central Mediterranean coastal site. *Atmospheric Environment,* 42**,** 5365-5373.

GLEASON, J. F., SINHA, A. & HOWARD, C. J. 1987. Kinetics of the gas-phase reaction HOSO2+O2- HO2+SO3. *Journal of Physical Chemistry,* 91**,** 719-724.

GONG, S. L., BARRIE, L. A. & BLANCHET, J. P. 1997. Modeling sea-salt aerosols in the atmosphere .1. Model development. *Journal of Geophysical Research-Atmospheres,* 102**,** 3805-3818.

GOVERNMENT, T. 2008. The Air Quality Assessment and Management Regulation. *Official Gazette Date/Number: 06.06.2008/26898.*

GRAF, H. F., FEICHTER, J. & LANGMANN, B. 1997. Volcanic sulfur emissions: Estimates of source strength and its contribution to the global sulfate distribution. *Journal of Geophysical Research-Atmospheres,* 102**,** 10727-10738.

GROSSI, C. M. & BRIMBLECOMBE, P. 2002. The effect of atmospheric pollution on building materials. *Journal De Physique Iv,* 12**,** 197-210.

GUIEU, C., LOYE-PILOT, M. D., RIDAME, C. & THOMAS, C. 2002. Chemical characterization of the Saharan dust end-member: Some biogeochemical implications for the western Mediterranean Sea. *Journal of Geophysical Research-Atmospheres,* 107.

GULLU, G., DOGAN, G. & TUNCEL, G. 2005. Atmospheric trace element and major ion concentrations over the eastern Mediterranean Sea: Identification of anthropogenic source regions. *Atmospheric Environment,* 39**,** 6376-6387.

GULLU, G., OLMEZ, I. & TUNCEL, G. 2004. Source apportionment of trace elements in the Eastern Mediterranean atmosphere. *Journal of Radioanalytical and Nuclear Chemistry,* 259**,** 163-171.

GULLU, G. H., OLMEZ, I., AYGUN, S. & TUNCEL, G. 1998. Atmospheric trace element concentrations over the eastern Mediterranean Sea: Factors affecting temporal variability. *Journal of Geophysical Research-Atmospheres,* 103**,** 21943-21954.

GUNAYDIN, G. C., TUNCEL, G. & MELAS, D. 2003. Sources regions affecting chemical composition of aerosols and precipitation in the eastern Mediterranean atmosphere determined using trajectory statistics. *In:* MELAS, D. & SYRAKOV, D. (eds.) *Air Pollution Processes in Regional Scale.*

GÜLLÜ, G. H., ÖLMEZ, İ. & TUNCEL, G. 2000. Temporal variability of atmospheric trace element concentrations over the eastern Mediterranean Sea. *Spectrochimica Acta Part B: Atomic Spectroscopy,* 55**,** 1135-1150.

HACISALIHOGLU, G., ELIYAKUT, F., OLMEZ, I., BALKAS, T. I. & TUNCEL, G. 1992. Chemical-composition of particles in the Black-Sea atmosphere. *Atmospheric Environment Part a-General Topics,* 26**,** 3207-3218.

HAYWOOD, J. & BOUCHER, O. 2000. Estimates of the direct and indirect radiative forcing due to tropospheric aerosols: A review. *Reviews of Geophysics,* 38**,** 513-543.

HEGDE, P., SUDHEER, A. K., SARIN, M. M. & MANJUNATHA, B. R. 2007. Chemical characteristics of atmospheric aerosols over southwest coast of India. *Atmospheric Environment,* 41**,** 7751-7766.

HEMANN, J. G., BRINKMAN, G. L., DUTTON, S. J., HANNIGAN, M. P., MILFORD, J. B. & MILLER, S. L. 2009. Assessing positive matrix factorization model fit: a new method to estimate uncertainty and bias in factor contributions at the measurement time scale. *Atmospheric Chemistry and Physics,* 9**,** 497-513.

HERMAN, J. R., BHARTIA, P. K., TORRES, O., HSU, C., SEFTOR, C. & CELARIER, E. 1997. Global distribution of UV-absorbing aerosols from Nimbus 7/TOMS data. *Journal of Geophysical Research D: Atmospheres,* 102**,** 16911-16922.

HERUT, B., NIMMO, M., MEDWAY, A., CHESTER, R. & KROM, M. D. 2001. Dry atmospheric inputs of trace metals at the Mediterranean coast of Israel (SE Mediterranean): sources and fluxes. *Atmospheric Environment,* 35**,** 803-813.

HIEN, P. D., BINH, N. T., TRUONG, Y., NGO, N. T. & SIEU, L. N. 2001. Comparative receptor modelling study of TSP, PM2 and PM2-10 in Ho Chi Minh City. *Atmospheric Environment,* 35**,** 2669-2678.

HJORTENKRANS, D. S. T., BERGBACK, B. G. & HAGGERUD, A. V. 2007. Metal emissions from brake linings and tires: Case studies of Stockholm, Sweden 1995/1998 and 2005. *Environmental Science & Technology,* 41**,** 5224-5230.

HLAVAY, J., POLYAK, K. & WESEMANN, G. 1992. Particle-size distribution of mineral phases and metals in dusts collected at different workplaces. *Fresenius Journal of Analytical Chemistry,* 344**,** 319-321.

HOPKE, P. K., BARRIE, L. A., LI, S. M., CHENG, M. D., LI, C. & XIE, Y. 1995a. Possible Sources and Preferred Pathways for Biogenic and Non-Seasalt Sulfur for the High Arctic. *Journal of Geophysical Research-Atmospheres,* 100**,** 16595-16603.

HOPKE, P. K., LELI, C., CISZEK, W. & LANDSBERGER, S. 1995b. The use of bootstrapping to estimate conditional probability fields for source locations of airborne pollutants. *Chemometrics and Intelligent Laboratory Systems,* 30**,** 69-79.

IM, U., MARKAKIS, K., KOCAK, M., GERASOPOULOS, E., DASKALAKIS, N., MIHALOPOULOS, N., POUPKOU, A., KINDAP, T., UNAL, A. & KANAKIDOU, M. 2012. Summertime aerosol chemical composition in the Eastern Mediterranean and its sensitivity to temperature. *Atmospheric Environment,* 50**,** 164-173.

IM, U., MARKAKIS, K., UNAL, A., KINDAP, T., POUPKOU, A., INCECIK, S., YENIGUN, O., MELAS, D., THEODOSI, C. & MIHALOPOULOS, N. 2010. Study of a winter PM episode in Istanbul using the high resolution WRF/CMAQ modeling system. *Atmospheric Environment,* 44**,** 3085-3094.

IPCC 2001. Climate Change 2001. *Intergovernmental Panel on Climate Change***,** Cambridge University Press, London.

JACOB, D. J. 2000. Heterogeneous chemistry and tropospheric ozone. *Atmospheric Environment,* 34**,** 2131-2159.

JANG, H. N., SEO, Y. C., LEE, J. H., HWANG, K. W., YOO, J. I., SOK, C. H. & KIM, S. H. 2007. Formation of fine particles enriched by V and Ni from heavy oil combustion: Anthropogenic sources and drop-tube furnace experiments. *Atmospheric Environment,* 41**,** 1053-1063.

JAPAR, S. M., BRACHACZEK, W. W., GORSE, R. A., NORBECK, J. M. & PIERSON, W. R. 1986. The contribution of elemental carbon to the optical-properties of rural atmospheric aerosols. *Atmospheric Environment,* 20**,** 1281-1289.

KALIVITIS, N., E. GERASOPOULOS, M. VREKOUSSIS, G. KOUVARAKIS, N. KUBILAY, N. HATZIANASTASSIOU, I. VARDAVAS & MIHALOPOULOS, N. 2007. Dust transport over the eastern mediterranean derived from total ozone mapping spectrometer, aerosol robotic network, and surface measurements. *Journal of Geophysical Research D: Atmospheres* 112**,** art. no. D03202

KALLOS, G., ASTITHA, M., KATSAFADOS, P. & SPYROU, C. 2007. Long-range transport of anthropogenically and naturally produced particulate matter in the Mediterranean and North Atlantic: Current state of knowledge. *Journal of Applied Meteorology and Climatology,* 46**,** 1230-1251.

KARACA, F., ALAGHA, O., ERTURK, F., YILMAZ, Y. Z. & OZKARA, T. 2008. Seasonal variation of source contributions to atmospheric fine and coarse particles at suburban area in Istanbul, Turkey. *Environmental Engineering Science,* 25**,** 767-781.

KARACA, F., ALAGHA, O. & ERTÜRK, F. 2005. Statistical characterization of atmospheric PM10 and PM2.5 concentrations at a non-impacted suburban site of Istanbul, Turkey. *Chemosphere,* 59**,** 1183-1190.

KARACA, F., ANIL, I. & ALAGHA, O. 2009. Long-range potential source contributions of episodic aerosol events to PM10 profile of a megacity. *Atmospheric Environment,* 43**,** 5713-5722.

KARACA, F. & CAMCI, F. 2010. Distant source contributions to PM10 profile evaluated by SOM based cluster analysis of air mass trajectory sets. *Atmospheric Environment,* 44**,** 892-899.

KARAKAS, D., OLMEZ, I., TOSUN, S. & TUNCEL, G. 2004. Trace and major element compositions of Black Sea aerosol. *Journal of Radioanalytical and Nuclear Chemistry,* 259**,** 187-192.

KARAKAŞ, S. Y. & TUNCEL, S. G. 1997. Chemical characteristics of atmospheric aerosols in a rural site of northwestern Anatolia. *Atmospheric Environment,* 31**,** 2933-2943.

KARANASIOU, A. A., SISKOS, P. A. & ELEFTHERIADIS, K. 2009. Assessment of source apportionment by Positive Matrix Factorization analysis on fine and coarse urban aerosol size fractions. *Atmospheric Environment,* 43**,** 3385-3395.

KARTHIKEYAN, S., JOSHI, U. M. & BALASUBRAMANIAN, R. 2006. Microwave assisted sample preparation for determining water-soluble fraction of trace elements in urban airborne particulate matter: Evaluation of bioavailability. *Analytica Chimica Acta,* 576**,** 23-30.

KEENE, W. C., PSZENNY, A. A. P., GALLOWAY, J. N. & HAWLEY, M. E. 1986. Sea-salt correlations and interpretation of constituent ratios in marine precipitation. *Journal of Geophysical Research,* 91**,** 6647-6658.

KHAN, A. J., LI, J. J., DUTKIEWICZ, V. A. & HUSAIN, L. 2010. Elemental carbon and sulfate aerosols over a rural mountain site in the northeastern United States: Regional emissions and implications for climate change. *Atmospheric Environment,* 44**,** 2364-2371.

KIEHL, J. T. & RODHE, H. 1995. *Modeling geographical and seasonal forcing due to aerosols.*

KIM, E., HOPKE, P. K. & EDGERTON, E. S. 2003. Source identification of Atlanta aerosol by positive matrix factorization. *Journal of the Air & Waste Management Association,* 53**,** 731-739.

KINDAP, T. 2008. Identifying the trans-boundary transport of air pollutants to the city of Istanbul under specific weather conditions. *Water Air and Soil Pollution,* 189**,** 279-289.

KINDAP, T. & KARACA, M. 2006. Avrupa kaynaklı aerosollerin Türkiye'ye taşınımı. *itüdergisi/d mühendislik,* 5**,** 3-12.

KINDAP, T., UNAL, A., CHEN, S. H., HU, Y., ODMAN, M. T. & KARACA, M. 2006. Long-range aerosol transport from Europe to Istanbul, Turkey. *Atmospheric Environment,* 40**,** 3536-3547.

KINDAP, T., UNAL, A., CHEN, S. H., HU, Y. T., ODMAN, T. & KARACA, M. 2007. Study of air pollutant transport in northern and western Turkey. *Air Pollution Modeling and Its Applications XVII,* 17**,** 656-658.

KITTO, M. E., ANDERSON, D. L., GORDON, G. E. & OLMEZ, I. 1992. Rare earth distributions in catalysts and airborne particles. *Environmental Science & Technology,* 26**,** 1368-1375.

KOCAK, M., KUBILAY, N., HERUT, B. & NIMMO, M. 2007a. Trace metal solid state speciation in aerosols of the Northern Levantine basin, East Mediterranean. *Journal of Atmospheric Chemistry,* 56**,** 239-257.

KOCAK, M., KUBILAY, N. & MIHALOPOULOS, N. 2004. Ionic composition of lower tropospheric aerosols at a Northeastern Mediterranean site: implications regarding sources and long-range transport. *Atmospheric Environment,* 38**,** 2067-2077.

KOCAK, M., MIHALOPOULOS, N. & KUBILAY, N. 2007b. Chemical composition of the fine and coarse fraction of aerosols in the northeastern Mediterranean. *Atmospheric Environment,* 41**,** 7351-7368.

KOCAK, M., MIHALOPOULOS, N. & KUBILAY, N. 2007c. Contributions of natural sources to high PM10 and PM2.5 events in the eastern Mediterranean. *Atmospheric Environment,* 41**,** 3806-3818.

KOCAK, M., MIHALOPOULOS, N. & KUBILAY, N. 2009. Origin and source regions of PM(10) in the Eastern Mediterranean atmosphere. *Atmospheric Research,* 92**,** 464-474.

KOCAK, M., THEODOSI, C., ZARMPAS, P., IM, U., BOUGIATIOTI, A., YENIGUN, O. & MIHALOPOULOS, N. 2011. Particulate matter (PM(10)) in Istanbul: Origin, source areas and potential impact on surrounding regions. *Atmospheric Environment,* 45**,** 6891-6900.

KOÇAK, M., THEODOSI, C., ZARMPAS, P., SÉGURET, M. J. M., HERUT, B., KALLOS, G., MIHALOPOULOS, N., KUBILAY, N. & NIMMO, M. 2012. Influence of mineral dust transport on the chemical composition and physical properties of the Eastern Mediterranean aerosol. *Atmospheric Environment,* 57**,** 266-277.

KRAM, P., HRUSKA, J. & DRISCOLL, C. T. 1998. Beryllium chemistry in the Lysina catchment, Czech Republic. *Water Air and Soil Pollution,* 105**,** 409-415.

KRUG, E. C. & FRINK, C. R. 1983. Acid-rain on acid soil - a new perspective. *Science,* 221**,** 520-525.

KUBILAY, N., NICKOVIC, S., MOULIN, C. & DULAC, F. 2000. An illustration of the transport and deposition of mineral dust onto the eastern Mediterranean. *Atmospheric Environment,* 34**,** 1293-1303.

KUBILAY, N., OGUZ, T., KOCAK, M. & TORRES, O. 2005. Ground-based assessment of Total Ozone Mapping Spectrometer (TOMS) data for dust transport over the northeastern Mediterranean. *Global Biogeochemical Cycles,* 19.

KULKARNI, P., CHELLAM, S. & MITTLEFEHLDT, D. W. 2007. Microwave-assisted extraction of rare earth elements from petroleum refining catalysts and ambient fine aerosols prior to inductively coupled plasma-mass spectrometry. *Analytica Chimica Acta,* 581**,** 247-259.

LAMBERT, G., CLOAREC, M. F. & PENNISI, M. 1988. Volcanic output of SO2 and trace metals: A new approach. *Geochimica Et Cosmochimica Acta,* 52**,** 39-42.

LANDSBERGER, S. & CREATCHMAN, M. 1999. Elemental Analysis of Airborne Particles. *Gordon and Breach Science Publishers.*

LEE, J. H. & HOPKE, P. K. 2006. Apportioning sources of PM2.5 in St. Louis, MO using speciation trends network data. *Atmospheric Environment,* 40**,** S360-S377.

LELIEVELD, J., BERRESHEIM, H., BORRMANN, S., CRUTZEN, P. J., DENTENER, F. J., FISCHER, H., FEICHTER, J., FLATAU, P. J., HELAND, J., HOLZINGER, R., KORRMANN, R., LAWRENCE, M. G., LEVIN, Z., MARKOWICZ, K. M., MIHALOPOULOS, N., MINIKIN, A., RAMANATHAN, V., DE REUS, M., ROELOFS, G. J., SCHEEREN, H. A., SCIARE, J., SCHLAGER, H., SCHULTZ, M., SIEGMUND, P., STEIL, B., STEPHANOU, E. G., STIER, P., TRAUB, M., WARNEKE, C., WILLIAMS, J. & ZIEREIS, H. 2002. Global air pollution crossroads over the Mediterranean. *Science,* 298**,** 794-799.

LI, C. L., KANG, S. C. & ZHANG, Q. G. 2009. Elemental composition of Tibetan Plateau top soils and its effect on evaluating atmospheric pollution transport. *Environmental Pollution,* 157**,** 2261-2265.

LI, J. J., KHAN, A. J. & HUSAIN, L. 2002. A technique for determination of black carbon in cellulose filters. *Atmospheric Environment,* 36**,** 4699-4704.

LIAO, H., ADAMS, P. J., CHUNG, S. H., SEINFELD, J. H., MICKLEY, L. J. & JACOB, D. J. 2003. Interactions between tropospheric chemistry and aerosols in a unified general circulation model. *Journal of Geophysical Research-Atmospheres,* 108.

LIKENS, G. E., DRISCOLL, C. T. & BUSO, D. C. 1996. Long-term effects of acid rain: Response and recovery of a forest ecosystem. *Science,* 272**,** 244-246.

LIN, C. W., YEH, J. F. & KAO, T. C. 2008. Source characterization of total suspended particulate matter near a riverbed in Central Taiwan. *Journal of Hazardous Materials,* 157**,** 418-422.

LIU, W., HOPKE, P. K. & VANCUREN, R. A. 2003. Origins of fine aerosol mass in the western United States using positive matrix factorization. *Journal of Geophysical Research-Atmospheres,* 108.

LUPU, A. & MAENHAUT, W. 2002. Application and comparison of two statistical trajectory techniques for identification of source regions of atmospheric aerosol species. *Atmospheric Environment,* 36**,** 5607-5618.

LURIA, M., PELEG, M., SHARF, G., TOVALPER, D. S., SPITZ, N., BENAMI, Y., GAWII, Z., LIFSCHITZ, B., YITZCHAKI, A. & SETER, I. 1996. Atmospheric sulfur over the east Mediterranean region. *Journal of Geophysical Research-Atmospheres,* 101**,** 25917-25930.

MAHLER, A.-B. T., K. YIN, D. SPRIGG, W. A. 2006. Dust transport model validation using satellite- and ground-based methods in the southwestern United States. *Proceedings of SPIE, the International Society for Optical Engineering,* 6299.

MAMANE, Y., PERRINO, C., YOSSEF, O. & CATRAMBONE, M. 2008. Source characterization of fine and coarse particles at the East Mediterranean coast. *Atmospheric Environment,* 42**,** 6114-6130.

MANALIS, N., GRIVAS, G., PROTONOTARIOS, V., MOUTSATSOU, A., SAMARA, C. & CHALOULAKOU, A. 2005. Toxic metal content of particulate matter (PM10), within the Greater Area of Athens. *Chemosphere,* 60**,** 557-566.

MARCAZZAN, G. M. B., BONELLI, P., DELLA BELLA, E., FUMAGALLI, A., RICCI, R. & PELLEGRINI, U. 1993. Study of regional and long-range transport in an Alpine station by PIXE analysis of aerosol particles. *Nuclear Instruments and Methods in Physics Research Section B: Beam Interactions with Materials and Atoms,* 75**,** 312-316.

MARGITAN, J. J. 1984. Mechanism of the atmospheric oxidation of sulfur-dioxide - catalysis by hydroxyl radicals. *Journal of Physical Chemistry,* 88**,** 3314-3318.

MARKAKIS, K., IM, U., UNAL, A., MELAS, D., YENIGUN, O. & INCECIK, S. 2012. Compilation of a GIS based high spatially and temporally resolved emission inventory for the greater Istanbul area. *Atmospheric Pollution Research,* 3**,** 112-125.

MASON, B. 1966. Principles of Geochemitry. *(third edition). John Willey, New York, NY.*

MASON, B. & MOORE, C. B. 1982. Principles of Geochemistry. fourth ed. Wiley.

MAZZEI, F., D'ALESSANDRO, A., LUCARELLI, F., NAVA, S., PRATI, P., VALLI, G. & VECCHI, R. 2008. Characterization of particulate matter sources in an urban environment. *Science of the Total Environment,* 401**,** 81-89.

MCQUEEN, J. T. & DRAXLER, R. R. 1994. Evaluation of model back trajectories of the Kuwait oil fires smoke plume using digital satellite data. *Atmospheric Environment,* 28**,** 2159-2174.

MENG, Z., DABDUB, D. & SEINFELD, J. H. 1997. Chemical coupling between atmospheric ozone and particulate matter. *Science,* 277**,** 116-119.

MIAN, I. A., BEGUM, S., RIAZ, M., RIDEALGH, M., MCCLEAN, C. J. & CRESSER, M. S. 2010. Spatial and temporal trends in nitrate concentrations in the River Derwent, North Yorkshire, and its need for NVZ status. *Science of the Total Environment,* 408**,** 702-712.

MINGUILLON, M. C., QUEROL, X., BALTENSPERGER, U. & PREVOT, A. S. H. 2012. Fine and coarse PM composition and sources in rural and urban sites in Switzerland: Local or regional pollution? *Science of the Total Environment,* 427**,** 191-202.

MOLTENI, F., BUIZZA, R., PALMER, T. N. & PETROLIAGIS, T. 1996. The ECMWF ensemble prediction system: Methodology and validation. *Quarterly Journal of the Royal Meteorological Society,* 122**,** 73-119.

MORENO, T., QUEROL, X., ALASTUEY, A., DE LA ROSA, J., DE LA CAMPA, A. M. S., MINGUILLON, M., PANDOLFI, M., GONZALEZ-CASTANEDO, Y., MONFORT, E. & GIBBONS, W. 2010. Variations in vanadium, nickel and lanthanoid element concentrations in urban air. *Science of the Total Environment,* 408**,** 4569-4579.

MOZURKEWICH, M. 1993. The Dissociation-Constant of Ammonium-Nitrate and Its Dependence On Temperature, Relative-Humidity and Particle-Size. *Atmospheric Environment Part a-General Topics,* 27**,** 261-270.

MUNZUR, B. & TUNCEL, G. 2008. Chemical Composition of Atmospheric Particles in the Aegean Region. *Master of Thesis, Department of Environmental Engineering, Middle East Technical University, Ankara.*

MURPHY, D. M., THOMSON, D. S. & MIDDLEBROOK, A. M. 1997. Bromine, iodine, and chlorine in single aerosol particles at Cape Grim. *Geophysical Research Letters,* 24**,** 3197-3200.

MYLONA, S. 1996. Sulphur dioxide emissions in Europe 1880-1991 and their effect on sulphur concentrations and depositions. *Tellus Series B-Chemical and Physical Meteorology,* 48**,** 662-689.

NATUSCH, D. F. S., WALLACE, J. R. & EVANS, C. A. 1974. Toxic trace-elements - preferential concentration in respirable particles. *Science,* 183**,** 202-204.

NAZIR, R., SHAHEEN, N. & SHAH, M. H. 2011. Indoor/outdoor relationship of trace metals in the atmospheric particulate matter of an industrial area. *Atmospheric Research,* 101**,** 765-772.

NENES, A., PANDIS, S. N. & PILINIS, C. 1999. Continued development and testing of a new thermodynamic aerosol module for urban and regional air quality models. *Atmospheric Environment,* 33**,** 1553-1560.

NICKOVIC, S., PAPADOPOULOS, A., KAKALIAGOU, O. & KALLOS, G. 2001. Model for prediciton of desert dust cycle in the atmosphere. *Journal of Geophysical Research* 106**,** 18113-18129.

NICOLAS, J. F., GALINDO, N., YUBERO, E., PASTOR, C., ESCLAPEZ, R. & CRESPO, J. 2009. Aerosol Inorganic Ions in a Semiarid Region on the Southeastern Spanish Mediterranean Coast. *Water Air and Soil Pollution,* 201**,** 149-159.

OKAY, C., AKKOYUNLU, B. O. & TAYANC, M. 2002. Composition of wet deposition in Kaynarca, Turkey. *Environmental Pollution,* 118**,** 401-410.

OLMEZ, I. & GORDON, G. E. 1985. Rare Earths: Atmospheric Signatures for Oil-Fired Power Plants and Refineries. *Science,* 229**,** 966-968.

OWEN, R. C. 2003. A Climatological Study of Transport to the PICO-NARE Site Using Atmospheric Backward Trajectories. *Civil and Environmental Engineering. Michigan Technological University, Master of Science, Houghton, MI. .*

ÖZTÜRK, F. & TUNCEL, G. 2009. Investigation of Short and Long Term Trends in the Eastern Mediterranean Aerosol Composition. *PhD Dissertation, Department of Environmental Engineering, Middle East Technical University, Ankara.*

ÖZTÜRK, F., ZARARSıZ, A., DUTKIEWICZ, V. A., HUSAIN, L., HOPKE, P. K. & TUNCEL, G. 2012. Temporal variations and sources of Eastern Mediterranean aerosols based on a 9-year observation. *Atmospheric Environment,* 61**,** 463-475.

PAATERO, P. 1997. Least squares formulation of robust nonnegative factor analysis. *Chemometrics and Intelligent Laboratory Systems,* 37**,** 15-35.

PAATERO, P. & HOPKE, P. K. 2003. Discarding or downweighting high-noise variables in factor analytic models. *Analytica Chimica Acta,* 490**,** 277-289.

PAATERO, P. & TAPPER, U. 1993. Analysis of different modes of factor analysis as least squares fit problems. *Chemometrics and Intelligent Laboratory Systems,* 18**,** 183-194.

PAATERO, P. & TAPPER, U. 1994. Positive matrix factorization: a non-negative factor model with optimal utilization of error estimates of data values. *Environmetrics,* 5**,** 111-126.

PACYNA, J. M. & PACYNA, E. G. 2001. An assessment of global and regional emissions of trace metals to the atmosphere from anthropogenic sources worldwide *Environmental Reviews,* 9**,** 269-298.

PAKKANEN, T. A. 1996. Study of formation of coarse particle nitrate aerosol. *Atmospheric Environment,* 30**,** 2475-2482.

PAKKANEN, T. A., KERMINEN, V. M., LOUKKOLA, K., HILLAMO, R. E., AARNIO, P., KOSKENTALO, T. & MAENHAUT, W. 2003. Size distributions of mass and chemical components in street-level and rooftop PM1 particles in Helsinki. *Atmospheric Environment,* 37**,** 1673-1690.

PANDIS, S. N. & SEINFELD, J. H. 1989. Sensitivity analysis of a chemical mechanism for aqueous-phase atmospheric chemistry. *Journal of Geophysical Research-Atmospheres,* 94**,** 1105-1126.

PANDOLFI, M., GONZALEZ-CASTANEDO, Y., ALASTUEY, A., DE LA ROSA, J. D., MANTILLA, E., DE LA CAMPA, A. S., QUEROL, X., PEY, J., AMATO, F. & MORENO, T. 2011. Source apportionment of PM10 and PM2.5 at multiple sites in the strait of Gibraltar by PMF: impact of shipping emissions. *Environmental Science and Pollution Research,* 18**,** 260-269.

PAPADIMAS, C. D., HATZIANASTASSIOU, N., MIHALOPOULOS, N., KANAKIDOU, M., KATSOULIS, B. D. & VARDAVAS, I. 2009. Assessment of the MODIS Collections C005 and C004 aerosol optical depth products over the Mediterranean basin. *Atmospheric Chemistry and Physics,* 9**,** 2987-2999.

PEKEY, H. & DOGAN, G. 2013. Application of positive matrix factorisation for the source apportionment of heavy metals in sediments: A comparison with a previous factor analysis study. *Microchemical Journal,* 106**,** 233-237.

PEKNEY, N. J. & DAVIDSON, C. I. 2005. Determination of trace elements in ambient aerosol samples. *Analytica Chimica Acta,* 540**,** 269-277.

PEREZ, C., NICKOVIC, S., BALDASANO, J. M., SICARD, M., ROCADENBOSCH, F. & CACHORRO, V. E. 2006. A long Saharan dust event over the western

Mediterranean: Lidar, Sun photometer observations, and regional dust modeling. *Journal of Geophysical Research* 111.

PERRONE, M. R., PIAZZALUNGA, A., PRATO, M. & CAROFALO, I. 2011. Composition of fine and coarse particles in a coastal site of the central Mediterranean: Carbonaceous species contributions. *Atmospheric Environment,* 45**,** 7470-7477.

PLAISANCE, H., GALLOO, J. C. & GUILLERMO, R. 1997. Source identification and variation in the chemical composition of precipitation at two rural sites in France. *Science of the Total Environment,* 206**,** 79-93.

POLISSAR, A. V., HOPKE, P. K., PAATERO, P., KAUFMANN, Y. J., HALL, D. K., BODHAINE, B. A., DUTTON, E. G. & HARRIS, J. M. 1999. The aerosol at Barrow, Alaska: long-term trends and source locations. *Atmospheric Environment,* 33**,** 2441-2458.

POPE, C. A. 2000. Review: Epidemiological basis for particulate air pollution health standards. *Aerosol Science and Technology,* 32**,** 4-14.

POPE, C. A., BATES, D. V. & RAIZENNE, M. E. 1995. Health-effects of particulate air-pollution - time for reassessment. *Environmental Health Perspectives,* 103**,** 472-480.

POPE, C. A. & DOCKERY, D. W. 2006. Health effects of fine particulate air pollution: Lines that connect. *Journal of the Air & Waste Management Association,* 56**,** 709-742.

POPE, C. A., SCHWARTZ, J. & RANSOM, M. R. 1992. Daily mortality and PM10 pollution in Utah Valley. *Archives Environmental Health,* 47**,** 211-217.

PUESCHEL, R. F. 1995. Atmospheric Aerosol. *In: Singh, H.B. (Ed.), .Van Nostrand Reinhold, New York***,** 120-175.

PULLES, T., VAN DER GON, H. D., APPELMAN, W. & VERHEUL, M. 2012. Emission factors for heavy metals from diesel and petrol used in European vehicles. *Atmospheric Environment,* 61**,** 641-651.

QUEROL, X., ALASTUEY, A., PEY, J., CUSACK, M., PEREZ, N., MIHALOPOULOS, N., THEODOSI, C., GERASOPOULOS, E., KUBILAY, N. & KOCAK, M. 2009. Variability in regional background aerosols within the Mediterranean. *Atmospheric Chemistry and Physics,* 9**,** 4575-4591.

REFF, A., EBERLY, S. I. & BHAVE, P. V. 2007. Receptor modeling of ambient particulate matter data using positive matrix factorization: Review of existing methods. *Journal of the Air & Waste Management Association,* 57**,** 146-154.

REIMANN, C. & DE CARITAT, P. 2005. Distinguishing between natural and anthropogenic sources for elements in the environment: regional geochemical surveys versus enrichment factors. *Science of the Total Environment,* 337**,** 91-107.

REVUELTA, M. A., HARRISON, R. M., NUNEZ, L., GOMEZ-MORENO, F. J., PUJADAS, M. & ARTINANO, B. 2012. Comparison of temporal features of sulphate and nitrate at urban and rural sites in Spain and the UK. *Atmospheric Environment,* 60**,** 383-391.

RHODES, E. P., REN, Z. Y. & MAYS, D. C. 2012. Zinc Leaching from Tire Crumb Rubber. *Environmental Science & Technology,* 46**,** 12856-12863.

RIVERA RIVERA, N. I., BLEIWEISS, M. P., HAND, J. L. & GILL, T. E. 2006. Characterization of dust storms sources in southwestern U.S. and northern Mexico using remote sensing imagery. *American Meteorological Society, 14th Conference on Satellite Meteorology and Oceanography*.

RODRIGUEZ, S., QUEROL, X., ALASTUEY, A., KALLOS, G. & KAKALIAGOU, O. 2001. Saharan dust contributions to PM10 and TSP levels in Southern and Eastern Spain. *Atmospheric Environment,* 35**,** 2433-2447.

RUSSELL, A. G., CASS, G. R. & SEINFELD, J. H. 1986. On some aspects of nighttime atmospheric chemistry. *Environmental Science & Technology,* 20**,** 1167-1172.

SAMET, J. M., DOMINICI, F., CURRIERO, F. C., COURSAC, I. & ZEGER, S. L. 2000. Fine particulate air pollution and mortality in 20 US Cities, 1987-1994. *New England Journal of Medicine,* 343**,** 1742-1749.

SAMURA, A., AL-AGHA, O. & TUNCEL, S. G. 2003. Study of Trace and Heavy Metals in Rural and Urban Aerosols of Uludağ and Bursa (Turkey). *Water, Air and Soil Pollution: Focus,* 3**,** 111-129.

SANDRONI, V., SMITH, C. M. M. & DONOVAN, A. 2003. Microwave digestion of sediment, soils and urban particulate matter for trace metal analysis. *Talanta,* 60**,** 715-723.

SAVOIE, D. L., PROSPERO, J. M. & NEES, R. T. 1987. Nitrate, non-sea-salt sulfate, and mineral aerosol over the northwestern Indian-Ocean. *Journal of Geophysical Research-Atmospheres,* 92**,** 933-942.

SCHWARTZ, J., DOCKERY, D. W. & NEAS, L. M. 1996. Is daily mortality associated specifically with fine particles? *Journal of the Air and Waste Management Association* 46**,** 927–939.

SCIARE, J., BARDOUKI, H., MOULIN, C. & MIHALOPOULOS, N. 2003. Aerosol sources and their contribution to the chemical composition of aerosols in the Eastern Mediterranean Sea during summertime. *Atmospheric Chemistry and Physics,* 3**,** 291-302.

SCIARE, J., OIKONOMOU, K., CACHIER, H., MIHALOPOULOS, N., ANDREAE, M. O., MAENHAUT, W. & SARDA-ESTEVE, R. 2005. Aerosol mass closure and reconstruction of the light scattering coefficient over the Eastern Mediterranean Sea during the MINOS campaign. *Atmospheric Chemistry and Physics,* 5**,** 2253-2265.

SCIARE, J., OIKONOMOU, K., FAVEZ, O., LIAKAKOU, E., MARKAKI, Z., CACHIER, H. & MIHALOPOULOS, N. 2008. Long-term measurements of carbonaceous aerosols in the Eastern Mediterranean: evidence of long-range transport of biomass burning. *Atmospheric Chemistry and Physics,* 8**,** 5551-5563.

SEINFELD, J. H. & PANDIS, S. N. 2006. Atmospheric Chemistry and Physics - From Air Pollution to Climate Change (2nd Edition). John Wiley & Sons.

SEN, O. 1997. Inversions and air pollution in Istanbul. *International Journal of Environment and Pollution,* 8**,** 158-163.

SEN, O. 1998. Air pollution and inversion features in Istanbul. *International Journal of Environment and Pollution,* 9**,** 371-383.

SEN, O., SAHIN, F., SAYLAN, L. & INCECIK, S. 1997. *The effects of surface and elevated inversions on the air pollution in Istanbul.*

SHAW, P. 2008. Application of aerosol speciation data as an in situ dust proxy for validation of the Dust Regional Atmospheric Model (DREAM). *Atmospheric Environment,* 42**,** 7304-7309.

SINGH, M., JAQUES, P. A. & SIOUTAS, C. 2002. Size distribution and diurnal characteristics of particle-bound metals in source and receptor sites of the Los Angeles Basin. *Atmospheric Environment,* 36**,** 1675-1689.

SONG, C. H. & CARMICHAEL, G. R. 1999. The aging process of naturally emitted aerosol (sea-salt and mineral aerosol) during long range transport. *Atmospheric Environment,* 33**,** 2203-2218.

SPECIATE, E. 2012. U.S. EPA. "SPECIATE: EPA's repository of total organic compound and particulate matter speciated profiles for a variety of sources for use in source

apportionment studies". *U.S. Environmental Protection Agency OAQPS,* Research Triangle Park, NC, 1999.

STERNBECK, J., SJODIN, A. & ANDREASSON, K. 2002. Metal emissions from road traffic and the influence of resuspension - results from two tunnel studies. *Atmospheric Environment,* 36**,** 4735-4744.

STOCKWELL, W. R. & CALVERT, J. G. 1983. The mechanism of the HO-SO2 reaction. *Atmospheric Environment,* 17**,** 2231-2235.

STOHL, A. 1998. Computation, accuracy and applications of trajectories - A review and bibliography. *Atmospheric Environment,* 32**,** 947-966.

STOHL, A. & KOFFI, N. E. 1998. Evaluation of trajectories calculated from ECMWF data against constant volume balloon flights during ETEX. *Atmospheric Environment,* 32**,** 4151-4156.

STOHL, A., WOTAWA, G., SEIBERT, P. & KROMPKOLB, H. 1995. Interpolation errors in wind fields as a function of spatial and temporal resolution and their impact on different types of kinematic trajectories. *Journal of Applied Meteorology,* 34**,** 2149-2165.

STOIBER, R. E., WILLIAMS, S. N. & HUEBERT, B. 1987. Annual contribution of sulfur dioxide to the atmosphere by volcanoes. *Journal of Volcanology and Geothermal Research,* 33**,** 1-8.

SZIGETI, T., MIHUCZ, V. G., ÓVÁRI, M., BAYSAL, A., ATıLGAN, S., AKMAN, S. & ZÁRAY, G. 2012. Chemical characterization of PM2.5 fractions of urban aerosol collected in Budapest and Istanbul. *Microchemical Journal***,** doi: 10.1016/j.microc.2012.05.029.

TANG, I. N. & MUNKELWITZ, H. R. 1993. Composition and temperature-dependence of the deliquescence properties of hygroscopic aerosols. . *Atmospheric Environment Part a-General Topics,* 27**,** 467-473.

TAUBMAN, B. F., HAINS, J. C., THOMPSON, A. M., MARUFU, L. T., DODDRIDGE, B. G., STEHR, J. W., PIETY, C. A. & DICKERSON, R. R. 2006. Aircraft vertical profiles of trace gas and aerosol pollution over the mid-Atlantic United States: Statistics and meteorological cluster analysis. *Journal of Geophysical Research-Atmospheres,* 111.

TAYANC, M., KARACA, M., SARAL, A. & ERTURK, F. 1998. *Study of the decrease of air pollution concentration levels with the meteorological factors in Istanbul.*

TAYLOR, S. R. 1964. Abundance of chemical elements in the continental crust: a new table. *Geochimica Et Cosmochimica Acta,* 28**,** 1273-1285.

TECER, L. H., TUNCEL, G., KARACA, F., ALAGHA, O., SUREN, P., ZARARSIZ, A. & KIRMAZ, R. 2012. Metallic composition and source apportionment of fine and coarse particles using positive matrix factorization in the southern Black Sea atmosphere. *Atmospheric Research,* 118**,** 153-169.

TEGEN, I. & LACIS, A. A. 1996. Modeling of particle size distribution and its influence on the radiative properties of mineral dust aerosol. *Journal of Geophysical Research,* 101**,** 19237-19244.

THEODOSI, C., IM, U., BOUGIATIOTI, A., ZARMPAS, P., YENIGUN, O. & MIHALOPOULOS, N. 2010a. Aerosol chemical composition over Istanbul. *Science of the Total Environment,* 408**,** 2482-2491.

THEODOSI, C., MARKAKI, Z., TSELEPIDES, A. & MIHALOPOULOS, N. 2010b. The significance of atmospheric inputs of soluble and particulate major and trace metals to the eastern Mediterranean seawater. *Marine Chemistry,* 120**,** 154-163.

THORPE, A. & HARRISON, R. M. 2008. Sources and properties of non-exhaust particulate matter from road traffic: A review. *Science of the Total Environment,* 400**,** 270-282.

TIDBLAD, J. & KUCERA, V. 1998. Materials damage. In: Fenger, J., Hertel, O., Palmgren, F. (Eds.), Urban Air Pollution, European Aspects. Kluwer Academic Publishers, Dordrecht**,** 343-361.

TODD, M. C., KARAM, D. B., CAVAZOS, C., BOUET, C., HEINOLD, B., BALDASANO, J. M., CAUTENET, G., KOREN, I., PEREZ, C., SOLMON, F., TEGEN, I., TULET, P., WASHINGTON, R. & ZAKEY, A. 2008. Quantifying uncertainty in estimates of mineral dust flux: An intercomparison of model performance over the Bodele Depression, northern Chad. *Journal of Geophysical Research-Atmospheres,* 113.

TRAPP, J. M., MILLERO, F. J. & PROSPERO, J. M. 2010. Temporal variability of the elemental composition of African dust measured in trade wind aerosols at Barbados and Miami. *Marine Chemistry,* 120**,** 71-82.

TUNCEL, G., ARAS, N. K. & ZOLLER, W. H. 1989. Temporal variations and sources of elements in the South Pole atmosphere 1. Nonenriched and moderately enriched elements. *Journal of Geophysical Research-Atmospheres,* 94**,** 13025-13038.

TURK, Y. A. & KAVRAZ, M. 2010. The relation between some meteorological factors and air pollutants in Trabzon city. *Fresenius Environmental Bulletin,* 19**,** 721-729.

TURKUM, A., PEKEY, B., PEKEY, H. & TUNCEL, G. 2008. Comparison of sources affecting chemical compositions of aerosol and rainwater at different locations in Turkey. *Atmospheric Research,* 89**,** 306-314.

UNECE 2007. Strategies and Policies for Air pollution Abadement:Review 2006. *United Nations New York Geneva.*

URL 1. Retrieved January 16, 2013 from web site:
http://www.unece.org/env/lrtap/lrtap_h1.html

UYGUR, N., KARACA, F. & ALAGHA, O. 2010. Prediction of sources of metal pollution in rainwater in Istanbul, Turkey using factor analysis and long-range transport models. *Atmospheric Research,* 95**,** 55-64.

VERMA, S. K., DEB, M. K., SUZUKI, Y. & TSAI, Y. I. 2010. Ion chemistry and source identification of coarse and fine aerosols in an urban area of eastern central India. *Atmospheric Research,* 95**,** 65-76.

VIANA, M., KUHLBUSCH, T. A. J., QUEROL, X., ALASTUEY, A., HARRISON, R. M., HOPKE, P. K., WINIWARTER, W., VALLIUS, A., SZIDAT, S., PREVOT, A. S. H., HUEGLIN, C., BLOEMEN, H., WAHLIN, P., VECCHI, R., MIRANDA, A. I., KASPER-GIEBL, A., MAENHAUT, W. & HITZENBERGER, R. 2008a. Source apportionment of particulate matter in Europe: A review of methods and results. *Journal of Aerosol Science,* 39**,** 827-849.

VIANA, M., LOPEZ, J. M., QUEROL, X., ALASTUEY, A., GARCIA-GACIO, D., BLANCO-HERAS, G., LOPEZ-MAHIA, P., PINEIRO-IGLESIAS, M., SANZ, M., SANZ, F., CHI, X. & MAENHAUT, W. 2008b. Tracers and impact of open burning of rice straw residues on PM in Eastern Spain. *Atmospheric Environment,* 42**,** 1941-1957.

VIEIRA, B. J., FREITAS, M. C. & WOLTERBEEK, H. T. 2012. Elemental composition of air masses under different altitudes in Azores, central north Atlantic. *Journal of Radioanalytical and Nuclear Chemistry,* 291**,** 63-69.

WANG, Y., ZHUANG, G. S., ZHANG, X. Y., HUANG, K., XU, C., TANG, A. H., CHEN, J. M. & AN, Z. S. 2006. The ion chemistry, seasonal cycle, and sources of PM2.5 and TSP aerosol in Shanghai. *Atmospheric Environment,* 40**,** 2935-2952.

WANG, Y. Q., ZHANG, X. Y. & DRAXLER, R. R. 2009. TrajStat: GIS-based software that uses various trajectory statistical analysis methods to identify potential sources from long-term air pollution measurement data. *Environmental Modelling & Software,* 24, 938-939.

WARD, J. H. 1963. Hierarchical Grouping to Optimize an Objective Function. *Journal of the American Statistical Association,* 58, 236-&.

WATSON, J. G. 2002. Visibility: Science and regulation. *Journal of the Air & Waste Management Association,* 52, 628-713.

WATSON, J. G. & CHOW, J. C. 2007. Receptor models for source apportionment of suspended particles: in Introduction to Environmental Forensics (Second Edition). Murphy, B. L. and Morrison, R. D. (Eds.), CRC Press, Sand Diego, CA. , Chapter 8, Pages 273-310,IX-X.

WATSON, J. G., CHOW, J. C. & HOUCK, J. E. 2001. PM2.5 chemical source profiles for vehicle exhaust, vegetative burning, geological material, and coal burning in Northwestern Colorado during 1995. *Chemosphere,* 43, 1141-1151.

WATSON, J. G., ZHU, T., CHOW, J. C., ENGELBRECHT, J., FUJITA, E. M. & WILSON, W. E. 2002. Receptor modeling application framework for particle source apportionment. *Chemosphere,* 49, 1093-1136.

WEDEPOHL, K. H. 1995. The composition of the continental-crust. *Geochimica Et Cosmochimica Acta,* 59, 1217-1232.

WEHRENS, R., PUTTER, H. & BUYDENS, L. M. C. 2000. The bootstrap: a tutorial. *Chemometrics and Intelligent Laboratory Systems,* 54, 35-52.

XIE, Y. L., HOPKE, P. K., PAATERO, P., BARRIE, L. A. & LI, S. M. 1999. Identification of source nature and seasonal variations of arctic aerosol by positive matrix factorization. *Journal of the Atmospheric Sciences,* 56, 249-260.

YANG, K. X., SWAMI, K. & HUSAIN, L. 2002. Determination of trace metals in atmospheric aerosols with a heavy matrix of cellulose by microwave digestion-inductively coupled plasma mass spectroscopy. *Spectrochimica Acta Part B-Atomic Spectroscopy,* 57, 73-84.

YıKMAZ, R. F. & TUNCEL, G. 2010. Development of GIS Based Trajectory Statistical Analysis Method to Identify Potential Sources of Regional Air Pollution. *Master of Thesis, Department of Environmental Engineering, Middle East Technical University, Ankara.*

YIN, D., NICKOVIC, S., BARBARIS, B., CHANDY, B. & SPRIGG, W. A. 2005. Modeling wind-blown desert dust in the southwestern United States for public health warning: A case study. *Atmospheric Environment,* 39, 6243-6254.

YIN, D., NICKOVIC, S. & SPRIGG, W. A. 2007. The impact of using different land cover data on wind-blown desert dust modeling results in the southwestern United States. *Atmospheric Environment,* 41, 2214-2224.

ZENDER, C. S., MILLER, R. L. & TEGEN, I. 2004. Quantifying mineral dust mass budgets: Terminology, constraints and current estimates. *EOS-AGU,* 85, 509– 512.

ZENG, Y. & HOPKE, P. K. 1989. A study of the sources of acid precipitation in Ontario, Canada. *Atmospheric Environment,* 23, 1499-1509.

ZHAO, W. X. & HOPKE, P. K. 2006. Source investigation for ambient PM2.5 in Indianapolis, IN. *Aerosol Science and Technology,* 40, 898-909.

ZHUANG, H., CHAN, C. K., FANG, M. & WEXLER, A. S. 1999. Formation of nitrate and non-sea-salt sulfate on coarse particles. *Atmospheric Environment,* 33, 4223-4233.

ZOLLER, W. H., GLADNEY, E. S. & DUCE, R. A. 1974 Atmospheric concentrations and sources of trace metals at the South Pole. *Science,* 183**,** 199–201.

CURRICULUM VITAE

PERSONAL INFORMATION
Surname, Name: Genç Tokgöz, D. Deniz
Date of birth: 7th February 1979
Nationality: Turkish
Marital Status: Married
email: dgtokgoz@hotmail.com

EDUCATION
Georgia Institute of Technology, School of Civil and Environmental Engineering, USA. *Visiting Scholar*, April 2010 to April 2011.
Middle East Technical University, Ankara. *Master of Science in Environmental Engineering*, September 2003 to October 2005.
Middle East Technical University, Ankara. *Bachelor of Science in Environmental Engineering*, September 1997 to July 2002.

WORK EXPERIENCE
Middle East Technical University, Ankara. Research Assistant, April 2004-February 2013.

AWARDS and FELLOWSHIP
The Scientific and Technological Research Council of Turkey (TUBITAK), International Doctoral Research Fellowship, 2010-2011.
M.S. Program Honour Student of the Department of Environmental Engineering in the Academic Year 2003-2004.
TEV Scholarship, 1997- 2002.

RESEARCH INTERESTS
Atmospheric chemistry
Air pollution and control
Air pollution meteorology
Long range transport of air pollutants
Precipitation chemistry
Air quality modeling: source and receptor models